Aus dem Max von Pettenkofer-Institut für Hygiene und Medizinische Mikrobiologie

Institut der Ludwig-Maximilians-Universität München

Vorstand: Prof. Dr. med. Sebastian Suerbaum

Influence of environmental cues on virulence factor regulation of Enterohemorrhagic *Escherichia coli*

Dissertation

Zum Erwerb des Doktorgrades der Naturwissenschaften an der Medizinischen Fakultät der Ludwig-Maximilians-Universität München

vorgelegt von

Benedikt Frederik Camille Graf von Armansperg

aus

München, Deutschland

2024

Mit Genehmigung der Medizinischen Fakultät
der Ludwig-Maximilians-Universität München

Betreuerin:	Prof. Dr. Barbara Stecher-Letsch
Zweitgutachter(in):	Prof. Dr. Alexander Dietrich
Dekan:	Prof. Dr. med. Thomas Gudermann
Tag der mündlichen Prüfung:	17. Dezember 2024

Eidesstattliche Versicherung

Graf von Armansperg, Benedikt Frederik Camille

Name, Vorname

Ich erkläre hiermit an Eides statt, dass ich die vorliegende Dissertation mit dem Thema

Influence of environmental cues on virluence factor regulation of Enterohemorrhagic Escherichia coli

selbständig verfasst, mich außer der angegebenen keiner weiteren Hilfsmittel bedient und alle Erkenntnisse, die aus dem Schrifttum ganz oder annähernd übernommen sind, als solche kenntlich gemacht und nach ihrer Herkunft unter Bezeichnung der Fundstelle einzeln nachgewiesen habe.

Ich erkläre des Weiteren, dass die hier vorgelegte Dissertation nicht in gleicher oder in ähnlicher Form bei einer anderen Stelle zur Erlangung eines akademischen Grades eingereicht wurde.

Gräfelfing, 21.04.2025 — Ort, Datum

Benedikt von Armansperg — Unterschrift Doktorandin/Doktorand

Danksagung

An dieser Stelle möchte ich mich herzlich bei allen bedanken, die zum Gelingen dieser Doktorarbeit beigetragen haben.

Mein besonderer Dank gilt meiner Doktormutter, Frau Professorin Bärbel Stecher. Deine fachliche Unterstützung, Geduld und unermüdliches Engagement haben maßgeblich zum Erfolg dieser Arbeit beigetragen. Deine wertvollen Ratschläge, vertrauen in meine Arbeit und konstruktive Kritik haben mich stets motiviert und meinen wissenschaftlichen Horizont erweitert. Vielen Dank, dass du mir die Möglichkeit gegeben hast, unter deiner Leitung an sehr interessanten Themen zu forschen, mich weiterzuentwickeln und viel Neues zu erlernen.

Des Weiteren möchte ich mich bei der gesamten Arbeitsgruppe Stecher bedanken. Die freundliche und kollegiale Arbeitsatmosphäre hat diese Zeit für mich besonders bereichernd gemacht. Jeder Einzelne von euch hat durch seine Hilfsbereitschaft und seinen Teamgeist dazu beigetragen, dass ich mich stets unterstützt und wertgeschätzt gefühlt habe. Besonders möchte ich mich bei Diana Ring bedanken. Vielen Dank für deine Unterstützung und Hilfe bei der Suche nach Geräten oder Chemikalien im Labor. Ohne deine Organisation wäre meine Arbeit um einiges schwieriger geworden.

A big thank you also to my three friends Anna, Alex and Marta. Without our great and loyal community in Office 034, my time as a doctoral student would only have been half as fun. This also applies to the two latecomers to this community, Lisa and Marla. The many interesting discussions about our scientific problems and questions, but also our everyday problems, has enriched my working time and made it easier to overcome setbacks. Our after-work activities in particular, such as cooking together, have brought us closer together and created wonderful traditions.

Mein besonderer Dank geht an meine Familie. I would especially like to highlight my wife Florencia and my daughter Emma. You were always by my side and encouraged me to continue, particularly during the exhausting final phase of my work. Your support was crucial in enabling me to complete my doctoral thesis. Auch bei meinen Eltern Wolfgang und Nikola, und Brüdern Dominik und Frederik möchte ich herzlichst bedanken für eure tatkräftige Unterstützung nicht nur während der Doktorandenzeit, sondern weiter darüber hinaus. Danke das ihr an mich geglaubt habt und mir diesen Lebensweg ermöglicht habt.

Tabel of Content

List of Tables

List of Figures

Abbreviations

°C	Degree Celsius	HUSEC	hemolytic uremic syndrome-associated *Escherichia coli*
µM	micro molar	M	Molar
ABX	Antibiotic treatment	MAD	Median absolute deviation
AE	Attaching and effacing lesions	min	minute
ATC	Anatomical Therapeutic Chemical	MitoC	Mitomycin C
CFU	Colony forming units	mM	Millimolar
CR	Colonization resistance	n.s.	Not significant
ddH20	Double-distilled water	o.n.	Overnight
DMSO	Dimethyl sulfoxide	OD_{600}	Optical density at 600nm
DNA	Deoxyribonucleic acid	OD_{max}	Maximal optical density at 600nm
E. coli	*Escherichia coli*	PBS	Phosphate-buffered saline
EAEC	Enteroaggregative *Escherichia coli*	PCR	Polymerase chain reaction
EDTA	Ethylenediaminetetraacetic acid	qPCR	Quantitative real-time polymerase chain reaction
EHEC	Enterohaemorrhagic *Escherichia coli*	RLU	Relative light unit
ER	Endoplasmatic reticulum	ROS	Reactive oxygen species
FAM	6-carboxyfluoresceine	rpm	Rounds per minute
Gb3	Globotriaosylceramide	rRNA	Ribosomal ribonucleic acid
gDNA	Genomic DNA	RT	Room temperature
GI	Gastrointestinal	rz-score	Robust Z-score
Gluc	*Gaussia principes* luciferase	s	second
h	Hour	SD	Standard deviation
H_2O_2	Hydrogen peroxide	SSMD	Strictly standardized mean difference
HEX	6-carboxyhexafluoresceine	STEC	Shiga-toxin producing *Escherichia coli*
HTS	High-throughput screen	SW	signal window
HUS	Hemolytic-uremic syndrome	Z'	z-score

Summary

Enterohemorrhagic *Escherichia coli* (EHEC) is a major food-borne human pathogen causing severe gastrointestinal disease, particularly acute diarrhoea, and haemorrhagic colitis, with an elevated risk in children and elderly. Both age groups have a higher risk to develop severe complications, including the development of haemolytic uremic syndrome (HUS), a life-threatening condition closely associated with the production of Shiga toxin 2 (Stx2) by the pathogen. Certain host factors, including age, gender and an elevated immune response towards Stx2, have been associated with an increased risk of HUS development. Likewise, Stx2 production is promoted by the induction of bacterial stress response like the SOS response mediated via RecA. Therefore, the use of certain antibiotics as therapy for EHEC infection are contraindicated. Furthermore, other environmental risk factors for the development of HUS are poorly characterized. The aim of this thesis was to investigate the role of environmental factors including human-targeted drugs and the microbiome in influencing the expression of EHEC virulence genes, particularly Stx2 production.

To address these aims, I established a high-throughput assay to systematically analyse the impact of various compounds on *stx2* expression. Utilizing an *E. coli* C600-based luciferase reporter strain (CW^{gluc}), I optimized the assay for scalability and reproducibility.

A range of human-targeted drugs has been shown to have antibacterial activity. Hence, I hypothesized that drugs may also influence *stx2* expression. I used the established assay to screen a comprehensive chemical library of Food and Drug Administration (FDA) and European Medicines Agency (EMA)-approved human-targeted drugs for their effects on *stx2* expression. Several compounds with either stimulatory or inhibitory effects on Stx2 production were identified and confirmed through several validation processes. Notably, certain antibiotic classes like quinolones and fluoroquinolones were highly represented among *stx2* inducing compounds, as well as beta-lactam antibiotics, belonging to the cephalosporin and penicillin cluster. Chemotherapeutic compounds evoked a significant inducing effect on *stx2*, especially the compounds dacarbazine and streptozotocin. Additionally, acetylsalicylic acid (aspirin), a widely taken medication, showed clear signs of *stx2* inducing effects. On the other hand, several compounds showed inhibitory effects on *stx2* expression. Especially antibiotics

inhibiting the protein biosynthesis like azithromycin or clarithromycin had a strong inhibitory effect. But also, non-antibiotic compounds like levodopa showed inhibition of *stx2* expression. Overall, this screen identified both, *stx2* inducing and inhibiting compounds, pointing at potential risk factors to develop severe disease on the one hand, and possible therapeutic avenues for mitigating HUS development on the other.

Additionally, I analysed microbiome datasets from faecal samples of patients obtained during the haemolytic uremic syndrome associated *E. coli* (HUSEC) outbreak in Northern Germany in 2011 to identify microbiome-based risk factors indicating disease severity. The analysis revealed distinct microbiota signatures associated with HUS, pointing at a potential role of specific bacterial taxa in modulating EHEC virulence or disease outcome. In particular, the presence of bacteria encoding the genotoxin colibactin (*pks* island), which was previously shown to induce *stx2* expression *in vitro*, was elevated within the HUS patient group. These data may point at a potential mechanism which increases the patient risk to develop HUS.

In conclusion, this thesis provides significant insights into the interplay of environmental cues, the intestinal microbiota, and EHEC pathogenesis. The established high-throughput assay to quantify Stx2 production in live bacteria offers a valuable tool for further research into Stx2 regulation and the identification of potential drug-based interventions. The findings underscore the importance of considering microbiome composition and drug interactions in managing EHEC infections and preventing HUS. This holistic approach could pave the way for more effective and personalized treatments, ultimately improving patient outcomes in the fight against EHEC-related diseases.

Zusammenfassung

Enterohämorrhagische Escherichia coli (EHEC) ist ein wichtiger lebensmittelbedingter Krankheitserreger beim Menschen, der schwere Magen-Darm-Erkrankungen verursacht, insbesondere akuten Durchfall und hämorrhagische Kolitis, wobei das Risiko bei Kindern und älteren Menschen erhöht ist. Beide Altersgruppen haben ein höheres Risiko, schwere Komplikationen zu entwickeln, einschließlich des hämolytisch-urämischen Syndroms (HUS), einer lebensbedrohlichen Erkrankung, die eng mit der Produktion von Shiga-Toxin 2 (Stx2) durch den Erreger verbunden ist. Bestimmte Wirtsfaktoren, wie Alter, Geschlecht und eine erhöhte Immunantwort auf Stx2, sind mit einem erhöhten Risiko für die Entwicklung von HUS verbunden. Ebenfalls wird die Produktion von Stx2 durch die Induktion von bakteriellen Stressreaktionen wie der durch RecA vermittelten SOS-Antwort gefördert. Daher ist die Anwendung bestimmter Antibiotika zur Behandlung von EHEC-Infektionen kontraindiziert. Andere Umweltfaktoren, die das Risiko für die Entwicklung von HUS beeinflussen, sind jedoch schlecht untersucht. Ziel dieser Dissertation war es, die Rolle von Umweltfaktoren, einschließlich der auf den Menschen ausgerichtete Medikamente und das Mikrobiom, bei der Beeinflussung der Expression von EHEC-Virulenzgenen, insbesondere der Stx2-Produktion, zu untersuchen.

Um diese Ziele zu erreichen, habe ich einen Hochdurchsatz-Assay entwickelt, um systematisch die Auswirkungen verschiedener Verbindungen auf die *stx2*-Expression zu analysieren. Unter Verwendung eines auf *E. coli* C600 basierenden Luciferase-Reporter-Stamms (CW^{gluc}) optimierte ich den Assay hinsichtlich Skalierbarkeit und Reproduzierbarkeit.

Eine Reihe von auf den Menschen ausgerichtete Medikamente zeigen antibakterielle Aktivität. Daher vermutete ich, dass diese Medikamente auch die *stx2*-Expression beeinflussen könnten. Ich verwendete den etablierten Assay, um eine umfassende Bibliothek von auf den Menschen ausgerichtete Medikamente, die von der Food and Drug Administration (FDA) und der Europäischen Arzneimittel-Agentur (EMA) zugelassenen sind, auf ihre Auswirkungen auf die *stx2*-Expression zu screenen. Mehrere Verbindungen mit entweder stimulierenden oder hemmenden Effekten auf die Stx2-Produktion wurden identifiziert und durch mehrere Validierungsprozesse bestätigt. Bemerkenswert war, dass bestimmte Antibiotikaklassen wie Chinolone und

Fluorchinolone stark unter den *stx2*-induzierenden Verbindungen vertreten waren, ebenso wie Beta-Lactam-Antibiotika, die zur Cephalosporin- und Penicillin-Gruppe gehören. Chemotherapeutische Verbindungen, insbesondere Dacarbazin und Streptozotocin, zeigten einen signifikanten induzierenden Effekt auf *stx2*. Auch Acetylsalicylsäure (Aspirin), ein oft angewendetes Medikament, zeigte einen deutlichen *stx2*-induzierende Effekt. Auf der anderen Seite zeigten mehrere Verbindungen einen *stx2*-Expression hemmenden Effekt. Insbesondere Antibiotika, die die Proteinbiosynthese hemmen, wie Azithromycin oder Clarithromycin, hatten eine stark hemmende Wirkung. Aber auch nicht-antibiotische Verbindungen wie Levodopa zeigten eine Hemmung der *stx2*-Expression. Insgesamt identifizierte dieser Screen sowohl *stx2*-induzierende als auch -hemmende Verbindungen, was auf potenzielle Risikofaktoren für die Entwicklung schwerer Krankheitsverläufe einerseits und mögliche therapeutische Ansätze zur Minderung der HUS-Entwicklung andererseits hinweist.

Zusätzlich analysierte ich Mikrobiom-Datensätze aus Stuhlproben von Patienten, die während des Ausbruchs von HUSEC (hämolytisch-urämisches Syndroms assoziierten *E. coli*) in Norddeutschland im Jahr 2011 gesammelt wurden, um mikrobiombasierte Risikofaktoren zu identifizieren, die auf die Schwere der Erkrankung hinweisen. Die Analyse zeigte unterschiedliche Mikrobiota-Signaturen, die mit HUS assoziiert waren, und deutete auf eine potenzielle Rolle bestimmter Bakterienarten bei der Modulation der EHEC-Virulenz oder des Krankheitsverlaufs hin. Insbesondere war die Präsenz von Bakterien, die das Genotoxin Colibactin (*pks*-Insel) kodieren, von welchem zuvor gezeigt wurde, dass es die *stx2*-Expression *in vitro* induziert, innerhalb der HUS-Patientengruppe erhöht. Diese Daten könnten auf einen potenziellen Mechanismus hinweisen, der das Risiko der Patienten, HUS zu entwickeln verstärkt.

Zusammenfassend liefert diese Dissertation bedeutende Einblicke in das Zusammenspiel von Umweltfaktoren, dem intestinalen Mikrobiom und der EHEC-Pathogenese. Der etablierte Hochdurchsatz-Assay zur Quantifizierung der Stx2-Produktion in lebenden Bakterien bietet ein wertvolles Werkzeug für die weitere Forschung über die Regulation von Stx2 und zur Identifizierung potenzieller medikamentöser Interventionen. Die Ergebnisse unterstreichen die Bedeutung der Berücksichtigung der Mikrobiomzusammensetzung und der Wechselwirkungen von Medikamenten bei der Behandlung von EHEC-Infektionen und der Prävention von

HUS. Dieser ganzheitliche Ansatz könnte den Weg für effektivere und personalisierte Behandlungen ebnen und letztlich die Ergebnisse für die Patienten im Kampf gegen EHEC-bedingte Erkrankungen verbessern.

1. Introduction

1.1 Enterohemorrhagic *Escherichia coli* pathogenesis

Shiga toxin-producing *Escherichia coli* (STEC) or Verotoxin-producing *Escherichia coli* (VTEC), both synonyms although the latter term is rather outdated, are pathogenic strains of *E. coli* that produce Shiga toxins (Stx1 and Stx2). They can cause severe foodborne illnesses in humans (Terajima *et al.*, 2017). There are about 200 different serotypes of STEC, but the majority of STEC infections can be associated with 11 of them (Quiñones *et al.*, 2012). Serotyping is based on the identification of O and H antigens. The O antigen is part of the lipopolysaccharide on the outer membrane, while the H antigen is associated with the flagella. Different serovars of *E. coli* exhibit diverse combinations of these antigens, contributing to their variability in virulence and pathogenicity (Blanco *et al.*, 2004; Park and Park, 2021). For example, the serovar O157 is one of the most studied and recognized Enterohemorrhagic *E. coli* (EHEC) strains due to its association with numerous outbreaks and severe disease (Pennington, 2010; Farrokh *et al.*, 2013). However, many other serovars, such as O26, O45, O103, O111, O121 and O145, also possess virulence factors that enable them to cause similar illnesses (Stigi *et al.*, 2012).

The pathogenicity of *E. coli* strains is often categorized into six different pathotypes based on their virulence factors and disease mechanisms (Kaper, Nataro and Mobley, 2004). In addition to EHEC, other notable pathotypes include enteropathogenic *E. coli* (EPEC), which causes diarrhoea primarily in children by forming characteristic attaching and effacing lesions without producing Stx; enteroaggregative *E. coli* (EAEC), known for its ability to form a biofilm on the intestinal mucosa leading to persistent diarrhoea; enteroinvasive *E. coli* (EIEC), associated with Crohn's disease due to its ability to invade intestinal epithelial cells and replicate intracellularly; enterotoxigenic *E. coli* (ETEC), causes watery diarrhoea and is the main cause of traveller's diarrhoea and uropathogenic *E. coli* (UPEC), which is a leading cause of urinary tract infections due to its specialized virulence factors for colonizing the urinary tract (Nataro and Kaper, 1998; Kaper, Nataro and Mobley, 2004). The concept of pathotypes highlights the diverse mechanisms by which *E. coli* strains can cause disease, reflecting their genetic variability and adaptability (Geurtsen *et al.*, 2022).

EHEC is a subset of STEC that is particularly associated with severe disease manifestations such as haemorrhagic colitis and haemolytic uremic syndrome (HUS). EHEC strains are characterized by the presence of *stx* genes (*stx1*, *stx2*) and the locus of enterocyte effacement (LEE) pathogenicity island, which encodes a type III secretion system essential for intestinal colonization and the formation of attaching and effacing lesions (Croxen *et al.*, 2013).

It represents a serious public health concern worldwide (Griffin and Karmali, 2017), mainly characterized by serotype O157:H7, which is the predominant source of *E. coli* foodborne outbreaks (Karmali, Gannon and Sargeant, 2010). These pathogens can lead to a variety of clinical symptoms, from abdominal cramps to the characteristic symptom of bloody diarrhoea which can develop into the serious condition of haemolytic uremic syndrome (HUS) (Karmali *et al.*, 1983; Karmali, 1989; Griffin and Tauxe, 1991). Children and elderly people in particular are at high risk of a complicated course of EHEC infection (Welinder-Olsson and Kaijser, 2005; Guillard *et al.*, 2015).

The main reservoir of EHEC in nature is the digestive tract of cattle. Adult cows do not fall ill from EHEC but show an asymptomatic colonization (Woodward *et al.*, 1999; Wray *et al.*, 2000). Unlike in humans, where EHEC preferentially colonizes the large intestine, in cattle EHEC establishes itself at the rectal-anal junction (RAJ), a site that remains largely insensitive to the effects of Stx (Naylor *et al.*, 2003). This difference in toxin susceptibility and colonization preference leads to EHEC infection in cattle without clinical manifestations, possibly underlining the important role of cattle in transmitting zoonotic EHEC infections. Cattle transmit EHEC to humans by excreting the pathogen in their faeces. A subgroup within the EHEC excreting animals, generally known as "super shedders", contribute disproportionately to the total bacterial load and could possibly be responsible for over 95% of all excreted EHEC bacteria (Omisakin *et al.*, 2003). Humans become infected with EHEC mainly through the consumption of contaminated products, such as meat and dairy products (Armstrong, Hollingsworth and Morris, 1996), or through the ingestion of contaminated water and vegetables (Hilborn *et al.*, 1999; Olsen *et al.*, 2002; Luna-Guevara *et al.*, 2019)(Hilborn *et al.*, 1999; Olsen *et al.*, 2002; Luna-Guevara *et al.*, 2019). Only a very low infectious dose is required (> less than 100 CFU) (Paton and Paton, 1998; Gilligan, 1999).

The linchpin of EHEC pathogenicity lies in the production of Stx, a potent cytotoxin that can induce apoptosis and simultaneously stop host protein synthesis (Sandvig, 2001).

Within the human host, EHEC establishes its area of activity in the large intestine (Phillips *et al.*, 2000). Here the Stx, once released by the pathogen, targets endothelial cells carrying the surface receptor globotriaosylceramide-3 (Gb3), an observation first described by Lingwood and colleagues in 1987 (Lingwood *et al.*, 1987). The close interaction between Stx and Gb3 receptor serves as a portal through which the toxin enters the bloodstream and ultimately disseminates to various organ systems, amplifying its deleterious effects (Sandvig, 2001). The selective distribution of Gb3 receptors in different tissues and cell types is decisive for the pathology of the disease mediated by the toxin. In humans, the renal glomerular endothelium proves to be a stronghold of Gb3 expression (Feitz *et al.*, 2021). This unique property makes it highly susceptible to Stx-induced damage, ultimately leading to acute renal failure, thrombocytopenia and microangiopathic haemolytic anaemia, the hallmark features of HUS (Karmali *et al.*, 1983).

1.1.1 HUSEC outbreak Germany 2011

In 2011, Germany experienced one of the largest haemolytic uremic syndrome-associated *E. coli* (HUSEC) outbreaks worldwide. There were a total of 3816 hospitalized patients, 845 of whom developed HUS and as many as 53 died (Frank *et al.*, 2011). Contaminated fenugreek sprouts were ultimately identified as the source of infection. The suspected fenugreek sprouts were traced back to a batch of seeds from Egypt, highlighting the global dimensions of food supply chains and the challenges of ensuring food safety across borders (Buchholz *et al.*, 2011).

This outbreak, with its epicentre in the north of the Germany, led to a major public health crisis as many infected people had to be treated in hospital and the number of severe cases (HUS) was unusually high. The identified pathogen of this outbreak was *E. coli* O104:H4, a hybrid strain. Molecular analysis played a crucial role in characterizing the outbreak strain and determining its unique genetic composition (Mellmann *et al.*, 2011). This strain has a high genetic similarity to enteroaggregative *E. coli* (EAEC) but also combines elements for STEC like a Stx2 prophage. The genetic background of that strain is the result of extensive genetic recombination events like horizontal gene transfer. The *stx2a* gene, integrated into the bacterial genome via a prophage, significantly increases the strain's pathogenic potential, especially due to

the presence of EAEC's strong adhesion capabilities mediated by aggregative adherence fimbriae type I (AAF/I) (Rohde *et al.*, 2011; Schiller *et al.*, 2021). The presence of a plasmid carrying multiple antibiotic resistance genes further complicated treatment (Mellmann et al., 2011). This combination of virulence factors made this *E. coli* especially virulent and was responsible for the many severe cases during the outbreak (Bielaszewska *et al.*, 2011; Rasko *et al.*, 2011). This strain highlights the role of recombination in the evolution of virulent bacterial pathogens.

In the following years, several association studies were carried out with the aim of finding risk factors for the development of HUS during a STEC infection. These studies focused in particular on clinical parameters such as blood values or symptoms of the disease (Wong *et al.*, 2012; Zoufaly *et al.*, 2013).

1.1.2 Virulence factors encoded in EHEC strains

EHEC strains can cause severe gastrointestinal infections in humans. Central to the pathogenicity of EHEC are a variety of virulence factors that together enable the bacteria to colonize the intestinal mucosa, escape the host's defence mechanisms and cause damage to the host epithelium (Pakbin, Brück and Rossen, 2021). A key virulence factor is the production of Stx. This is the subject of a separate chapter in this thesis (1.1.2 Shiga toxin).

The Locus of Enterocyte Effacement (LEE) is a pathogenicity island that is chromosomally encoded in almost all EHEC strains associated with severe disease (Luck *et al.*, 2005). This genetic element encodes for several proteins that play a central role in the pathogenesis of EHEC infection and is tightly controlled by a variety of regulators, e.g. Ler, RpoS, QseR and IsrR (Elliott *et al.*, 2000; Kendall, Rasko and Sperandio, 2010; Franzin and Sircili, 2015; Kumar *et al.*, 2022). These key proteins include the components of a type III secretion system (TTSS), intimin (an adhesion molecule), its receptor Tir (translocated intimin receptor) and various TTSS effector proteins (Kobayashi *et al.*, 2013; Franzin and Sircili, 2015). Together, these elements orchestrate the formation of attaching and effacement (ae) lesions on the intestinal epithelial layer, a characteristic feature of EHEC infections. This process involves the reorganization of the actin cytoskeleton of the host cell, resulting in the loss of microvilli and the formation of pedestal-like structures (Shimada *et al.*, 1999; Mallick *et al.*, 2014).

The LEE Island is critical for the tight attachment of EHEC to the epithelium, which promotes intestinal colonization and ultimately contributes to the severity of the disease.

Intimin and it's receptor Tir, encoded by the *eaeA* and *tir* genes in LEE, play a critical role in the development of adhesive and effacing (A/E) lesions (Frankel *et al.*, 1998). The receptor Tir is first transported into the host cell by the type III secretion system of the bacteria, and it is presented into the host cell membrane. Intimin, an outer membrane protein, facilitates tight binding to the host cell by binding to Tir (Kenny *et al.*, 1997). This strong association of Tir with intimin and the subsequent signal transduction results in the reorganization of the cytoskeleton of the cell (Pakbin, Brück and Rossen, 2021). Another virulence factor, the enterohaemolysin of EHEC (Ehx), contributes to the pathogenicity of EHEC strains. This protein forms pores in host cells and may promote tissue damage during infection. On blood agar it induces haemolysis (Bielaszewska *et al.*, 2012a; Schwidder, Heinisch and Schmidt, 2019). In addition, the enzyme catalase-peroxidase encoded by *katP* provides a defence against oxidative stress, a crucial adaptation for EHEC in the oxidative environment of the host intestine (Brunder, Schmidt and Karch, 1996). In addition to these well-characterized virulence factors, EHEC strains can possess various adhesins, such as type 1 fimbriae, P-fimbriae, S-fimbriae and F1845 (McWilliams and Torres, 2014). These filamentous structures extend from the bacterial surface and enable the bacteria to adhere to specific receptors on host cells. Type 1 fimbriae are particularly abundant and mediate binding to mannose-containing glycoproteins found on the surface of many eukaryotic cells. This adhesion is regulated by phase variation in the promoter of *fimA* (Enami *et al.*, 1999; Iida *et al.*, 2001).

All described virulence factors are not only influenced by EHEC itself, but also by the host microbiota and metabolic products provided by the diet. The gut microbiota can produce metabolites such as short-chain fatty acids (SCFAs) upon fermentation of dietary proteins and fibre. SCFAs act as signalling molecules and influence gene expression and virulence of EHEC (Pifer *et al.*, 2018; Gelalcha *et al.*, 2022). Small extracellular molecules (<3 kDa) produced by a complex human microbiota, especially by *Bacteroides thetaiotaomicron*, have been shown to repress *stx2* mRNA expression (De Sablet *et al.*, 2009).

In addition, food components such as galacturonic acid, derived from digested pectin, can influence the virulence potential of EHEC. First it serves EHEC as carbon source for initial colonisation. Later on, the lack of this sugar acid sensed by ExuR leads to transcriptional activation of the LEE (Jimenez *et al.*, 2020). Another metabolite that influences EHEC virulence is fucose, which is derived from the degradation of host glycans. The presence of fucose, detected by FusK, leads to repression of LEE by FusR (Pacheco *et al.*, 2012). Not only metabolites, but also neurotransmitters such as serotonin have an influence on the expression of virulence genes. The accumulation of serotonin in the intestinal lumen sensed by CpxA decreases LEE expression (Kumar *et al.*, 2020). Another group of molecules, bile salts, present in the human intestine, are reported to decrease LEE gene transcription and increase iron uptake pathways in EHEC. By this regulatory mechanism, EHEC might prepare itself for the small intestine to overcome the antimicrobial effects of bile and at the same time prepare for the low iron availability (Hamner *et al.*, 2013).

1.1.3 Shiga toxin

Stx1 and Stx2 are important virulence factors in EHEC. It was first identified by Kiyoshi Shiga in *Shigella dysenteriae serotype I* (Trofa *et al.*, 1999). For the first time in 1983, *E. coli* was reported to produce Stx too (O'Brien and LaVeck, 1983). Synonym terms used for Stx are Shiga-like toxin, verocytotoxin or verotoxin. These names come from the fact, that Stx has cytotoxic activity against Vero cells in culture (Pacheco and Sperandio, 2012).

There are two different antigenic forms of Stx, Stx1 and Stx2, which can be grouped according to their biological activity and sequence identity (share 56% amino acid sequence homology). The two Stx forms have a similar mode of action but different immunological characteristics. Both antigenic forms have several subtypes. For Stx1 four subtypes Stx1a, Stx1c, Stx1d and Stx1e have been reported, while for Stx2 fifteen subtypes Stx2a – Stx2o are known. The Stx1 subtypes have a high amino acid similarity (> 90%) in their group, while the subtypes of Stx2 are considerably more heterogenous in the amino acid similarity between the different subtypes. In general, Stx2 subtypes are more toxic (up to 1000-fold) and more often related with human infections compared to Stx1 subtypes (Jackson *et al.*, 1987; Fuller *et al.*, 2011; Wang

et al., 2024). The division of *stx* into the various subtypes is based on the phylogenetic sequence-based relatedness of the holotoxin. A PCR based subtyping method was developed by Scheutz et al., with which new *stx* can be assigned to their respective Stx subtype (Scheutz *et al.*, 2012).

The two Stx variants are AB_5 toxins, which means that they consist of an A subunit (32 kDa) and 5 identical B subunits (7.7 kDa). The A subunit is the catalytically active part of the toxin. It exerts its toxic effect by inhibiting protein synthesis and inducing cell apoptosis in eukaryotic cells (Fraser *et al.*, 2004; Tesh, 2010; Lee, Park and Lee, 2022). The expression of Stx is the main trigger for haemolytic uremic syndrome (HUS) in EHEC infected patients, especially the subtypes Stx2a and Stx2c are highly associated with the life threatening HUS (Louise and Obrig, 1995; Obrig, 2010; Matussek *et al.*, 2023). One EHEC strain can harbour one or more *stx*, up to four *stx1* or *stx2* in one strain have been detected, of the same subtype or a combination of different subtypes (Tahamtan, Hayati and Namavari, 2010; Pinto *et al.*, 2021). Always one *stx* operon is encoded in the sequence of an inducible, lysogenic, lambda-like bacteriophage (prophage). An EHEC strain with several *stx* has therefore multiple *stx* encoding prophages.

How Shiga toxin crosses the gut barrier is not fully understood yet, but recent findings in an intestine layer model show that Stx can cross the 3-layer model (colonic epithelia, myofibroblasts and extracellular matrix (ECM) on the apical side and ECM and colonic microvascular endothelia on the basolateral side) used in the study (Bova *et al.*, 2023). Stx translocation from the gut lumen into the circulatory system is increased by paracellular as well as transcellular mechanisms like Gb3 dependent endocytosis and pinocytosis (Hurley *et al.*, 1999; Schüller, 2011; Garimano, Amaral and Ibarra, 2019). After invasion into the circulatory system, Shiga toxins travel via bloodstream to their effector organs e.g. kidney and brain (Ståhl *et al.*, 2015; Chan and Ng, 2016; Lee and Tesh, 2019). In humans, glycosphingolipid globotriaosylceramide (Gb3, CD77) is the cellular receptor for Stx.

The pentameric B subunit of the toxin binds to the receptor. The A subunit enters the cell cytoplasm of the eukaryotic cell via a retrograde pathway (Sandvig *et al.*, 2010). This leads to the internalization of the receptor-toxin complex and further vesicular transport to the Golgi apparatus and endoplasmic reticulum (ER). In this process, the A subunit is cleaved and thus activated and transported into the cytosol of the cell.

There it removes an adenine moiety from the 28S rRNA of the 60S ribosome, which leads to the inhibition of protein synthesis (End0 *et al.*, 1988; Lee, Cherla and Tesh, 2010; Chan and Ng, 2016). Besides inhibiting the protein biosynthesis, Stx induces at the ER the stress response leading to activation of apoptotic pathways (Smith *et al.*, 2003; Lee *et al.*, 2007).

1.1.3.1 Regulation of Shiga toxin2

Stx2 is encoded on the genome of lambdoid bacteriophages (e.g. 933W & 933J) (O'Brien *et al.*, 1984; Rodríguez-Rubio *et al.*, 2021). Lysogenic phage's have a life cycle that includes several intermediate steps (**Fig. 1**). In general, two different modes of replication can be distinguished, the lytic and the lysogenic mode (Campbell, 2003; Zhang *et al.*, 2022). Both begin with the attachment of the phage to the host cell and the injection of the phage DNA from the capsid into the cytoplasm of the host cell. In the lytic mode, transcription, and translation of phage genes in the cell cytoplasm takes place immediately after injection. Afterwards, the phage particles assemble, and the host cell is lysed. This process releases many new bacteriophages, which in turn can infect new host bacteria. In the lysogenic life mode, the phage DNA integrates into the chromosome of the host bacterial strain. It remains there silently as a prophage, where it is copied together with the host cell DNA during replication (Rodríguez-Rubio *et al.*, 2021). One possible explanation why *E. coli* retains the *stx2*-encoding prophage is the *nanS-p* gene, encoded in the phage genome, which functions as an esterase that can metabolize sialic acids. Sialic acid is found in the gastrointestinal tract of cattle, the major reservoir for EHEC (Zuppi *et al.*, 2020). The prophage remains in its lysogenic state until it is induced and thus enters the lytic life cycle. There are various environmental cues that can initiate prophage induction, for example host cell DNA damage, low pH, ions, oxidative stress, and antibiotics (Pacheco and Sperandio, 2012; Filipiak, Łoś and Łoś, 2020; Rodríguez-Rubio *et al.*, 2021). These triggers initiate the bacterial SOS response which is signalled via the protein RecA (Maslowska, Makiela-Dzbenska and Fijalkowska, 2019). However, prophage induction can also occur independently of RecA (Imamovic and Muniesa, 2012).

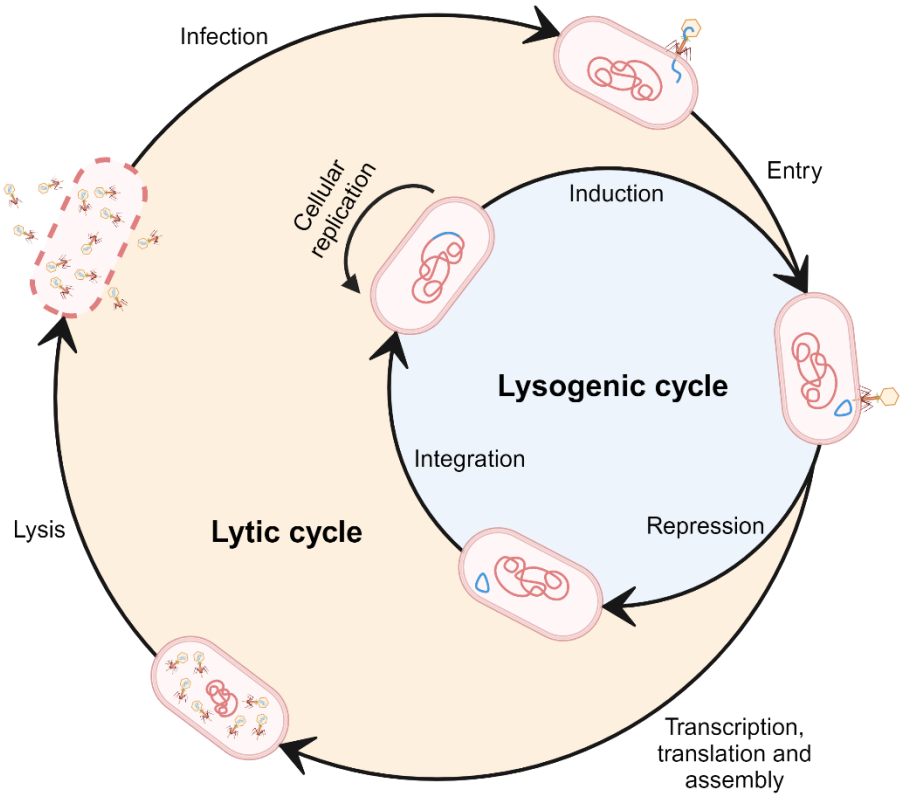

Figure 1. Replication modes of lambdoid bacteriophages.
Upon encountering the host bacterial cell surface, the phage particle attaches via its tail tip, allowing the phage DNA to enter. This process leaves an empty protein shell on the cell's exterior. In some infected bacteria, the phage DNA undergoes transcription, translation, and replication (lytic cycle). Rolling-circle replication generates linear double-stranded DNA (dsDNA), which is combined with the phage protein shells. Bacteria cell lysis is followed by the release of phage progeny. In other infected bacterial cells, phage replication is suppressed, and phage DNA integrates into the bacterial chromosome as prophage (lysogenic cycle). This creates a lysogenic bacterium in which the phage can replicate indefinitely. Through an outside trigger the phage can be induced returning to the lytic cycle by excising its DNA from the chromosome. Figure was created using BioRender

CI is the phage encoded repressor that binds to the operators of the phage promoters (P_L & P_R) and thus keeps the prophage in its lysogenic state. RecA induces the autocleavage of CI which leads to the transcription of the initial phage genes, including an antiterminator (N). This antiterminator enables the polymerases to read over the terminator regions, which in turn lead to the expression of the late phase antiterminator Q and consequently to the expression of the late phase genes. Among the late phase genes are the *stx2*, but also the genes (*S,R*) which are necessary for cell lysis (**Fig. 2**). The Stx2 and the phages assemble in the host cell cytoplasm. Lysis of the host cell releases the phages and the toxin (Pacheco and Sperandio, 2012; Rodríguez-Rubio *et al.*, 2021).

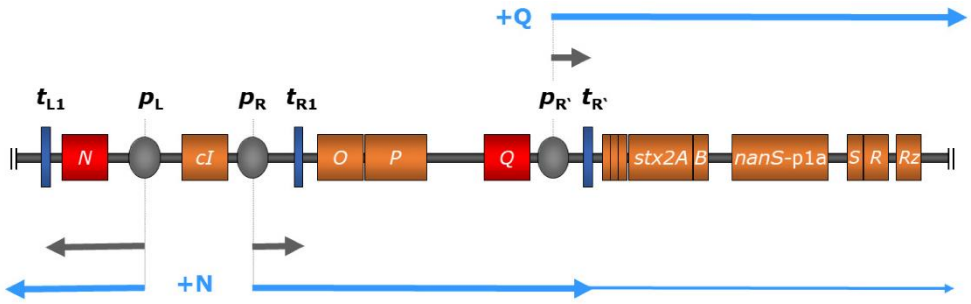

Figure 2. Regulation of Shiga toxin carrying prophage 933W of *E. coli* O157:H7 strain EDL933. Regulation of *stx2* expression involves several key genes (highlighted in orange). In the lysogenic mode, transcription of the phage is suppressed by the *cI*-encoded repressor, which binds to operator sites within the early promoters P_L and P_R (grey arrows). Transcriptional termination is further enforced by downstream terminators (t_{L1}, t_{R1}, $t_{R'}$; dark blue). Upon phage induction, the *cI*-encoded repressor undergoes autocleavage, allowing transcription initiation at P_L. This prompts the production of phage-encoded antiterminator N (red). The antiterminator facilitates polymerase read-through at downstream terminators like t_{L1} and t_{R1}. This paves the way for expression of the late-phase antiterminator Q (red), which promotes transcription from the late-phase promoter $P_{R'}$. This mechanism helps to surpass the terminator $t_{R'}$, enabling expression of downstream genes including *stx2* as well as the cell lysis genes S and R (indicated by light blue arrows). (*Adapted from* Rodriguez-Rubio *et. al.,* 2021)

1.1.4 Haemolytic uremic syndrome

In 1955, haemolytic uremic syndrome (HUS) was described for the first time as the cause of death of five patients (GASSER *et al.*, 1955). However, it took until 1985 to confirm the link between HUS and STEC (Karmali *et al.*, 1985). The main pathogen for bacterial-induced HUS is Shiga toxin-producing *E. coli*, although there are other bacteria such as *Shigella dysenteriae serotype 1* that can produce Shiga toxin (O'Brien *et al.*, 1983; Cody and Dixon, 2019).

Most patients infected with EHEC show first symptoms after three days. The first manifestations include abdominal pain, diarrhoea, and nausea (Karch, 2001). The reason for the symptoms is the inflammation of the colon. The next phase of the disease begins on day 5 - 6 post-infection (p.i.) once EHEC infection and subsequent colitis have manifested themselves, leading to bloody stools (Harkins, McAllister and Reynolds, 2020). This is due to the production of Stx2 in the intestinal lumen, which disrupts the intestinal epithelial cells and causes blood to enter the lumen. At this point, most patients seek clinical treatment. The majority of patients (~90%) recover from the infection after about 5-10 days and have no further symptoms. A small subset of patients (~10%) however, develop complications leading to HUS (**Fig. 3**). In children or women, the risk of developing HUS is higher. In the HUS affected patients, Stx2 is systemically distributed attacking organs with Gb3 positive cells (kidney, brain, and gut)

(Salvadori and Bertoni, 2013; Chan and Ng, 2016). This leads to microangiopathic haemolytic anaemia, high blood pressure, thrombocytopenia, and acute kidney injury (Cody and Dixon, 2019). The mortality rate in HUS patients is 2-7% (Verweyen *et al.*, 2000). Survivors often struggle with long-term sequelae such as chronic renal failure, proteinuria, and diabetes mellitus (Pundziene *et al.*, 2015; Vaterodt *et al.*, 2018).

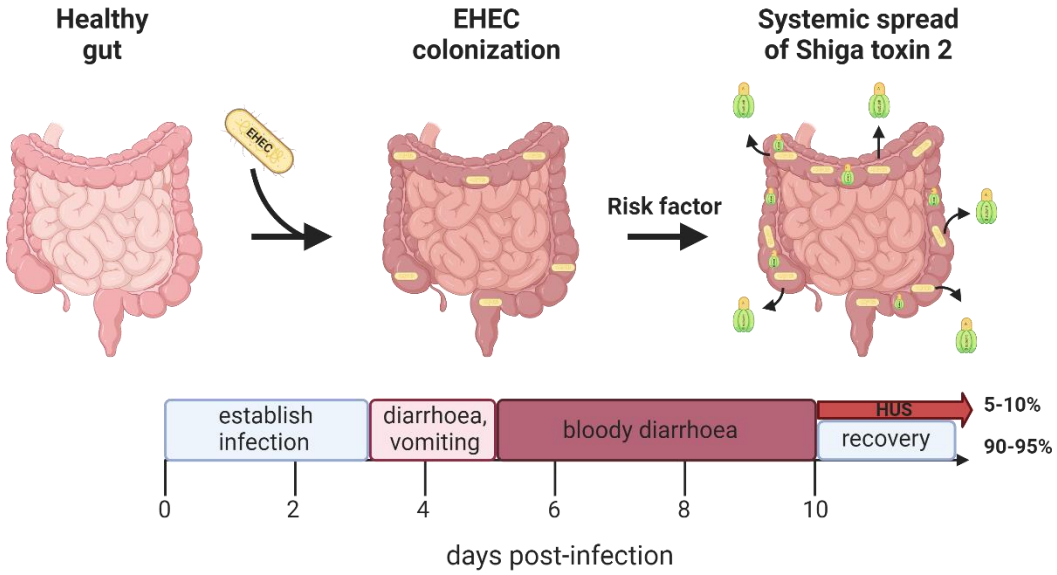

Figure 3. EHEC infection, from disease onset to haemolytic uremic syndrome (HUS) development.
EHEC only needs a low infection dose to colonize the human gut. After 3 days of infection, the first symptoms are abdominal pain and diarrhoea due to inflammation of the colon. Day 5 – 6 p.i. the EHEC infection has manifested itself and the patient has bloody diarrhoea. The reason for that is the production of Stx in the intestinal lumen, leading to the disruption of the epithelial cells and the systemic spread of Stx. 90% of EHEC infected patients recover without long term symptoms, while a subset of 5 – 10% of the patients develop the life threating HUS. Figure was created using BioRender.

Several risk factors including age and gender are known from the literature that favour the development of HUS in patients with an EHEC infection (Dundas *et al.*, 2001; Zoufaly *et al.*, 2013). Physiological parameters that are predictive for the development of HUS are C reactive protein level > 1.2 mg/dl, elevated white blood cell counts (more than 11 x 10^9/l) and a body temperature above 38 °C (Ikeda *et al.*, 2000; Hirata, Kenzaka and Akita, 2020). Other risk factors for the development of HUS include the use of antimotility agents, specific antibiotics and antidiarrheal agents at the beginning of infection (Butler *et al.*, 1987; Cimolai *et al.*, 1990; Wong *et al.*, 2000).

1.1.4.1 Treatment options

There is no generally recommended causal therapy for haemorrhagic colitis to prevent the development of HUS. To date, the most important form of treatment for patients with a severe EHEC infection is supportive therapy to alleviate the symptoms of the disease. This includes hospitalization of the patient, preferably in a specialized clinic, intravenous fluid expansion to prevent dehydration and, if necessary, nutritional support (Joseph *et al.*, 2020; Fatima and Aziz, 2023). These measures alone have greatly reduced the mortality rate of HUS in recent decades. Nevertheless, research into effective treatment strategies continues. Different targets (on the host side or EHEC specific) are being investigated to develop a targeted therapeutic intervention for EHEC infections (Bova and Melton-Celsa, 2022).

One approach is immunomodulatory intervention in the patient. In one study, immunoadsorption therapy had positive effects on the neurological damage prevention of HUS patients (Greinacher *et al.*, 2011). Blocking the complement system with antibodies (eculizumab) showed protective effects in EHEC infected children (Lapeyraque *et al.*, 2011). Further monoclonal antibodies designed to bind and capture Stx were developed (Mejías *et al.*, 2016; Moxley *et al.*, 2017). To date, none of the antibodies has succeeded in achieving a positive Stx-binding effect in various animal models. One of the reasons for this could be the short period of time during which Stx circulates freely in the body and is therefore accessible for antibodies (Henrique *et al.*, 2022).

A second approach is the development of a vaccine as a preventive strategy. A vaccine, targeting several EHEC virulence factors elicited a strong immune response upon vaccination in mice and protected against an EHEC infection (Gu *et al.*, 2009). Another polypeptide vaccine containing the last 32 amino acids of the Stx2 A_2 subunit (non-toxic) and the complete B subunit of Stx2 lead to protective immunity in a mouse model (Bentancor *et al.*, 2009). A different group developed a plant-based Stx vaccine. After consumption of the toxoid-expressing plant cells, this vaccine completely protected mice against a challenge with Stx2 (Wen *et al.*, 2006).

Besides, the retrograde transport of Stx into host cells expressing the Gb3 receptor is a potential drug target. Tamoxifen and Retro-2, both inhibitors of retrograde trafficking,

have a positive effect on survival and general health of mice in EHEC infection mouse studies (Secher *et al.*, 2015; Selyunin *et al.*, 2019).

The administration of antibiotics during an EHEC infection is controversially discussed. There are several studies that identified certain antibiotic classes that lead to the induction of Stx and thus may increase the risk of HUS (Grif *et al.*, 1998a; Wong *et al.*, 2000; Safdar *et al.*, 2002). Other antibiotics (e.g. azithromycin, fosfomycin) are mentioned as safe for the treatment of EHEC infected patients (Ikeda *et al.*, 1999; Zhang *et al.*, 2009). Based on the available data, the administration of antibiotics during a potential EHEC infection is generally not recommended. Further studies, like the one by Mühlen *et al.* which could show that ampicillin, kanamycin and tetracycline cleared bacterial infection in their mouse model (Mühlen et al., 2020), are needed to rule out the possibility that the "safe" antibiotics do not induce Stx2 and thereby cause HUS.

All these new approaches offer a great prospect of having an effective drug to treat EHEC infections in the future. Until then, it is up to clinicians to weigh up the risks and benefits of the various treatment options, considering individual patient factors such as age, gender, previous illnesses and stage of infection.

1.2 The influence of human-targeted drugs on the intestinal microbiota

In the last decade, studying the effects of drugs designed for human use on commensal gut bacteria has become a critical area of investigation. This is particularly relevant given the complex relationship between the human body and its resident microbial communities and the development of diseases linked to microbiota dysbiosis (Degruttola *et al.*, 2016; Elias-Oliveira *et al.*, 2020). Commensal gut bacteria play a crucial role in maintaining host health by contributing to nutrient uptake, colonization resistance against pathogens, metabolic processes, and regulation of the immune system (Ogunrinola *et al.*, 2020).

The broad-spectrum antimicrobial activity of antibiotics has been well documented for many years (Blaser, 2011; Dubourg *et al.*, 2014). On the one hand, antibiotics are still among the most effective drugs for bacterial infections. On the other hand, the lack of specificity to the pathogen and broad spectrum activity is a major problem as it leads

to collateral damage of commensal intestinal bacteria (Zimmermann and Curtis, 2019; Patangia *et al.*, 2022). In recent years, the antimicrobial properties of non-antibiotic human-targeted drugs on commensal bacteria have been investigated in more detail. Certain groups of compounds have been shown to have particularly antimicrobial properties (Maier *et al.*, 2018a; Algavi and Borenstein, 2023). These include proton pump inhibitors (PPIs), antipsychotics, which have a profound negative impact on gut bacteria. The action of PPIs on commensals are on the one hand the direct inhibition of the bacteria by the drug, on the other hand the change in gastric pH which is influences the growth of bacteria in this organ (Kiecka and Szczepanik, 2023; Zhang *et al.*, 2023). Another class of drugs which has a significant impact on gut bacteria are immunomodulatory agents. These drugs can induce major dysbiosis, which can cause disease, or can significantly alter the host immune response (Cohen, Ruff and Longbrake, 2021; Faucher *et al.*, 2022). Another aspect regarding the effects of medication on the human microbiota is polypharmacy. As people are getting older, it is not uncommon for a person to take several different medications (at least 5) at the same time over a longer period. This phenomenon is known as polypharmacy. The interactions between, and cumulative effects of medications on bacteria remains an active area of research (Nagata *et al.*, 2022; Gemikonakli *et al.*, 2023).

Because of this new awareness, research efforts are underway to develop strategies to reverse or mitigate these unintended side effects of medication. For example probiotics have shown promise in restoring and maintaining a healthy gut microbiome during and after drug treatment (Storr and Stengel, 2021; Purdel *et al.*, 2023). In summary, the impact of human-targeted drugs on commensal gut bacteria is poorly investigated, due to a complex mechanism of action and may, as consequence, be currently difficult to assess. A variety of drugs can significantly alter the composition and function of the gut microbiome and thereby potentially impact host health. As research in this area progresses, there is the prospect of discovering novel therapeutic approaches that do not perturb but perhaps even support the symbiotic relationship between the human body and its resident microbial communities.

1.3 The influence of the gastrointestinal microbiota during enteric bacterial infections

The complex interactions between the human gut microbiome and bacterial pathogens are based on various mechanisms. The gut microbiome consists of about 10^14 bacteria, over 90% of which belong to the four phyla *Actinomycetota*, *Bacteroidota*, *Bacillota* and *Pseudomonadota* (Thursby and Juge, 2017; Oren and Garrity, 2021). Although bacteria represent the main biomass, archaea, eukaryotes and viruses are also a functionally important part of the gut microbiome (Ursell *et al.*, 2012). The gastrointestinal microbiota acts as a crucial line of defence against bacterial infections by limiting available nutrients, inhibiting pathogens (with e.g. bacteriocins), and stimulating the host immune system (Hammami *et al.*, 2012; Eberl *et al.*, 2021; Khan *et al.*, 2021). For example, commensal *E. coli* can prevent colonization of EHEC through the production of colicins (Schamberger and Diez-Gonzalez, 2002). In contrast, following successful EHEC gut colonisation, colicinogenic *E. coli*, capable of producing microcins and member of the gut microbiota carrying the *pks* island (encoding for colibactin) have been reported to induce prophage and *stx2* expression (Toshima *et al.*, 2007; Mosso *et al.*, 2019; Silpe *et al.*, 2022). Certain bacteria of the intestinal microbiome, such as *Enterococcus faecalis* and *Bacteroides thetaiotaomicron,* can also increase the expression of EHEC virulence genes and thus contribute to colonization (Martins *et al.*, 2022a).

On the other hand, specific bacterial species within the microbiome (e.g. *Bifidobaceria*) can provide protection by inhibiting the adhesion of EHEC to intestinal epithelial cells (Vazquez-Gutierrez *et al.*, 2016). This protective property of the gut microbiome, known as colonization resistance (CR), is crucial to prevent enteric bacterial infections.

Despite the CR phenotype, bacterial pathogens have developed strategies to overcome the barriers of the gut microbiome. In particular, the ability of pathogens to find suitable niches in the gut is crucial for the establishment of infections (Khan *et al.*, 2021). EHEC has adaptation strategies and virulence factors that enable it to colonize the intestine despite an intact microbiome (Vogt *et al.*, 2023). EHEC senses riboflavin, indole, L-malate, and nicotinamide produced by the gut microbiota and adapts the expression of its LEE virulence genes accordingly (Kumar *et al.*, 2022; Liu *et al.*, 2022;

B. Liu *et al.*, 2023; Yang *et al.*, 2023). The intestinal microbiota therefore has different effects on EHEC during the infection process.

1.4 Available Shiga toxin reporter strains

EHEC poses a significant threat to public health and leads to serious foodborne illnesses. Due to the lack of a curative treatment strategy, there is a great research interest in STEC to find novel and alternative treatments. As wild-type EHEC belongs to biosafety level (BSL)-3**, working with these organisms is only allowed in specialized laboratories. This makes research more difficult, with limitations of handling and scaling of experiments. EHEC reporter strains, in which virulence factors such as the Shiga toxin itself are replaced by a reporter gene, are very useful tools as lack of *stx* genes renders the strains BSL-2. Not only does this make handling easier and safer, but the possibilities for experiments are also more diverse. For example, new drugs can be tested more easily, or the dynamics of infection can be more thoroughly investigated.

One Stx2 reporter strain is the eGFP-tagged *E. coli* O157:H4 (STEC O104:H4 *Δstx2::gfp::amp*^{r}). This reporter is designed to study *stx2* expression on a single cell basis. In the study by (Fang *et al.*, 2017), this reporter was used to investigate the influence of bacterial stress on phage and *stx2* expression. The use of fluorescent markers facilitates rapid detection and improves efficiency.

The activity of Stx2 can also be measured indirectly in an assay. Stx2 inhibits protein biosynthesis in cells. Measuring a GFP florescence signal which is reduced by Stx2 activity indirectly reflects the activation of the toxin (Rasooly *et al.*, 2017).

Another strategy involves the use of the *lacZ* gene (β-galactosidase) as a reporter gene. Here, *stx2* is replaced by *lacZ* in a STEC (Kimmitt, Harwood and Barer, 2000b). The readout is carried out either via indicator plates (blue/white screening) or via the β-galatosidase assay. This reporter is a very cost-effective screening variant, especially as first screen to determine whether a particular molecule triggers *stx2* expression.

In addition to fluorophore or colour-based reporter strains, luminescence-based reporter systems have also become increasingly important. The *luxCDABE* operon of

Photorhabdus luminescens was in part chromosomally and plasmid encoded within an EHEC strain. This reporter emits bioluminescence when the *stx1 or stx2* locus is induced (Shimizu *et al.*, 2011).

Despite the availability of these different reporter systems, there is still a need to develop Stx2 reporters that have improved sensitivity and scalability, and more naturally represent the kinetics of *stx2* expression.

Another luminescence-based reporter is the CW^{gluc} strain. This strain fulfils sensitivity and scalability. Here, the *stx2A* is exchanged against the luciferase of *Gaussia princeps* (Gluc) functioning as reporter gene leaving the downstream encoded phage lytic genes S and R untouched (**Fig. 4**). The activation of the prophage lytic cycle, for example by mitomycin C (MitoC), also leads to expression of *gluc*, and release of Gluc into to the culture supernatant upon cell lysis. Gluc mediated luminescence can be quantified in the supernatant. The signal is linearly proportional to the amount of released Gluc. It was shown that this mimics very well the release kinetics of Stx2 form *E. coli* (Koeppel *et al.*, 2021).

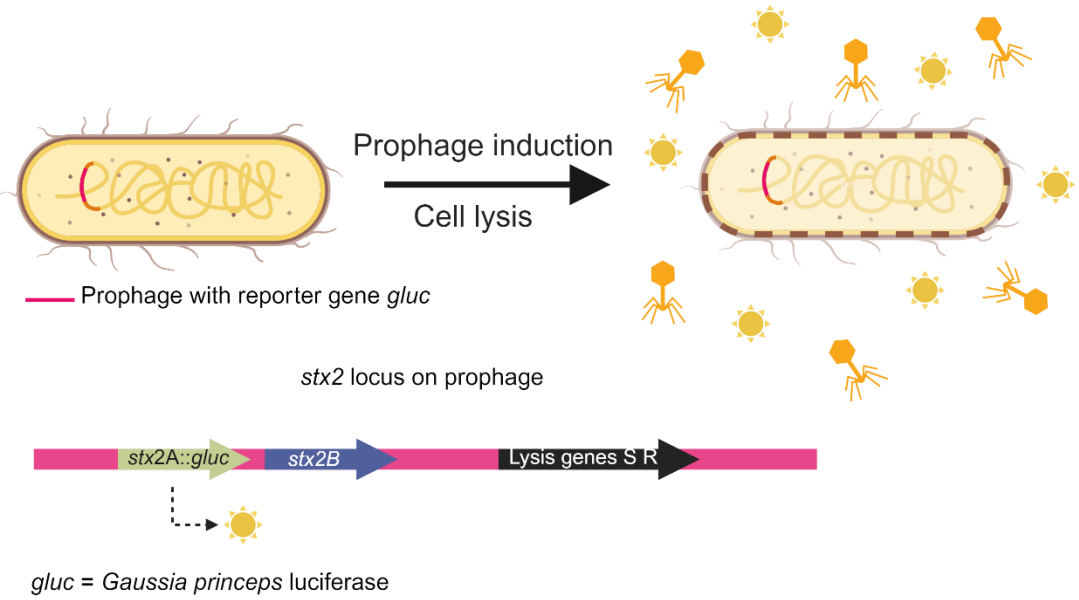

Figure 4. Design and function of the reporter strain CW^{gluc}.
Genetic organization (bottom figure) of the reporter gene *Gaussia* luciferase (*gluc*., light green arrow) in the lysogenic Shiga toxin 2 (*stx2*) encoding prophage 933W in the background strain *E.coli* C600W34. The lysis genes S and R (black arrow) are intact enabling bacterial cell lysis upon phage/reporter induction. Induction of the prophage leads to production of the luciferase (yellow) and phages (orange). With the subsequent cell lysis, the luciferase and the newly formed phages are released (upper figure). Figure was created using BioRender.

This new reporter should be particularly useful to comprehensively analyse the influence of environmental and host factors, potentially including drugs, small metabolites, and the microbiota, on Stx2 release and thus contribute to the identification of risk factors and novel therapies for Stx2-mediated pathologies.

The availability of all these Stx2 reporters offers a variety of advantages, from live cell imaging to cost-effective screening methods. Research and development in this area has the potential to improve our ability to treat EHEC patients, detect and contain contamination on food and improve our understanding of disease progression and advancement towards HUS.

2. Aims of this thesis

Enterohemorrhagic *Escherichia coli* is a food-borne human pathogen, which frequently causes outbreaks. It is one of the major pathogens leading to acute diarrhoea and haemorrhagic colitis, especially in children and elderly people. Only a subset of EHEC infected patients develop the life threatening HUS, which is linked to Stx, in particular Stx2. So far, no causal therapy against HUS exists and the cues leading to the development of HUS remain unclear as well as the signals activating *stx2* production in the human gut. Since recent outbreaks were linked with the appearance of more virulent strains, there is a high need to explore the risk factors responsible for developing HUS during an EHEC infection.

The aim of my thesis was to **examine how various environmental cues influence the virulence factor regulation of EHEC**, especially the production of Shiga toxin 2. To elucidate this question, I focused on:

1. **Establishing a high-throughput assay to systematically analyse the effects of compounds on *stx2* expression.** The *stx2* reporter strain CW^{gluc} shall be employed to analyse environmental factors like drugs, small molecules or microbiota-derived toxins and metabolites in a safe and reproducible manner. To this end, I planned using an already available luciferase reporter CW^{gluc} and further developing this reporter for easy and scalable readout. For this purpose, I will test different incubation times of the reporter strain with the drugs, changing concentrations of the positive control mitomycin C as well as optimizing the readout, i.e. luciferase activity detection.
2. **Applying the assay to screen human-targeted drugs for stimulatory or inhibitory effects on *stx2* expression and bacterial release.** In the main part of my thesis, I aimed to analyse the influence of human-targeted drugs on the growth behaviour and Shiga toxin 2 release of EHEC. For this purpose, I will screen a chemical library of U.S. Food and Drug Administration (FDA)-approved & European Medicines Agency (EMA)-approved compounds on the established assay. I will also confirm the activity of identified compounds in follow-up experiments using alternative assays.
3. **Addressing the influence of factors promoting *stx2* expression in faecal microbiome datasets from the 2011 HUSEC outbreak in Germany.** The final

aim of this project is to test for *stx2* inducing effects in metagenomics samples from a cohort of HUSEC infected patients and controls, obtained during an outbreak in Germany in 2011 and to test for correlations between microbiota derived signals and disease severity.

By addressing these aims, this thesis will significantly advance our understanding of the interplay between environmental cues and EHEC pathogenesis. The outcomes may potentially lead to the development of innovative treatment and prevention approaches of HUS in EHEC infected human patients.

3. Materials and Methods

3.1 Materials

3.1.1 Devices

Table 1. List of devices

Device	Manufacturer
Balance 1712 MP8	Sartorius Lab Instruments (Göttingen)
Balance KB 500-2	Kern & Sohn GmbH (Balingen)
BioPhotometer	Eppendorf (Wesseling-Berzdorf)
Centrifuge 5430R; rotor: 5430R	Eppendorf, Hamburg Germany
Centrifuge Heraeus multifuge X3R Rotor: 75003603	Heraeus, Hanau Germany
CLARIOstar	BMG (Ortenberg)
Gel Imaging System: GelDoc Go	Bio-Rad, Feldkirchen Germany
Microplate Reader Epoch 2	BioTek, Santa Clara US
Nanodrop	Thermo Fisher (St. Leon-Rot)
Roche LightCycler96	Roche
Thermocycler: peqstar 2X gradient	Peqlab, Erlangen Germany
Thermomixer C	Eppendorf, Hamburg Germany
Thermomixer comfort	Eppendorf, Hamburg Germany
Vortex Genie 2	Scientific Industries (USA)

3.1.2 Consumables

Table 2. List of consumables

Name	Supplier
1.5 ml plastic tubes (PCR grade)	Eppendorf, Wesseling-Berzdorf Germany
15 ml plastic tubes, V-bottom	Greiner Bio One, Frickenhausen Germany
50 ml plastic tubes, V-bottom	Greiner Bio One, Frickenhausen Germany
96 well plate (Nunc™ MicroWell™ round bottom)	ThermoFisher Scientific, Massachusetts US
Full white 96 well plate (Nunc™ MicroWell™ flat bottom)	ThermoFisher Scientific, Massachusetts US

96-well plates (flat bottom)	Sarstedt, Nümbrecht Germany
Parafilm	Sigma-Aldrich, Munich Germany

3.1.3 Chemicals, reagents, and kits

Table 3. List of chemicals, reagents, and kits

Name	Supplier
1 kb Gene Ruler DNA Ladder	Thermo Fisher Scientific, Karlsruhe, Germany
2 x FastStart Essential DNA Probes Master	Roche, Mannheim, Germany
Acetazolamide	Tokyo Chemical Industry, Tokyo, Japan
Acetylsalicylic acid	Merck, Darmstadt, Germany
Acyclovir	Tokyo Chemical Industry, Tokyo, Japan
Agarose	Bio & Sell, Feucht, Germany
Aminocaproic acid	Tokyo Chemical Industry, Tokyo, Japan
Amiodarone hydrochloride	Tokyo Chemical Industry, Tokyo, Japan
Ampicillin	Roth, Karlsruhe, Germany
Antimycin A	Merck, Darmstadt, Germany
Ascorbic acid	Tokyo Chemical Industry, Tokyo, Japan
Azithromycin	Tokyo Chemical Industry, Tokyo, Japan
Azlocillin sodium salt	Merck, Darmstadt, Germany
BactoTM Agar	BD, Franklin Lakes, USA
Balsalazide Sodium	Tokyo Chemical Industry, Tokyo, Japan
CaCl2	Roth, Karlsruhe, Germany
Clarithromycin	Tokyo Chemical Industry, Tokyo, Japan
Clindamycin hydrochloride	Tokyo Chemical Industry, Tokyo, Japan
Clioquinol	Tokyo Chemical Industry, Tokyo, Japan
Clomiphene citrate (Z/E)	Sigma Aldrich, Taufkirchen, Germany
CloneJet PCR Cloning Kit	Thermo Scientific, Karlsruhe, Germany
Coelenterazine (CTZ)	Synchem, Felsberg, Germany
Dacarbazine	Tokyo Chemical Industry, Tokyo, Japan
ddH_2O	Tokyo Chemical Industry, Tokyo, Japan
Disulfiram	Tokyo Chemical Industry, Tokyo, Japan

DMSO	Roth, Karlsruhe, Germany
Dream Taq Master Mix (2X)	ThermoFisher Scientific, Karlsruhe, Germany
EDTA	Biomol, Hamburg, Germany
Efavirenz	Tokyo Chemical Industry, Tokyo, Japan
Esmolol hydrochloride	Prestwick Chemical Libraries, Orléans, France
Ethanol absolute	Sigma-Aldrich, St. Louis, USa
Ethidium bromide, 1% solution	AppliChem, Darmstadt, Germany
Floxuridine	Tokyo Chemical Industry, Tokyo, Japan
GeneJET Gel Extraction and DNA Cleanup Micro Kit	Thermo Fisher Scientific, Karlsruhe, Germany
Glycerol	Carl Roth, Karlsruhe, Germany
Guaiacol	Tokyo Chemical Industry, Tokyo, Japan
Imatinib	Tokyo Chemical Industry, Tokyo, Japan
Imipenem	Prestwick Chemical Libraries, Orléans, France
Indatraline hydrochloride	Merck, Darmstadt, Germany
Isopropanol	Roth, Karlsruhe, Germany
Kanamycinsulfate	Roth, Karlsruhe, Germany
Ketorolac tromethamine	Tokyo Chemical Industry, Tokyo, Japan
Levodopa	Tokyo Chemical Industry, Tokyo, Japan
Lincomycin hydrochloride	Tokyo Chemical Industry, Tokyo, Japan
Loading Buffer	Thermo Fisher Scientific, Karlsruhe, Germany
Lymecycline	Merck, Darmstadt, Germany
Meglumine	Tokyo Chemical Industry, Tokyo, Japan
Mepivacaine hydrochloride	Tokyo Chemical Industry, Tokyo, Japan
Metronidazole	Tokyo Chemical Industry, Tokyo, Japan
Mevastatin	Tokyo Chemical Industry, Tokyo, Japan
Miconazole	Tokyo Chemical Industry, Tokyo, Japan
Mitomycin C	Roth, Karlsruhe, Germany
Moroxidine hydrochloride	Tokyo Chemical Industry, Tokyo, Japan
NaCl	Carl Roth, Karlsruhe, Germany

Niacin	Tokyo Chemical Industry, Tokyo, Japan
Nicotinamide	Tokyo Chemical Industry, Tokyo, Japan
Niridazole	Prestwick Chemical Libraries, Orléans, France
NucleoSpin Gel and PCR Clean-Up Kit	Macherey-Nagel, Düren, Germany
NucleoSpin Plasmid Mini Kit	Macherey-Nagel, Düren, Germany
Pentobarbital	Merck, Darmstadt, Germany
Pinaverium bromide	Prestwick Chemical Libraries, Orléans, France
Piperacetazine	Prestwick Chemical Libraries, Orléans, France
Q5 High-Fidelity DNA polymerase	New England Biolabs, Ipswich, England
Qiagen Plasmid Plus Midi Kit	Qiagen, Hilden, Germany
Quinethazone	Prestwick Chemical Libraries, Orléans, France
Raclopride	Prestwick Chemical Libraries, Orléans, France
Saquinavir mesylate	Merck, Darmstadt, Germany
Sertindole	Prestwick Chemical Libraries, Orléans, France
Sildenafil/ Viagra	Tokyo Chemical Industry, Tokyo, Japan
Stavudine	Prestwick Chemical Libraries, Orléans, France
Sterile water (Ampuwa)	Fresenius Kabi Deutschland GmbH
Streptozotocin	Prestwick Chemical Libraries, Orléans, France
Sulmazole	Prestwick Chemical Libraries, Orléans, France
Tridihexethyl chloride	Prestwick Chemical Libraries, Orléans, France
Trimipramine maleate salt	Prestwick Chemical Libraries, Orléans, France
Tris	MP Biomedicals, Irvine, USA

Trypticase Soy Broth	Thermo Fisher Scientific, Karlsruhe, Germany
Tryptone	Carl Roth, Karlsruhe, Germany
Valproic acid	Tokyo Chemical Industry, Tokyo, Japan
Yeast Extract	Carl Roth, Karlsruhe, Germany
Yeast extract	Carl Roth, Karlsruhe, Germany
Yeast tRNA solution	Roche, Mannheim, Germany
Zardaverine	Prestwick Chemical Libraries, Orléans, France
Zidovudine/ AZT	Tokyo Chemical Industry, Tokyo, Japan

3.1.4 Media

Media were prepared according to the following recipes with desalted water and autoclaved at 121 °C for 20 min.

Table 4. List of media

Media	Components	Gramm per liter
LB Medium	NaCl	5 g
	Yeast extract	5 g
	Tryptone	10 g
LB Agar	NaCl	5 g
	Yeast extract	5 g
	Tryptone	10 g
	Agar	15 g
Peptone-/glycerol solution	Peptone	10 g
	Glycerol	50 g

3.1.5 Buffers

Table 5. List of buffers

	Components	Final concentration
Gluc Assay Buffer	Tris-HCl	10 mM
	NaCl	600 mM
	EDTA	1 mM
	Coelenterazine	15 µM
10 x Phosphate Buffered Saline (PBS)	NaCl	80 g
	KCl	2 g
	Na_2HPO_4	6.1 g
	KH_2PO_4	2.4 g
$CaCl_2$ Buffer	$CaCl_2$	0.1 M

The powder or liquids were fill up with ddH_2O to the calculated end volume and for the Gluc Assay buffer the pH was adjust to 7.8 with HCl. Coelenterazine was dissolved in methanol to yield a stock concentration of 10 mM and stored at –80 °C. The Coelenterazine was added to the Gluc Assay buffer right before use.

3.1.6 Bacterial strains

Table 6. List of bacterial strains

Strain	Genotype	Designation	Reference
CW^{gluc}	*E. coli* C600 lysogen of 933W *stx2A::gluc*^{M43LM100L}*aphT, Kan*^{R}	JLG5	(Koeppel *et al.*, 2021)
E. coli DH5α	F$^-$ φ80*lac*ZΔM15 Δ(*lac*ZYA-*arg*F)U169 *rec*A1 *end*A1 *hsd*R17(r_K^-, m_K^+) *pho*A *sup*E44 λ$^-$*thi*-1 *gyr*A96 *rel*A1	DH5α	(Grant *et al.*, 1990)
E.coli Mt1B1		Mt1B1	DSM 28618

3.1.7 Software

Table 7. List of software

Software	Developer/Publication
Affinity Designer	Serif, Notthingham, England
Biorender	Biorender, Toronto, Canada
Gen 5 microplate reader and imager software	BioTek, Santa Clara, USA
GraphPad Prism 8 (Version 9.5.1)	GraphPad Software, Boston, USA
HiTSeekR	(List *et al.*, 2016a)
LightCycler 96	Roche, Mannheim, Germany
Microsoft Office	Microsoft, Redmond, USA
Rstudio	Posit PBC, Boston, USA
SnapGene	GSL Biotech LLC, San Diego, USA

3.2 Methods

3.2.1 Bacterial cultivation

If not differently stated, bacteria were grown in LB medium containing the appropriate antibiotic in an incubator at 37 °C while shaking at 180 rpm overnight (o.n.).. At the next day, the o.n. culture was diluted 1:20 with fresh LB medium and incubated in the same conditions as before until mid-log phase (OD_{600} 0.5). At this point the bacterial culture was ready to be used for different experiments.

3.2.2 Chemocompetent *E. coli* DH5α

500 µl o.n. culture of *E. coli* DH5α was added into 50 ml fresh LB in a 250 ml shaking flask. Cells were incubated at 30 °C until OD_{600} of 0.3 was reached. The culture was transferred into two new falcon tubes and placed on ice for 10 min. After the 10 min, the tubes were centrifuged at 1,000 x g for 30 min at 4 °C. Supernatant was discarded and cells resuspended in 15 ml ice cold $CaCl_2$ (0.1 M) and placed again on ice for 10 min. After the 10 min, the tubes were centrifuged at 1,000 x g for 10 min at 4 °C. This whole step was repeated. After the last centrifugation step 2 ml of the ice cold $CaCl_2$

solution was added to the bacteria pellet. The cells were resuspended, and aliquots were made and snap frozen in liquid nitrogen. The aliquots were stored at – 80 °C.

3.2.2.1 Generation of frozen stocks of reporter strain CW^{gluc}

The Reporter strain (CW^{gluc}) from a frozen glycerol stock was streaked out on LB agar plates containing kanamycin (30 µg/ml) and incubated o.n. at 37 °C. The next day a single colony was transferred into 5 ml LB medium containing kanamycin (30 µg/ml) and incubated in an incubator (180 rpm) o.n. at 37 °C. 99 ml LB medium containing kanamycin (30 µg/ml) were inoculated with 1 ml of this o.n. culture and incubated at 37 °C while shaking (180 rpm) until OD_{600} of 0.5. Next, the bacteria got harvested via centrifugation at 4000 x g for 5 min at 4 °C. After centrifugation the supernatant was removed, and the bacterial pellet was resuspended with a peptone-/gylcerol solution to an OD_{600} of 0.65. 1 ml aliquots were made and snap frozen in liquid nitrogen. The aliquots were stored at – 80 °C. Viability of the bacteria was tested every month via plating on LB agar plates containing kanamycin (30 µg/ml) and counting CFU/ml as well as growing the reporter strain in liquid culture (LB containing kanamycin (30 µg/ml)).

3.2.2.2 Preparation of reporter strain culture for screening

For the screen of one 96-well plate, one frozen aliquot of the reporter strain was rapidly defrosted at 37 °C in a ThermoMixer® and then inoculated into 5 ml LB medium containing kanamycin (30 µg/ml). The culture was incubated shaking at 180 rpm at 37 °C until OD_{600} of 0.5. The culture was centrifuged (4000 x g, 5 min, 4 °C) and washed with PBS (5 ml) 3 times (4000 x g for 5 min at 4 °C). After the last washing step, PBS was removed, and LB medium was added to the bacterial pellet (end OD_{600} 0.1). Bacteria where then used to inoculate plates containing compounds.

3.2.3 Prestwick Chemical Library® screen

3.2.3.1 Compound dilution and preparation of the 96-well compound replica plates

The Prestwick Chemical Library® (**Suppl. Tabel 2**) was stored at -80 °C in 14 96-well master plates, each had 8 empty wells for controls. The compounds had a concentration of 2 mM and were dissolved in 100% DMSO. From each master plate, a dilution plate was prepared, out of which 4 replica plates containing 40 µM compound concentration were generated for compound screening, giving a total of 56 96-well plate to screen. To ensure compound stability, the 4 replica plates were created the same week they were screened and stored at -20 °C.

The dilution plates were prepared by adding 245 µl LB medium and 5 µl compound (conc. 2 mM) of the corresponding master plate. Compound concentration in the dilution plate was 40 µM in 250 µl. Into the 8 control wells on the dilution plate 5 µl DMSO (100%) was added, additionally into 3 control wells 1 µg/ml MitoC (3 µM) was distributed. This led to one LB control, 3 positive (1 µg/ml MitoC) and 4 negative controls. From the dilution plate containing in total 250 µl, 4 round bottom replica plates were pipetted, each well containing 50 µl of LB with compound at a concentration of 40 µM or controls. These replica plates were sealed with a foil and the 96-well plate lid and stored at -20 °C.

3.2.3.2 Screening of compound plates

The day of measurement, a replica plate was thawn at RT and the foil was removed. The reporter culture was freshly prepared. 50 µl of the reporter strain culture (OD_{600} 0.1; see 3.2.1.2) was added into of each well of the replica plate (apart from the LB control). The result was an OD_{600} of 0.05 for the reporter and a compound concentration of 20 µM in a total volume of 100 µl. The positive control was the reporter in combination with 500 ng/ml MitoC, whereas the negative control was the reporter with DMSO alone. This round bottom 96-well plate with the lid was incubated in a BioTek EPOCH2 plate reader for 17 h at 37 °C. Every 15 min OD_{600} was measured.

Before each OD measurement the plate was shaken for 30 s in a double orbital way at 180 rpm.

3.2.3.3 Gluc luciferase assay

After 17 h growth, the 96-well replica plate was centrifuged at 4000 x g for 5 min at 4 °C. After centrifugation, 20 µl of the supernatant from each well were transferred into a new full white 96-well plate to determine luminescence. Beforehand the Gluc assay buffer was freshly prepared with the addition of coelenterazine (12.5 µM) to the buffer solution. 30 µl of Gluc assay buffer were injected into each well containing 20 µl supernatant, luminescence measurement was performed at 560 nm emission wavelength and subsequently quenching was performed by injecting 100 µl of 96% ethanol per well and thereafter 3 sec of 500 rpm double orbital shaking. Quenching of the reaction by ethanol prevented luminescence crosstalk into neighbouring wells by denaturing the Gluc luciferase.

CLARIOstar setting:	**Injection timing:**
Top optic	Settling time = 0 s
Gain = 2000	Injection start time Gluc assay buffer = 0 s (pump 1)
Focal height = 11 mm	Injection start time 96% Ethanol = 5.3 s (pump 2)
Measurement start time = 3 s	Shaking time (double orbital, 500 rpm) = 3 s (after pump 2)
No. of intervals = 1	Pump speed 300/300
Measurement interval time = 2 s	

3.2.3.4 Analysis of the Prestwick Chemical Library® screen

The screening data of all 56 compound plates was collected in a .csv file. The maximum OD_{600} reached for each growth curve was determined (OD_{max}). The quantified luminescence (RLU) from each well was divided by the corresponding OD_{max}

value and thus a quotient (RLU/OD_{max}) was calculated, which sets the luminescence in relation to the reporter growth ergo available biomass to produce the Gluc luciferase.

These raw data was then processed and analysed using the software tool HiTSeekR (https://exbio.wzw.tum.de/hitseekr/ (List *et al.*, 2016b), an online software for analysis of high-throughput screens. The goal was the identification of Shiga toxin active compounds also called hits in the tool. In the beginning the data was log_2 transformed and the input options were set. This step was followed by quality control, data normalization and as a last step hit discovery. The exact parameters chosen are described in paragraph 4.2.3.

3.2.4 Shiga toxin active compounds 96-well plates

161 Shiga toxin active compounds (**Suppl. Table 1**) were taken from the entirety of the Prestwick Chemical Library® and newly arrayed into 96-well plates. 5 µl of each identified compound was transferred from the 2 mM Prestwick Chemical Library® master plate into the new 96-well plate. The 5 µl compound solutions were diluted with 245 µl LB medium (1:50) leading to a compound concentration of 40 µM. Out of this dilution plate 4 96-well round bottom replica plate were pipetted, in which each well contained 50 µl. These 4 plates were stored at -20 °C.

3.2.5 Enzymatic activity test of *Gaussia princeps* luciferase

To test if the enzymatic activity of the luciferase was directly impaired by the compounds, 5 ml LB medium containing kanamycin (30 µg/ml) were inoculated with one colony of the reporter strain CW^{gluc} and incubated o.n. at 37 °C while shaking at 180 rpm. From the o.n. culture a day culture was prepared in 20 ml LB medium with an OD_{600} of 0.05. This culture was incubated for 2 h at 37°C while shaking at 180 rpm before MitoC (500 ng/ml final concentration) was added. After MitoC addition the culture was incubated for 4 h at 37°C while shaking at 180 rpm. After the 4 h, the bacterial culture was centrifugated at 2,000 x g at 4 °C for 10 min. 50 µl of the supernatant was added into each well of the newly array 96-well compound plates (section 3.2.4) giving a total volume of 100 µl and a final compound concentration of

20 µM. The 96-well plates were incubated for 30 min at 37 °C in an incubator. After the incubation, 10 µl out of each well were taken and pipetted into a new white 96 well plate. These plates were used to measure the luciferase activity and determine whether there is a direct effect of the compounds on the enzyme.

3.2.6 Test for inhibition of *stx2* expression

The test of potential Shiga toxin inhibitors was conducted as follows. A pre-culture of the reporter strain CW^{gluc} from a frozen aliquot (paragraph 3.2.1.1) was rapidly defrosted at 37 °C in a ThermoMixer® and then inoculated into 5 ml LB medium. The culture was incubated for 2 h at 37 °C while shaking at 180 rpm. The pre-culture was centrifuged (4000 x g, 5 min, 4 °C) and supernatant discarded. The pellet was resuspended in LB medium (end OD_{600} 0.1) containing 50 ng/ml MitoC. 50 µl of this bacterial suspension was added into each well of prepared 96-well compound plates (paragraph 3.2.3). Final concentration in each well was 20 µM for the compound and 25 ng/ml MitoC. This 96-well plate with lid was incubated in a BioTek EPOCH2 plate reader for 17 h at 37 °C. Every 15 min OD_{600} was measured. Before each OD measurement the plate was shaken for 30 s in a double orbital way at 180 rpm. After the 17 h incubation time, the Gluc luciferase assay (paragraph 3.2.2.4) was performed.

3.2.7 Concentration-dependent re-screen

The compounds for the concentration-dependent test were obtained from different manufacturers (**Table 3**). All 52 compounds (**Table 8**) were dissolved and diluted with 100% DMSO to a working concentration of 60 mM. For each compound, 10 different concentrations were tested (2.5 µM –1280 µM). The DMSO compound solution was diluted in LB medium. The First dilution was 1:23.44 which achieved a compound concentration of 2560 µM. From there a 2-fold dilution series in LB medium was done. After each dilution step, the new compound solution was vortexed to assure even compound distribution. 8 different compounds were tested on one round bottom 96-well plate, each row having one compound. The Shiga toxin inducing compounds were on separate plates than the inhibiting ones. 250 µl of each of the 10 different compound concentrations were added into each well of a 96-well plate in columns 2 – 11 leaving

columns 1 and 12 empty for controls. In these empty wells LB medium containing 1% DMSO was added. In this scheme 5 master plates containing inducing compounds and 2 master plates with inhibiting compounds were pipetted. These master plates were stored at – 80 °C. Out of each master plate 4 replica plates were created at the time of measurement. The replica plates were screened one by one, and in the meantime the rest of the plates were stored at – 20 °C.

Table 8. List of compounds for the concentration-dependent screen

Compound	Substance class	Cellular target	Impact on Shiga toxin expression
Acetylsalicylic acid	Nonsteroidal anti-inflammatory drugs	Inhibits activity of cyclooxygenase (COX) 1 & 2	Inducing
Acyclovir	Nucleoside analogue	Viral enzyme thymidine kinase	Inducing
Aminocaproic acid	Antifibrinolytics	Enzyme plasmin	Inducing
Amiodarone hydrochloride	Antiarrhythmics	Ion channels in the heart	Inducing
Ascorbic acid	Organic compounds (vitamins)	Various enzymes and processes	Inducing
Balsalazide Sodium	5-aminosalicylates (ASAs)	Inflamed tissue in colon and rectum	Inducing
Clioquinol	Hydroxyquinolines	Interference with metal metabolism of microorganisms	Inducing
Clomiphene citrate (Z/E)	Selective estrogen receptor modulators (SERMs)	Estrogen receptor in hypothalamus	Inducing
Dacarbazine	Alkylating agents	DNA	Inducing

Esmolol hydrochloride	Beta-blockers	Beta-adrenergic receptors in the heart	Inducing
Floxuridine	Antimetabolite chemotherapeutic agents	DNA	Inducing
Guaiacol	Phenolic compound	Respiratory system	Inducing
Imatinib	Tyrosine kinase inhibitors	BCR-ABL tyrosine kinase	Inducing
Indatraline hydrochloride	Dopamine reuptake inhibitor	Dopamine transporter	Inducing
Ketorolac tromethamine	Nonsteroidal anti-inflammatory drug	Inhibits activity of cyclooxygenase (COX) 1 & 2	Inducing
Meglumine	Contrast agent	No specific cellular target	Inducing
Mepivacaine hydrochloride	Local anesthetics	Voltage-gated sodium channels	Inducing
Mevastatin	Statins	HMG-CoA reducatase	Inducing
Niacin	Vitamins B	Various enzymes and processes	Inducing
Nicotinamide	Vitamins B	Various enzymes and processes	Inducing
Niridazole	Antiparasitic drugs	Interference with metabolism of parasitic organisms	Inducing
Pentobarbital	Barbiturate drugs	Gamma-aminobutyric acid (GABA-A) receptor	Inducing
Pinaverium bromide	Antispasmodic drugs	Smooth muscle cells in	Inducing

		gastrointestinal tract	
Piperacetazine	Phenothiazine antipsychotic drugs	Antagonism of dopamine receptors of CNS	Inducing
Quinethazone	Thiazide diuretics	Renal tubules	Inducing
Raclopride	Dopamine receptor antagonists	Dopamine D2 receptor	Inducing
Saquinavir mesylate	Protease inhibitors	HIV-1 protease enzyme	Inducing
Sertindole	Atypical antipsychotic drugs	Antagonism of dopamine receptors in CNS	Inducing
Sildenafil/ Viagra	Phosphodiesterase type 5 (PDE5) inhibitors	PDE5 enzyme	Inducing
Stavudine	Nucleoside reverse transcriptase inhibitors	Reverse transcriptase (virus)	Inducing
Streptozotocin	Alkylating agents	DNA	Inducing
Tridihexethyl chloride	Antimuscarinic drugs	Muscarinic acetylcholine receptors	Inducing
Trimipramine maleate salt	Tricyclic antidepressants	Inhibition of the reuptake of neurotransmitters	Inducing
Valproic acid	Antiepileptic drugs	Enhancement of GABA activity	Inducing
Zardaverine	Phosphodiesterase inhibitors	Phosphodiesterase	Inducing
Zidovudine/ AZT	Nucleoside reverse transcriptase inhibitors	Reverse transcriptase (virus)	Inducing

Acetazolamide	Carbonic anhydrase inhibitors	Carbonic anhydrase	Inhibiting
Antimycin A	Mitochondrial electron transport chain inhibitors	Complex III of electron transport chain	Inhibiting
Azithromycin	Macrolides	Bacterial ribosome	Inhibiting
Azlocillin sodium salt	Semisynthetic penicillin	Bacterial cell wall synthesis	Inhibiting
Clarithromycin	Macrolides	Bacterial ribosome	Inhibiting
Clindamycin hydrochloride	Lincosamide	Bacterial ribosome	Inhibiting
Disulfiram	Alcohol-sensitizing agents	Aldehyde dehydrogenase	Inhibiting
Efavirenz	Non-nucleoside reverse transcriptase inhibitors	Reverse transcriptase (virus)	Inhibiting
Imipenem	Carbapenems	Bacterial cell wall synthesis	Inhibiting
Levodopa	Dopaminergic agents	Conversion to dopamine in the brain	Inhibiting
Lincomycin hydrochloride	Lincosamide	Bacterial ribosome	Inhibiting
Lymecycline	Tetracycline	Bacterial ribosome	Inhibiting
Metronidazole	Nitroimidazole	DNA of anaerobic bacteria	Inhibiting
Miconazole	Antifungal agents	Fungal cell membrane	Inhibiting
Moroxidine hydrochloride	Antiviral agents	Target not fully elucidated	Inhibiting
Sulmazole	Antifungal agents	Fungal cell membrane	Inhibiting

3.2.7.1 *Stx2* expression inducing compounds

The replica plates for the re-screen of *stx2* expression inducing compounds were screened as described above (paragraph 3.2.1.2 + 3.2.2.2 + 3.2.2.3) with the following changes in the Gluc luciferase assay. After centrifugation, 10 µl of the supernatant of each well was transferred into a new full white 96-well plate to determine luminescence. Beforehand, the Gluc assay buffer was freshly prepared with the addition of coelenterazine (10 µM) to the buffer solution. 40 µl of Gluc assay buffer were injected into each well containing 10 µl supernatant, luminescence measurement was performed at 560 nm emission wavelength. Luminescence crosstalk into neighbouring wells was prevented by using an aperture spoon.

CLARIOstar setting:	**Injection timing:**
Top optic	Settling time = 0 s
Gain = 2000	Injection start time Gluc assay buffer = 0 s (pump 1)
Focal height = 11 mm	Pump speed 300
Measurement start time = 1.6 s	
No. of intervals = 1	
Measurement interval time = 0.5 s	

3.2.7.2 Shiga toxin expression inhibiting compounds

The replica plates for the concentration-dependent re-screen of Shiga toxin expression inhibitors were screened as described above (paragraph 3.2.5 + 3.2.2.3) with the following changes in the Gluc luciferase assay. After centrifugation, 10 µl of the supernatant of each well was transferred into a new 96-well plate. To the 10 µl supernatant 90 µl Gluc assay buffer without coelenterazine was added, resulting 1:10 dilution of the supernatant. 10 µl of this dilution was added into a new full white 96-well plate to determine luminescence. Beforehand, the Gluc assay buffer was freshly prepared with the addition of coelenterazine (10 µM) to the buffer solution. 40 µl of Gluc assay buffer were injected into each well containing 10 µl supernatant dilution, luminescence measurement was performed at 560 nm emission wavelength.

Luminescence crosstalk into neighbouring wells was prevented by using an aperture spoon.

CLARIOstar setting:	Injection timing:
Top optic	Settling time = 0 s
Gain = 2000	Injection start time Gluc assay buffer = 0 s (pump 1)
Focal height = 11 mm	Pump speed 300
Measurement start time = 1.6 s	
No. of intervals = 1	
Measurement interval time = 0.5 s	

3.2.8 Quantitative PCR for *uidA* and *clbB*

3.2.8.1 Generation of qPCR standards for *uidA* and *clbB*

Primers for PCR amplifying the fragment (2000 bp) of interest were chosen. *E. coli* Mt1B1 genomic DNA was used as templates for PCR to amplify the fragment of the gene of interest (*uidA*, *clbB*). The Q5 DNA polymerase was used due to the proofreading features. The PCR the product was visualised on a 1% agarose gel. The correct band size was purified using the NucleoSpin Gel and PCR Clean-Up Kit (following manufacturer protocol). DNA concentration was determined using Nanodrop. The fragment was cloned into pJET1.2/blunt cloning vector following the manufacturer protocol (CloneJet PCR Cloning Kit). The newly generated plasmid was transformed into chemocompetent DH5α. 1 µl of ligation product was added into 50 µl chemocompetent DH5α on ice and incubated for 30 min. Then the cells were heat shocked (30 sec, 42 °C) and immediately put on ice. 950 µl LB medium was added and then incubated for 1 h at 37 °C while shaking at 650 rpm. 50 µl bacterial culture was plated on LB agar plates containing ampicillin (100 µg/ml) and incubated at 37 °C o.n. At the next day single colonies were picked. 5 ml LB medium containing ampicillin (100 µg/ml) was inoculated with one single colony, this was repeated with 5 single colonies. The colony used for medium inoculation was streaked onto a new LB agar plate containing ampicillin (100 µg/ml). The inoculated medium was incubated o.n. at

37 °C while shaking at 180 rpm. At the next day, the bacteria were pelleted (5,000 x g, 5 min, 4 °C) and the plasmid was extracted using the Nucleospin Plasmid Mini Kit (following manufacturers protocol). Correct sequence of plasmid insert was verified using Sanger sequencing. From the colony with the correct insert a 100 ml LB medium (ampicillin 100 µg/ml) o.n. culture was done. At the next day, plasmid extraction was performed using the Qiagen Plasmid Plus Midi Kit and concentration determined via Nanodrop. Extracted plasmid got linearized using the restriction enzyme *HindIII* (single cutter; 1 µg plasmid in 50 µl restriction reaction, 1 h, 37 °C). The linearized plasmid was cleaned up with the NucleoSpin Gel and PCR Clean-up Kit and diluted with yeast tRNA solution (100 ng/µl) to concentrations between 10^8-10^{-2} gene copies/ml.

Table 9. Primers and probes used for uidA and clbB qPCR

Designation	Sequence 5' – 3'	Specificity	Purpose	Reference
Mt1B1_uidA_fw	ATGTTACGTCCTGT AGAAACCCCAAC	Mt1B1 *uidA*	Amplification of gene *uidA* (1812 bp)	In this study
Mt1B1_uidA_rev	TCATTGTTTGCCTC CCTGCTGC			In this study
Mt1B1_clbB_fw	GATTGCGATGCGG CATTGGC	Mt1B1 *clbB*	Amplification of gene *clbB* (2200 bp)	In this study
Mt1B1_clbB_rev	ACTTGTCGCCGTC AGCACT			In this study
uidA_Probe2	5' 6-FAM-TGACGCATGTCGC GCAAGACTGTAAC C-3'BHQ-1	*E.coli* housekeeping gene *uidA*	qPCR	In this study
qPCR_uidA_fw_2	TGCTCTACACCAC GCCGAATAC			In this study
qPCR_uidA_rev_2	ACATCACCATTTG CCACCACC			In this study
clbB_Probe3	5' HEX-CGCGTGGCCTCC ACACTGGAATATG -3'BHQ-1	Pks island gene *clbB*	qPCR	In this study
qPCR_clbB_fw_3	GTTCTCCGCTAAA ACACCC			In this study
qPCR_clbB_rev_3	TGCAATGTATAAG CCACATCC			In this study

3.2.8.2 Protocol for absolute quantitative PCR

Primer and probe (**Table 9**) for qPCR were designed with the software Primer Express using the sequence of the fragment of the gene of interest. For duplex qPCR, probes

were 5' labelled with either 6-carboxyfluorescein (FAM) or 6-carboxyhexafluorescein (HEX) and 3' labelled with the black hole quencher 1 (BHO-1). Standard curves for each primer probe pair were performed in triplicates. As DNA template linearized plasmid (paragraph 3.2.7.1) with known DNA quantity was used (10^8-10^{-2} gene copies/ml). From the three runs, the qPCR efficiency (85-95%) was derived using the standard curves. Sample DNA extracted from human feces was diluted with Gibco water to a final concentration of 2 ng/µl.

qPCR reaction with sample DNA was conducted as follows. The reaction was run as duplex assay in a Roche LightCycler96® system. One PCR reaction (total volume of 20 µl) contained 300 nM of each primer, 250 nM of the corresponding hydrolysis probe, 2 x FastStart Essential DNA Probes Master (10 µl) and 5 ng sample DNA (2 ng/µl) all combined in a qPCR specific 96-well plate. The following cycler program was used for the run; pre-incubation for 10 min at 95 °C, followed by 45 cycles of 15 s 95 °C and 60 s 60 °C. Fluorescence was recorded after each cycle. Standards in the 96-well plate were used together with the previously measured standard curves for absolute quantification of gene copies in sample DNA. Data were analysed with the LightCycler96® software package (Roche).

3.2.9 Statistical analysis

Statistical significance for each experiment is indicated in the individual plots and described in the figure legend. Statistical tests Kruskal-Wallis test, Fisher's exact test, one-way ANOVA test and Dunnett's multiple comparisons test were performed in GraphPad Prism. P values < 0.05 were considered as statistically significant (* P < 0.05, ** P < 0.01, *** P < 0.001, **** P< 0.0001).

3.2.10 Figures

The data shown in this thesis was plotted using GraphPad Prism or R studio. schematics were created using BioRender.

4. Results

4.1 Evaluation of the potential of the reporter strain CW^{gluc} to be employed for compound-screening

Because CW^{gluc} not only recapitulates excellently the kinetics of natural Stx2 release, but also integrates safety, usability, scalability, and a very good sensitivity, we wanted to verify that this reporter is very well suited to be applied in a high-throughput screen. For this reason, I selected a 96-well plate format, which is regularly used in high-throughput screens and robotic platforms. To verify, if the reporter strain would be applicable in such a set-up, optimal growth conditions were analysed. Inoculated LB medium with different starting OD_{600} (0.2, 0.1 and 0.05) of CW^{gluc}, in volumes of 100 µl or 200 µl per well were incubated at 37 °C for 6 h. Cell density was measured every 15 min (**Fig. 5**). The growth curves in 200 µl have overall higher OD_{600} values compared to the 100 µl, reaching values higher than 1. Also, the starting OD_{600} had a greater influence in 200 µl especially in the lag phase of the growth curves. In the lower volume, the reporter strain reached an end OD_{600} below 0.6. The reporter strain did not reach complete stationary phase for both volumes and starting ODs after the 6 hours of growth. In view of these results, I decided to use 100 µl for further screens in 96-well format, as this reduces the tested compounds used in a screen.

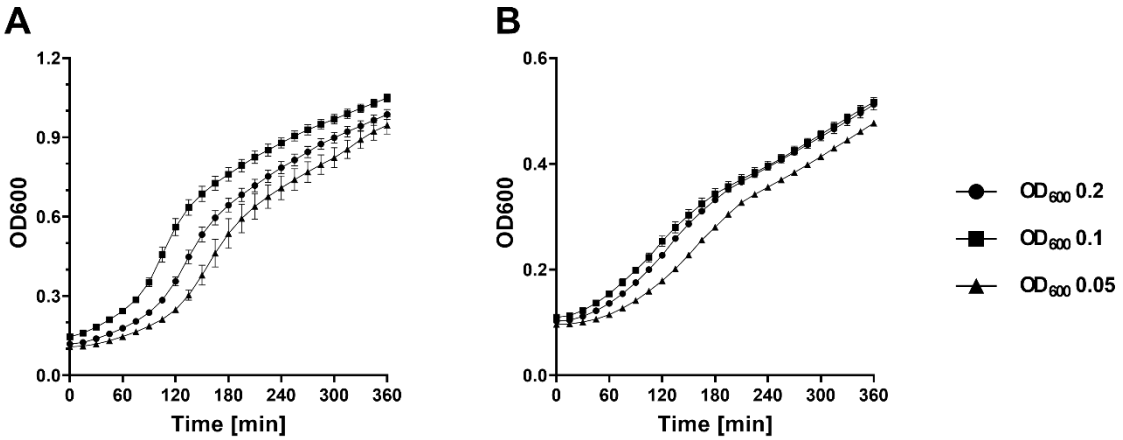

Figure 5. Characterization of *E. coli* CW^{gluc} reporter strain.
Preculture of *E. coli* CW^{gluc} was grown in LB medium until mid-log phase (OD_{600} ~ 0.5). After centrifugation, bacteria were suspended and diluted in LB to the three different starting OD_{600}: 0.2 (circles), 0.1 (squares) and 0.05 (triangles). The reporter strain was grown in (**A**) 200 µl or (**B**) 100 µl LB in a 96-well plate for 6h at 37°C. OD_{600} was measured every 15 min. The mean and standard deviation of OD_{600} for 3 independent technical replicates are plotted.

To induce *stx2* expression, I measured the growth of the reporter strain with different concentrations of MitoC (0, 62.5, 250 and 500 ng/ml) in 100 µl (**Fig. 6C and D**) or 200 µl volume (**Fig. 6A and B**) and a starting OD_{600} of 0.1 (**Fig. 6B and D**) or 0.2 (**Fig. 6A and C**). The reporter strain was incubated at 37°C for 6 h under all these different conditions. An observation which holds true for all four different conditions (different well volume and starting OD) was, that the lowest MitoC concentration of 62.5 ng/ml did not lead to a reduction in growth of the reporter. At 500 ng/ml MitoC in 100 µl well volume, the reporter strain showed the typical lysis curve indicating prophage induction.

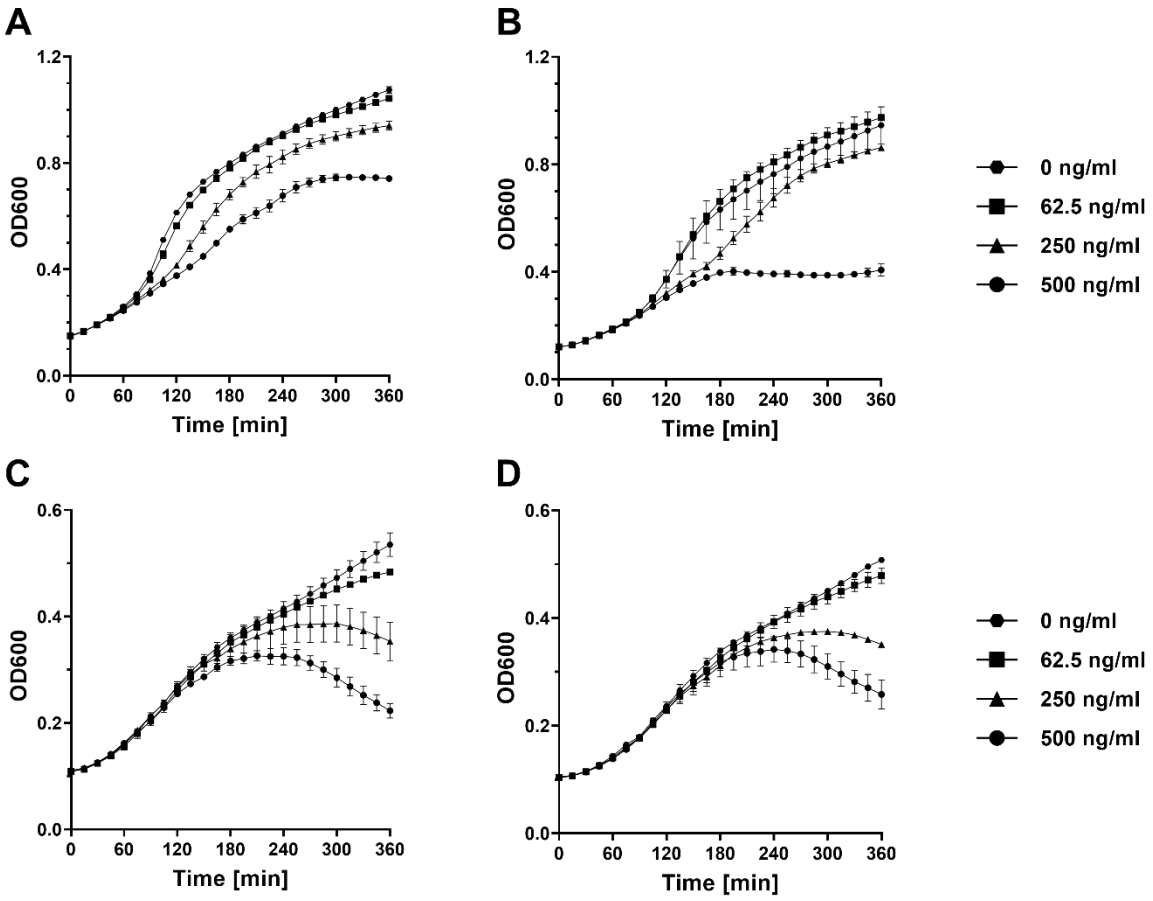

Figure 6. Characterization of *E. coli* CW^{gluc} growth in response to mitomycin C.
The precultured reporter strain was grown in (**A, B**) 200 µl or (**C, D**) 100 µl LB (hexagons) or LB supplemented with different concentrations of MitoC: 62.5 ng/ml (squares), 250 ng/ml (triangles), 500 ng/ml (circles) in a 96-well plate for 6h at 37°C. Two different starting OD_{600} (**A, C**) 0.2 and (**B, D**) 0.1 were tested. OD_{600} was measured every 15 min. The mean and standard deviation of 3 independent biological and technical replicates are plotted.

The growth behaviour of the reporter strain under chemical influence was only one possible readout for *stx2* expression. The stronger and more direct readout is the measurement of the luminescence in the culture supernatant. **Figure 7** shows the growth curves and relative light units (RLU) of the reporter grown in 100 µl well volume with a starting OD600 of 0.1 and four different MitoC concentrations (0, 62.5, 250 and 500 ng/ml). The luminescence values determined for 0 ng/ml and 62.5 ng/ml MitoC were nearly identical, similar to the growth behaviour of the reporter at these concentrations (**Fig. 6D**). A MitoC concentration of 250 ng/ml or 500 ng/ml led to a strong increase in luminescence exceeding the 10^6 RLU.

Therefore, I selected the following conditions for the future assays: Starting OD_{600} of 0.05, in a volume of 100 µl incubated at 37 °C. A concentration of 500 ng/ml of MitoC was selected for the future assays as positive control.

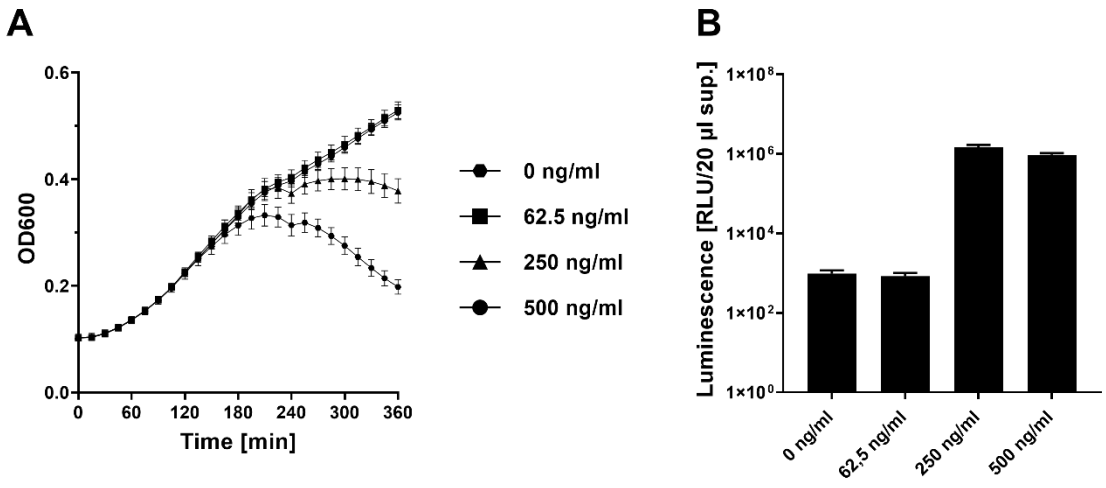

Figure 7 Evaluation of the influence of different mitomycin C concentrations on reporter activity in the culture supernatant.
The precultured of *E. coli* CW^{gluc} was grown in 100 µl LB (hexagons) or LB supplemented with increasing concentrations of MitoC: 62.5 ng/ml (squares), 250 ng/ml (triangles), 500 ng/ml (circles) in a 96-well plate for 6h at 37°C. The starting OD_{600} was 0.1. OD_{600} was measured every 15 min. (**A**) The mean and standard deviation of 3 independent biological and technical replicates are plotted. Afterward, the 96-well plate was centrifuged (5 min 1000 x g) to pellet the bacteria. 20 µL supernatant was taken and Gluc activity was determined as described in methods. (**B**) The mean relative light units (RLUs) and standard deviation for 3 independent biological and technical replicates are shown.

To evaluate if this reporter could be used in medium- and high-throughput screening assays, I calculated the signal window (SW) and Z'-factor, two parameters used to measure assay performance (Iversen *et al.*, 2012). The signal window provides the degree of separation between signals of active and inactive compounds. This allows

for a correct identification of active molecules with desired level of activity. A signal window value greater than 2 indicates good performance of the assay. The formula for the signal window is:

$$SW = \frac{\left(AVG_{max} - {3SD_{max}}/{\sqrt{n}}\right) - \left(AVG_{min} + {3SD_{min}}/{\sqrt{n}}\right)}{{SD_{max}}/{\sqrt{n}}} \geq 2$$

where AVG is the calculated mean of the maximal (max) and minimal (min) signal, SD the standard deviation and n the number of replicates for the test substance. The Z'-factor assesses the separation between the positive and negative control as well as the variability in an assay and by that provides a quantitative measure of how well positive and negative control can be discriminated. The possible range is from 0 to 1. Values above 0.4 are considered good performance of the assay.

$$Z' = \frac{\left(AVG_{max} - {3SD_{max}}/{\sqrt{n}}\right) - \left(AVG_{min} + {3SD_{min}}/{\sqrt{n}}\right)}{AVG_{max} - AVG_{min}} \geq 0.4$$

For our tests with the new reporter strain CW^{gluc}, I calculated for three independent 96-well plates signal windows in the range of 15 – 25 and an overall Z'-factor of 0.8. We concluded that the reporter strain is suitable for an assay in the 96-well format.

4.2 Influence of human-targeted drugs on *stx2* expression in a high-throughput screen

Human medication can have a strong antibiotic impact on bacteria in the gut microbiome (Maier *et al.*, 2018). Therefore, we hypothesized that human-targeted drugs may also promote EHEC *stx2* expression. To test this idea, I used the reporter strain CW^{gluc} and the Prestwick Chemical Library® (**Suppl. Table 2**), a commercially available source of compounds. This library contains more than 1200 FDA- and EMA-approved off-patent compounds with a big range of chemical and pharmacological diversity. We hypothesized that some of the human-targeted drugs would induce the bacterial SOS response and by that activate the Shiga toxin carrying prophage.

4.2.1 Creating a workflow for 96-well plate base compound screen

To have a consistent and reproducible workflow throughout the entire screening process (involving a total of 56 compound plates), I set-up a routine procedure for plate inoculation (**Fig. 8**). To normalize growth parameters of the reporter strain, I created a large batch of frozen CW^{gluc} aliquots with a final OD_{600} of 0.65 in LB glycerol medium. These stocks were stored at -80 °C and regularly checked for viability. At each day, one of these aliquots was rapidly defrosted at 37 °C in a ThermoMixer®. 5 ml of LB medium supplemented with 30 µg/ml kanamycin, to ensure only the reporter strain could grow, was inoculated with the stock and incubated at 37 °C until an OD_{600} of 0.5 was reached. At this point the cells were washed and diluted with LB medium to an OD_{600} of 0.1 ready to be pipetted onto the compound plate.

The master plates of the Prestwick Chemical Library® were stored at -80 °C for long term stability of the compounds. To screen the compound library, the chemicals were arrayed into dilution plates a few days before use. We created four replica plates out of each dilution plate, to ensure that at the end of the screen we have statistically significant results (see material and methods). All 96-well replica plates had 50 µl of a LB-compound (40 µM) suspension in each well. These plates were stored at -20 °C. At the day the plate was used for the experiment, one of the replica plates was thawed and each well got topped up with 50 µl prediluted reporter strain culture, yielding a final concentration of 20 µM of the compound and an OD_{600} of 0.05.

In the screen, growth (OD_{600}) in each well was measured for 17 hours at 37 °C in a plate reader. This time range gives the compounds enough time to penetrate the cells and potentially influence the *stx2* expression and also allows the culture to reach stationary phase. In addition, luciferase activity (luminescence) was quantified in the culture supernatant. With the addition of coelenterazine (CTZ) containing buffer, luminescence of each well was individually measured (RLU/20 µl supernatant) (**Fig. 8**).

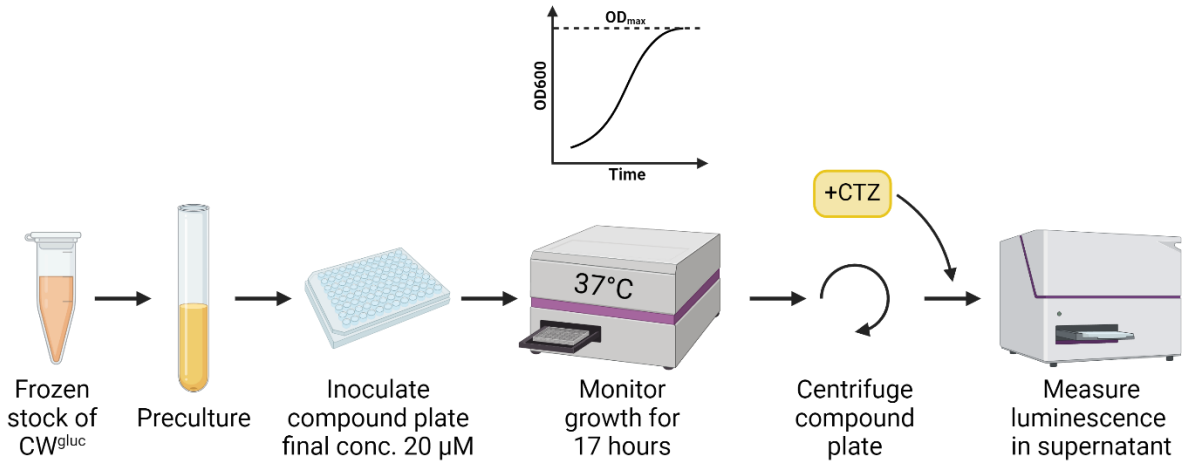

Figure 8. Workflow of the Prestwick Chemical Library screen.
Cryostocks of CW^{gluc} were rapidly thawed and used to generate a preculture, which was grown till mid-log phase (OD_{600} ~ 0.5). The culture was then diluted with LB to an OD_{600} of 0.1. 50 µl of the culture were added on top of the 50 µl compound-LB suspension to each well of the 96-well compound plate, leading to a final compound concentration of 20 µM in 100 µl. The plate was incubated in a plate reader at 37°C for 17 h while shaking and growth was measured as OD_{600} every 15 min. Afterwards, the 96-well plate was centrifuged for 5 min at 1000 x g and 20 µL of each well was transferred into a new white 96-well plate. The light produced by the Gluc was measured in each well after the automated addition of 30 µl Gluc buffer containing coelenterazine (RLU/20 µl sup). Figure was created using BioRender.

As a positive control, I choose 500 ng/ml MitoC, a reported *stx2* inducing compound, and as negative control, the reporter strain without compound, only containing DMSO (solvent for the compounds). To normalize luminescence relative to the amount of cells, I determined the maximum growth reached (OD_{max}) in each well and set this into relation to the quantified luminescence of that well (RLU/OD_{max}) (**Fig. 9A and B**).

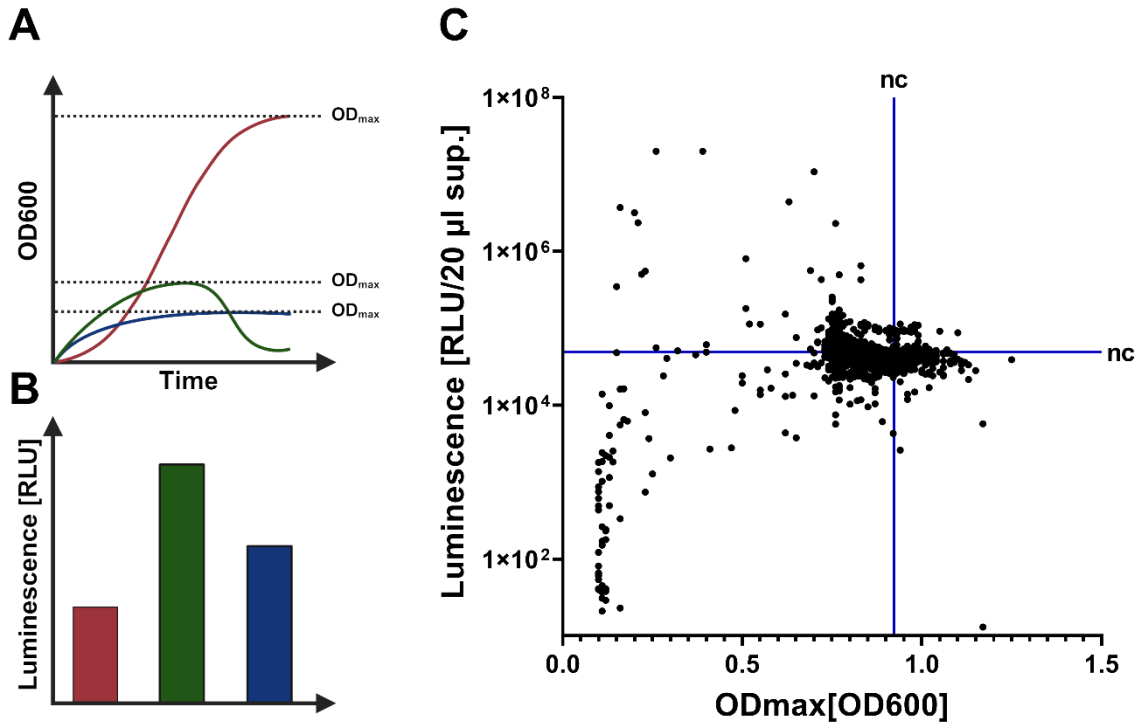

Figure 9. Overview of the results of the complete Prestwick Chemical Library screen.
(**A**) Shows graphicly examples of three different growth curves and their respective OD_{max} value (dotted line), which is the highest measured OD_{600} value for each growth curve. The OD_{max} value was chosen as parameter to represent the available CW^{gluc} biomass in a culture which can produce Gluc luciferase. (**B**) Indicates the luminescence measured in 20 µl culture supernatant as relative light units (RLU) for the three different cultures. (**C**) Shows the measured values for each compound in the Prestwick Chemical Library. On the x-axis the OD_{max} values of the screened compounds are plotted, while on the y-axis the corresponding luminescence values are plotted. Each point is the mean of 4 independent replicates. The vertical blue line indicates the OD_{max} value of the negative control (nc, no drug) and the horizontal blue line the luminescence value of the nc.

4.2.2 Screening of the Prestwick Chemical Library® for compounds influencing *stx2* expression

For the screen, one master plate at the time was measured and quadruplicates were analysed at consecutive days. This procedure was chosen to keep the time the chemicals were stored at -20 °C as short as possible. **Figure 9C** presents an overview of the results of all screened compounds. The mean OD_{max} for the 4 replicates of each compound is plotted on the x-axis, while the y-axis shows the corresponding mean luminescence value in the culture supernatant (RLU/20 µl). The two blue lines show the corresponding OD_{max} and luminescence value for the negative control. All compounds in the two left quadrants have an inhibitory effect on growth. Those in the

upper left quadrant led to increased luminescence, while those in the lower one, to decreased luminescence.

The effect of individual compounds on growth and luciferase production was diverse. **Figure 10** shows as example five compounds (ceftazidime, dirithromycin, rifaximin, novobiocin and pipemidic acid) to demonstrate the observed diversity of compounds effect in the screen. The controls we choose, CW^{gluc} with 500 ng/ml MitoC as positive and the CW^{gluc} alone as negative control, depict the high range of the assay (**Fig. 10C**). Growth curves and luminescence values of the reporter strain exposed to the 5 different compounds is shown in **figure 10A and B.** These examples show very clearly that luminescence cannot solely be predicted based on the growth behaviour of CW^{gluc}.

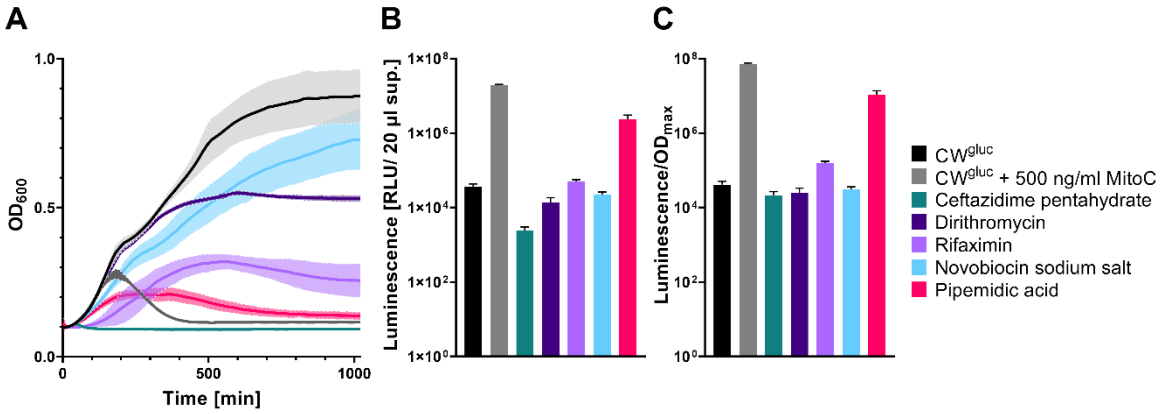

Figure 10. Example compounds that have different impact on *stx2* expression.
Example of CW^{gluc} exposed to 5 different compounds (ceftazidime pentahydrate, dirithromycin, rifaximin, novobiocin sodium salt & pipemidic acid) from the Prestwick Chemical Library® screen with their (**A**) growth curves (**B**) luminescence values per 20 µl supernatant and (**C**) the RLU/OD_{max} ratio from these two values. Additionally, the positive control (CW^{gluc} + 500 ng/ml MitoC) and negative control (CW^{gluc}) are shown. The mean and standard deviation of 4 independent replicates is shown.

4.2.3 Analysis of the screen data and validation of the hit compounds

To analyse the screening data, we employed an R Shiny tool called HiTSeekR (List *et al.*, 2016a). This software was designed for analysing a variety of different high-throughput screening data and includes all major steps, such as different quality controls and normalization options followed by "Hit" detection. **Figure 11** shows the analysis pipeline for the imported data, from quality control to normalization until hit detection.

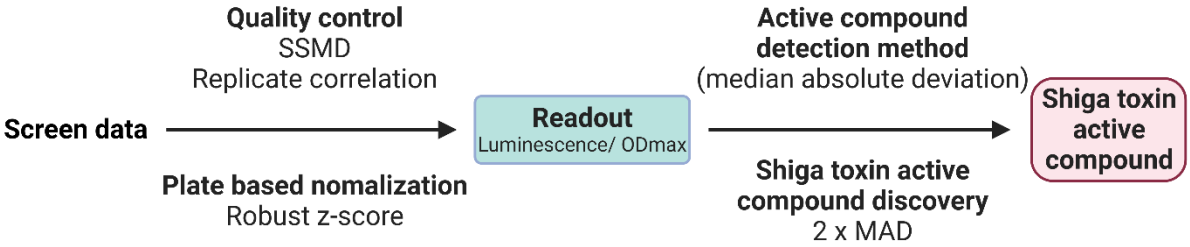

Figure 11. Identification of Shiga toxin 2 active compounds using HiTSeekR.
Steps of the data analysis from the Prestwick Chemical Library® screen using the R shiny software HiTSeekR. The data import is followed by quality testing (strictly standardized mean difference (SSMD), replicate correlation) and data normalization (robust z-score) on single 96-well plate basis. As readout parameter the quotient of luminescence divided by OD_{max} (RLU/OD_{max}) was taken. For defining active compounds with biological meaningful impact on *stx2* expression (pos. or neg.) a threshold of 2-fold median absolute deviation (MAD) of the robust z-score normalized plate median of the whole screen was chosen. Figure was created using BioRender.

To verify if the screening data was solid enough to get statistically sound results, several mathematical quality control steps were performed, visualized through graphics provided by HiTSeekR. I performed correlation analysis between each of the quadruplicates. The r^2 values from linear regression varied between 0.88 and 0.97 which shoes a significant correlation between our replicates. Next, I confirmed that the signal-to-noise ratio was high enough to be able to identify active compounds ("hits"). We chose to use the strictly standardized mean difference (SSMD) as preferred parameter. The SSMD were μ_1 and μ_2 are the means and σ_1 and σ_2 the variance of the positive (reporter with 500 ng/ml MitoC) and negative (reporter without compound) control was calculated as follows:

$$SSMD = \frac{\mu_1 - \mu_2}{\sqrt{\sigma_1^2 + \sigma_2^2}}$$

$$SSMD: strictly\ standarized\ mean\ difference$$

$$\mu: Mean$$

$$\sigma: Variance$$

This value describes not only the difference but also the variability of both control populations. A SSMD > 3 states that the mean difference is at least three times the standard deviation of the differences between the positive and negative control. The positive and negative control on each compound plate achieved a SSMD of 20 or higher. Since all the quality-based parameters (plate signal variation, row and column

effects, replicate correlation and SSMD) of the HTS were good, I next normalized the data using the robust z-score (rz) as plate-based normalization method.

The rz, with x_i corresponds to the sample value, med(x) corresponds to the plate median and MAD is the median absolute deviation (see below), was calculated as follows:

$$rz = \frac{|x_i - med(x)|}{MAD}$$

$$rz: Robust\ z-score$$
$$med(x) = Median$$

The advantage compared to the often-used z-score is that the plate median is taken instead of the plate mean, which makes it favourable in a screen where high signal differences on one plate are expected since outliers do not have a strong influence.

The last step in data analysis was the detection of active compounds ("hits"). As hit detection method, we choose to use two times the Median absolute deviation (MAD) as threshold at which a measured effect is considered significant. The MAD has an increased robustness compared to the standard deviation since the median is used instead of the mean. The MAD with x_i corresponds to the sample value and $\bar{x}$ to the plate median is calculated as follows:

$$MAD = 1.4296 \times med(|x_i - \bar{x}|)$$

$$MAD: Median\ absolute\ deviation$$
$$med: Median$$
$$\bar{x}: Median$$

Figure 12 provides an overview of all screened compounds with the upper and lower hit detection threshold (2x MAD) visualized as black line (Cutoff). This cut-off resulted in 161 primary hits (**Suppl. Table 1**) from all screened compounds, which is an active compound rate of approximately 13.4%. With 2x MAD we went for a lower cut-off than often used in HTS due to the strong biological effect Stx2 has once produced in an EHEC infected patient.

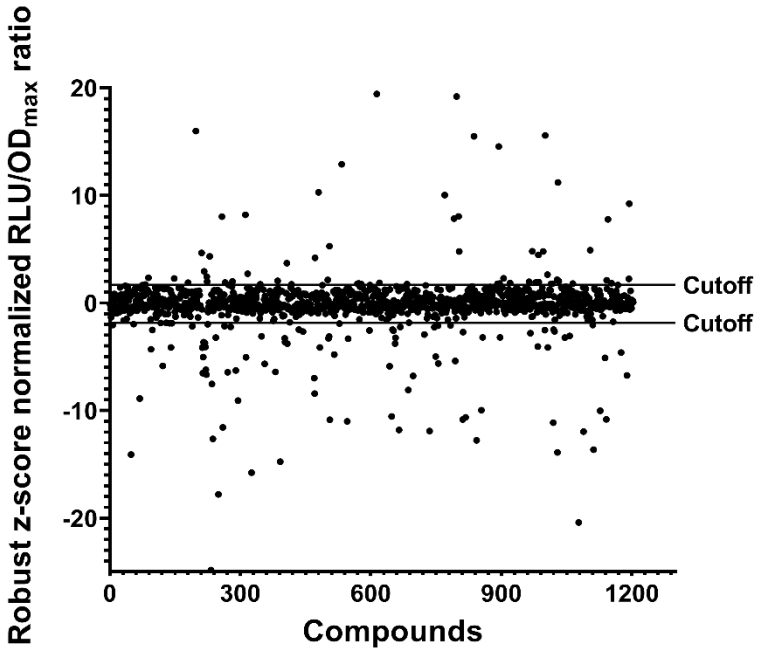

Figure 12. Overview of robust z-score normalized RLU/OD$_{max}$ ratio from the compound screen. Compounds are depicted on the x-axis, the y-axis shows the robust z- score (rz-score) normalized ratio RLU/OD$_{max}$. Each point represents the rz-score normalized ratio of RLU/OD$_{max}$ of one compound, which is the result of 4 independent measurements. The two horizontal lines represent the chosen cutoffs (2x median absolute deviation) for identifying Stx2 active compounds.

In the next step, I validated these 161 primary hits. I examined the ability of these 161 compounds to interfere with the enzymatic function of *Gaussia princeps* luciferase (Gluc), and thereby causing a bias in the measured values. If a compound interferes with the enzymatic function of Gluc, the luminescence signal in the supernatant would be higher or lower than the luminescence signal of the untreated supernatant, leading to false hits. The 161 primary hits were newly arrayed into 96-well plates, each well apart from control wells had 50 µl of a LB compound (40 µM) suspension in it. An overnight culture of the reporter stain CW^{gluc} was diluted with LB to an OD$_{600}$ of 0.05. After 2 hours of incubation at 37 °C *gluc* expression was induced with 500 ng/ml MitoC and incubation was continued for another 4 hours. At this point the bacterial culture was centrifuged, and the supernatant was checked for Gluc activity via luminescence detection. After the confirmation that Gluc was active, each well of the newly arrayed compound plates got topped up with 50 µl of this Gluc containing supernatant. The compound plates were incubated for 30 min at 37 °C in an incubator. Afterwards luminescence was quantified in 10 µl of this suspension and compared to the control

wells (supernatant containing active Gluc without compound influence) (**Fig. 13**). This experiment was performed in duplicates.

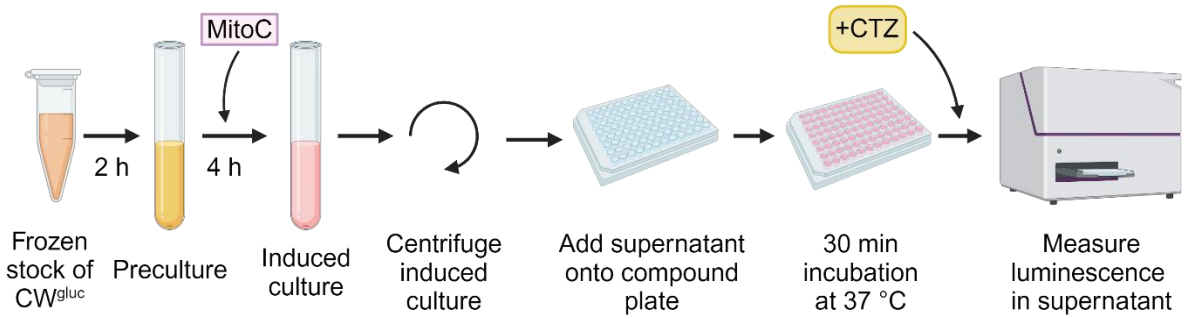

Figure 13. Workflow of the enzymatic activity test for the *Gaussia* luciferase.
Cryostocks of CW^{gluc} were rapidly thawed and used to generate a preculture, which was grown till mid-log phase (OD_{600} ~ 0.5). Then, the culture was diluted with LB to an OD_{600} of 0.05 and 500 ng/ml MitoC was added. This culture was incubated for 4 h at 37°C in order to induce luciferase production. After 4 h the culture was centrifuged, and the supernatant tested for luciferase activity (Gluc assay). 50 µl of the supernatant containing luciferase was added on top of the 50 µl compound-LB suspension to each well of the newly arrayed 96-well compound plate, leading to a final compound concentration of 20 µM. This 96-well plate was incubated at 37 °C for 30 min to ensure a possible interaction between the compounds and the luciferase. After incubation, 10 µL of each well was transferred into a new white 96-well plate. Gluc activity in each well was measured after the automated addition of 40 µl Gluc buffer containing coelenterazine and compared to the control well where no compound was influencing Gluc activity. Compounds influencing Gluc activity, detected by luminescence values higher or lower than 3x the standard deviation of the control values, where discarded from further testing. Figure was created using BioRender

Validation of the hit compounds for interfering with Gluc activity resulted in the exclusion of 21 compounds (**Table 10**) from the list of 161 Stx2 active compounds, leaving 140 compounds.

Table 10. List of compounds interfering with *Gaussia princeps* luciferase activity

Sample	Substance class	Cellular target
Alexidine dihydrochloride	Antiseptic	Mitochondria
Benzbromarone	Uricosuric Agent	Urate Transporter 1 (URAT1)
Chicago sky blue 6B	Dye	N/A
Chloroxine	Antimicrobial	Bacterial DNA
Closantel	Anthelmintic	Mitochondria
Danazol	Steroid	Androgen Receptor
Daunorubicin hydrochloride	Antibiotic	Topoisomerase II
Diethylstilbestrol	Synthetic Estrogen	Estrogen Receptor

Entacapone	COMT Inhibitor	Catechol-O-Methyltransferase (COMT)
Fosinopril	ACE Inhibitor	Angiotensin-Converting Enzyme (ACE)
Gliquidone	Sulfonylurea	ATP-sensitive Potassium Channel
Hexachlorophene	Disinfectant	Cell Membrane
Hexestrol	Synthetic Estrogen	Estrogen Receptor
Liothyronine	Thyroid Hormone	Thyroid Hormone Receptor
Luteolin	Flavonoid	Various Enzymes
Merbromin	Antiseptic	Bacterial Cell Membrane
Rifapentine	Antibiotic	RNA Polymerase
Tiratricol triiodothyroacetic acid	Thyroid Hormone	Thyroid Hormone Receptor
Tribenoside	Vasoprotective Agent	Vascular Endothelium
Verteporfin	Photosensitizer	Photodynamic Therapy Target
Zafirlukast	Leukotriene Receptor Antagonist	Leukotriene Receptor

4.2.4 Classification of Shiga toxin 2 active compounds

The Anatomical Therapeutic Chemical (ATC) classification system classifies compounds into their respective groups according to the organ or system they act on and the compound properties and use case (*Anatomical Therapeutic Chemical (ATC) Classification*). The pie chart in **figure 14** illustrates the distribution of compounds in the Prestwick Chemical Library® according to their ATC classification. Of note, the cardiovascular system (C) and nervous system (N) are the two predominant ATC groups, each accounting for approximately 13% of the total compound spectrum.

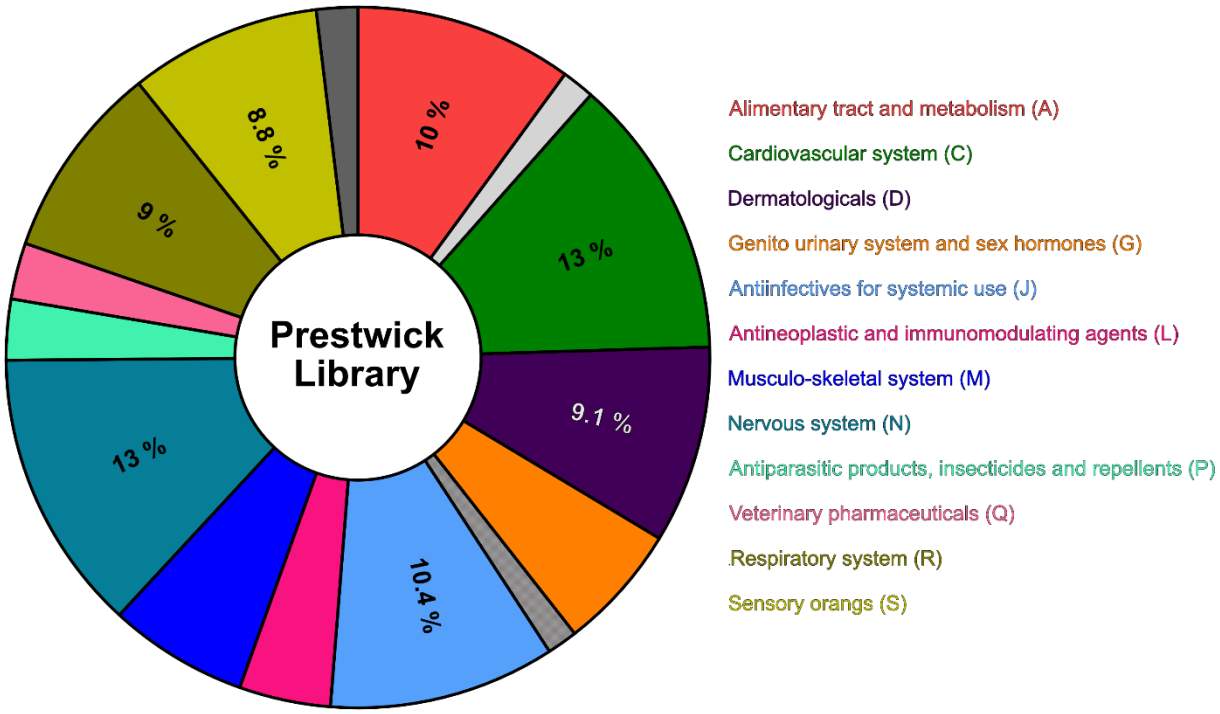

Figure 14. Categorization of the compounds of the Prestwick Chemical Library® in the Anatomical Therapeutic Chemical (ATC) classification system.
Each pie slice represents one ATC group. The percentage indicates how highly the respective ATC group is represented in the Prestwick Chemicals Library®. For the coloured pie slices the one letter ATC code is given. A: Alimentary tract and metabolism; C: Cardiovascular system; D: Dermatologicals; G: Genito urinary system and sex hormones; J: Antiinfectives for systemic use; L: Antineoplastic and immunomodulating agents; M: Musculo-skeletal system; N: Nervous system; P: Antiparasitic products, insecticides, and repellents; Q: Veterinary drug; R: Respiratory system; S: Sensory organs.

We assigned the 140 validated Stx2 active compounds (hits) to their respective ATC groups (**Fig. 15**), with some compounds belonging to multiple ATC groups. In blue is shown the relative distribution of the Prestwick Chemical Library® compounds to the different ATC groups and in orange the distribution of the 140 Stx2 active compounds. A closer look at the hits classified into different ATC groups revealed a significant peak of relative abundance within the group of anti-infectives for systemic use (J), which comprises nearly 40% of all active compounds. This proportion exceeds the expected equally distributed relative representation of this ATC group compared with the library, a deviation that is statistically significant by the Fisher exact test (p-value 0.0001). Similarly, the sensory organs ATC group (S) shows a significantly increased relative abundance of approximately 15% among the 140 hits (p-value 0.01). In contrast, the Cardiovascular system (C), Musculo-skeletal system (M), Nervous system (N), and Various (V) ATC groups show a significant underrepresentation in the list of active compounds (* p-value 0.05, **** p-value 0.0001). The majority of other ATC groups show an even distribution of relative frequency between the Prestwick Chemical

library® and the active compounds group. An exception is ATC group H (Systemic hormonal preparations, excl. sex hormones and insulins), which in contrast has no hits at all in the screen.

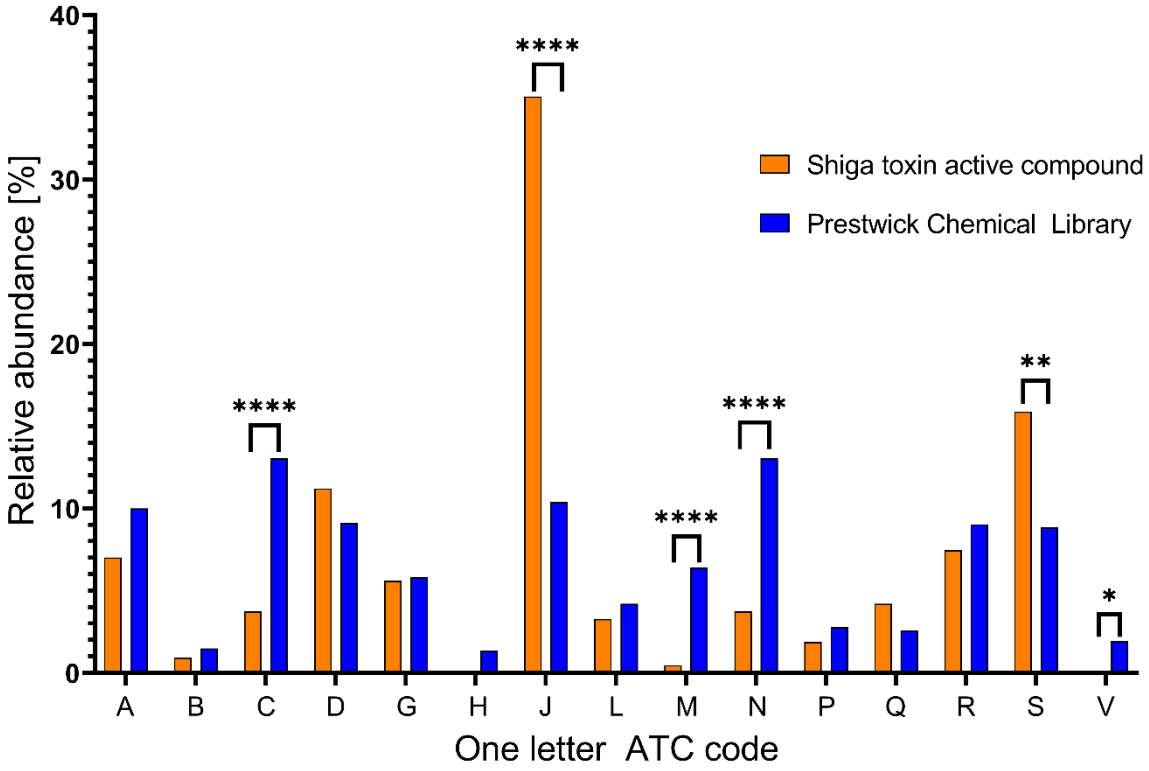

Figure 15. Relative abundance of ATC groups among Shiga toxin 2 active compounds compared to the Prestwick chemical library®.

The 140 Stx2 active compounds were categorized according to the ATC classification system. In orange, the relative abundance of the respective ATC group in the total of Stx 2 active compounds is shown. In comparison, the relative abundance of each ATC group in the Prestwick Chemical Library® is shown in blue. On the x-axis, each group is shown as one letter ATC code. A: Alimentary tract and metabolism; B: Blood and blood forming organs; C: Cardiovascular system; D: Dermatologicals; G: Genito urinary system and sex hormones; H: Systemic hormonal preparations, excl. sex hormones and insulins; J: Antiinfectives for systemic use; L: Antineoplastic and immunomodulating agents; M: Musculo-skeletal system; N: Nervous system; P: Antiparasitic products, insecticides, and repellents; Q: Veterinary drug; R: Respiratory system; S: Sensory organs; V: Various. The y-axis shows the relative abundance in percentage. To determine a significant over- or underrepresentation of an ATC group between the two clusters, the Fisher's Exact Test was used (* $p < 0.05$, ** $p < 0.01$, **** $p < 0.0001$).

4.2.5 Determination of inducing or inhibiting effect on *stx2* expression

The HiTSeekR analysis provides a list of compounds that are above or below the hit detection threshold (2x MAD), but does not classify the compounds into inducing or inhibiting Stx2 production. In order to identify which compounds induce or inhibit expression of the toxin, the results of two experimental setups need to be combined.

A general statement that can be made by looking at **figure 9C** is, that the compounds that affected *stx2* expression in our screening process can be divided into two distinct groups. One group includes compounds that induces toxin expression, resulting in a higher luminescence signal compared to the negative control, while the other includes compounds that appear to inhibit toxin production, resulting in a lower luminescence level compared to the negative control.

To verify that among the Stx2 active compounds are inhibitors of *stx2* expression, all active compounds were re-analysed in an alternative experimental setup. Here, I pre-induced *stx2* expression at a low level by adding a final concentration of 25 ng/ml MitoC to the reporter strain culture prior to the addition of the compounds (**Fig. 16**). The rest of the workflow was the same as in the initial screen. Previously, we had shown that a MitoC concentration of 25 ng/ml led to a measurable increase in luminescence in our reporter strain but did not inhibit its growth too severely (**Fig. 17**). From this, we concluded that prior induction of stx2 expression would facilitate the readout of potentially Stx2 inhibitory compounds. This re-screen targeting Stx2 inhibiting compounds was performed in duplicates.

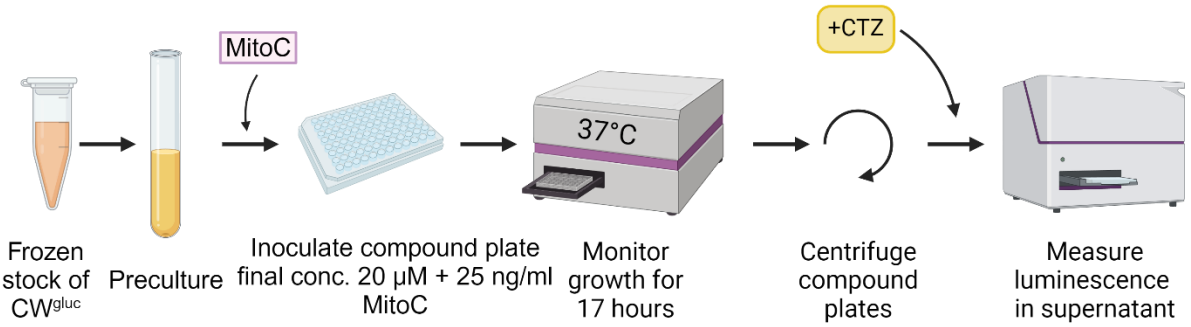

Figure 16. Workflow to determine inhibitory effect of compounds on stx2 expression.
Cryostocks of CW^{gluc} were rapidly thawed and used to generate a preculture, which was grown till mid-log phase (OD_{600} ~ 0.5). Then, the culture was diluted with LB to an OD_{600} of 0.1 and 50 ng/ml MitoC was added to induce luciferase expression. 50 µl of the culture with MitoC was added on top of the 50 µl compound-LB suspension to each well of the 96-well compound plate, leading to a final compound concentration of 20 µM and a final MitoC concentration of 25 ng/ml. The plate was incubated in a plate reader at 37°C for 17 h while shaking and growth was measured as OD_{600} every 15 min. Afterwards, the 96-well plate was centrifuged for 5 min at 1000 x g and 10 µL of each well was transferred into a new white 96-well plate. Gluc activity in each well was measured after the automated addition of 40 µl Gluc buffer containing coelenterazine (RLU/10 µl sup). Figure was created using BioRender.

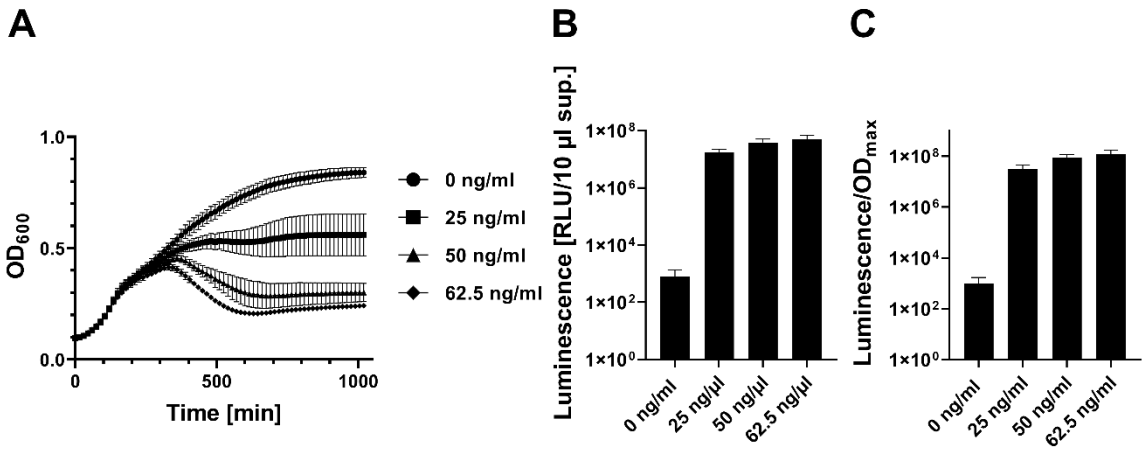

Figure 17. Induction of *stx2* with low concentrations of mitomycin C.
(**A**) Growth curves of the reporter strain CW^{gluc} with different MitoC concentrations: 0 ng/ml (circles), 25 ng/ml (squares), 50 ng/ml (triangles) and 62.5 ng/ml (diamonds) grown at 37 °C for 17 h. (**B**) Luciferase activity measured in 10 µl of the supernatant shown as relative light units (RLU). (**C**) Ratio of the luminescence value to OD_{max} of the respective growth curve is depicted. Shown is the mean and StD of three technical replicates.

Combining these two results, the 140 Stx2 active compounds could be divided into 97 *stx2* expression inducing compounds and 43 potential *stx2* expression inhibitors due to their luminescence values.

4.2.5.1 Compounds inducing *stx2* expression

The distribution of these 97 *stx2* expression inducing compounds in the ATC classification system can be seen in **figure 18**. The biggest ATC group in the 97 compounds is the ATC group J (Antiinfectives for systemic use) representing around 30% of *stx2* expression inducing compounds (p-value 0.0001). Other not significantly overrepresented ATC groups in comparison to their distribution in the Prestwick Chemical Library® are ATC group G (Genito urinary system and sex hormones), Q (Veterinary drug) and R (Respiratory system). Strongly underrepresented ATC groups among the *stx2* expression inducing compounds are the groups C (Cardiovascular system), H (Systemic hormonal preparations, excl. sex hormones and insulins), M (Musculo-skeletal system), N (Nervous system) and V (Various).

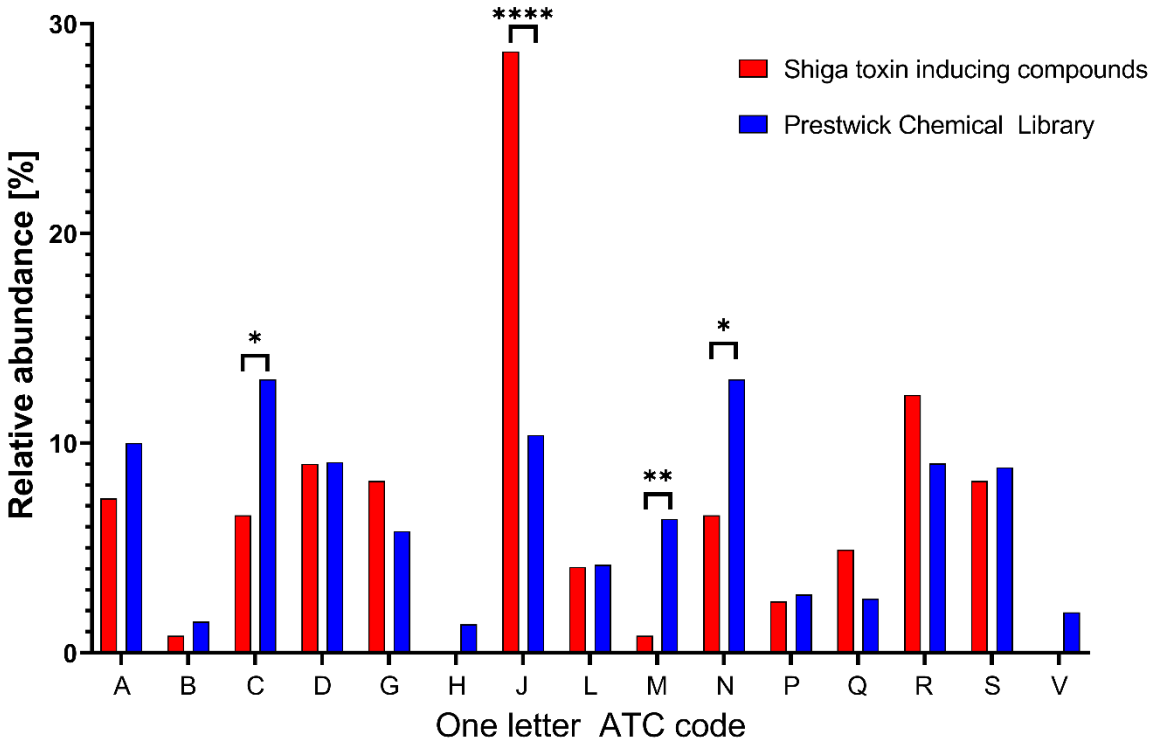

Figure 18. Relative abundance of ATC groups among *stx2* inducing compounds compared to Prestwick chemical library®.
The 97 *stx2* inducing compounds were categorized according to the ATC classification system. In red the relative abundance of the respective ATC groups in the total of *stx2* inducing compounds is shown. In comparison, the relative abundance of each ATC group in the Prestwick Chemical Library® is shown in blue. On the x-axis, the one letter ATC code for each ATC group is depicted, while the y-axis shows the relative abundance in percentage. See figure 15 for group names. To determine a significant over- or underrepresentation of an ATC group between the two clusters, the Fisher's Exact Test was performed (* $p < 0.05$, ** $p < 0.01$, **** $p < 0.0001$).

In the initial screen, all compounds were tested at a concentration of 20 µM. To cover a broader range of potential effects, we next performed experiments testing the effect of a selected list of compounds at ten different concentrations ranging from 2.5 µM to 1,280 µM per compound. For the concentration-dependent screen, we selected 36 out of the 97 originally identified *stx2* expression inducing compounds (**Table 8**). The selection of the 36 compounds was based on several criteria. First, we choose compounds which showed a strong increase in *stx2* expression in the initial screen like niridazole or streptozotocin. As a second criteria we choose compounds, which had an estimated intestine concentration in humans (values taken from Maier *et al.*, 2018) much higher than the 20 µM used in our initial screen for example meglumine (1451 µM) and esmolol hydrochloride (2511 µM). As a third criteria, we selected compounds that are frequently used by people who feel sick like acetylsalicylic acid or ascorbic acid. The 36 compounds were purchased from different manufacturers (**Table 3**) and then dissolved in DMSO. For the concentration dependent screen, 96-well master plates were generated with eight compounds, each at ten different concentrations. I again measured four replicates per master plate. To facilitate a comprehensive evaluation of the effect of each concentration on *stx2* induction, the ratio between the measured luminescence signal and the maximum measured OD_{600} value in the growth curve was calculated (RLU/OD_{max}).

Since a compound concentration range of 2.5 µM - 1,280 µM was to be measured, and the associated DMSO concentration per well would be at the highest compound concentrations a bit above 2%, which is higher than in the initial screen (less than 1%), we still had to ensure that the elevated DMSO concentrations would not affect our reporter strain. We investigated the effect of DMSO on the growth of the reporter strain and measured the luminescence under 6 different DMSO concentration (1%, 2%, 4%, 6%, 8%, 10%). **Figure 19A, B** and **C** show the growth of the reporter strain, the measured luminescence and the quotient of luminescence divided by OD_{max} with the different DMSO concentrations. Since the DMSO concentration in the concentration-dependent compound screen exceeds 2% only in the highest concentration, the measured DMSO concentrations of 1% and 2% are most important for our analysis. The growth curve of the reporter with 2% DMSO was slightly lower than with 1% DMSO, but still in a tolerance range when the standard deviations of the two growth curves are taken into account (**Fig. 19A**). Regarding the luminescence measured in the culture supernatant, the difference between the two concentrations was very subtle

(**Fig. 19B**), so that the quotient RLU by OD_{max} reached a very similar value for the two DMSO concentrations (**Fig. 19C**). Taking all these data together, we concluded that the DMSO concentration in the highest compound concentration of the concentration-dependent screen does not significantly affect the reporter strain.

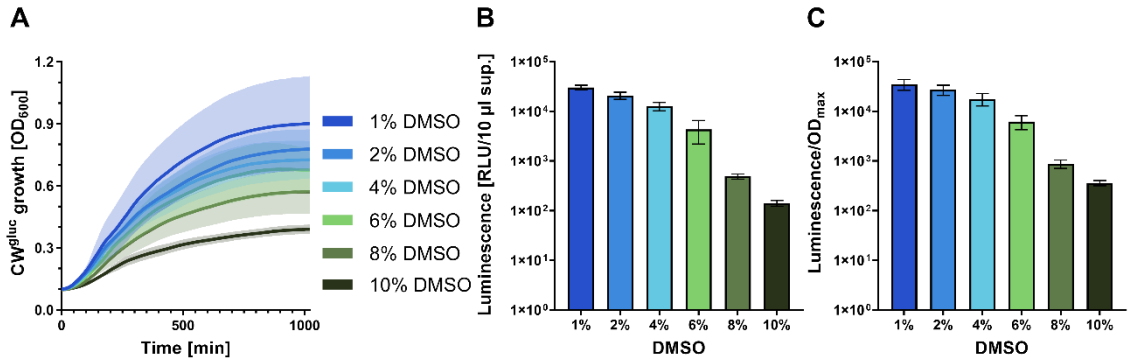

Figure 19. Effect of DMSO on the reporter strain CW^{gluc}.
(**A**) Growth curves of the reporter strain with different DMSO concentrations at 37 °C for 17 h is shown. Each colour represents a different DMSO concentration. For each growth curve, the mean and StD of three independent biological replicates is shown. (**B**) Luciferase activity measured in 10 µl of the supernatant shown as relative light units. Each bar reflects the mean and StD of 3 independent biological replicates. (**C**) Ratio of the luminescence value to OD_{max} of the respective growth curve. Shown is the mean and StD of three replicates.

Overall, we encountered very different results in the concentration-dependent study. For 19 of the 36 compounds, we could no longer reproduce the previously observed effect of *stx2* induction at any of the measured concentrations. **Figure 20A - H** shows eight representative examples from the 36 rescreened compounds (**Suppl. Fig. 1**). The blue bar in each plot marks the 20 µM concentration used in the initial screen. The light orange bar in each plot is the negative control, the reporter strain without the influence of any compound. Ascorbic acid, guaiacol and pentobarbital (**Fig. 20B, C and F**) are three examples of compounds where none of the measured compound concentrations exceeded the quotient value luminescence divided by OD_{max} of the negative control. Another group we identified, were compounds for which the *stx2* inducing effect was only slightly dependent on the concentration. For example, meglumine as well as quinethazone (**Fig. 20D and G**) showed the same *stx2* inducing effect across all measured concentrations with only small variations. Acetylsalicylic acid and especially niridazole are two examples of compounds that showed an increase in *stx2* induction at lower compound concentrations (< 20 µM). While the calculated quotient RLU by OD_{max} for acetylsalicylic acid at a compound concentration

of 2.5 µM comes close to 50,000 (one-third higher than negative control, **Fig. 20a**), there is a more pronounced increase in the ratio for niridazole, which peaked at just under $2.5x10^7$ at a compound concentration of 10 µM. This is almost a factor of 650 higher than the negative control (**Fig. 20E**). As a final group, there were also compounds for which the ratio of luminescence to OD_{max} increased at higher compound concentrations. Sertindole (**Fig. 20H**) is an example of this group. It reached a ratio peak of nearly $2.8x10^5$ at a compound concentration of 640 µM, a factor of 550 higher than the negative control.

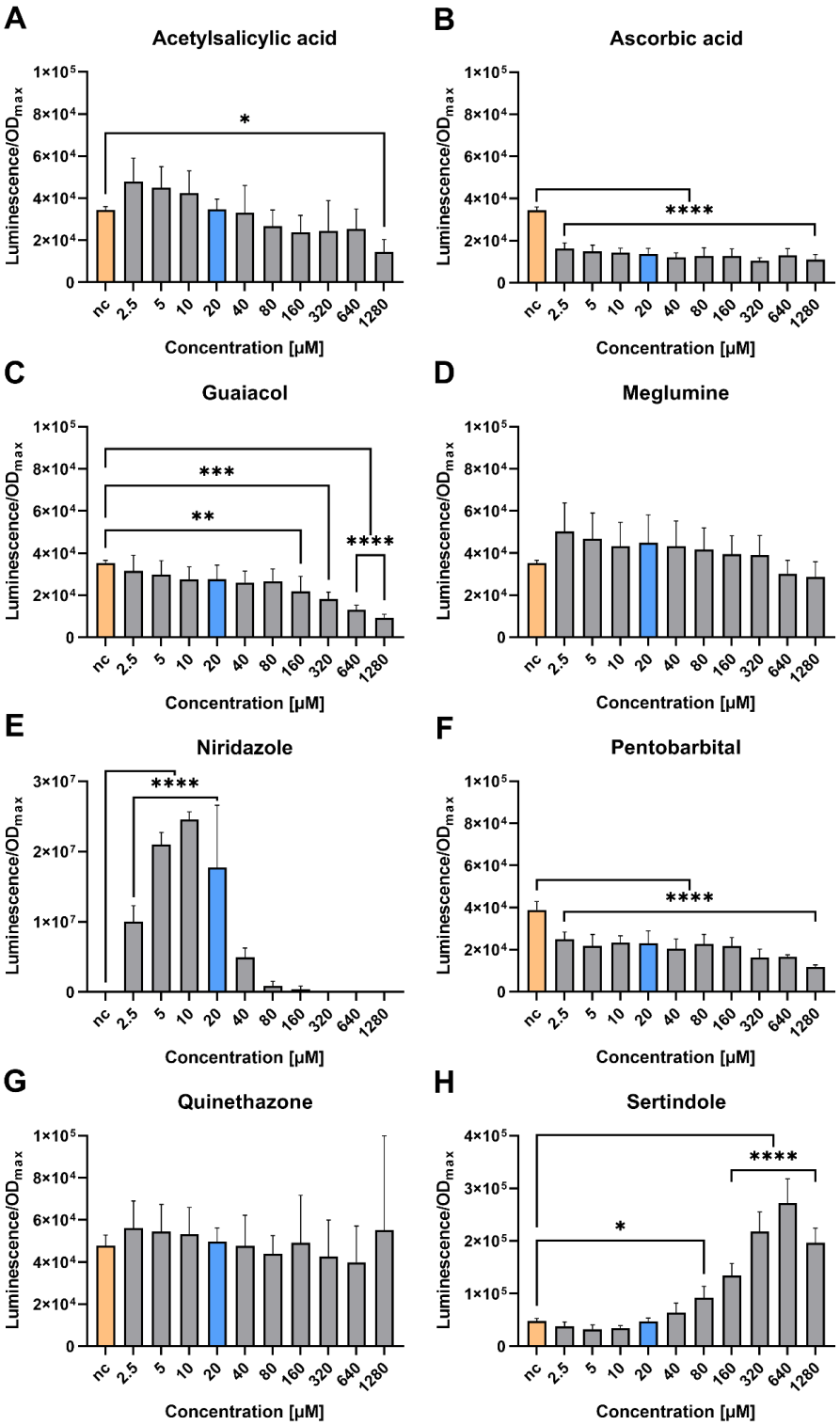

Figure 20. Dose-dependent influence of *stx2*-inducing compounds on CW^{gluc}.
Luminescence/OD$_{max}$ values of the reporter strain exposed to increasing concentrations (2.5 µM - 1.280 µM) of different compounds (**A**) acetylsalicylic acid, (**B**) ascorbic acid, (**C**) guaiacol, (**D**) meglumine, (**E**) niridazole, (**F**) pentobarbital, (**G**) quinethazone and (**H**) sertindole. The blue bar marks the concentration used in the initial screen (20 µM). The orange bar indicates Luminescence/OD$_{max}$ ratio of the negative control (no compound). Shown is the mean and StD of four independent experiments. Statistical analysis using one-way ANOVA followed by Dunnett multiple comparison test was performed (* $p < 0.05$, ** $p < 0.01$, *** $p < 0.001$, **** $p < 0.0001$).

The corresponding OD_{max} values for each of the ten different concentrations of the eight compounds previously shown, can be seen in **figure 21**. Niridazole has a strong negative effect on CW^{gluc} growth at higher compound concentrations (> 40 µM). At lower concentrations, the bactericidal effect decreases, allowing the reporter strain to grow. The result of this growth, led to one of the highest luminescence signals in the concentration-dependent screen (**Fig. 20E**). It should be noted, however, that a significant increase in *stx2* expression is not necessarily accompanied by a pronounced reduction in growth of the reporter strain. The compound sertindole also reduces the growth of the reporter strain to a lesser extent, but still has a significantly higher *stx2* expression level than the negative control. Meglumine as well as acetylsalicylic acid hardly affect CW^{gluc} growth at the concentrations measured in each case. The same can be said for quinethazone, although here at a concentration of 1,280 µM caused growth inhibition. However, this inhibition is put into perspective by the high standard deviation for this OD_{max} value. As in the initial screen, there were compounds in the concentration-dependent screen that appeared to enhance reporter growth. The growth of the reporter was increased by guaiacol to a small extent, and ascorbic acid and pentobarbital to a considerable extent. This effect was concentration independent (**Fig. 21**).

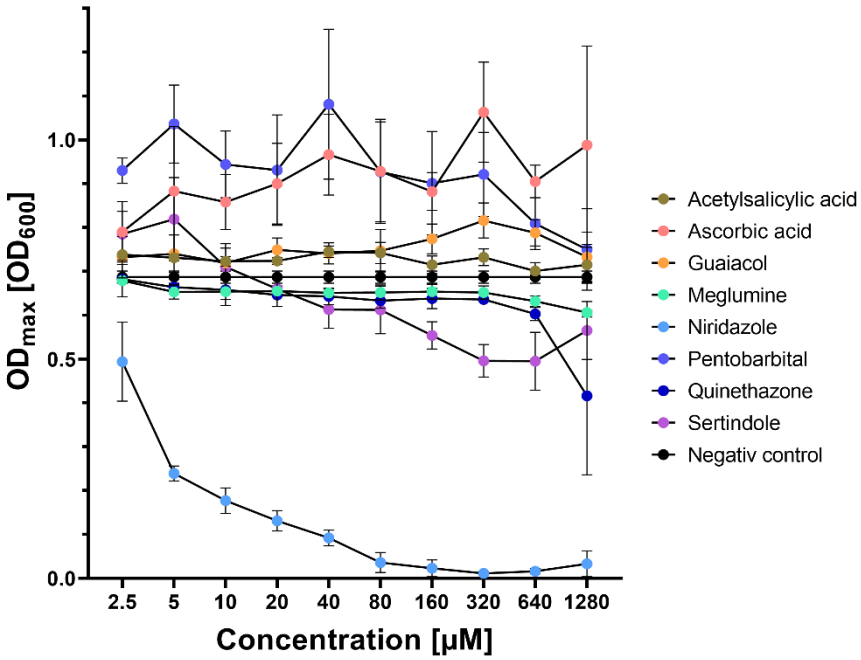

Figure 21. Influence on CW^{gluc} growth of *stx2*-inducing compounds at different concentrations. OD$_{max}$ of each growth curve of the reporter strain in the dose-dependent assay of the selected *stx2*-inducing compounds. Shown is the OD$_{max}$ of each compound at increasing compound concentrations (2.5 µM – 1,280 µM). The eight different compounds are colour coded differently. The OD$_{max}$ of the negative control (no compound) is shown in black. Mean and StD of four independent experiments are depicted.

4.2.5.2 ATC classification group Antineoplastic and Immunomodulating agents (L) comprises Shiga toxin 2-inducing compounds

After the initial screen, we not only categorized the Stx2-active compounds into their respective ATC group memberships (**Fig. 15**), but also analysed the extent to which these compounds enhanced Stx2 production. We noticed that streptozotocin (49-fold higher luminescence compared to negative control) and dacarbazine (46-fold higher luminescence compared to negative control) had one of the most pronounced inducing effects on *stx2* expression compared with all compounds screened. These two compounds belong to the ATC classification group L (Antineoplastic and immunomodulatory agents). We then analysed whether other active compounds in the initial screen belonged to ATC group L and assigned them to the different subgroups (**Table 11**) within the ATC classification group L. This gave us a good overview of the

distribution of these compounds among the different subgroups (**Fig. 22A**). It became apparent that the *stx2* expression inducing compounds were not evenly distributed across all subgroups, but mainly clustered in some subgroups, namely nitrosoureas (L01AD), other alkylating agents (L01AX), pyrimidine analogues (L01BC), protein kinase inhibitors (L01XE), antiestrogens (L02BA), and enzyme inhibitors (L02BG). This prompted us to focus on compounds belonging to group L in subsequent studies, and to investigate other ATC group L compounds in addition to the Prestwick Chemical Library® to gain a more comprehensive understanding of their inducing effects on *stx2* (**Table 12**).

Table 11. ATC-group L subgroups

ATC Code	Group Namen	Compounds in Prestwick Chemical Library®	Stx2 active compounds
L01AA	Nitrogen mustard analogues	3	0
L01AB	Alkyl sulfonates	1	0
L01AD	Nitrosoureas	1	1
L01AX	Other alkylating agents	2	1
L01BA	Folic acid analogues	2	0
L01BB	Purine analogues	5	1
L01BC	Pyrimidine analogues	5	1
L01CA	Vinca alkaloids and analogues	1	0
L01CB	Podophyllotoxin derivatives	1	0
L01CD	Taxanes	2	0
L01DB	Anthracyclines and related substances	4	0
L01XB	Methylhydrazines	1	0
L01XE	Protein kinase inhibitors	4	1
L01XX	Other antineoplastic agents	11	0
L02AA	Estrogens	4	0
L02BA	Anti-estrogens	4	1
L02BB	Anti-androgens	3	0

L02BG	Enzyme inhibitors	5	1
L04AA	Selective immunosuppressants	1	0
L04AD	Calcineurin inhibitors	1	0
L04AX	Other immunosuppressants	4	0

Table 12. Additional ATC group L compounds

Compound	ATC Code	ATC group name
5-Azacitidine	L01BC	Pyrimidine analogues
Clofarabine	L01BB	Purine analogues
3-Deazauridine	-	-
Decitabine	L01BC	Pyrimidine analogues
Nelarabine	L01BB	Purine analogues

Again, I performed a concentration-dependent analysis of Stx2 active compounds within ATC group L, which included those from the initial screening as well as additional ones (**Table 12**). The concentration range extended from 2.5 µM to 1,250 µM. A recurring phenomenon from previous experiments was also observed, some of the Stx2 active compounds identified in the initial screen did not have the same expression inducing effect in the concentration-dependent analysis. Seven of the thirteen compounds screened did not exceed the luminescence/OD_{max} ratio of the negative control at a concentration of 20 µM (**Fig. 22C, D, E, G, J, L and M**). ATC subgroup L01BC, pyrimidine analogues, had the most representatives in this screen, with five compounds. Of note, the *stx2*-inducing effect was highly variable among the different representatives of this subgroup. Cytarabine (**Fig. 22E**) showed no inducing effect, whereas 5-azacitidine and floxuridine (**Fig. 22A and I**) showed remarkably strong effects, peaking at 160 µM and 640 µM, respectively. In comparison, the two compounds decitabine and 5-fluorouracil both induced *stx2* expression, although to a lesser extent than the former compounds. Decitabine had the strongest effect on expression at a concentration of 320 µM, while 5-fluorouracil had the highest peak at 80 µM (**Fig. 22H and K**). Thus, decitabine had a 2.9-fold, 5-fluorouracil a 3.8-fold, floxuridine a 5-fold, and 5-azacitidine an 11-fold higher quotient of RLU by OD_{max} than the reporter strain (n.c.). The ten measured concentrations of the five compounds did

not reveal a clear trend in terms of their inducing effect on *stx2* expression. In general, a stronger inducing effect was observed in the ATC group L01BC (Pyrimidine analogues) at higher compound concentrations (>20 µM). However, this observation could not be generalized, as shown by the example of floxuridine (**Fig. 22I**), where a decrease in the quotient RLU by OD_{max} was observed in the concentration range from 80 µM to 320 µM. Consistent with the initial screen, I again found very strong inducing effects among the rescreened compounds from ATC group L (Antineoplastic and immunomodulating agents), particularly for the compounds dacarbazine and streptozotocin. Dacarbazine belongs to ATC subgroup L01AX, designated as "Other alkylating agents," while streptozotocin belongs to subgroup L01AD, designated as "Nitrosoureas." While for streptozotocin (**Fig. 22N**) the strongest effect was measured at 20 µM, the same concentration which was used in the initial screen, for dacarbazine (**Fig. 22F**) a significant increase of the inducing effect on *stx2* expression was detectable at concentrations above 20 µM, with a peak at 40 µM. The measured values imply that dacarbazine exhibited an over 200-fold and streptozotocin an over 375-fold higher RLU/OD_{max} quotient than the negative control.

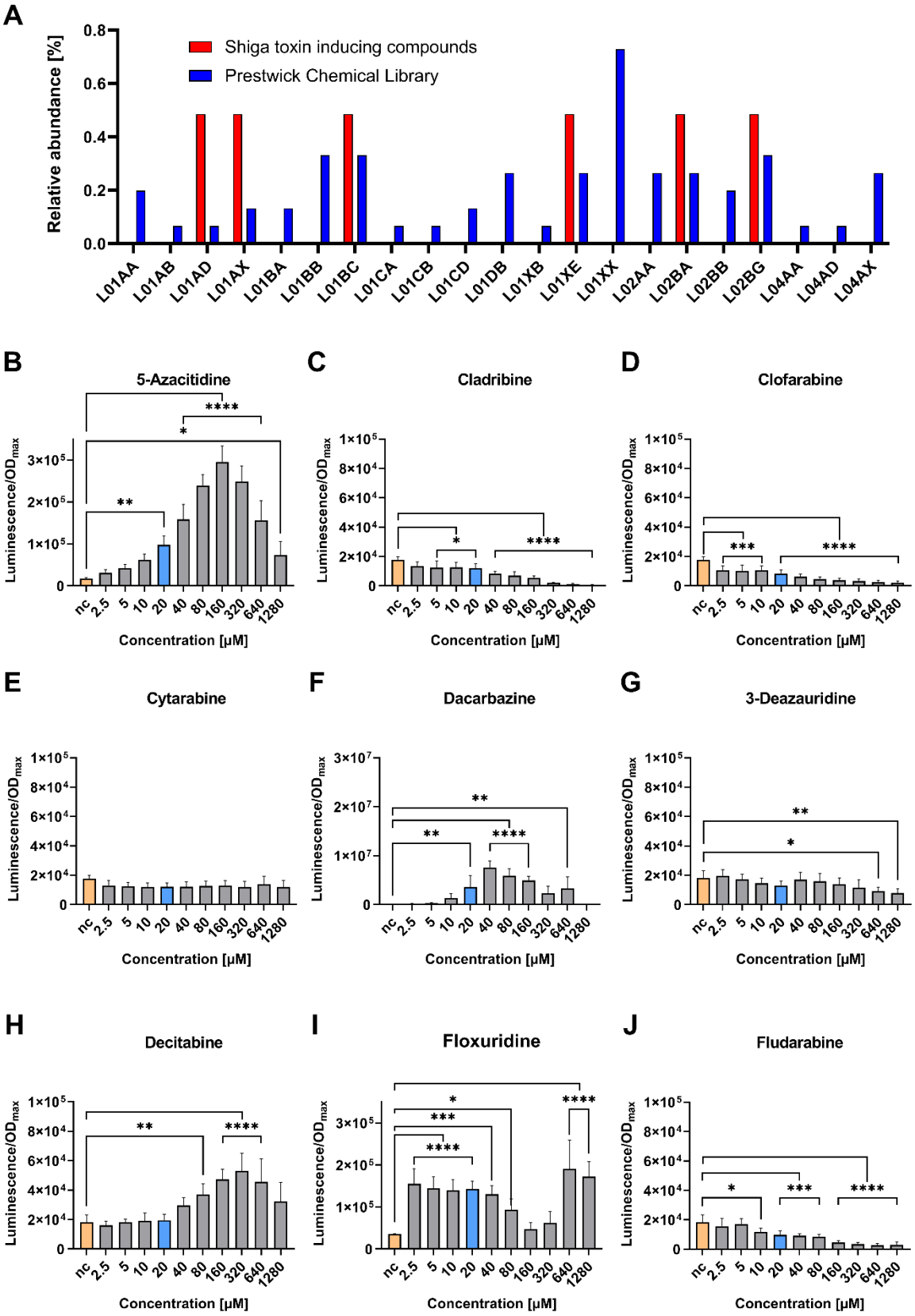
A
Relative abundance [%]
Shiga toxin inducing compounds
Prestwick Chemical Library
L01AA
L01AB
L01AD
L01AX
L01BA
L01BB
L01BC
L01CA
L01CB
L01CD
L01DB
L01XB
L01XE
L01XX
L02AA
L02BA
L02BB
L02BG
L04AA
L04AD
L04AX
B
5-Azacitidine
C
Cladribine
D
Clofarabine
E
Cytarabine
F
Dacarbazine
G
3-Deazauridine
H
Decitabine
I
Floxuridine
J
Fludarabine
Luminescence/OD max
Concentration [µM]
nc
2.5
5
10
20
40
80
160
320
640
1280

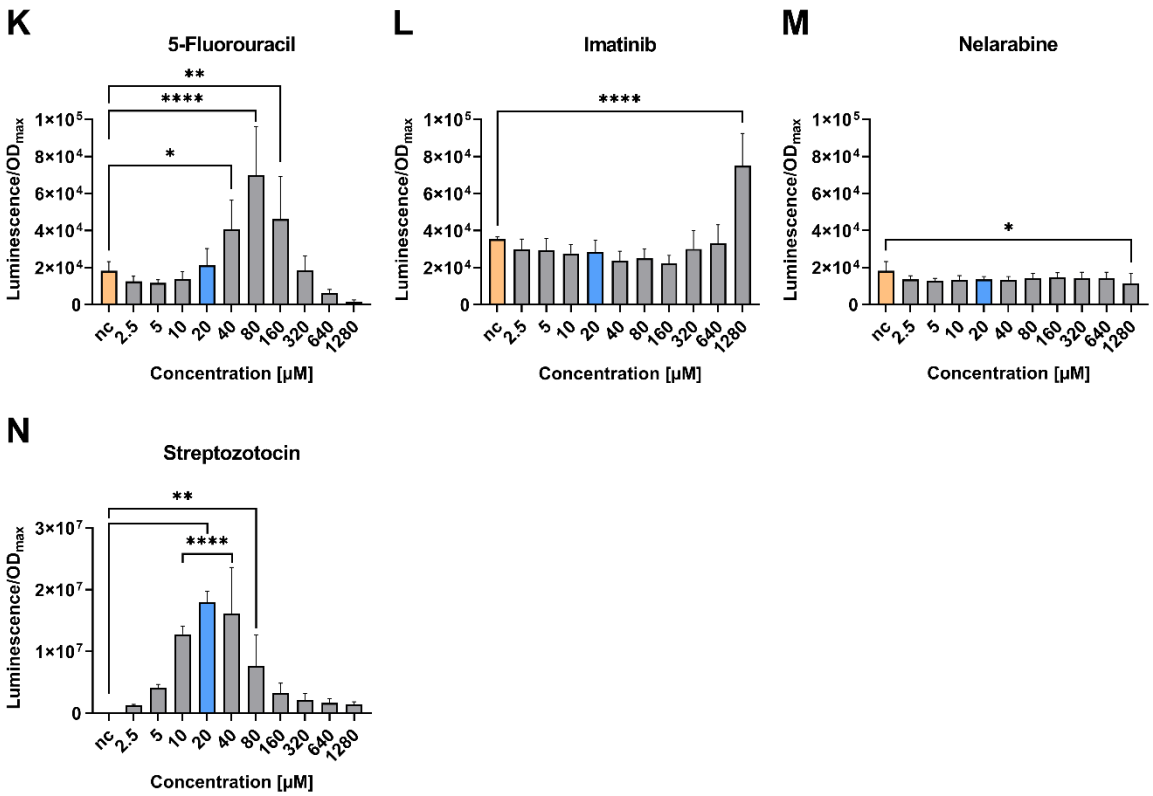

Figure 22. Effect of ATC group L compounds on stx2 induction at different concentrations. (A) Compounds with stx2 induction properties classified in ATC group L were further subdivided into the different 4th level ATC L (Antineoplastic and immunomodulating agents) subgroups (L01AA: Nitrogen mustard analogues, L01AB: Alkyl sulfonates, L01AD: Nitrosoureas, L01AX: Other alkylating agents, L01BA: Folic acid analogues, L01BB: Purine analogues, L01BC: Pyrimidine analogues, L01CA: Vinca alkaloids and analogues, L01CB: Podophyllotoxin derivatives, L01CD: Taxanes, L01DB: Anthracyclines and related substances, L01XB: Methylhydrazines, L01XE: Protein kinase inhibitors, L01XX: Other antineoplastic agents, L02AA: Estrogens, L02BA: Anti-estrogens, L02BB: Anti-androgens, L02BG: Enzyme inhibitors, L04AA: Selective immunosuppressants, L04AD: Calcineurin inhibitors, L04AX: Other immunosuppressants).The y-axis shows the relative abundance of each group in percentage. In red the relative abundance of the respective ATC L subgroup in the total of stx2-inducing compounds is shown. In comparison, the relative abundance of each ATC L subgroup in the Prestwick Chemical Library® is shown in blue. (B-N) Influence of ATC group L compounds on stx2 induction plotted as the ratio of Luminescence/ODmax (B: 5-azacitidine, C: cladribine, D: clofarabine, E: cytarabine, F: dacarbazine, G: 3-deazauridine, H: decitabine, I: floxuridine, J: fludarabine, K: 5-fluorouracil, L: imatinib, M: nelarabine, N: streptozotocin). The reporter strain was exposed to increasing concentrations (2.5 µM - 1,280 µM) of each compound. The blue bar corresponds to the concentration used in the initial screen (20 µM). The orange bar indicates RLU/ODmax of the negative control (no compound). Shown is the mean and StD of four independent experiments. Statistical analysis using one-way ANOVA followed by Dunnett multiple comparison test was performed (* $p < 0.05$, ** $p < 0.01$, *** $p < 0.001$, **** $p < 0.0001$).

4.2.5.3 Potential inhibitors of *stx2* expression

Out of the 140 stx2 active compounds, 43 were classified as potential inhibitors (section 4.2.5). For compounds in this group, I determined lower luminescence levels in the culture supernatant compared to the negative control. **Figure 23** illustrates the impact of six compounds from this group (clarithromycin, clindamycin, imipenem,

levodopa, lincomycin & metronidazole) on the reporter strain at a concentration of 20 µM, measured in the initial screen. Growth curves (**Fig. 23A**) and measured luminescence values (**Fig. 23B**) are depicted in comparison to the negative control (in grey), reporter strain without compound exposure. In **figure 23C**, the ratio of luminescence by OD_{max} (RLU/OD_{max}) is presented. Clarithromycin had the highest inhibitory effect on Stx2 in the initial screen, followed by metronidazole, clindamycin, imipenem, lincomycin and levodopa. **Figure 24** shows the ATC group distribution for the potential 43 Stx2-inhibitory compounds.

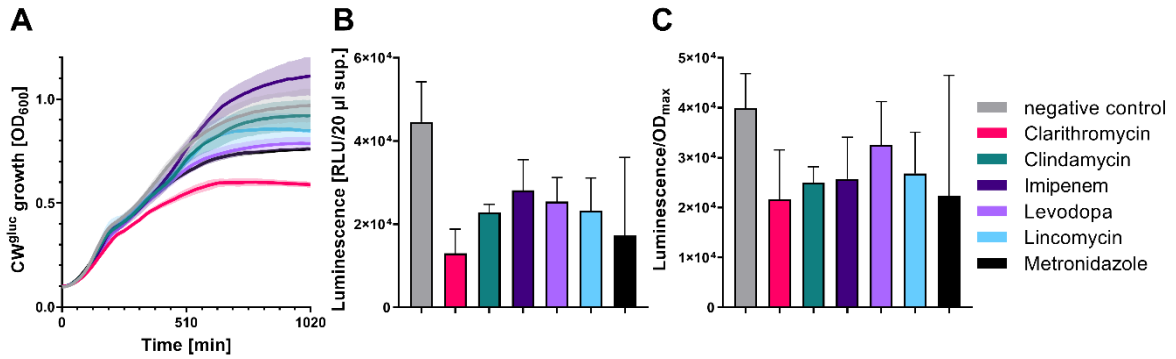

Figure 23. Inhibitory effect of compounds on stx2 expression.
Six (clarithromycin, clindamycin, imipenem, levodopa, lincomycin metronidazole) potentially stx2 inhibitory compounds from the initial screening are shown. The compounds were used at a concentration of 20 µM. The negative control, in grey, is the reporter strain CW^{gluc} without compound influence. The mean and standard deviation of 4 independent biological replicates are shown in each case. (A) Growth curves of the reporter strain exposed to each compound incubated at 37°C for 17h in a plate reader. (B) Luciferase activity measured in 20 µl supernatant shown as relative light units (RLU). (C) Ratio of the luminescence/ODmax of the respective growth curve. Shown is the mean and StD of four independent biological replicates.

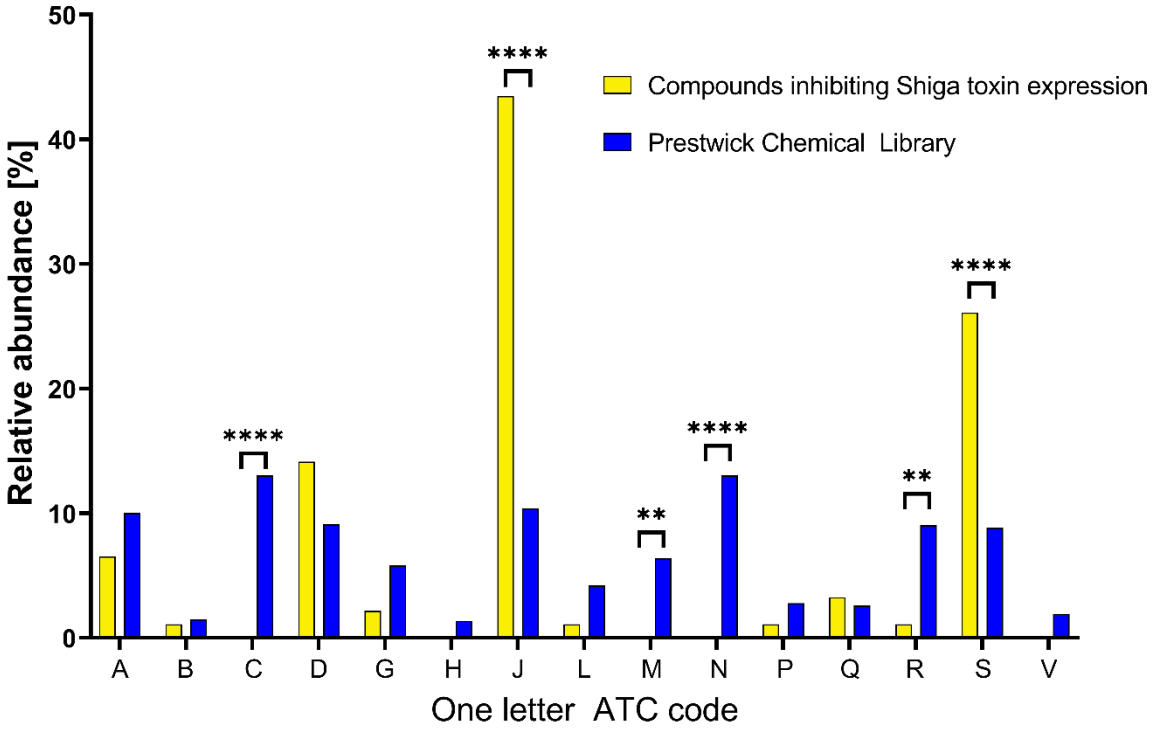

Figure 24. Relative abundance of ATC groups among *stx2* expression inhibitors compared to the Prestwick Chemical Library®.
The 43 possible inhibitors were classified into the ATC classification system. In yellow is the relative abundance of the respective ATC groups among the inhibitors. In comparison, the relative abundance of each ATC group in the Prestwick Chemical Library® is shown in blue. On the x-axis, the one letter ATC code is depicted for each ATC group. See figure 15 for group names. To determine a significant over- or underrepresentation of an ATC group between the two clusters, the Fisher's Exact Test was performed (** $p < 0.01$, **** $p < 0.0001$).

For a concentration-dependence screen of potential *stx2* expression inhibitors, compounds that led to a strong reduction in quantified luminescence, while only minimally inhibiting the reporter growth, were selected. This resulted in 6 potential *stx2* expression inhibitors: antimycin A, azithromycin, dihydrostreptomycin sulfate, efavirenz, lymecycline, and roxithromycin. In order to investigate more potential Stx2 inhibitors, we filtered the list of Stx2 active compounds for those that had an estimated intestine concentration well above > 20 µM and kept the above mentioned criteria. In the end, we had a combined list of 18 potential *stx2* expression inhibitors, 16 of which we purchased for further analysis (two were excluded due to availability issues) (**Table 13**).

The 16 compounds were diluted in DMSO for further use. With these, I tested the effect on the reporter strain at 10 different concentrations (2.5 µM – 1,280 µM) in the setup

with pre-inducing *stx2* expression by adding 25 ng/ml MitoC final concentration into the reporter strain culture (**Fig. 16**).

Table 13. Shiga toxin inhibitory compounds for concentration-dependent screen

Compound	Estimated intestine conc. in humans [µM]	Substance Class	Cellular target
Acetazolamide	375.0	Sulfonamides	Carbonic anhydrase
Antimycin A	-	Antibiotic (macrolide)	Electron transport chain (cytochrome bc1 complex)
Azithromycin	111.3	Antibiotic (macrolide)	50S ribosomal subunit
Azlocillin sodium salt	2,068.3	Antibiotic (penicillin)	Bacterial cell wall synthesis
Clarithromycin	222.8	Antibiotic (macrolide)	50S ribosomal subunit
Clindamycin hydrochloride	108.4	Antibiotic (lincosamide)	50S ribosomal subunit
Disulfiram	281.0	Aldehyde dehydrogenase inhibitor	Aldehyde dehydrogenase
Efavirenz	316.8	Non-nucleoside reverse transcriptase inhibitor	HIV-1 reverse transcriptase
Imipenem	2,227.0	Antibiotic (carbapenem)	Bacterial cell wall synthesis
Levodopa	422.6	Dopamine precursor	Dopamine receptors
Lincomycin hydrochloride	376.2	Antibiotic (lincosamide)	50S ribosomal subunit

Lymecycline	331.9	Antibiotic (tetracycline)	30S ribosomal subunit
Metronidazole	730.3	Antibiotic (nitroimidazole)	DNA synthesis
Miconazole	480.6	Antifungal	Ergosterol synthesis
Moroxidine hydrochloride	481.5	Antiviral	RNA synthesis
Sulmazole	-	Phosphodiesterase inhibitor	Phosphodiesterase

Figure 25A - P shows the 16 compounds tested for *stx2* expression inhibition. 12 out of these 16 compounds, acetazolamide, antimycin A, azithromycin, azlocillin, clarithromycin, clindamycin, disulfiram, imipenem, levodopa, lincomycin, metronidazole and moroxidine (**Fig. 25A, B, C, D, E, F, G, I, J, K, M and O**), showed an inhibitory effect on *stx2* expression in a concentration-dependent manner. The grey bars in the plots represent the respective OD_{max} values at the corresponding compound concentration. The positive control (pc) is the reporter strain grown in LB with the addition of 25 ng/ml MitoC. The red line depicts the produced luminescence in percent calculated as a ratio of luminescence/OD_{max} from the compound at the indicated concentration divided by luminescence/OD_{max} from the positive control. 100% means a Luminescence/OD_{max} ratio equal to the positive control and the closer it gets to 0%, the lower the quotient of luminescence versus OD_{max} of the respective compound compared to the positive control is. Azithromycin (2% luminescence production left), clarithromycin (9% luminescence production left) and imipenem (14% luminescence production left) had a very strong inhibitory effect on *stx2* expression already at 2.5 µM, while the growth of the reporter strain was only slightly affected (**Fig. 25A, E and I**).

Azlocillin (7% – 0.3% luminescence production left) and clindamycin (10% – 0.5% luminescence production left) had the greatest inhibitory effect at 10-40 µM. At this concentration, growth of the reporter strain was not affected by clindamycin but started to get reduced by azlocillin (**Fig. 25D and F**). Acetazolamide, antimycin A, disulfiram, levodopa, lincomycin, metronidazole and moroxidine showed concentration-

dependent inhibition of *stx2* expression (**Fig. 25A, B, G, J, K, M and O**). The higher the compound concentration got, the more *stx2* expression was inhibited. The inhibitory influence of disulfiram on *stx2* expression increased gradually and reached 100% inhibition at a concentration of 160 µM (**Fig. 25G**). For levodopa, the strongest reducing effect on *stx2* expression was at the highest concentration measured (1,280 µM), were only 3% luminescence production compared to the pc was left (**Fig. 25J**). For lincomycin the situation was very similar but with strong inhibition already at lower concentrations. Maximum inhibition of *stx2* expression was reached at 80 µM, were not even 1% luminescence production compared to the pc was left (**Fig. 25K**). Compared to the previous three, acetazolamide, antimycin A, metronidazole and moroxidine never reached a full inhibition (**Fig. 25A, B, M and O**). The strongest inhibitory effect on stx2 expression for all four compounds was reached at the highest measured concentration (1,280 µM). Acetazolamide had 10%, antimycin A had 2%, metronidazole had 13% and moroxydine had 24% luminescence production compared to the pc left. All four had in common, that they only slightly affect the growth of the reporter strain. Efavirenz, lymecycline, miconazole and sulmazole did not show clear signs of stx2 expression inhibition or gave no clear phenotype regarding reporter strain growth (**Fig. 25H, L N and P**).

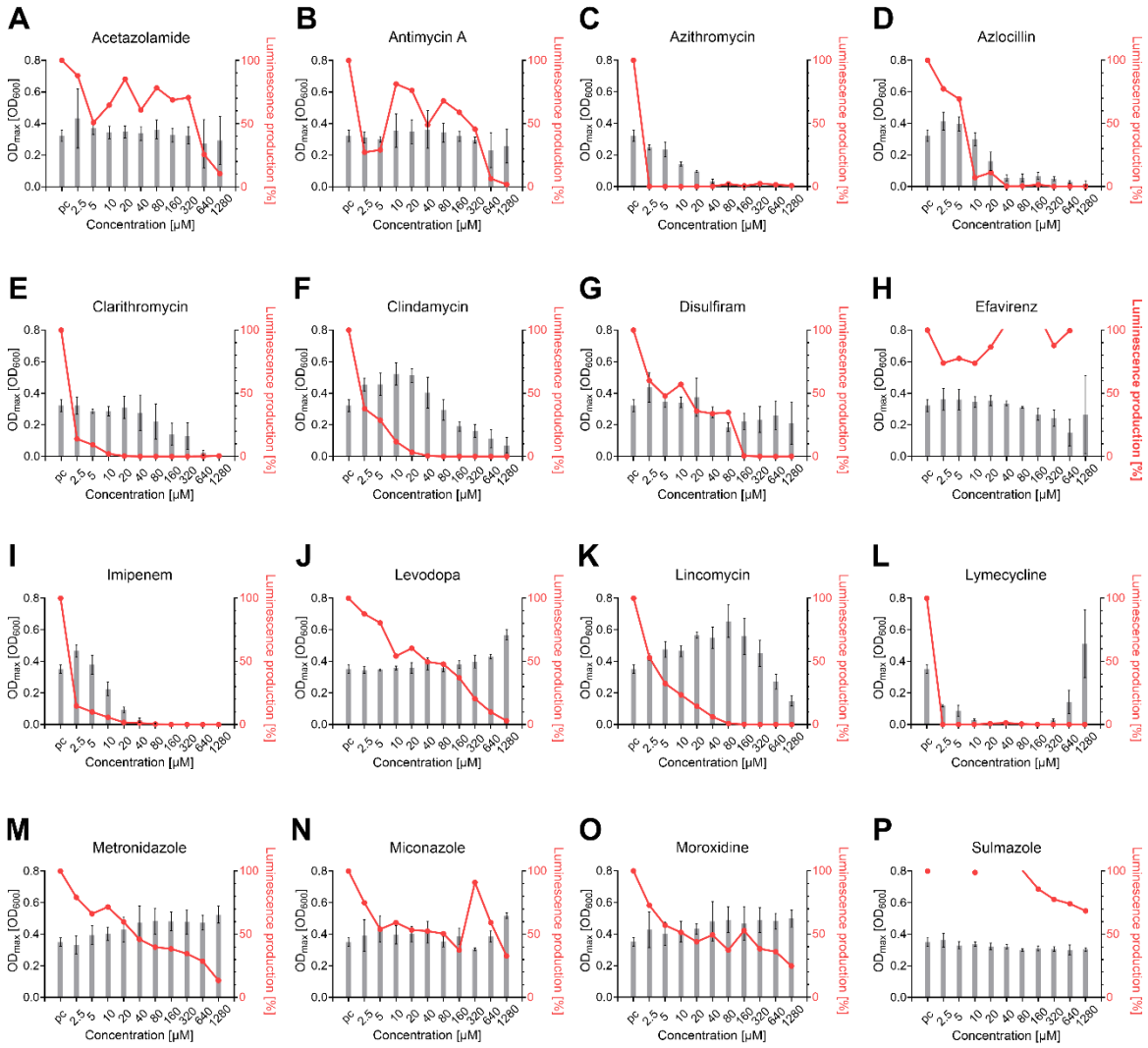

Figure 25. Inhibitory effect of compounds on the *stx2* expression at different concentrations. Panels (**A-P**) show in gray bars the OD_{max} (left y-axis) of the growth curves of the reporter strain grown in LB containing 25 ng/ml MitoC and the corresponding concentration (2.5 µM - 1,280 µM) of the indicated compound. In red, the percentage of luminescence production is indicated (right y-axis). It is calculated by dividing the RLU/OD_{max} from each compound at each concentration with the RLU/OD_{max} of the positive control. The x-axis shows the positive control (pc) and the 10 different compound concentrations. The reporter strain incubated in LB with 25 ng/ml MitoC is the pc. The 16 compounds used are (**A**) acetazolamide, (**B**) antimycin A, (**C**) azithromycin, (**D**) azlocillin, (**E**) clarithromycin, (**F**) clindamycin, (**G**) disulfiram, (**H**) efavirenz, (**I**) imipenem, (**J**) levodopa, (**K**) lincomycin, (**L**) lymecycline, (**M**) metronidazole, (**N**) miconazole, (**O**) moroxydine and (**P**) sulmazole. Shown is the mean and StD of four independent experiments. For the workflow of the assay see figure 16.

The corresponding luminescence/OD_{max} ration for all the 16 measured compounds at 10 different concentrations (2.5 µM– 1,280 µM) can be seen in **figure 26A - P**. The blue bar in each plot marks the 20 µM concentration used in the initial screen. The light red bar in each plot is the positive control, the reporter strain under the influence of 25 ng/ml MitoC.

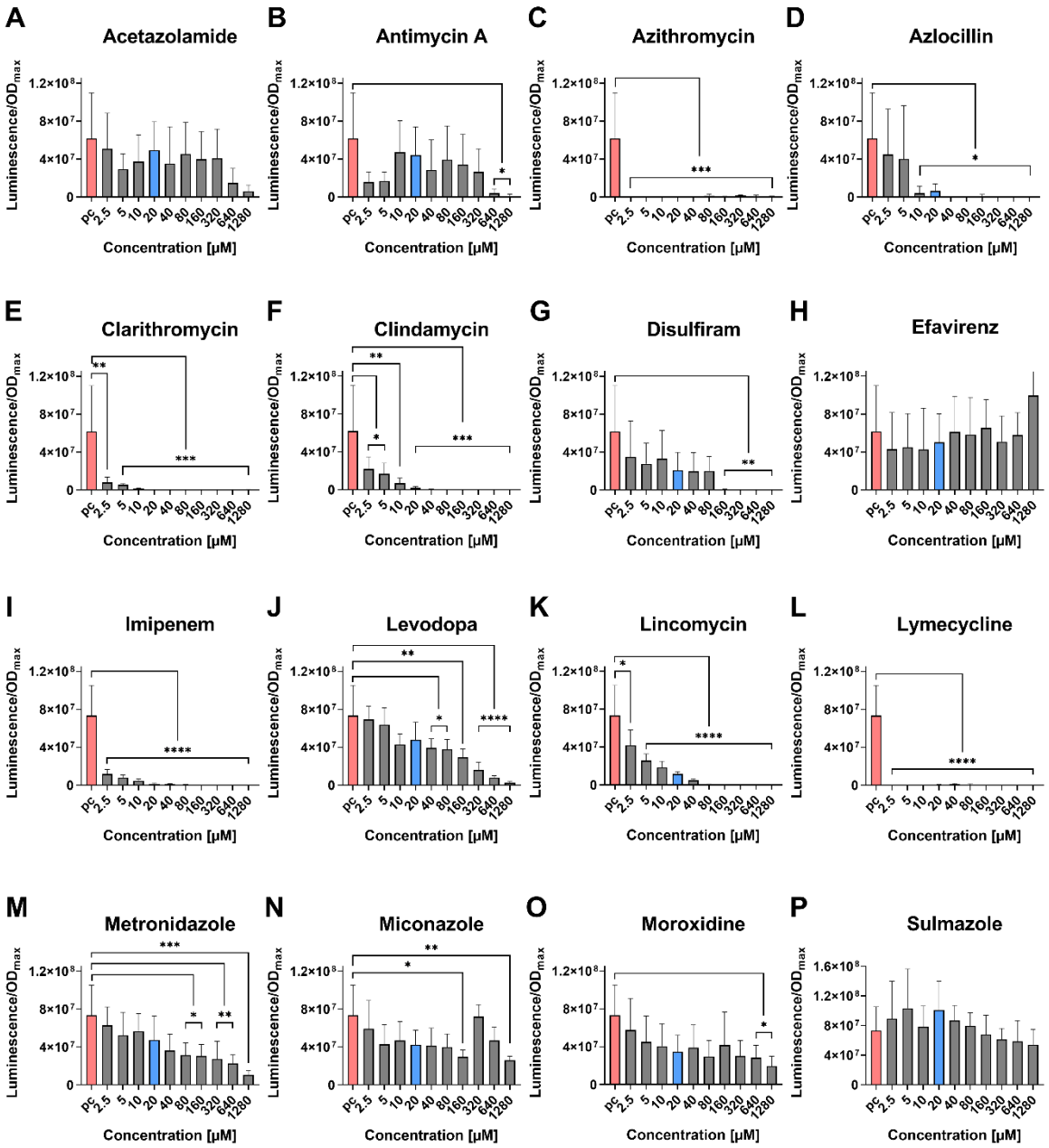

Figure 26. Inhibitory effect of compounds on *stx2* expression at different concentrations as Luminescence/OD$_{max}$.

(**A-P**) Influence of inhibitory compounds on *stx2* expression as depicted by the ratio of Luminescence/OD$_{max}$ (**A**) acetazolamide, (**B**) antimycin A, (**C**) azithromycin, (**D**) azlocillin, (**E**) clarithromycin, (**F**) clindamycin, (**G**) disulfiram, (**H**) efavirenz, (**I**) imipenem, (**J**) levodopa, (**K**) lincomycin, (**L**) lymecycline, (**M**) metronidazole, (**N**) miconazole, (**O**) moroxydine and (**P**) sulmazole). The reporter strain was exposed to 25 ng/ml MitoC and increasing concentrations (2.5 µM - 1,280 µM) of each compound. The blue bar corresponds to the concentration used in the initial screen (20 µM). The red bar indicates RLU/OD$_{max}$ of the positive control (pc, only MitoC). Shown is the mean and StD of four independent experiments. Statistical analysis using one-way ANOVA followed by Dunnett multiple comparison test was performed (* $p < 0.05$, ** $p < 0.01$, *** $p < 0.001$, **** $p < 0.0001$).

4.2.6 Compounds that strongly inhibit cell growth

Looking at the initial screen, focusing only on cell growth, I found some antibacterial compounds, such as ceftazidime (**Fig. 10**) and ciprofloxacin which resulted in a strong growth reduction of the reporter and therefore low luminescence values. Ciprofloxacin is an antimicrobial known to induce *stx2* expression (Walterspiel *et al.*, 1992; Bielaszewska *et al.*, 2012a; Wong *et al.*, 2012; Mühlen and Dersch, 2020). This compound (as well as others known to induce *stx2* expression) suppressed growth of the reporter strain at the concentration of 20 µM used in the screen. This might have led to false classification of these compounds (either no hit or possibly inhibitors). To test if these compounds would have an effect on the reporter at lower concentration, I retested 19 representative compounds from the library that inhibited growth at lower concentrations (0.04 µM, 0.16 µM, 0.267 µM & 20 µM) (**Table. 14**). **Figure 27A** shows the OD_{max} values of the respective antibiotics for all four measured concentrations. A clear increase in the OD_{max} value at lower compound concentrations was observed. Ciprofloxacin led to an OD_{max} value below OD_{600} of 0.4 even at the lowest concentration tested. In general, the tested antibiotics can be divided into two groups. The first group greatly reduces the growth of the reporter strain even at the low concentrations, while the second group does not do so until 20 µM. Also, in **figure 27B** where the ratio of RLU by OD_{max} is shown, the division into these two groups can be detected, although here the separation is not as clear. Antibiotics that strongly inhibit the growth of the reporter at lower concentrations (resulting in lower OD_{max}) show a greater ratio RLU/OD_{max}. At lower concentrations, most of the compounds showed a *stx2* inducing effect. Some of these compounds could be found in the Hit list, both as inducing or inhibiting compounds. Trimethoprim, for example, was not found in the Hit list but clearly showed an inducing effect. The compounds that were included in the Hit list and re-tested here are indicated with an (*) in **Suppl. Table 1**. These results highlight the importance of re-testing compounds that strongly inhibit cell growth.

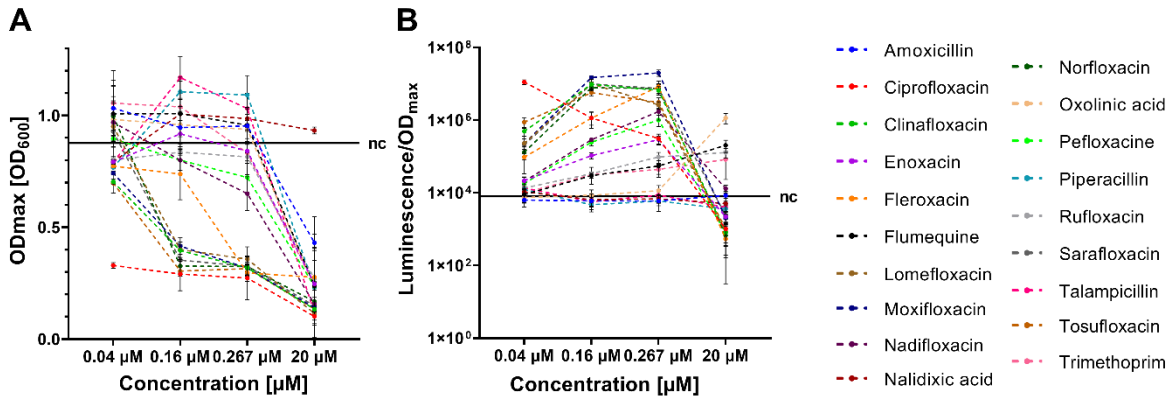

Figure 27. Impact of antibiotics on bacterial growth and activity at lower compound concentrations.

19 antibiotics (contained in the Prestwick Chemical Library®) were tested at four concentrations (0.04 µM, 0.16 µM, 0.267 µM & 20 µM). Each antibiotic (ABX) is shown in a different colour. (**A**) OD_{max} value of each growth curve of the reporter strain at the four different ABX concentrations. (**B**) Ratio of Luminescence in 20 µl supernatant divided by OD_{max} (RLU/OD_{max}) for the different ABX and concentrations. Mean values and standard deviation are plotted and consist of 4 independent replicates.

Table 14. List of antibiotics re-screened at lower concentrations (< 20 µM)

Chemical name	Substance class	Cellular target
Ciprofloxacin hydrochloride monohydrate	Fluoroquinolone	Bacterial gyrase
Oxolinic acid	Quinolone	Bacterial gyrase
Flumequine	Quinolone	Bacterial gyrase
Trimethoprim	Dihydrofolate reductase inhibitors	Dihydrofolate reductase
Norfloxacin	Fluoroquinolone	Bacterial gyrase
Lomefloxacin hydrochloride	Fluoroquinolone	Bacterial gyrase
Sarafloxacin	Fluoroquinolone	Bacterial gyrase
Amoxicillin	Penicillin's	Inhibits bacterial cell wall synthesis
Nadifloxacin	Fluoroquinolone	Bacterial gyrase
Pefloxacin	Fluoroquinolone	Bacterial gyrase
Tosufloxacin hydrochloride	Fluoroquinolone	Bacterial gyrase
Moxifloxacin	Fluoroquinolone	Bacterial gyrase and topoisomerase IV

Rufloxacin	Fluoroquinolone	Bacterial gyrase
Fleroxacin	Fluoroquinolone	Bacterial gyrase
Enoxacin	Fluoroquinolone	Bacterial gyrase
Nalidixic acid sodium salt	Quinolone	Bacterial gyrase
Piperacillin sodium salt	Penicillin's	Inhibits bacterial cell wall synthesis
Clinafloxacin	Fluoroquinolone	Bacterial gyrase
Talampicillin hydrochloride	Penicillin's	Inhibits bacterial cell wall synthesis

4.3 Analysis of faecal samples from patients of the 2011 HUSEC outbreak in Germany

In the final part of my thesis, we focus on the study of patient samples that were collected during the large outbreak of haemolytic uremic syndrome-associated *Escherichia coli* (HUSEC) in Germany in 2011. The focus of the investigation was to process and analyse metadata and microbiota datasets from the study. Subsequently, the intent was to correlate specific microbiota signatures and the collected metadata to the patient's risk to develop HUS in the course of gastrointestinal HUSEC infection. Sample preparation and metadata collection was completed at the start of this thesis and was done in part by former group members. The analyses presented here were performed by me in collaboration with Dr. Abilash Chakravarthy Durai Raj.

The HUSEC outbreak occurred in northern Germany during May and June 2011, was characterized by significant expansion, with approximately four thousand persons reported as infected with HUSEC. Among hospitalized patients, a substantial proportion were diagnosed with HUS, and tragically, 53 died from the infection (Rki, 2011). The origin of the pathogen was linked to contaminated fenugreek germs (Food and Authority, 2011; King *et al.*, 2011). The disease was exacerbated by the emergence of an novel *E. coli* pathotype, known as EHEC O104:H4 or HUSEC, which encodes both *stx2* and the AAF/I type fimbriae of enteroaggregative *E. coli* (EAEC) (Karch *et*

al., 2012), facilitating its close attachment to intestinal epithelial cells (Bielaszewska *et al.*, 2011).

4.3.1 Patient distribution and collected metadata

The dataset was generated from faecal samples collected from patients from Hamburg (N=201), which experienced symptoms of a GI infection. As a control, stool samples were collected from healthy individuals (N=20). **Figure 28** shows the patient distribution among the different disease groups. Out of the 201 patients (118 female, 83 male), 149 were determined *stx2* positive by PCR (STEC+), while 52 patients were negative (STEC-). The latter potentially suffered from a GI disease of different unknown aetiology (no EHEC/HUS). Of the 149 Stx2 positive patients 79 developed HUS (HUS), 70 did not (EHEC).

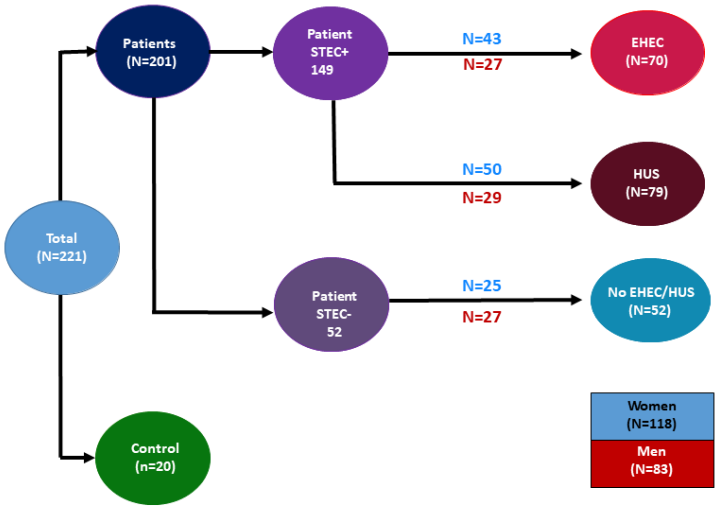

Figure 28. Overview of patient groups in HUSEC study.
201 Patients were hospitalized during the 2011 haemolytic uremic syndrome (HUS)-associated *Escherichia coli* (HUSEC) outbreak in northern Germany. 149 tested positive for *stx2* encoding *E. coli* (STEC+). 70 of these had only gastrointestinal EHEC (enterohaemorrhagic *E. coli*) infection, while 79 patients developed HUS. 52 patients were symptomatic, but no STEC was detected (no EHEC/HUS; infection/inflammation of unknown aetiology) The 20 controls are faecal samples of healthy individuals from a different part of Germany. This figure was created by Dr. Abilash Chakravarthy Durai Raj

Besides the STEC status of the patient's, other parameters like faecal colour and texture were recorded (faecal colour: bloody, green, normal and control; faecal texture: firm, soft, liquid and control). Moreover, microbiota composition was analysed by 16S rRNA amplicon sequencing. **Figure 29** gives an overview over the relative abundance

of different bacterial taxa at phylum level for each patient. The three outer rings show the metadata associated with each individual, from inside to outside the disease status, the faecal colour and faecal texture. We observed that Firmicutes was the most prevalent phyla in most of the samples across the disease conditions while Proteobacteria were predominantly found in patients classified as EHEC or HUS.

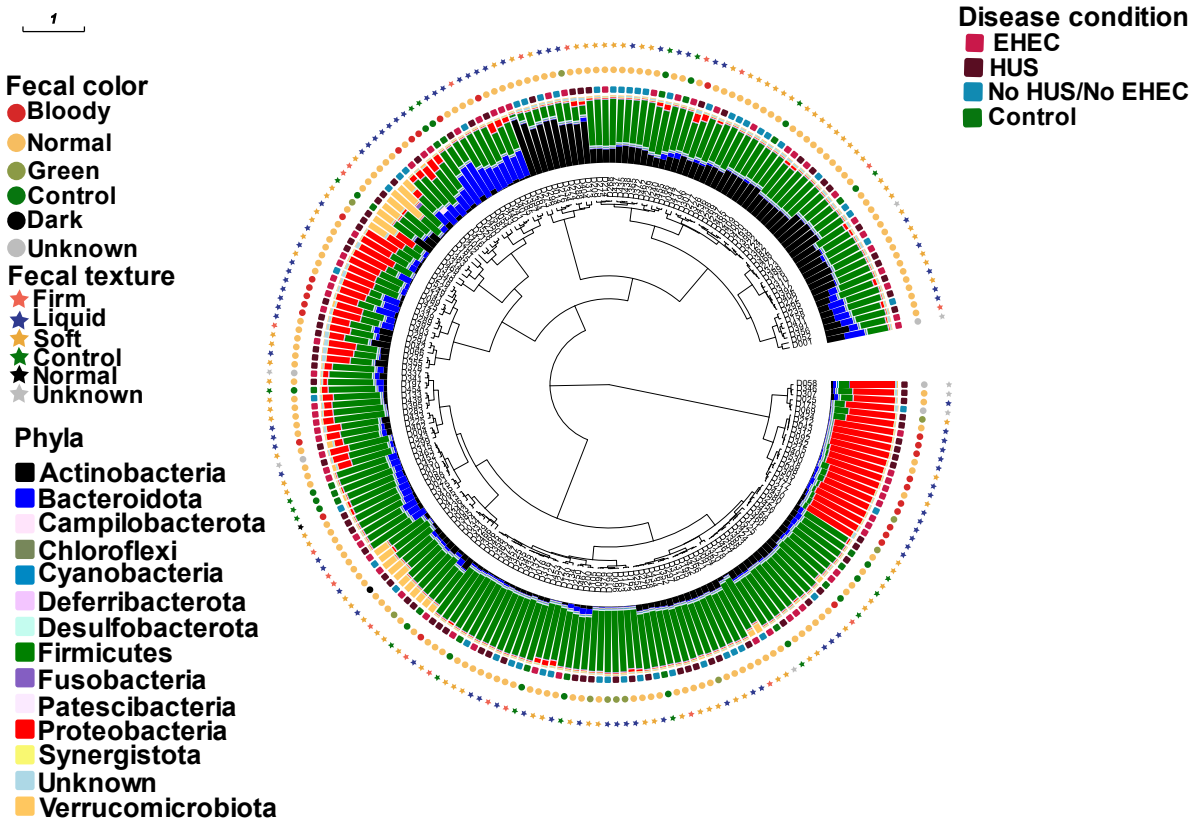

Figure 29. Phylum-level microbiome composition in faecal samples of individual patients and controls in combination with metadata.
Phylum-level faecal microbial community composition is shown as a circular stacked barplot. A distance matrix was obtained from the normalized phyla profile using the function dist() from stats package in R. Hierarchical clustering was done on this distance matrix using hclust() function from stats package in R by setting the argument method ="ward.D2". Then, a phylogenetic tree was created using as.phylo.hclust function from ape packages using the hierarchical cluster as input. The outer rings around it represent faecal texture, faecal colour, and disease condition (from outside to inside) from individual patient samples. This figure was created by Dr. Abilash Chakravarthy Durai Raj

4.3.2 LEfSe analysis of the microbiome data

We first performed linear discriminant analysis effect size (LEfSe, Segata *et al.*, 2011) analysis comparing healthy control samples versus STEC-positive (EHEC + HUS group) from the HUSEC study to identify potential microbiome members as biomarkers facilitating the infection (**Fig. 30**). Healthy individuals had the orders *Bifidobacteriales*

as well as several orders of the class *Clostridia* (*Christensenellales*, *Clostridia_UCG_014*, *Monoglobales* & *Oscillospirales*) overrepresented compared to STEC-positive patients. From a different study of STEC infected patients, it is already reported that these individuals have a lower abundance of *Bifidobacteriales* as well as *Clostridiales* (Gigliucci *et al.*, 2018). The STEC-positive patients had an overrepresentation of the orders *Enterobacterales* as well as *Staphylococcales* (class *Bacilli*). In the previous mentioned study, they found that the order *Lactobacillales* (class *Bacilli*) was dominating in the patient group.

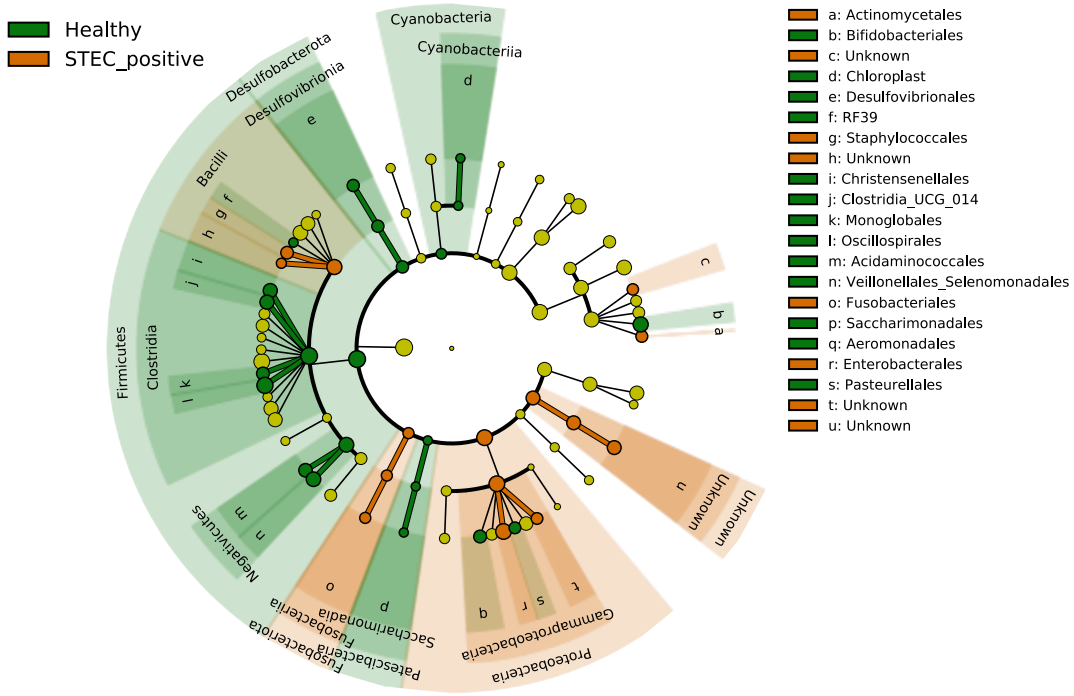

Figure 30. Faecal microbiome biomarkers correlating with STEC infection or healthy patients. LEfSe analysis was performed to identify taxa that are significantly enriched in the faecal microbiota of STEC pos. patients compared to healthy controls. We considered bacterial taxa at different taxonomic levels with a log LDA score ≥ 1 and a Kruskal-Wallis test between classes ≤ 0.05 as significantly enriched in either group (healthy: green, STEC: brown; in the cladogram).

Next, we performed LEfSe analysis with the EHEC samples against the HUS samples to detect potential bacterial families or genus that drive or prevent the development of HUS (**Fig. 31**). In the EHEC patient group *Lachnospiraceae_UCG_008* and *Prevotellaceae* were more abundant than in the HUS group. These bacterial families are known to produce short chain fatty acids like butyrate and acetate. It was previously

reported that the production of short chain fatty acids has *in vitro* and *in vivo* an inhibitory effect on EHEC growth as well as Stx production (Takahashi *et al.*, 2004a; Carey *et al.*, 2008a). The patients with HUS had members of the class *Bacilli* overrepresented compared to the EHEC group. One family out of these members is *Enterococcaceae* with the genus *Enterococcus*. *Enterococcus faecalis* has been reported to induce EHEC virulence in an *in vitro* cell culture setting (Martins *et al.*, 2022a).

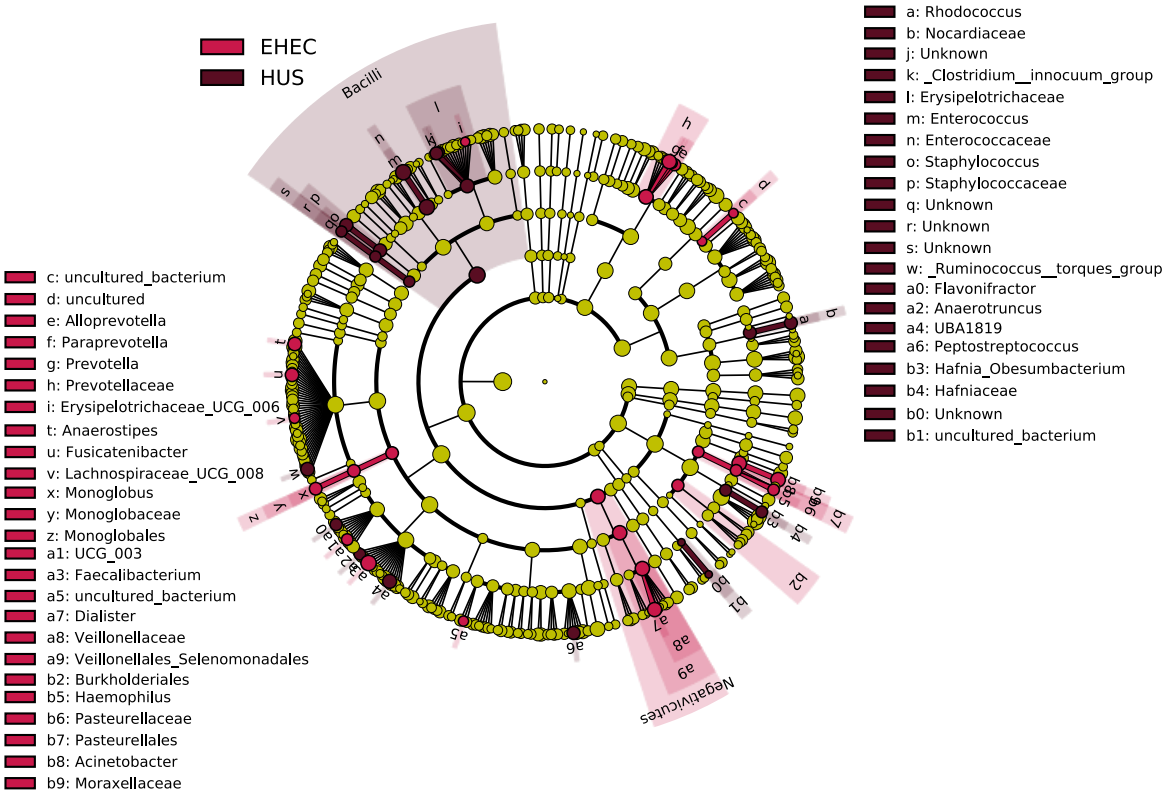

Figure 31. Faecal microbiome biomarkers correlating with HUS development or EHEC infection. LEfSe analysis was performed to identify taxa significantly enriched in the faecal microbiota of STEC pos. patients (EHEC) compared to STEC pos. patients developing HUS (HUS). We consider bacterial taxa at different taxonomic levels with a log LDA score ≥ 1 and a Kruskal-Wallis test between classes of ≤ 0.05 as significantly enriched in either group (EHEC: red, HUS: dark red; in the cladogram).

4.3.3 Investigating the potential impact of Colibactin on the development of HUS

In a recently published paper (Silpe *et al.*, 2022) the bacterial toxin colibactin was linked to the induction of prophages including *stx2* phages. Colibactin (*clbB*) is a known

genotoxin encoded by the *pks* gene island (Dougherty and Jobin, 2021) and widely distributed among members of *Enterobacteriaceae* (Putze *et al.*, 2009). It was reported that *E. coli* harbouring the *pks* gene island have a strong impact on the microbial diversity at day 35 in mice, leading to lower levels of Firmicutes (Tronnet *et al.*, 2020).

We hypothesized that, colibactin expression by other members of the microbiota during EHEC/ HUSEC infections could increase the patient's risk developing HUS due to higher intestinal Stx2 levels. We designed a quantitative PCR assay to measure the *clbB* gene copies in the first taken faecal sample of the patients from the HUSEC outbreak and the healthy controls. ClbB is a type 1 polyketide synthase encoded in the *pks* gene island. To quantify total *E. coli* loads in the samples, we determined housekeeping gene copies of *uidA*. For *uidA* copies, we found significant differences between control and the EHEC group (p-value 0.01), while there was no significant difference between the control and HUS group (**Fig. 32A**). **Figure 32B** shows the *clbB* copies per µl for the three different groups (control, EHEC & HUS). There was a significant difference between the control and the HUS group (p-value 0.05) but no significant different in the *clbB* copies between the control and EHEC group. No significant difference in *clbB* copies per µl was found between the EHEC and HUS disease groups. For all three groups (control, EHEC and HUS), all the tested samples had detectable *uidA* loads (**Fig. 33A**). 31.6% of control samples had detectable *clbB* loads. 45.7% (32 patients out of 70) of patients in the EHEC group had detectable *clbB* loads, whereas this value was 55.7% (44 patients out of 79) in the HUS group (**Fig. 33B**). These results indicate that the abundance of the *clbB* gene could increase the risk of developing HUS but cannot be the sole explanation for it.

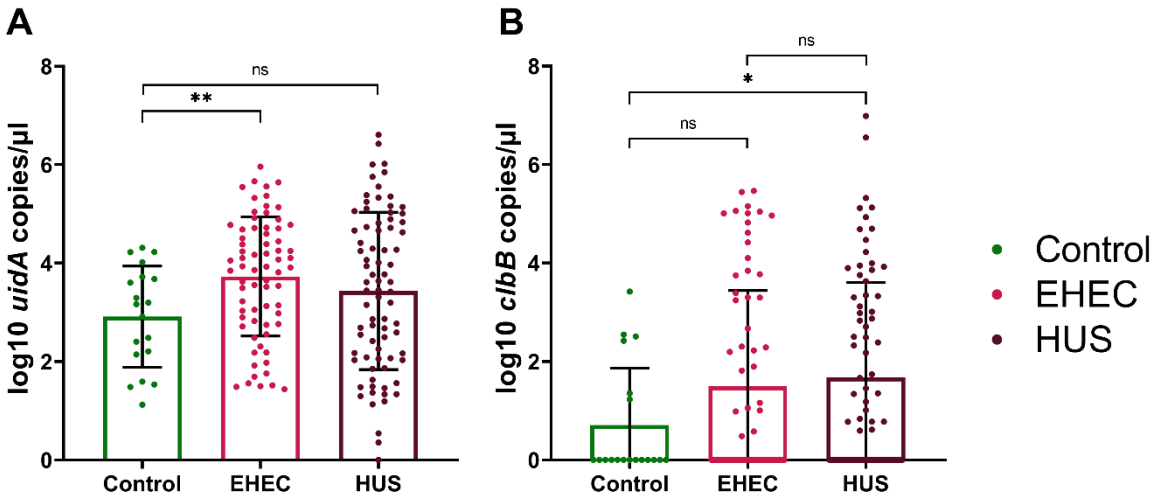

Figure 32. Abundance of *uidA* & *clbB* gene copies among patients.
Faecal DNA extracted from samples of healthy individuals and the two patient groups EHEC and HUS were tested via quantitative PCR for *uidA* (as a *E. coli* housekeeping gene) and *clbB* (test for the colibactin containing *pks* island). The logarithmic gene copy number per µl of extracted DNA of the respective gene, (**A**) *uidA*, (**B**) *clbB*, per patient is indicated, divided into the three disease groups. Mann-Whitney test was performed as statistical analysis (* $p < 0.05$, ** $p < 0.01$).

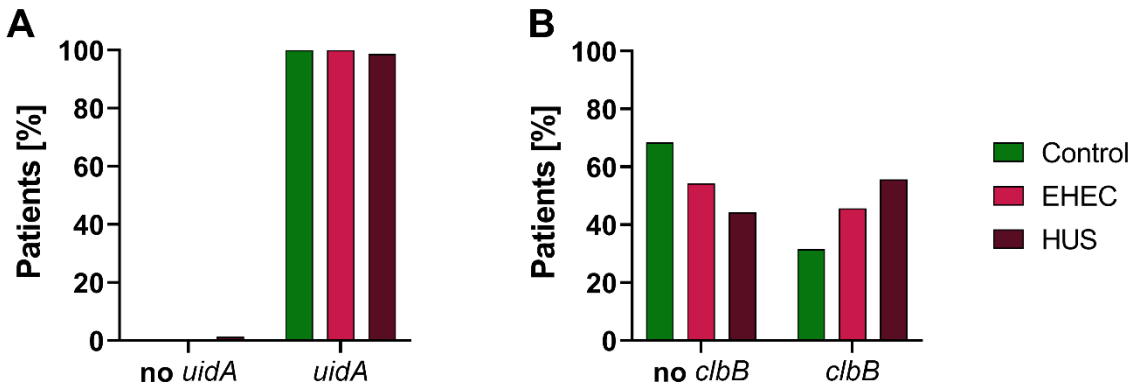

Figure 33. *uidA* and *clbB* positive patients among the tested samples.
Percentage of samples from each group in which (**A**) *uidA* or (**B**) *clbB* was detected. Percent of patients who were *uidA*/*clbB* negative or positive in quantitative PCR divided into the three groups control, EHEC and HUS. The y-axis indicates the percentage of patients.

5. Discussion

Enterohemorrhagic *Escherichia coli* is a food-borne human pathogen, which is involved in many outbreaks worldwide, leading to acute diarrhoea and haemorrhagic colitis. The appearance of new hybrid strains, harbouring virulence factors from different *E. coli* pathotypes have led to an increased fatality rate during outbreaks (Santos *et al.*, 2020; Pokharel, Dhakal and Dozois, 2023). One major virulence factor is the prophage encoded *stx*2, which causes life-threatening complications such as HUS (Ogura *et al.*, 2015). The lack of a causal therapy for HUS patients and the poor knowledge of risk factors leading to HUS development, underline the need for further research elucidating these questions (Orth *et al.*, 2008).

In this thesis we have analysed the effect of human-targeted drugs on the expression of *stx2*, as well as possible microbial signatures related to HUS and the link between colibactin and the risk of developing HUS from samples obtained from the HUSEC outbreak in Germany in 2011.

5.1 Important reporter strain features and assay parameters

The development of reporter strains to study virulence factors facilitates working under safe laboratory conditions (Bumann and Valdivia, 2007; Vannini *et al.*, 2012; Sukumar *et al.*, 2014). The key innovation of CW^{gluc} lies in its ability to accurately mimic the release kinetics of Stx2 from *E. coli* while providing safety, ease of use, scalability, and high sensitivity (Koeppel *et al.*, 2021). Other Stx2 reporter strains have successfully utilised a wide variety of reporter genes that replace the *stx2* gene to allow toxin expression studies without relying on high biosafety level (BSL-3) facilities (Kimmitt, Harwood and Barer, 2000b; Shimizu *et al.*, 2011; Nowicki *et al.*, 2016). For example, a beta-galactosidase reporter was used by Kimmitt *et al*. to analyse *stx2* inducing antimicrobial agents. The blue/ white colony screening is limited in its sensitivity, while the beta-galactosidase activity assay lacks the needed scalability. The benefit is, that both readouts are well known and cheap. Nowicki *et al*. used a green fluorescent protein Stx2 reporter to evaluate the *stx2* inhibiting potential of plant derived small molecules. While with this reporter single cell analysis is possible, it lacks the Stx2 release kinetics upon prophage induction. A bioluminescent reporter, utilizing the

luxCDABE genes of *Photorhabdus luminescences* was used by Shimizu *et al.* to examine the expression profile of Stx2 when in contact with intestinal epithelial cells and macrophages. This reporter mimics the expression pattern of *stx2* well but for that a plasmid is needed in the bacterial cell to have the necessary genes available. All these reporters have drawbacks for our application needs in terms of scalability, dynamic range, and the visualisation of natural kinetic patterns of Stx2 release. The newly created Stx2 reporter CW^{gluc} does have some drawbacks too. Since we use a luciferase as reporter gene, a substrate, in this case coelenterazine, is needed for the luminescence readout. This requires an extra step during the assay to avoid chemical interference during the initial growth. Another drawback compared to some other reporters, even though irrelevant for our application purposes, is that no single cell analysis is possible.

5.1.1 Establishment of a high-throughput screening system

In order to standardize the screening to systematically analyse the effect of small compounds on *stx2* expression, growth conditions as well as *stx2* readout had to be stablished. I optimized the growth of the reporter strain by varying starting cell density (OD), culture volumes, incubation times and compound concentrations (**Fig. 5, 6 and 7**). Adjusting the luciferase readout assay was also necessary to obtain a reproducible and standardized detection method. Several concentrations of MitoC were tested (**Fig. 6 and 7**). Stimulation of the reporter strain with 500 ng/ml MitoC resulted in a high increase in luminescence in the culture supernatant (**Fig. 7**) and was therefore selected as positive control for the screen. It is well established that MitoC is an effective inducer for *stx2*-encoding prophages (Aertsen, Faster and Michiels, 2005; Filipiak, Łoś and Łoś, 2020). Our selected MitoC concentration achieved one of the highest measured luminescence signals in the screen, proving the high induction potential for *stx2* by MitoC. The chosen concentration is lower than the usual concentration used (1 µg/ml) to induce prophages, but as Filipiak *et al*. pointed out the susceptibility and prophage induction outcome can vary depending on the *E. coli* as well as the prophage carrying *stx2* (Łoś *et al.*, 2009; Filipiak, Łoś and Łoś, 2020). We achieved with our C600 *E. coli* background and the *stx2*-encoding prophage 933W the best results for our assay with the 500 ng/ml MitoC.

In our negative control we observed a luminescence signal, even though no compound was added (**Fig 7**). We saw that even without MitoC stimulation, an increase in luminescence could be detected in the culture supernatant. We attributed this effect to background reporter gene expression during bacterial growth. Reportedly, spontaneous prophage induction has been observed to occur within a subset of bacterial population (Shimizu, Ohta and Noda, 2009). Nevertheless, spontaneous induction occurs at a low frequency (Loś *et al.*, 2012). The background luminescence was low enough, especially in contrast to our positive control. Due to this background induction of the reporter strain, subtle inducing effects of compounds being tested in the reporter assay were neglected.

We included the growth behaviour (OD_{max}) under the influence of the different compounds in our evaluation on the inducing potential of each compound. This was an important parameter since it helped us compare the measured luminescence signals and set these values in relation to biomass, which stands for the potential to produce the luciferase. The downside of this approach was, that compounds greatly reducing growth could give misleading results (**Fig. 27**).

All in all, I was able to establish a high-throughput assay to systematically analyse the effects of small compounds on *stx2* expression employing the Stx2 reporter strain CW^{gluc}.

In terms of future implications, the opportunity to apply the reporter CW^{gluc} for HTS opens up possibilities for further research on host and microbial factors as well as compounds altering *stx2* expression and potential therapeutic interventions (Mühlen and Dersch, 2020; Mengistu and Mengesha, 2023). This is particularly relevant as HTS's play an essential role in the development of new drugs, enabling rapid screening of compound libraries for inhibitors of Stx2 or identification of bacterial virulence factors involved in toxin production (Aheme, McDonald and Workman, 2002).

5.2 Human-targeted drugs influencing *stx2* expression

Our study provides an insight into the inducing properties of a broad range of compounds on the expression of *stx2*. Many compounds are analysed for the first time in this context. The screen of the Prestwick Chemical Library® identified a range of chemical compounds inducing *stx2* expression, while others had an inhibitory effect. A total of 161 primary hits were detected. The most prominent ATC classification system group among the hits is Group J (Anti-infectives for systemic use), which accounts for 35% of Stx2 active substances (**Fig. 15**). This is not surprising, as most antibiotics fall into this group. Antibiotics have previously been linked to both induction and inhibition of *stx2* expression, emphasising their dual nature in toxin regulation (McGannon, Fuller and Weiss, 2010). In addition, our study highlights the importance of ATC group S (Sensory organs) in Stx2 modulation, with approximately 15% of active compounds classified into this group (**Fig. 15**).

Initially, we focused on the 97 *stx2*-inducing compounds of the Prestwick Chemical Library®, as these could lead to the development of HUS (Mayer *et al.*, 2012). A closer look at the distribution of these compounds among the different ATC groups showed an overrepresentation of ATC group J (Anti-infectives for systemic use) (**Fig. 18**). Furthermore, compounds of ATC groups G (Genito-urinary system and sex hormones), Q (Veterinary drugs) and R (Respiratory tract) were highly represented among the *stx2*-inducing compounds. Veterinary drugs in particular could play a special role, as cattle have been identified as the primary STEC reservoir (Ekong, Sanderson and Cernicchiaro, 2015; Munns *et al.*, 2015). Thus, most infections occur through the consumption of raw meat or other foods cross-contaminated by cattle faeces (Rangel *et al.*, 2005). The use of veterinary drugs to prevent this transmission to humans could lead to the increased expression of *stx2* in some cases. A similar phenomenon has already been observed in meat processing, where salt concentrations used to preserve the product caused an increase in Stx2 production (Harris *et al.*, 2012). These results suggest that certain ATC groups may have a higher risk of inducing *stx2*, which has important implications for clinical practice and drug safety. In contrast, ATC groups C (cardiovascular system), M (musculoskeletal system), and N (nervous system) show a significant underrepresentation among the Stx2 active compounds (**Fig. 18**). Thus, these drugs can be safely applied in EHEC infected patients whose cardiovascular system and especially the central nervous system are often severely affected by Stx2

(Obata *et al.*, 2008; Neu *et al.*, 2023; Pinto, Celi and Goldstein, 2023). Nevertheless, a lower number of Stx2 active compounds was present for each of these three ATC groups. As our screen only contained a selection of compounds from the respective ATC groups, it is not possible to make any statements for the entirety of compounds of these ATC groups regarding the influence of *stx2* expression.

The ATC group distribution for compounds inhibiting *stx2* expression (**Fig. 24**) looks very different compared to the one of the *stx2* inducing compounds. A common nominator between the two groups is the overrepresentation of ATC group J (Anti-infectives for systemic use). Next to ATC group J, ATC group S (Sensory organs) is significantly overrepresented in inhibiting compounds.

5.2.1 Compounds inducing Stx2 production

5.2.1.1 Compounds from ATC group J “Anti-infective for systemic use”

It is generally not recommended to use antibiotics in the treatment of EHEC infected patients (Eppinger *et al.*, 2022; Tarr and Freedman, 2022). Antibiotics such as ampicillin, azithromycin, kanamycin, rifaximin and tetracycline which are categorised in the literature as non-*stx*-inducing could potentially be used in the treatment of EHEC patients in the future, but a consensus has not yet been reached (Bielaszewska *et al.*, 2012b; Freedman *et al.*, 2016; Mühlen *et al.*, 2020b). In general, antibiotics that target the DNA replication lead to *stx2* induction, while the ones targeting the cell wall, transcription or translation seem to not induce *stx2* expression (McGannon, Fuller and Weiss, 2010).

In our screen several quinolone (oxolinic acid, flumequine, nalidixic acid sodium salt, pipemidic acid, cinoxacin and rifampicin) and fluoroquinolone (ciprofloxacin, norfloxacin, lomefloxacin, sarafloxacin, nadifloxacin, pefloxacin, tosufloxacin, moxifloxacin, rufloxacin, fleroxacin, enoxacin, clinafloxacin and rufloxacin) antibiotics were identified as *stx2* inducing (**Suppl. Table 1**). The *stx2* inducing effect for these two antibiotic classes *in vitro* as well as *in vivo* is very well documented (Zhang *et al.*, 2000; Bielaszewska *et al.*, 2012b; Mühlen and Dersch, 2020). These examples show

in a straightforward fashion, that our reporter CW^{gluc} and the screening assay yield reliable results in terms of finding *stx2* inducing compounds.

For some of the antibiotics in our screen, subinhibitory concentrations (<20 µM) were necessary to show *stx2* induction, as higher concentrations had a bactericidal effect on our reporter strain and led to mislabelling of the compounds (**Fig. 27**).

One of the examples is trimethoprim. Re-testing the compound at lower concentrations allowed us to confirm that trimethoprim, an antifolate inhibiting the dihydrofolate reductase, induces *stx2* expression (McGannon, Fuller and Weiss, 2010; Mühlen *et al.*, 2020a) (**Fig. 27**).

We identified some beta-lactam (belonging to the cephalosporin and penicillin cluster) antibiotics (cephalothin sodium salt, cefaclor hydrate, cefsulodin sodium salt, cefoxitin sodium salt, ticarcillin sodium, benzylpenicillin and phenethicillin) (**Suppl. Table 1**), which inhibit the cell wall synthesis, as *stx2* inducing, while others (amoxicillin, piperacillin sodium salt, talampicillin hydrochloride) did not induce the *stx2* (**Fig. 27**). This two-faced reaction of beta-lactams antibiotics towards *stx2* induction is reported in the literature as well (Yoh, Frimpong and Honda, 1997; Grif *et al.*, 1998b; McGannon, Fuller and Weiss, 2010; Mühlen *et al.*, 2020a; Y. Liu *et al.*, 2023). This dual nature of beta-lactam antibiotics might be more related to the reaction of an individual STEC strain and the Stx carried by that strain to the antibiotic, than the antibiotic itself.

We identified two beta-lactamase inhibitors (sulbactam and clavulanate potassium salt) as *stx2* inducing compounds (**Suppl. Table 1**). To our knowledge this has not been reported yet, since often these compounds are used in combination with beta-lactam antibiotics and not alone. There is a rising problem of EHEC strains harbouring beta-lactamases in their genome expanding the antibiotic resistance of these strains (Valat *et al.*, 2012; Ramatla *et al.*, 2024). The potential *stx2* inducing effect of beta-lactamase inhibitors would make the dual treatment with beta-lactam antibiotics a risk factor for the patient health. Therefore, in case of beta-lactam resistant EHEC strains the use of lactamase inhibitors should be avoided. Further tests are needed to confirm the *stx2* inducing potential of lactamase inhibitors and the implications that has on possible treatment strategies for EHEC infections.

Nitrofurantoin, a nitrofuran antibiotic with multiple cellular targets was identified as *stx2* inducing by us (**Suppl. Table 1**). The *stx2* inducing effect of nitrofurantoin has not yet

been reported, but the DNA damaging properties and following that, the activation of the SOS response is known in the literature (Chittò *et al.*, 2020; Revitt-Mills *et al.*, 2022). In a study with *Vibrio cholerae* el tor strain SLH22(J) the prophage inducing capacity of nitrofurantoin have been shown (Rahman, Pal and Chatterjee, 1993). Therefore, it is highly likely that nitrofurantoin induces the SOS response by DNA damage and that this leads to the induction of *stx2*.

Rifampicin, a rifamycin antibiotic that inhibits the bacterial DNA-dependent RNA-polymerase was found to be *stx2* inducing in our screen (**Suppl. Table 1**). The *stx2* induction level was on the low end of our hits, nevertheless rifampicin induced Stx2 production significantly. This finding contradicts other findings, where rifampicin did not induce *stx2* expression and was proposed to be used in the treatment of EHEC infected patients (Rahal *et al.*, 2011). In a recent paper by Ramstad *et al.* rifampicin did not induce *stx2* expression in the majority of STEC tested strains. Nevertheless, they found two strains, both from the serotype O104:H4, where the exposure to rifampicin lead to *stx2* induction (Ramstad *et al.*, 2021). A study from 2015 focusing on the effect of rifampicin on *E. coli* O104:H4 outbreak strain D3774/C22711 reported that MIC and MBC level of the antibiotic do not lead to *stx2* induction, while sub-MIC level result in higher transcription level of *stx2*. This increase in stx2 expression was independent of the SOS response, since *recA* transcription levels stayed low (Fadlallah *et al.*, 2015). These papers together show that the effect of rifampicin on *stx2* expression highly depends on the strain and the used drug concentration. A uniformly evaluation regarding the effect on Stx2 production cannot be made.

5.2.1.2 Compounds from ATC group L “Antineoplastic and immunomodulating agents”

An observation from our initial screen, which was confirmed in the concentration-dependent screen was, that compounds from ATC group L had one of the strongest *stx2* inducing effect. The interactions of *E. coli* and other bacteria with chemotherapeutic drugs are well studied, focussing mainly on the effects that bacteria exert on the drugs (Lehouritis *et al.*, 2015; Attwaters, 2022), while other reports evaluate the antibacterial properties of chemotherapeutic drugs (Hamilton-Miller, 1984; Campbell, Gagnon and Rubin, 2019).

In particularly two compounds, streptozotocin and dacarbazine, were identified as potent inducers of *stx2* expression within ATC group L in our screen (**Fig. 22F and N**). Streptozotocin is a nitrosourea compound structurally similar to glucose, which is taken up by beta cells of the mammalian pancreas. Inside the cell it creates DNA damage through alkylating the DNA molecule. In a study by Lengeler in 1980, in which the antibacterial property of streptozotocin on *E. coli* was investigated, it is pointed out that after the uptake, streptozotocin is phosphorylated and accumulates intracellularly in its toxic phosphorylated form. At the same time intracellular disintegration of streptozotocin forms diazomethane, which compromises bacterial DNA (Lengeler, 1980). DNA damage triggers the SOS response and could thus explain the strong *stx2* induction (Kimmitt, Harwood, & Barer, 2000). Dacarbazine on the other hand is a triazene derivative with DNA alkylating activity. It methylates in human cells the DNA at a guanine residue, leading to the disruption of DNA replication. It is not unlikely that the same happens in bacterial cells, leading to DNA damage and thus *stx2* expression in EHEC.

A number of ATC group L compounds showed concentration-dependent effects on *stx2* expression, with notable variations observed among members of the pyrimidine analogue subgroup (L01BC). Cytarabine, a nucleoside analogue of cytidine, which leads to the inhibition of DNA synthesis in human cells showed no *stx2* inducing effect in the concentration-dependent rescreen (**Fig. 22E**). On the other hand, 5-azacitidine, another cytidine analogue, and floxuridine, a nucleoside analogue to uridine, altered expression levels of *stx2* in a concentration-dependent manner (**Fig. 22B and I**). Floxuridine, inhibits thymidylate synthase, blocking the conversion to deoxythymidine as well as DNA synthesis in human cells. For 5-azacitidine, the *E. coli* transcriptome was shown to be altered via an DNA methylation-dependent mechanism, as well as DNA damage response mechanisms (Militello *et al.*, 2016). This mechanism could lead to the induction of *stx2* in EHEC. For floxuridine, antibacterial activity against *Streptococcus suis* was reported. Floxuridine increased the permeability of the cytoplasm membrane and inhibited the expression of virulence genes in *S. suis* (Li *et al.*, 2023). In *S. aureus* floxuridine reduces the virulence factor expression and lead to induction of prophages, which indicate DNA damage (Yeo *et al.*, 2018). Floxuridine, as pyrimidine analogue, might lead to DNA synthesis inhibition in EHEC and thus the induction of SOS response followed by *stx2* expression. The compound cytarabine, which was not *stx2*-inducing in the concentration-dependent screen, was found not to

be antibacterial for *E. coli*, which is in line with our findings from the concentration-dependent screen (Hamilton-Miller, 1984; Campbell, Gagnon and Rubin, 2019). This shows that compounds from the same ATC subgroup can have very different effects on bacteria even though their effect in human cells might be similar.

The general mechanism of action of chemotherapeutic drugs, DNA damage, can largely be transferred to bacteria (Woods and Turchi, 2013; Sumabe *et al.*, 2021). Why are not all compounds of ATC group L *stx2* inducing? We cannot answer this clearly, but possible reasons could be a natural resistance of the reporter strain to certain compounds (Sayin *et al.*, 2023), efflux pumps that transport the compounds out of the cell (Nishino *et al.*, 2021) or that the compounds do not enter or bind to the bacterial cell in the first place. Another explanation could be the needed conversion from a pro-drug to the active form by human enzymes. These enzymes or equivalents could be lacking in bacteria and therefore the drug would not be transformed to the active form.

In light of increasing antibiotic resistance and the urgent need for new therapeutic approaches, chemotherapeutic drugs are considered as antibiotic alternatives (Ventola, 2015; Alaoui Mdarhri *et al.*, 2022). The study by Borsa *et al.* sheds light on the possibility of using chemotherapeutic drugs e.g. floxuridine as therapeutic agents for bacterial infections using *Staphylococcus aureus* as example pathogen (Borsa *et al.*, 2023). In another study streptozotocin and floxuridine were used as treatment against *S. aureus* in a murine model of blood infection (Yeo *et al.*, 2018).

While previous studies have mainly focused on the cytotoxic and antibacterial effects of chemotherapeutic drugs, our study provides new insights into their potential to modulate bacterial virulence. The identification of streptozotocin and dacarbazine as potent inducers of *stx2* expression expands our understanding of the interplay between chemotherapy and bacterial pathogenesis and the risk of Stx2-related complications in cancer patients. The clustering of *stx2*-inducing compounds within certain subgroups of ATC group L suggests potential common mechanisms. This underlines the need for mechanistic studies to understand the signalling pathways involved in *stx2* induction by chemotherapeutic drugs. As promising as anti-cancer drugs may appear as antibiotic alternatives, it should always be considered and investigated whether undesirable side effects could occur due to the regulation of virulence factors like Stx2.

5.2.1.3 Additional *stx2* inducing compounds

Acetylsalicylic acid, better known under the name Aspirin, was *stx2* inducing in our screen (**Fig. 20A**). It is a nonsteroidal anti-inflammatory drug used to reduce pain, fever and inflammation. The discovery of *stx2* induction is supported by the literature. There are several studies in which salicylate is shown to be ROS-inducing (Price, Lee and Gustafson, 2000; Wang, El Meouche and Dunlop, 2017). ROS can trigger the bacterial SOS response and thus induce *stx2* (Podlesek and Žgur Bertok, 2020).

Another compound, that has been identified by us as *stx2* inducing is clomiphene citrate (**Suppl. Fig. 1**). Clomiphene is a nonsteroidal triphenylethylene derivative, which is used for the treatment of infertility in women. It induces ovulation (Brown and Farquhar, 2016). Clomiphene citrate causes DNA strand breaks in *E. coli*, but the bacterial SOS response is not induced and therefore neither is *recA* (Ohnishi *et al.*, 1986). The RecA-independent induction of the lambdoid prophages as well as the induction of *stx2* are known in the literature (Rozanov, D'Ari and Sineoky, 1998; Imamovic and Muniesa, 2012). Thus, clomiphene citrate could induce *stx2* despite not activating the SOS response.

Guaiacol, an anti-diarrhoeal drug used particularly in Japan, was identified as *stx2* inducing in our initial screen (Baba and Tani, 2001). However, this observation could not be verified in the concentration-dependent screen (**Fig. 20C**). Guaiacol is a component of *Juniperus oxycedrus*. A study from 2018 on essential oils reported that guaiacol next too other essential oils and their components trigger the stress response in *E. coli*. The observed protein profile of *E. coli* treated with guaiacol is similar to the one of *E. coli* treated with tetracycline. The mechanism by which guaiacol acts is not known, but it could influence protein biosynthesis (Božik *et al.*, 2018). Additionally, guaiacol has been reported to inhibit biofilm formation but other publications contradict this observation (Cooper, 2013; Kim *et al.*, 2016; Božik *et al.*, 2018). Thus, a more detailed investigation of the *stx2* inducing properties of guaiacol could be very relevant, especially considering that the first symptom of an EHEC infection is diarrhoea and guaiacol is used as a medication against that in Japan (Nguyen and Sperandio, 2012). If an EHEC infected person takes guaiacol in the belief that it will treat the diarrhoea, but instead induces the expression of *stx2*, this would lead to a drastic health risk.

In 2021, a study was published that reported the activation of the SOS response and Stx production by psychoactive drugs (Crane, Salehi and Alvarado, 2021). We too have identified a psychoactive compound, sertindole, as a strong *stx2* inducer (**Fig. 20H**). Sertindole is a serotonin-dopamine antagonist, which blocks their receptors in the brain. In a publication from 2023, the antibacterial and antibiofilm activity of sertindole against *Staphylococcus aureus* was reported, which supports our result (Tang *et al.*, 2023). Due to its lipophilic chemical structure, it can surpass the membrane lipid layer. In *S. aureus*, sertindole leads to blockade of the protein biosynthesis by affecting amino acids synthesis and ribosome formation. In addition, it compromised the cell wall integrity of *S. aureus*. Even though *S. aureus* is a gram-positive bacterium, sertindole could very well have the same cell damaging effects on *E. coli*.

For another compound, zidovudine, which is known to induce SOS response and trigger Stx production, we were able to confirm strong *stx2* induction in our screens (**Suppl. Fig. 1**) (Mamber, Brookshire and Forenza, 1990; Crane, Salehi and Alvarado, 2021). Zidovudine is a thymidine analogue, which is used as antiretroviral medication. It inhibits the reverse transcriptase of the virus by integrating into the growing viral DNA chain. The bacterial SOS response in EHEC is triggered by DNA chain termination, which leads to the inhibition of DNA replication (Elwell *et al.*, 1987). Zidovudine as a substitution for other antimicrobials in the treatment of e.g. salmonellosis has shown promising results in *Salmonella* clearance *in vitro* and *in vivo* (Casado *et al.*, 1999; Nascimento, Silva and Fernandes, 2008). However, as a treatment strategy for STEC infections, zidovudine would be not suited due to its *stx2* induction properties. This illustrates once again how difficult it is to develop a promising therapy against STEC infections.

5.2.2 Human-targeted drugs inhibiting *stx2* expression

Given the limited treatment options for STEC infections, the discovery of compounds that could inhibit the expression of *stx2* represents a promising approach for therapeutic intervention. The most promising regulatory pathway to target is the inhibition of the bacterial SOS response. In our study, we applied a comprehensive

screening approach to identify potential inhibitors of *stx2* expression. Our results shed light on novel compounds that exhibit significant inhibitory effects on *stx2* expression.

Clarithromycin (macrolide antibiotic, inhibits protein synthesis), clindamycin (lincosamide antibiotic, inhibits protein synthesis), imipenem (β-lactam antibiotic, inhibits cell wall synthesis), levodopa (precursor of catecholamines, increases dopamine concentration in brain), lincomycin (lincosamide antibiotic, inhibits protein synthesis) and metronidazole (antibiotic and antiprotozoal, inhibits nucleic acid synthesis), showed a significant inhibition of *stx2* expression in the initial screen (**Fig. 23**). By simultaneously treating the reporter with MitoC, which leads to the induction of *stx2* expression, we were able to increase the sensitivity of our assay in subsequent experiments due to the increased production of Stx2 (**Fig. 16**). This helped us in the identification of compounds inhibiting *stx2* expression. This approach, which has been used in other studies (Wigle *et al.*, 2009), identified additional compounds to the ones from the initial screen of potential Stx2 inhibitors. These compounds are antimycin A (fungicidal antibiotic, inhibits oxidative respiration), azithromycin (macrolide antibiotic, inhibits protein synthesis), dihydrostreptomycin sulfate (aminoglycoside antibiotic, inhibits protein synthesis), efavirenz (antiretroviral medication, inhibits reverse transcriptase), lymecycline (tetracycline antibiotic, inhibits protein snythesis), oxethazaine (local anesthetic), pivmecillinam hydrochloride (penicillin antibiotic, inhibits cell wall synthesis) and roxithromycin (macrolide antibiotic, inhibits protein synthesis) (**Fig. 25 and 26**).

The Stx2 inhibitory effect of several compounds we have identified (clarithromycin, clindamycin, lincomycin, azithromycin, lymecycline and roxithromycin) might be due to their inhibitory effect on translation. A previous study showed that transcriptional and translational inhibitors block the SOS response and thus prevent *stx2* expression (Berger *et al.*, 2019). This could be the mechanism of action for the above-mentioned compounds in our study (**Fig. 25 and 26**). The strength of Stx2 inhibition by the compounds were often concentration dependent. Clarithromycin for example, showed strong inhibition of *stx2* expression even at low concentrations (**Fig. 25E and 26E**). This finding is consistent with a study from 1997, in which Stx production was also inhibited at a low concentration of clarithromycin (Nakata *et al.*, 1997). An *in vitro* study by Murakami *et al.* confirmed that clindamycin and roxithromycin reduced the release of Stx (Murakami *et al.*, 2000). Beta-Lactam antibiotics such as imipenem

(carbapenems) are not *stx2*-inducing, unlike other antibiotic classes. This has already been shown *in vitro* and in mouse experiments (Grif et al., 1998; McGannon et al., 2010; Mühlen et al., 2020). Here, the death of the bacteria could lead to the reduction of Stx2 production. This general idea that beta-lactam antibiotics do not induce *stx2* expression should be taken with a grain of salt and the focus should rather be on the specific antibiotic and their effects on Stx2.

For the compound's disulfiram, levodopa, metronidazole and moroxidine, which all showed a concentration-dependent inhibition of Stx2 in our screen (**Fig. 25G, J, M and O**), we are not aware of any mechanisms of action that could explain their effect on *stx2* expression. Individual reports that link these compounds to *E. coli* are always in a different context. For example, disulfiram alone did not inhibit the growth of *E. coli*, but it enhanced the effect of antibiotics against resistant Gram-negative bacteria (Lanz *et al.*, 2023).

It is known that levodopa is converted to dopamine by bacteria in the gut and can therefore no longer enter the human brain as a drug (Yamanishi *et al.*, 2022). In a study from 2023, changes in the gut microbiome and the accumulation of antibiotic resistance genes caused by levodopa were reported (Sheng *et al.*, 2023). This contrasts with a previous study, which found no changes in the gut microbiota due to exposure to levodopa (Palacios *et al.*, 2021). It is therefore not trivial to find an explanation for our observed effect of levodopa. A possible, but unconfirmed, explanation for Stx2 inhibition by levodopa could arise from the knowledge of two other studies. Freestone *et al.* showed that the growth of *E. coli* O157:H7 is enhanced by dopamine (Freestone, Haigh and Lyte, 2007) and that the two-component regulator sensor kinase QseC is probably responsible for this. This sensor kinase also regulates *stx* in EHEC (Hughes *et al.*, 2009; Mellies and Lorenzen, 2014). However, whether the Stx2 inhibitory effect of levodopa is actually related to extracellular degradation to dopamine and signalling by QseC remains unclear and requires further investigation.

A study from 1995 reports on the mode of action of metronidazole on *E. coli*. In the study, metronidazole leads to DNA strand breaks, which would lead to *stx2* expression. On the contrary, we found Stx2 inhibition. The DNA strand breaks can be negated by MetA, which also protects *E. coli* under heat stress (Dachs, Abratt and Woods, 1995; Schink *et al.*, 2022). In another study in which metronidazole was administered to mice, there was no negative effect on *E. coli* viability or cell count (Reznikov and McDonald,

1983). Therefore, the effects of metronidazole on *E. coli* do not appear to be uniform and always depend on the experimental settings and oxygen concentration due to the required reduction under anaerobic conditions. Hence, it is unclear why *stx2* expression was inhibited by metronidazole in our case. A possible explanation for the outcome could be that metronidazole or its metabolites could directly interfere with the regulatory elements or promoters responsible for *stx2* expression and by that inhibit the production.

The SOS response, which is responsible for *stx2* induction, also plays a crucial role in the evolution of antibiotic resistance (Podlesek and Žgur Bertok, 2020; Yakimov, Bakhlanova and Baitin, 2021). Therefore, other studies have already searched for inhibitors affecting proteins that are involved in the bacterial SOS response. In 2018, a collaboration between industry and academia found inhibitors of LexA autoproteolysis (Mo *et al.*, 2018). For the second important protein of the SOS response, RecA, inhibitors of ATPase activity as well as for the RecA-induced autoproteolysis of LexA, were found (Sexton *et al.*, 2010; Bunnell *et al.*, 2017). Our compounds with unknown inhibitory mechanism could also affect proteins needed in the SOS response pathway. Further experiments are needed to confirm this possibility.

Comparison of our results with existing literature revealed several remarkable findings and novelties regarding Stx2 inhibition. Our study expands the knowledge by revealing additional compounds with similar inhibitory properties, but also compounds with previously unknown Stx2 inhibitory properties. Of particular interest was the identification of non-antibiotic compounds, such as levodopa and disulfiram, as potential inhibitors of *stx2* expression. Further research is needed to clarify the molecular mechanisms of the inhibitory effects of these compounds and to evaluate their efficacy in further *in vitro* and *in vivo* studies. Furthermore, the concentration-dependent nature of the observed inhibitory effects highlights the importance of optimizing dosing regimens, if these compounds turn out to be part in possible treatment regimens for STEC infections, to maximize efficacy and minimize potential adverse effects. The ability of certain compounds, such as clarithromycin and imipenem, to exert strong inhibitory effects on *stx2* expression at relatively low concentrations suggests their potential for use in combination therapies with other antibiotics against STEC infections. Additional studies addressing this question are needed to potentially develop a treatment strategy.

5.2.3 Evaluation of the Prestwick Chemical Library® screen

With the integration of advanced analytical tools (HiTSeekR), we identified 161 primary hits among the screened compounds, which is a hit rate of 13.4% (**Fig. 11**). This is a high value for a compound screen, due to the low cutoff we set (2x MAD, **Fig. 12**) (Shun *et al.*, 2011; Zhu *et al.*, 2013). In a mouse study, it was shown that HUS development is concentration-dependent and that Stx2 amounts greater than 100 ng/kg body weight are needed for clinical signs for HUS (Dennhardt *et al.*, 2018). In a baboon model for Stx-mediated HUS, which may represent the Gb3 receptor distribution and expression pattern of human better than mice, the intravenous injection of 25 ng/kg Stx2 every 12 h resulted in HUS (Siegler *et al.*, 2003). Human patient data regarding the amount of Stx2 needed to induce clinical symptoms is not as clear, since they are a lot of factors like Gb3 receptor expression, STEC strain and health condition of the patient that vary between the patients. With this hit detection cut-off, we wanted to make sure to be able to also detect compounds exhibiting subtle effects on *stx*2 expression, since we believe that already small changes in *stx2* expression have a big impact on patient's health.

The subsequent validation process, which aimed to identify hit compounds that inhibited the enzymatic activity of *Gaussia princeps* luciferase, resulted in 21 compounds being excluded from the hit list (**Table 10**). This is 1.75% of the compounds originally screened and thus within an expected range of luciferase inhibitors in a compound library (Ho *et al.*, 2013; Auld and Inglese, 2018).

We were able to confirm the *stx2* inducing effect observed at 20 µM in the initial screen for 39% of the compounds in the concentration-dependent screen. For 56% of the compounds tested in the concentration-dependent screen, we were able to detect an induction of *stx2* expression when all 10 measured concentrations were included. A hit confirmation rate of around 50% is rather low compared to the expected confirmation rate of 80% or better given by the good Z-factor of 0.8 and signal to noise ration well above 10 (Zhang, Chung and Oldenburg, 2000; Zhijin Wu, Dongmei Liu and Yunxia Sui, 2008). The selection of a rather low cutoff (2x MAD) could lead to more false positive compounds as with a cutoff of 3x MAD. Furthermore, inhibition of cell growth by the compounds leads to misinterpretation of the results. Some compounds that were identified as inhibitors, at lower concentrations were in fact inducers (as

previously reported). This was also true for compounds that were not identified as Hits. Therefore, we cannot exclude a high amount of false negative Hits (**Fig. 9C**, dots in the far left of the bottom left quadrant). A fixed concentration normally used in HTS might mask the real effect of some compounds but is a necessary compromise to be able to screen high numbers of compounds.

Another reason could be the compounds themselves. Preparation and long-term storage of compounds also play a significant role in their stability (Nickolai *et al.*, 1985).

It is important to note that our study has some limitations. Firstly, the experiments were conducted *in vitro*, which may not fully reflect all aspects of the interaction between the compounds and the bacterial host organism. In addition, the experiments were conducted with a specific strain of *E. coli* (CW^{gluc}), which may limit the transferability of the results to other pathogenic *E. coli* strains or other bacterial species.

Moving forward, the findings of the entire study on the impact of human-targeted drugs on *stx2* expression hold significant implications for both basic science and clinical practice. From a basic science perspective, elucidating the mechanisms underlying drug-induced modulation of *stx2* expression will provide valuable insights into bacterial gene regulation and virulence. This knowledge can inform the development of targeted strategies to disrupt toxin production in pathogenic bacteria, offering novel avenues for therapeutic intervention. For clinical practice, understanding the impact of human-targeted drugs on *stx2* expression has important implications for patient management. Patients receiving certain medications may accidentally worsen EHEC infections by promoting toxin production. Additionally, the identification of drugs capable of inhibiting *stx2* expression opens up the possibility of repurposing existing medications for therapeutic use against EHEC infections.

5.3 Microbiome-based markers for HUS development

The 2011 outbreak of HUSEC in Germany marked a significant public health crisis, with thousands infected and a substantial mortality rate. Understanding the microbiota signatures associated with disease is crucial for elucidating factors contributing to disease severity and guiding therapeutic interventions (Hou *et al.*, 2022; Madhogaria, Bhowmik and Kundu, 2022). In this study, we analysed faecal samples collected from

HUSEC infected patients during the outbreak, focusing on correlating microbiota profiles with disease outcomes, particularly the risk of developing HUS.

Notably, we observed distinct microbiota signatures associated with different disease states, including healthy controls, STEC-positive patients (including both EHEC and HUS groups), and patients with HUS. Comparison of healthy controls with STEC-positive patients revealed an overrepresentation of Enterobacterales and Staphylococcales in the latter (**Fig. 30**). An increase in abundance of Enterobacterales is often correlated with dysbiosis and inflammation, which in turn helps pathogens like HUSEC to bloom (Baldelli *et al.*, 2021; Bujňáková, Puvača and Ćirković, 2022). There are several reasons for the upgrowth of Enterobacterales in an inflamed gut. The inflammatory responses of the host mediated by the epithelial cells and neutrophils lead to the production of reactive oxygen (ROS) and nitrogen species (RNS), which Enterobacterales can utilize as electron acceptor for anaerobic respiration (Stecher, 2015). The increase of oxygen in the gut lumen, due to metabolic changes in the enterocytes, facilitates the increase of these facultative anaerobes and reduce the strictly anaerobic bacteria even more (Rigottier-Gois, 2013; Moreira de Gouveia, Bernalier-Donadille and Jubelin, 2024). All these gut environmental changes together disrupts the colonization resistance of the gut and pave the way for enteropathogens like HUSEC to colonize (Stecher *et al.*, 2010). Additionally, these pathogens have adopted to the host immune responses and can therefore evade them (J. Worley, 2023).

Consistent with previous studies, the abundance of beneficial taxa like Bifidobacteriales and Clostridiales in individuals help to prevent STEC-infection, therefore the reduced abundance increases the chances of infection (Asahara *et al.*, 2004; Gagnon *et al.*, 2004; Takahashi *et al.*, 2004b; Yoshimura, Matsui and Itoh, 2010; Vazquez-Gutierrez *et al.*, 2016). This is in line with a study from 2018, where they also analysed faecal samples from STEC-infected patients and found a lower abundance of members of Bifidobacteriales and Clostridiales (Gigliucci *et al.*, 2018). These observed differences underscore the notion, that certain bacterial taxa may facilitate or prevent HUSEC infection and disease symptoms. The main mechanism by which these bacteria inhibit STEC infection is the production of short-chain fatty acids (SCFAs) like acetate, butyrate, and propionate or lactate and the consequently pH drop (Sherman *et al.*, 2005; Zhang *et al.*, 2020; Kadry, El-Antrawy and El-Ganiny, 2023). On

the other hand, there are also reports indicating that not the production of SCFA but rather the enhancement of the local immune response leads to the protective phenotype (Ogawa *et al.*, 2001).

Our analysis identified specific bacterial families associated with the development or prevention of HUS. Lachnospiraceae_UCG_008 and Prevotellaceae were more abundant in EHEC patients compared to HUS patients (**Fig. 31**). These families are known to produce SCFAs (Chen *et al.*, 2017; Vacca *et al.*, 2020), which exhibit inhibitory effects on Shiga toxin production or translocation from the gut lumen to the blood (Carey *et al.*, 2008b; Fukuda *et al.*, 2011). In contrast, there are reports contradicting the beneficial effect of SCFA. Low level of butyrate enhance LEE gene expression, whereas elevated levels of butyrate enhanced the cell-killing capacity of Stx (Nakanishi *et al.*, 2009; Zumbrun *et al.*, 2013). Conversely, patients with HUS showed an overrepresentation of Bacilli compared to the EHEC group (**Fig. 31**). Of particular interest is *Enterococcus faecalis*, which has been reported to increase EHEC virulence (Curtis *et al.*, 2014; Martins *et al.*, 2022b). This suggests a potential role of SCFA-producing bacteria in mitigating HUS development and highlights the complex interplay between microbiota composition and disease outcomes.

Moreover, we investigated the potential impact of colibactin, a genotoxin encoded by the *pks* gene island, on HUS development. Previous studies have linked colibactin expression to alterations in microbial diversity and increased activation of DNA repair pathways (Tronnet *et al.*, 2020; Mousa, 2022). Silpe *et al.* showed that colibactin can trigger the SOS response, induce a variety of prophages and lead to an increase of Stx production in a *Citrobacter rodentium* strain harbouring an *stx2* prophage (Silpe *et al.*, 2022). Our results indicate a significant difference in presence of colibactin gene (*clbB*) between healthy controls and HUS patients (**Fig. 32**), with 55.7% of HUS patients exhibiting detectable *clbB* levels (**Fig. 33**). This observation of increased *clbB* levels in the HUS group compared to healthy controls is at least partially due to increase abundance of *Enterobacteriaceae* in this group, e.g. *E. coli,* shown through the control gene *uidA* (**Fig. 32 and 33**). These elevated *clbB* levels indicate a potential association between colibactin expression and HUS development via *stx2* encoding prophage induction. We can not 100% rule out, that the *clbB* probe binds unspecific to other DNA sequences in the faecal sample and therefore lead to false positive results in the samples. Further *in vivo* studies in a defined microbiome background, consisting

of several bacterial species in addition to bacteria containing the *pks* gene island, are needed to prove and elucidate the mechanism of Stx2 production due to colibactin and the consequently development of HUS.

There are other bacteria produced toxins, which could induce the Stx production in STEC infected patients. Another genotoxin, tilimycin, which is produced by *Klebsiella* spp., is a known mutagen (Pö *et al.*, 2023). Tilimycin leads to DNA alkylation followed by DNA strand breakage (Alexander *et al.*, 2020). It was reported by Kienesberger *et al.*, that tilimycin alters the taxonomic composition in the murine gut and that subinhibitory concentrations can induce the SOS response in *E. coli* (Kienesberger *et al.*, 2022). This would lead to the induction of *stx* and therefore result in the development of HUS.

On the other hand, bacterial toxins could also have a protective effect for STEC infected patients. Another category of toxins produced by bacteria are bacteriocins e.g. colicins or microcins which are predominantly produced by *Enterobacteriaceae* (Rebuffat, 2011). Such colicins and microcins have numerous cytotoxic mechanisms as mode of action, including pore forming capacity, degradation of peptidoglycan precursory, RNAse and DNAse activity (Marković *et al.*, 2022). These toxins inhibit the growth or kill competing bacterial species and are therefore considered as alternative to antibiotics (Cotter, Ross and Hill, 2012; Yang *et al.*, 2014). It was shown, for example, that colicinogenic *E. coli* can inhibit the growth of several STEC from different serotypes O26, O111, O128, O145 and O157:H7 (Jordi *et al.*, 2001; García *et al.*, 2023). Therefore, the presents of toxin producing bacteria in STEC infected patients does not have to implicate an increased risk for the development of HUS, but a better understanding of the impact such bacteria have on the STEC infection would be very beneficial for future patients.

Our study contributes to the growing body of literature illuminating the role of microbiota dysbiosis in STEC infection and HUS development. By identifying specific microbiota signatures associated with disease outcomes, we provide valuable insights into potential biomarkers and therapeutic targets for prevention or mitigating HUS development and severity.

In conclusion, our study emphasizes the significance of microbiota analysis of patient samples in unravelling the mechanisms underlying HUSEC infection and HUS

development. Further research is needed to validate our findings in larger cohorts and elucidate the mechanistic basis of microbiota-mediated modulation of HUS susceptibility. Ultimately, exploiting these insights may pave the way for the development of new therapeutic strategies aimed at improving clinical outcomes in HUSEC-infected patients.

5.4 End conclusion and future perspectives

Over the past years, the research on human-targeted drugs and their influence on the microbiome has undergone a significant evolution. Recent research has unveiled the complex interactions between these drugs and the human microbiome, leading to a more holistic understanding of the impact human-targeted drugs have on gut bacteria and vice versa. This led my research on EHEC, focusing on environmental factors like human-targeted drugs or the gut microbiome and their impact on Stx2 regulation. With this study we have increased the knowledge on factors influencing Stx2 production and pointed out potential risk factors for patients during an EHEC infection, by identifying drugs that increase Stx2 production. Expanding this study to other toxins could lead to improved treatments and reduction of severe disease. On the other hand, we showed that there is a possibility for drug repurposing in the search for a therapy against EHEC, due to *stx2* expression inhibitors we identified, which could prevent the production of Stx2, lowering the risk of HUS development. Furthermore, our results indicate that the microbiome composition, especially possible toxin producing bacteria, are potential drivers for a more severe infection progress. Implementation of routine search for these microbes before treatment could prevent unwanted side effects due to increased toxin production, since also non-antibiotic drugs can have a big impact on the expression pattern of virulence factors. The validation of our *stx2* inducing compounds in an *in vivo* set-up would bring us one step closer to expanding the list of drugs which should be avoided during EHEC infections. The approach of a dual treatment with an antibiotic and a *stx2* expression inhibitor as possible treatment during an EHEC infection is an interesting idea to follow up on.

In the last 10 years there is a more holistic view that considers the pathogen, the patient, and their microbiome as a dynamic and interconnected system. This perspective acknowledges that the pathogen's virulence and the patient's susceptibility

are influenced by a multitude of factors, including the microbiome composition and function, the patient's genetic predispositions, and the pharmacological environment created by other medications the patient may be taking. This holistic understanding opens new avenues for more effective and personalized treatments, ultimately improving patient outcomes in the fight against infectious diseases.

6. References

Aertsen, A., Faster, D. and Michiels, C. W. (2005) 'Induction of Shiga Toxin-Converting Prophage in Escherichia coli by High Hydrostatic Pressure', *Applied and Environmental Microbiology*. American Society for Microbiology (ASM), 71(3), p. 1155. doi: 10.1128/AEM.71.3.1155-1162.2005.

Aheme, G. W., McDonald, E. and Workman, P. (2002) 'Finding the needle in the haystack: Why high-throughput screening is good for your health', *Breast Cancer Research*. BioMed Central, 4(4), pp. 148–154. doi: 10.1186/BCR440/FIGURES/2.

Alaoui Mdarhri, H. *et al.* (2022) 'Alternatives Therapeutic Approaches to Conventional Antibiotics: Advantages, Limitations and Potential Application in Medicine', *Antibiotics*. Multidisciplinary Digital Publishing Institute (MDPI), 11(12). doi: 10.3390/ANTIBIOTICS11121826.

Alexander, E. M. *et al.* (2020) 'Biosynthesis, Mechanism of Action, and Inhibition of the Enterotoxin Tilimycin Produced by the Opportunistic Pathogen Klebsiella oxytoca', *ACS infectious diseases*. ACS Infect Dis, 6(7), pp. 1976–1997. doi: 10.1021/ACSINFECDIS.0C00326.

Algavi, Y. M. and Borenstein, E. (2023) 'A data-driven approach for predicting the impact of drugs on the human microbiome', *Nature Communications 2023 14:1*. Nature Publishing Group, 14(1), pp. 1–13. doi: 10.1038/s41467-023-39264-0.

Anatomical Therapeutic Chemical (ATC) Classification (no date). Available at: https://www.who.int/tools/atc-ddd-toolkit/atc-classification (Accessed: 15 January 2024).

Armstrong, G. L., Hollingsworth, J. and Morris, J. G. (1996) 'Emerging foodborne pathogens: Escherichia coli O157:H7 as a model of entry of a new pathogen into the food supply of the developed world', *Epidemiologic reviews*. Epidemiol Rev, 18(1), pp. 29–51. doi: 10.1093/OXFORDJOURNALS.EPIREV.A017914.

Asahara, T. *et al.* (2004) 'Probiotic Bifidobacteria Protect Mice from Lethal Infection with Shiga Toxin-Producing Escherichia coli O157:H7', *Infection and Immunity*. American Society for Microbiology, 72(4), pp. 2240–2247. doi: 10.1128/IAI.72.4.2240-2247.2004/ASSET/19A22E13-289E-404C-B5AB-292334F44CB1/ASSETS/GRAPHIC/ZII0040411680005.JPEG.

Attwaters, M. (2022) 'Gut bugs disrupt cancer drugs', *Nature Reviews Microbiology 2022 20:12*. Nature Publishing Group, 20(12), pp. 704–704. doi: 10.1038/s41579-022-00812-y.

Auld, D. S. and Inglese, J. (2018) 'Interferences with Luciferase Reporter Enzymes', *Assay Guidance Manual*. Eli Lilly & Company and the National Center for Advancing Translational Sciences. Available at: https://www.ncbi.nlm.nih.gov/books/NBK374281/ (Accessed: 9 February 2024).

Baba, T. and Tani, T. (2001) '[Wood creosote: a historical study and its preparation in combination with herbal drugs].', *Yakushigaku Zasshi*, 36(1), pp. 10–17. Available at: https://europepmc.org/article/med/11776992 (Accessed: 15 February 2024).

Baldelli, V. *et al.* (2021) 'The Role of Enterobacteriaceae in Gut Microbiota Dysbiosis in Inflammatory Bowel Diseases', *Microorganisms*. Multidisciplinary Digital Publishing Institute (MDPI), 9(4). doi: 10.3390/MICROORGANISMS9040697.

Bentancor, L. V. *et al.* (2009) 'A DNA vaccine encoding the enterohemorragic Escherichia coli shiga-like toxin 2 A2 and B subunits confers protective immunity to shiga toxin challenge in the murine model', *Clinical and Vaccine Immunology*. American Society for Microbiology, 16(5), pp. 712–718. doi: 10.1128/CVI.00328-08/ASSET/D96E6E6E-5475-4308-9B27-E7A844EDFA65/ASSETS/GRAPHIC/ZCD0050935270003.JPEG.

Berger, M. *et al.* (2019) 'Transcriptional and Translational Inhibitors Block SOS Response and Shiga

Toxin Expression in Enterohemorrhagic Escherichia coli', *Scientific Reports 2019 9:1*. Nature Publishing Group, 9(1), pp. 1–9. doi: 10.1038/s41598-019-55332-2.

Bielaszewska, M. *et al.* (2011) 'Characterisation of the Escherichia coli strain associated with an outbreak of haemolytic uraemic syndrome in Germany, 2011: A microbiological study', *The Lancet Infectious Diseases*. Elsevier, 11(9), pp. 671–676. doi: 10.1016/S1473-3099(11)70165-7.

Bielaszewska, M. *et al.* (2012a) 'Effects of antibiotics on Shiga toxin 2 production and bacteriophage induction by epidemic Escherichia coli O104:H4 strain', *Antimicrobial agents and chemotherapy*. Antimicrob Agents Chemother, 56(6), pp. 3277–3282. doi: 10.1128/AAC.06315-11.

Bielaszewska, M. *et al.* (2012b) 'Effects of antibiotics on Shiga toxin 2 production and bacteriophage induction by epidemic Escherichia coli O104:H4 strain', *Antimicrobial Agents and Chemotherapy*. American Society for Microbiology1752 N St., N.W., Washington, DC, 56(6), pp. 3277–3282. doi: 10.1128/AAC.06315-11/ASSET/EA89F995-D60E-45AE-B007-129FD913A059/ASSETS/GRAPHIC/ZAC9991008730003.JPEG.

Blanco, M. *et al.* (2004) 'Serotypes, Virulence Genes, and Intimin Types of Shiga Toxin (Verotoxin)-Producing Escherichia coli Isolates from Cattle in Spain and Identification of a New Intimin Variant Gene (eae-ξ)', *Journal of Clinical Microbiology*. American Society for Microbiology (ASM), 42(2), p. 645. doi: 10.1128/JCM.42.2.645-651.2004.

Blaser, M. (2011) 'Stop the killing of beneficial bacteria', *Nature 2011 476:7361*. Nature Publishing Group, 476(7361), pp. 393–394. doi: 10.1038/476393a.

Borsa, B. A. *et al.* (2023) 'Therapeutic-oligonucleotides activated by nucleases (TOUCAN): A nanocarrier system for the specific delivery of clinical nucleoside analogues', *Journal of Controlled Release*. Elsevier, 361, pp. 260–269. doi: 10.1016/J.JCONREL.2023.07.057.

Bova, R. A. *et al.* (2023) 'Shiga Toxin (Stx) Type 1a and Stx2a Translocate through a Three-Layer Intestinal Model', *Toxins*. Toxins (Basel), 15(3). doi: 10.3390/TOXINS15030207.

Bova, R. A. and Melton-Celsa, A. (2022) 'Shiga toxin (Stx) type 2-induced increase in O-linked N-acetyl glucosamine protein modification: a new therapeutic target?', *EMBO molecular medicine*. EMBO Mol Med, 14(1). doi: 10.15252/EMMM.202115389.

Božik, M. *et al.* (2018) 'Stress response of Escherichia coli to essential oil components – insights on low-molecular-weight proteins from MALDI-TOF', *Scientific Reports 2018 8:1*. Nature Publishing Group, 8(1), pp. 1–9. doi: 10.1038/s41598-018-31255-2.

Brown, J. and Farquhar, C. (2016) 'Clomiphene and other antioestrogens for ovulation induction in polycystic ovarian syndrome', *The Cochrane Database of Systematic Reviews*. John Wiley and Sons, Inc. and the Cochrane Library, 2016(12). doi: 10.1002/14651858.CD002249.PUB5.

Brunder, W., Schmidt, H. and Karch, H. (1996) 'KatP, a novel catalase-peroxidase encoded by the large plasmid of enterohaemorrhagic Escherichia coli O157:H7', *Microbiology (Reading, England)*. Microbiology (Reading), 142 (Pt 11)(11), pp. 3305–3315. doi: 10.1099/13500872-142-11-3305.

Buchholz, U. *et al.* (2011) ' German Outbreak of Escherichia coli O104:H4 Associated with Sprouts ', *New England Journal of Medicine*. Massachusetts Medical Society, 365(19), pp. 1763–1770. doi: 10.1056/NEJMOA1106482/SUPPL_FILE/NEJMOA1106482_DISCLOSURES.PDF.

Bujňáková, D., Puvača, N. and Ćirković, I. (2022) 'Virulence Factors and Antibiotic Resistance of Enterobacterales', *Microorganisms*. Multidisciplinary Digital Publishing Institute (MDPI), 10(8). doi: 10.3390/MICROORGANISMS10081588.

Bumann, D. and Valdivia, R. H. (2007) 'Identification of host-induced pathogen genes by differential fluorescence induction reporter systems', *Nature Protocols 2007 2:4*. Nature Publishing Group, 2(4), pp. 770–777. doi: 10.1038/nprot.2007.78.

Bunnell, B. E. *et al.* (2017) 'Zinc blocks SOS-induced antibiotic resistance via inhibition of RecA in Escherichia coli', *PLOS ONE*. Public Library of Science, 12(5), p. e0178303. doi: 10.1371/JOURNAL.PONE.0178303.

Butler, T. *et al.* (1987) 'Risk factors for development of hemolytic uremic syndrome during shigellosis', *The Journal of Pediatrics*, 110(6), pp. 894–897. doi: 10.1016/S0022-3476(87)80405-5.

Campbell, A. (2003) 'The future of bacteriophage biology', *Nature reviews. Genetics*. Nat Rev Genet, 4(6), pp. 471–477. doi: 10.1038/NRG1089.

Campbell, O., Gagnon, J. and Rubin, J. E. (2019) 'Antibacterial activity of chemotherapeutic drugs against Escherichia coli and Staphylococcus pseudintermedius', *Letters in Applied Microbiology*. John Wiley and Sons Inc, 69(5), pp. 353–357. doi: 10.1111/LAM.13213.

Carey, C. M. *et al.* (2008a) 'The effect of probiotics and organic acids on Shiga-toxin 2 gene expression in enterohemorrhagic Escherichia coli O157:H7', *Journal of Microbiological Methods*, 73(2), pp. 125–132. doi: 10.1016/J.MIMET.2008.01.014.

Carey, C. M. *et al.* (2008b) 'The effect of probiotics and organic acids on Shiga-toxin 2 gene expression in enterohemorrhagic Escherichia coli O157:H7', *Journal of Microbiological Methods*. Elsevier, 73(2), pp. 125–132. doi: 10.1016/J.MIMET.2008.01.014.

Casado, J. L. *et al.* (1999) 'Zidovudine Therapy Protects against Salmonella Bacteremia Recurrence in Human Immunodeficiency Virus-Infected Patients', *The Journal of Infectious Diseases*. Oxford Academic, 179(6), pp. 1553–1556. doi: 10.1086/314749.

Chan, Y. S. and Ng, T. B. (2016) 'Shiga toxins: from structure and mechanism to applications', *Applied Microbiology and Biotechnology*. Springer Verlag, 100(4), pp. 1597–1610. doi: 10.1007/S00253-015-7236-3/TABLES/1.

Chen, T. *et al.* (2017) 'Fiber-utilizing capacity varies in Prevotella- versus Bacteroides-dominated gut microbiota', *Scientific Reports 2017 7:1*. Nature Publishing Group, 7(1), pp. 1–7. doi: 10.1038/s41598-017-02995-4.

Chittò, M. *et al.* (2020) 'Sub-Inhibitory concentrations of SOS-Response inducing antibiotics stimulate integrase expression and excision of pathogenicity islands in uropathogenic Escherichia coli strain 536', *International Journal of Medical Microbiology*. Urban & Fischer, 310(1), p. 151361. doi: 10.1016/J.IJMM.2019.151361.

Chopra, I. and Roberts, M. (2001) 'Tetracycline Antibiotics: Mode of Action, Applications, Molecular Biology, and Epidemiology of Bacterial Resistance', *Microbiology and Molecular Biology Reviews*. American Society for Microbiology, 65(2), pp. 232–260. doi: 10.1128/MMBR.65.2.232-260.2001/ASSET/B6E30F54-A22E-465F-9655-C334EC599313/ASSETS/GRAPHIC/MR0210009002.JPEG.

Cimolai, N. *et al.* (1990) 'Risk factors for the progression of Escherichia coli O157:H7 enteritis to hemolytic-uremic syndrome', *The Journal of Pediatrics*, 116(4), pp. 589–592. doi: 10.1016/S0022-3476(05)81609-9.

Cody, E. M. and Dixon, B. P. (2019) 'Hemolytic Uremic Syndrome', *Pediatric Clinics of North America*. W.B. Saunders, 66(1), pp. 235–246. doi: 10.1016/J.PCL.2018.09.011.

Cohen, I., Ruff, W. E. and Longbrake, E. E. (2021) 'Influence of Immunomodulatory Drugs on the Gut Microbiota', *Translational research : the journal of laboratory and clinical medicine*. NIH Public Access, 233, p. 144. doi: 10.1016/J.TRSL.2021.01.009.

Cooper, R. A. (2013) 'Inhibition of biofilms by glucose oxidase, lactoperoxidase and guaiacol: the active antibacterial component in an enzyme alginogel', *International Wound Journal*. Wiley, 10(6), p. 630. doi: 10.1111/IWJ.12083.

Cotter, P. D., Ross, R. P. and Hill, C. (2012) 'Bacteriocins — a viable alternative to antibiotics?', *Nature Reviews Microbiology 2012 11:2*. Nature Publishing Group, 11(2), pp. 95–105. doi: 10.1038/nrmicro2937.

Crane, J. K., Salehi, M. and Alvarado, C. L. (2021) 'Psychoactive Drugs Induce the SOS Response and Shiga Toxin Production in Escherichia coli', *Toxins*. Toxins (Basel), 13(7). doi: 10.3390/TOXINS13070437.

Croxen, M. A. *et al.* (2013) 'Recent Advances in Understanding Enteric Pathogenic Escherichia coli', *Clinical Microbiology Reviews*. American Society for Microbiology (ASM), 26(4), p. 822. doi: 10.1128/CMR.00022-13.

Curtis, M. M. *et al.* (2014) 'The Gut Commensal Bacteroides thetaiotaomicron Exacerbates Enteric Infection through Modification of the Metabolic Landscape', *Cell Host and Microbe*, 16, pp. 759–769. doi: 10.1016/j.chom.2014.11.005.

Dachs, G. U., Abratt, V. R. and Woods, D. R. (1995) 'Mode of action of metronidazole and a bacteroides fragilis meta resistance gene in escherichia coli', *Journal of Antimicrobial Chemotherapy*, 35(4), pp. 483–496. doi: 10.1093/JAC/35.4.483.

Degruttola, A. K. *et al.* (2016) 'Current understanding of dysbiosis in disease in human and animal models', *Inflammatory bowel diseases*. NIH Public Access, 22(5), p. 1137. doi: 10.1097/MIB.0000000000000750.

Dennhardt, S. *et al.* (2018) 'Modeling hemolytic-uremic syndrome: In-depth characterization of distinct murine models reflecting different features of human disease', *Frontiers in Immunology*. Frontiers Media S.A., 9(JUN), p. 347514. doi: 10.3389/FIMMU.2018.01459/BIBTEX.

Dougherty, M. W. and Jobin, C. (2021) 'Shining a light on colibactin biology', *Toxins*, 13(5), pp. 1–15. doi: 10.3390/toxins13050346.

Dubourg, G. *et al.* (2014) 'Culturomics and pyrosequencing evidence of the reduction in gut microbiota diversity in patients with broad-spectrum antibiotics', *International Journal of Antimicrobial Agents*. Elsevier, 44(2), pp. 117–124. doi: 10.1016/J.IJANTIMICAG.2014.04.020.

Dundas, S. *et al.* (2001) 'The central Scotland Escherichia coli O157:H7 outbreak: Risk factors for the hemolytic uremic syndrome and death among hospitalized patients', *Clinical Infectious Diseases*. Oxford Academic, 33(7), pp. 923–931. doi: 10.1086/322598/2/33-7-923-FIG002.GIF.

Eberl, C. *et al.* (2021) 'E. coli enhance colonization resistance against Salmonella Typhimurium by competing for galactitol, a context-dependent limiting carbon source', *Cell host & microbe*. Cell Host Microbe, 29(11), pp. 1680-1692.e7. doi: 10.1016/J.CHOM.2021.09.004.

Ekong, P. S., Sanderson, M. W. and Cernicchiaro, N. (2015) 'Prevalence and concentration of Escherichia coli O157 in different seasons and cattle types processed in North America: A systematic review and meta-analysis of published research', *Preventive Veterinary Medicine*. Elsevier B.V., 121(1–2), pp. 74–85. doi: 10.1016/j.prevetmed.2015.06.019.

Elias-Oliveira, J. *et al.* (2020) 'NLR and Intestinal Dysbiosis-Associated Inflammatory Illness: Drivers or Dampers?', *Frontiers in Immunology*. Frontiers Media S.A., 11, p. 562489. doi: 10.3389/FIMMU.2020.01810/BIBTEX.

Elliott, S. J. *et al.* (2000) 'The locus of enterocyte effacement (LEE)-encoded regulator controls expression of both LEE- and non-LEE-encoded virulence factors in enteropathogenic and enterohemorrhagic Escherichia coli', *Infection and Immunity*, 68(11), pp. 6115–6126. doi: 10.1128/IAI.68.11.6115-6126.2000.

Elwell, L. P. *et al.* (1987) 'Antibacterial activity and mechanism of action of 3'-azido-3'-deoxythymidine (BW A509U)', *Antimicrobial agents and chemotherapy*. Antimicrob Agents Chemother, 31(2), pp. 274–

280. doi: 10.1128/AAC.31.2.274.

Enami, M. *et al.* (1999) 'Expression of type I pili is abolished in verotoxin-producing Escherichia coli O157', *FEMS Microbiology Letters*. Oxford Academic, 179(2), pp. 467–472. doi: 10.1111/J.1574-6968.1999.TB08764.X.

End0, Y. *et al.* (1988) 'Site of action of a Vero toxin (VT2) from Escherichia coli O157:H7 and of Shiga toxin on eukaryotic ribosomes: RNA N-glycosidase activity of the toxins', *Wiley Online LibraryY Endo, K Tsurugi, T Yutsudo, Y Takeda, T Ogasawara, K IgarashiEuropean Journal of Biochemistry, 1988•Wiley Online Library*, 171(1–2), pp. 45–50. doi: 10.1111/j.1432-1033.1988.tb13756.x.

Eppinger, M. *et al.* (2022) 'Genome Sequence Analysis and Characterization of Shiga Toxin 2 Production by Escherichia coli O157:H7 Strains Associated With a Laboratory Infection', *Frontiers in Cellular and Infection Microbiology*. Frontiers Media S.A., 12, p. 888568. doi: 10.3389/FCIMB.2022.888568/BIBTEX.

Fadlallah, S. M. *et al.* (2015) 'Effect of rifampicin and gentamicin on shiga toxin 2 expression level and the SOS response in Escherichia coli O104:H4', *Foodborne Pathogens and Disease*. Mary Ann Liebert Inc., 12(1), pp. 47–55. doi: 10.1089/FPD.2014.1824.

Fang, Y. *et al.* (2017) 'Induction of Shiga Toxin-Encoding Prophage by Abiotic Environmental Stress in Food', *Applied and Environmental Microbiology*. American Society for Microbiology (ASM), 83(19). doi: 10.1128/AEM.01378-17.

Farrokh, C. *et al.* (2013) 'Review of Shiga-toxin-producing Escherichia coli (STEC) and their significance in dairy production', *International journal of food microbiology*. Int J Food Microbiol, 162(2), pp. 190–212. doi: 10.1016/J.IJFOODMICRO.2012.08.008.

Fatima, R. and Aziz, M. (2023) 'Enterohemorrhagic Escherichia coli', *StatPearls*. StatPearls Publishing. Available at: https://www.ncbi.nlm.nih.gov/books/NBK519509/ (Accessed: 20 November 2023).

Faucher, Q. *et al.* (2022) 'Is Intestinal Dysbiosis-Associated With Immunosuppressive Therapy a Key Factor in the Pathophysiology of Post-Transplant Diabetes Mellitus?', *Frontiers in Endocrinology*. Frontiers Media S.A., 13, p. 898878. doi: 10.3389/FENDO.2022.898878/BIBTEX.

Feitz, W. J. C. *et al.* (2021) 'Cell Biological Responses after Shiga Toxin-1 Exposure to Primary Human Glomerular Microvascular Endothelial Cells from Pediatric and Adult Origin', *International Journal of Molecular Sciences*. Multidisciplinary Digital Publishing Institute (MDPI), 22(11). doi: 10.3390/IJMS22115615.

Filipiak, M., Łoś, J. M. and Łoś, M. (2020) 'Efficiency of induction of Shiga-toxin lambdoid prophages in Escherichia coli due to oxidative and antibiotic stress depends on the combination of prophage and the bacterial strain', *Journal of Applied Genetics*. Springer, 61(1), pp. 131–140. doi: 10.1007/S13353-019-00525-8/FIGURES/2.

Food, E. and Authority, S. (2011) 'Tracing seeds, in particular fenugreek (Trigonella foenum-graecum) seeds, in relation to the Shiga toxin-producing E. coli (STEC) O104:H4 2011 Outbreaks in Germany and France', *EFSA Supporting Publications*. John Wiley & Sons, Ltd, 8(7), p. 176E. doi: 10.2903/SP.EFSA.2011.EN-176.

Frank, C. *et al.* (2011) ' Epidemic Profile of Shiga-Toxin–Producing Escherichia coli O104:H4 Outbreak in Germany ', *New England Journal of Medicine*. Massachusetts Medical Society, 365(19), pp. 1771–1780. doi: 10.1056/NEJMOA1106483/SUPPL_FILE/NEJMOA1106483_DISCLOSURES.PDF.

Frankel, G. *et al.* (1998) 'Enteropathogenic and enterohaemorrhagic Escherichia coli : more subversive elements', *Molecular Microbiology*. John Wiley & Sons, Ltd, 30(5), pp. 911–921. doi:

10.1046/J.1365-2958.1998.01144.X.

Franzin, F. M. and Sircili, M. P. (2015) 'Locus of Enterocyte Effacement: A Pathogenicity Island Involved in the Virulence of Enteropathogenic and Enterohemorragic Escherichia coli Subjected to a Complex Network of Gene Regulation', *BioMed Research International*. Hindawi Limited, 2015. doi: 10.1155/2015/534738.

Fraser, M. E. *et al.* (2004) 'Structure of shiga toxin type 2 (Stx2) from Escherichia coli O157:H7', *The Journal of biological chemistry*. J Biol Chem, 279(26), pp. 27511–27517. doi: 10.1074/JBC.M401939200.

Freedman, S. B. *et al.* (2016) 'Editor's choice: Shiga Toxin–Producing Escherichia coli Infection, Antibiotics, and Risk of Developing Hemolytic Uremic Syndrome: A Meta-analysis', *Clinical Infectious Diseases: An Official Publication of the Infectious Diseases Society of America*. Oxford University Press, 62(10), p. 1251. doi: 10.1093/CID/CIW099.

Freestone, P. P. E., Haigh, R. D. and Lyte, M. (2007) 'Specificity of catecholamine-induced growth in Escherichia coli O157:H7, Salmonella enterica and Yersinia enterocolitica', *FEMS Microbiology Letters*. Oxford Academic, 269(2), pp. 221–228. doi: 10.1111/J.1574-6968.2006.00619.X.

Fukuda, S. *et al.* (2011) 'Bifidobacteria can protect from enteropathogenic infection through production of acetate', *Nature*. Nature, 469(7331), pp. 543–549. doi: 10.1038/NATURE09646.

Fuller, C. A. *et al.* (2011) 'Shiga Toxin Subtypes Display Dramatic Differences in Potency', *Infection and Immunity*. American Society for Microbiology (ASM), 79(3), p. 1329. doi: 10.1128/IAI.01182-10.

Gagnon, M. *et al.* (2004) 'In vitro inhibition of Escherichia coli O157:H7 by bifidobacterial strains of human origin', *International Journal of Food Microbiology*. Elsevier, 92(1), pp. 69–78. doi: 10.1016/J.IJFOODMICRO.2003.07.010.

García, M. D. *et al.* (2023) 'Molecular and Genetic Characterization of Colicinogenic Escherichia coli Strains Active against Shiga Toxin-Producing Escherichia coli O157:H7', *Foods 2023, Vol. 12, Page 2676*. Multidisciplinary Digital Publishing Institute, 12(14), p. 2676. doi: 10.3390/FOODS12142676.

Garimano, N., Amaral, M. M. and Ibarra, C. (2019) 'Endocytosis, Cytotoxicity, and Translocation of Shiga Toxin-2 Are Stimulated by Infection of Human Intestinal (HCT-8) Monolayers With an Hypervirulent E. coli O157:H7 Lacking stx2 Gene', *Frontiers in Cellular and Infection Microbiology*. Frontiers Media S.A., 9, p. 494125. doi: 10.3389/FCIMB.2019.00396/BIBTEX.

GASSER, C. *et al.* (1955) '[Hemolytic-uremic syndrome: bilateral necrosis of the renal cortex in acute acquired hemolytic anemia].', *Schweizerische medizinische Wochenschrift*, 85(38–39), pp. 905–9. Available at: https://europepmc.org/article/med/13274004 (Accessed: 16 November 2023).

Gelalcha, B. D. *et al.* (2022) 'Regulation Mechanisms of Virulence Genes in Enterohemorrhagic Escherichia coli', *Foodborne Pathogens and Disease*. Mary Ann Liebert Inc., 19(9), pp. 598–612. doi: 10.1089/FPD.2021.0103/ASSET/IMAGES/LARGE/FPD.2021.0103_FIGURE4.JPEG.

Gemikonakli, G. *et al.* (2023) 'Polypharmacy With High Drug Burden Index (DBI) Alters the Gut Microbiome Overriding Aging Effects and Is Reversible With Deprescribing', *The Journals of Gerontology Series A: Biological Sciences and Medical Sciences*. Oxford University Press, 78(2), p. 213. doi: 10.1093/GERONA/GLAC195.

Geurtsen, J. *et al.* (2022) 'Genomics and pathotypes of the many faces of Escherichia coli', *FEMS Microbiology Reviews*. Oxford University Press, 46(6). doi: 10.1093/FEMSRE/FUAC031.

Gigliucci, F. *et al.* (2018) 'Metagenomic characterization of the human intestinal microbiota in fecal samples from STEC-infected patients', *Frontiers in Cellular and Infection Microbiology*. Frontiers Media S.A., 8(FEB), p. 25. doi: 10.3389/FCIMB.2018.00025/FULL.

Gilligan, P. H. (1999) 'Escherichia Coli: EAEC, EHEC, EIEC, ETEC', *Clinics in Laboratory Medicine*. Elsevier, 19(3), pp. 505–521. doi: 10.1016/S0272-2712(18)30101-X.

Grant, G. N. *et al.* (1990) 'Differential plasmid rescue from transgenic mouse DNAs into Escherichia coli methylation-restriction mutants.', *Proceedings of the National Academy of Sciences of the United States of America*. National Academy of Sciences, 87(12), p. 4645. doi: 10.1073/PNAS.87.12.4645.

Greinacher, A. *et al.* (2011) 'Treatment of severe neurological defi cits with IgG depletion through immunoadsorption in patients with Escherichia coli O104:H4-associated haemolytic uraemic syndrome: A prospective trial', *The Lancet*. Elsevier B.V., 378(9797), pp. 1166–1173. doi: 10.1016/S0140-6736(11)61253-1.

Grif, K. *et al.* (1998a) 'Strain-specific differences in the amount of Shiga toxin released from enterohemorrhagic Escherichia coli O157 following exposure to subinhibitory concentrations of antimicrobial agents', *European Journal of Clinical Microbiology and Infectious Diseases*. Springer Verlag, 17(11), pp. 761–766. doi: 10.1007/S100960050181/METRICS.

Grif, K. *et al.* (1998b) 'Strain-specific differences in the amount of Shiga toxin released from enterohemorrhagic Escherichia coli O157 following exposure to subinhibitory concentrations of antimicrobial agents', *European journal of clinical microbiology & infectious diseases : official publication of the European Society of Clinical Microbiology*. Eur J Clin Microbiol Infect Dis, 17(11), pp. 761–766. doi: 10.1007/S100960050181.

Griffin, P. M. and Karmali, M. A. (2017) 'Emerging Public Health Challenges of Shiga Toxin–Producing Escherichia coli Related to Changes in the Pathogen, the Population, and the Environment', *Clinical Infectious Diseases*. Oxford Academic, 64(3), pp. 371–376. doi: 10.1093/CID/CIW708.

Griffin, P. M. and Tauxe, R. V. (1991) 'The epidemiology of infections caused by Escherichia coli O157:H7, other enterohemorrhagic E. coli, and the associated hemolytic uremic syndrome', *Epidemiologic reviews*. Epidemiol Rev, 13(1), pp. 60–98. doi: 10.1093/OXFORDJOURNALS.EPIREV.A036079.

Gu, J. *et al.* (2009) 'Enterohemorrhagic Escherichia coli trivalent recombinant vaccine containing EspA, intimin and Stx2 induces strong humoral immune response and confers protection in mice', *Microbes and Infection*. Elsevier Masson, 11(10–11), pp. 835–841. doi: 10.1016/J.MICINF.2009.04.024.

Guillard, T. *et al.* (2015) 'Fatal case of hemolytic-uremic syndrome in an adult due to a rare serogroup O91 Entero hemorrhagic Escherichia coli associated with a Clostridium difficile infection. More than meets the eye'. doi: 10.1016/j.ijid.2015.06.015.

Hamilton-Miller, J. M. T. (1984) 'Antimicrobial activity of 21 anti-neoplastic agents', *Br. J. Cancer*, 49, pp. 367–369.

Hammami, R. *et al.* (2012) 'Anti-infective properties of bacteriocins: an update', *Cellular and Molecular Life Sciences 2012 70:16*. Springer, 70(16), pp. 2947–2967. doi: 10.1007/S00018-012-1202-3.

Hamner, S. *et al.* (2013) 'Bile Salts Affect Expression of Escherichia coli O157:H7 Genes for Virulence and Iron Acquisition, and Promote Growth under Iron Limiting Conditions', *PLOS ONE*. Public Library of Science, 8(9), p. e74647. doi: 10.1371/JOURNAL.PONE.0074647.

Harkins, V. J., McAllister, D. A. and Reynolds, B. C. (2020) 'Shiga-Toxin E. coli Hemolytic Uremic Syndrome: Review of Management and Long-term Outcome', *Current Pediatrics Reports*. Springer Science and Business Media, LLC, 8(1), pp. 16–25. doi: 10.1007/S40124-020-00208-7/TABLES/1.

Harris, S. M. *et al.* (2012) 'Salt at concentrations relevant to meat processing enhances Shiga toxin 2 production in Escherichia coli O157:H7', *International Journal of Food Microbiology*. Elsevier, 159(3), pp. 186–192. doi: 10.1016/J.IJFOODMICRO.2012.09.007.

Henrique, I. de M. *et al.* (2022) 'Therapeutic Antibodies Against Shiga Toxins: Trends and Perspectives', *Frontiers in Cellular and Infection Microbiology*. Frontiers Media S.A., 12, p. 825856. doi: 10.3389/FCIMB.2022.825856/BIBTEX.

Hilborn, E. D. *et al.* (1999) 'A multistate outbreak of Escherichia coli O157:H7 infections associated with consumption of mesclun lettuce', *Archives of Internal Medicine*, 159(15), pp. 1758–1764. doi: 10.1001/archinte.159.15.1758.

Hirata, C., Kenzaka, T. and Akita, H. (2020) 'Late onset of hemolytic uremic syndrome after the appearance of prodromal gastrointestinal tract symptoms', *Clinical Case Reports*. Wiley-Blackwell, 8(10), p. 1910. doi: 10.1002/CCR3.3020.

Ho, P. I. *et al.* (2013) 'Reporter enzyme inhibitor study to aid assembly of orthogonal reporter gene assays', *ACS Chemical Biology*. American Chemical Society, 8(5), pp. 1009–1017. doi: 10.1021/CB3007264.

Hou, K. *et al.* (2022) 'Microbiota in health and diseases', *Signal Transduction and Targeted Therapy 2022 7:1*. Nature Publishing Group, 7(1), pp. 1–28. doi: 10.1038/s41392-022-00974-4.

Hughes, D. T. *et al.* (2009) 'The QseC Adrenergic Signaling Cascade in Enterohemorrhagic E. coli (EHEC)', *PLOS Pathogens*. Public Library of Science, 5(8), p. e1000553. doi: 10.1371/JOURNAL.PPAT.1000553.

Hurley, B. P. *et al.* (1999) 'Shiga toxins 1 and 2 translocate differently across polarized intestinal epithelial cells', *Infection and Immunity*. American Society for Microbiology, 67(12), pp. 6670–6677. doi: 10.1128/IAI.67.12.6670-6677.1999/ASSET/52F76C17-B848-4F4E-A818-A3BFC08AA95A/ASSETS/GRAPHIC/II1290755002.JPEG.

Hutka, B. *et al.* (2021) 'The Nonsteroidal Anti-Inflammatory Drug Ketorolac Alters the Small Intestinal Microbiota and Bile Acids Without Inducing Intestinal Damage or Delaying Peristalsis in the Rat', *Frontiers in Pharmacology*. Frontiers Media S.A., 12, p. 664177. doi: 10.3389/FPHAR.2021.664177/FULL.

Iida, K. I. *et al.* (2001) 'Type 1 Fimbriation and Its Phase Switching in Diarrheagenic Escherichia coli Strains', *Clinical and Diagnostic Laboratory Immunology*. American Society for Microbiology (ASM), 8(3), p. 489. doi: 10.1128/CDLI.8.3.489-495.2001.

Ikeda, K. *et al.* (1999) 'Effect of early fosfomycin treatment on prevention of hemolytic uremic syndrome accompanying Escherichia coli O157:H7 infection.', *Clinical Nephrology*, 52(6), pp. 357–362. Available at: https://europepmc.org/article/med/10604643 (Accessed: 20 November 2023).

Ikeda, K. *et al.* (2000) 'Predictors for the development of haemolytic uraemic syndrome with Escherichia coli O157 : H7 infections : with focus on the day of illness', *Epidemiol. Infect*. Cambridge University Press, 124, pp. 343–349.

Imamovic, L. and Muniesa, M. (2012) 'Characterizing RecA-Independent Induction of Shiga toxin2-Encoding Phages by EDTA Treatment', *PLoS ONE*. PLOS, 7(2). doi: 10.1371/JOURNAL.PONE.0032393.

Iversen, P. W. *et al.* (2012) 'HTS Assay Validation 2 . Stability and Process Studies', *Assay Guidance Manual*, (Md), pp. 1–26.

J. Worley, M. (2023) 'Immune evasion and persistence in enteric bacterial pathogens', *Gut Microbes*. Taylor & Francis, 15(1). doi: 10.1080/19490976.2022.2163839.

Jackson, M. P. *et al.* (1987) 'Nucleotide sequence analysis of the structural genes for Shiga-like toxin I encoded by bacteriophage 933J from Escherichia coli', *Microbial Pathogenesis*, 2(2), pp. 147–153. doi: 10.1016/0882-4010(87)90106-9.

Jimenez, A. G. *et al.* (2020) 'Diet-derived galacturonic acid regulates virulence and intestinal colonization in enterohaemorrhagic Escherichia coli and Citrobacter rodentium', *Nature Microbiology*. Springer US, 5(2), pp. 368–378. doi: 10.1038/s41564-019-0641-0.

Jordi, B. J. A. M. *et al.* (2001) 'Sensitivity of Shiga toxin-producing Escherichia coli (STEC) strains for colicins under different experimental conditions', *FEMS Microbiology Letters*. Oxford Academic, 204(2), pp. 329–334. doi: 10.1111/J.1574-6968.2001.TB10906.X.

Joseph, A. *et al.* (2020) 'Shiga Toxin-Associated Hemolytic Uremic Syndrome: A Narrative Review', *Toxins*, 12(2), pp. 1–46. doi: 10.3390/toxins12020067.

Kadry, A. A., El-Antrawy, M. A. and El-Ganiny, A. M. (2023) 'Impact of short chain fatty acids (SCFAs) on antimicrobial activity of new β-lactam/β-lactamase inhibitor combinations and on virulence of Escherichia coli isolates', *The Journal of Antibiotics 2023 76:4*. Nature Publishing Group, 76(4), pp. 225–235. doi: 10.1038/s41429-023-00595-1.

Kaper, J. B., Nataro, J. P. and Mobley, H. L. T. (2004) 'Pathogenic Escherichia coli', *Nature Reviews Microbiology 2004 2:2*. Nature Publishing Group, 2(2), pp. 123–140. doi: 10.1038/nrmicro818.

Karch, H. (2001) 'The role of virulence factors in enterohemorrhagic Escherichia coli (EHEC)--associated hemolytic-uremic syndrome', *Seminars in thrombosis and hemostasis*. Semin Thromb Hemost, 27(3), pp. 207–213. doi: 10.1055/S-2001-15250.

Karch, H. *et al.* (2012) 'The enemy within us: lessons from the 2011 European Escherichia coli O104:H4 outbreak', *EMBO Molecular Medicine*. Springer, 4(9), p. 841. doi: 10.1002/EMMM.201201662.

Karmali, M. A. *et al.* (1983) 'SPORADIC CASES OF HAEMOLYTIC-URAEMIC SYNDROME ASSOCIATED WITH FAECAL CYTOTOXIN AND CYTOTOXIN-PRODUCING ESCHERICHIA COLI IN STOOLS', *The Lancet*. Elsevier, 321(8325), pp. 619–620. doi: 10.1016/S0140-6736(83)91795-6.

Karmali, M. A. *et al.* (1985) 'The Association Between Idiopathic Hemolytic Uremic Syndrome and Infection by Verotoxin-Producing Escherichia coli', *The Journal of Infectious Diseases*. Oxford Academic, 151(5), pp. 775–782. doi: 10.1093/INFDIS/151.5.775.

Karmali, M. A. (1989) 'Infection by verocytotoxin-producing Escherichia coli', *Clinical microbiology reviews*. Clin Microbiol Rev, 2(1), pp. 15–38. doi: 10.1128/CMR.2.1.15.

Karmali, M. A., Gannon, V. and Sargeant, J. M. (2010) 'Verocytotoxin-producing Escherichia coli (VTEC)', *Veterinary microbiology*. Vet Microbiol, 140(3–4), pp. 360–370. doi: 10.1016/J.VETMIC.2009.04.011.

Kendall, M. M., Rasko, D. A. and Sperandio, V. (2010) 'The LysR-type regulator QseA regulates both characterized and putative virulence genes in enterohaemorrhagic Escherichia coli O157:H7', *Molecular Microbiology*. John Wiley & Sons, Ltd, 76(5), pp. 1306–1321. doi: 10.1111/J.1365-2958.2010.07174.X.

Kenny, B. *et al.* (1997) 'Enteropathogenic E. coli (EPEC) Transfers Its Receptor for Intimate Adherence into Mammalian Cells', *Cell*. Cell Press, 91(4), pp. 511–520. doi: 10.1016/S0092-8674(00)80437-7.

Khan, I. *et al.* (2021) 'Mechanism of the Gut Microbiota Colonization Resistance and Enteric Pathogen Infection', *Frontiers in Cellular and Infection Microbiology*. Frontiers Media S.A., 11, p. 716299. doi: 10.3389/FCIMB.2021.716299/BIBTEX.

Kiecka, A. and Szczepanik, M. (2023) 'Proton pump inhibitor-induced gut dysbiosis and immunomodulation: current knowledge and potential restoration by probiotics', *Pharmacological Reports*. Springer, 75(4), p. 791. doi: 10.1007/S43440-023-00489-X.

Kienesberger, S. *et al.* (2022) 'Enterotoxin tilimycin from gut-resident Klebsiella promotes mutational evolution and antibiotic resistance in mice', *Nature Microbiology 2022 7:11*. Nature Publishing Group, 7(11), pp. 1834–1848. doi: 10.1038/s41564-022-01260-3.

Kim, Y. G. *et al.* (2016) 'Essential Oils and Eugenols Inhibit Biofilm Formation and the Virulence of Escherichia coli O157:H7', *Scientific reports*. Sci Rep, 6. doi: 10.1038/SREP36377.

Kimmitt, P. T., Harwood, C. R. and Barer, M. R. (2000a) 'Toxin gene expression by shiga toxin-producing Escherichia coli: the role of antibiotics and the bacterial SOS response.', *Emerging Infectious Diseases*. Centers for Disease Control and Prevention, 6(5), p. 458. doi: 10.3201/EID0605.000503.

Kimmitt, P. T., Harwood, C. R. and Barer, M. R. (2000b) 'Toxin gene expression by Shiga toxin-producing Escherichia coli: The role of antibiotics and the bacterial SOS response', *Emerging Infectious Diseases*, 6(5), pp. 458–465. doi: 10.3201/eid0605.000503.

King, L. A. *et al.* (2011) 'Outbreak of Shiga Toxin-Producing Escherichia coli O104:H4 Associated With Organic Fenugreek Sprouts'. doi: 10.1093/cid/cis255.

Kobayashi, N. *et al.* (2013) 'Virulence gene profiles and population genetic analysis for exploration of pathogenic serogroups of shiga toxin-producing escherichia coli', *Journal of Clinical Microbiology*, 51(12), pp. 4022–4028. doi: 10.1128/JCM.01598-13.

Koeppel, M. B. *et al.* (2021) 'Scalable reporter assays to analyze the regulation of stx2 expression in shiga toxin-producing enteropathogens', *Toxins*. MDPI AG, 13(8). doi: 10.3390/TOXINS13080534/S1.

Kumar, A. *et al.* (2020) 'The Serotonin Neurotransmitter Modulates Virulence of Enteric Pathogens', *Cell host & microbe*. Cell Host Microbe, 28(1), pp. 41-53.e8. doi: 10.1016/J.CHOM.2020.05.004.

Kumar, A. *et al.* (2022) 'Indole Sensing Regulator (IsrR) Promotes Virulence Gene Expression in Enteric Pathogens', *mBio*. American Society for Microbiology, 13(4). doi: 10.1128/MBIO.01939-22/SUPPL_FILE/MBIO.01939-22-ST002.DOCX.

Lanz, J. *et al.* (2023) 'Disulfiram: Mechanisms, Applications, and Challenges', *Antibiotics*. MDPI, 12(3). doi: 10.3390/ANTIBIOTICS12030524/S1.

Lapeyraque, A.-L. *et al.* (2011) 'Eculizumab in Severe Shiga-Toxin–Associated HUS', *New England Journal of Medicine*. New England Journal of Medicine (NEJM/MMS), 364(26), pp. 2561–2563. doi: 10.1056/NEJMC1100859/SUPPL_FILE/NEJMC1100859_DISCLOSURES.PDF.

Lee, K. S., Park, S. Y. and Lee, M. S. (2022) 'Host Cellular Response during Enterohaemorrhagic Escherichia coli Shiga Toxin Exposure', *Microbiol. Biotechnol. Lett.* Korean Society for Microbiology and Biotechnology, 50(4), pp. 441–456. doi: 10.48022/MBL.2209.09004.

Lee, M. S., Cherla, R. P. and Tesh, V. L. (2010) 'Shiga Toxins: Intracellular Trafficking to the ER Leading to Activation of Host Cell Stress Responses', *Toxins*. Multidisciplinary Digital Publishing Institute (MDPI), 2(6), p. 1515. doi: 10.3390/TOXINS2061515.

Lee, M. S. and Tesh, V. L. (2019) 'Roles of Shiga Toxins in Immunopathology', *Toxins*. Multidisciplinary Digital Publishing Institute (MDPI), 11(4). doi: 10.3390/TOXINS11040212.

Lee, S. *et al.* (2007) 'Shiga toxin 1 induces apoptosis through the endoplasmic reticulum stress response in human monocytic cells', *Wiley Online LibrarySY Lee, MS Lee, RP Cherla, VL TeshCellular microbiology, 2008•Wiley Online Library*, 10(3), pp. 770–780. doi: 10.1111/j.1462-5822.2007.01083.x.

Lehouritis, P. *et al.* (2015) 'Local bacteria affect the efficacy of chemotherapeutic drugs', *Scientific Reports 2015 5:1*. Nature Publishing Group, 5(1), pp. 1–12. doi: 10.1038/srep14554.

Lengeler, J. (1980) 'Analysis of the physiological effects of the antibiotic streptozotocin on Escherichia coli K 12 and other sensitive bacteria', *Archives of Microbiology*. Springer-Verlag, 128(2), pp. 196–203. doi: 10.1007/BF00406158.

Li, J. *et al.* (2023) 'Evaluating the Antibacterial and Antivirulence Activities of Floxuridine against Streptococcus suis', *International journal of molecular sciences*. Int J Mol Sci, 24(18). doi: 10.3390/IJMS241814211.

Lingwood, C. A. *et al.* (1987) 'Glycolipid binding of purified and recombinant Escherichia coli produced verotoxin in vitro.', *Journal of Biological Chemistry*. Elsevier, 262(18), pp. 8834–8839. doi: 10.1016/S0021-9258(18)47490-X.

List, M. *et al.* (2016a) 'Comprehensive analysis of high-throughput screens with HiTSeekR', *Nucleic Acids Research*, 44(14), pp. 6639–6648. doi: 10.1093/nar/gkw554.

List, M. *et al.* (2016b) 'Comprehensive analysis of high-throughput screens with HiTSeekR', *Nucleic acids research*. Nucleic Acids Res, 44(14), pp. 6639–6648. doi: 10.1093/NAR/GKW554.

Liu, B. *et al.* (2022) 'Escherichia coli O157:H7 senses microbiota-produced riboflavin to increase its virulence in the gut', *Proceedings of the National Academy of Sciences of the United States of America*. National Academy of Sciences, 119(48), p. e2212436119. doi: 10.1073/PNAS.2212436119/SUPPL_FILE/PNAS.2212436119.SD02.XLSX.

Liu, B. *et al.* (2023) 'Enterohaemorrhagic E. coli utilizes host- and microbiota-derived L-malate as a signaling molecule for intestinal colonization', *Nature Communications 2023 14:1*. Nature Publishing Group, 14(1), pp. 1–16. doi: 10.1038/s41467-023-43149-7.

Liu, Y. *et al.* (2023) 'Diagnosis and Treatment for Shiga Toxin-Producing Escherichia coli Associated Hemolytic Uremic Syndrome', *Toxins*. Multidisciplinary Digital Publishing Institute (MDPI), 15(1). doi: 10.3390/TOXINS15010010.

Loś, J. M. *et al.* (2012) 'Altruism of Shiga toxin-producing Escherichia coli: recent hypothesis versus experimental results', *Frontiers in Cellular and Infection Microbiology*. Frontiers Media SA, 2, p. 166. doi: 10.3389/FCIMB.2012.00166.

Łoś, J. M. *et al.* (2009) 'Differential efficiency of induction of various lambdoid prophages responsible for production of Shiga toxins in response to different induction agents', *Microbial Pathogenesis*. Academic Press, 47(6), pp. 289–298. doi: 10.1016/J.MICPATH.2009.09.006.

Louise, C. B. and Obrig, T. G. (1995) 'Specific interaction of Escherichia coli O157:H7-derived Shiga-like toxin II with human renal endothelial cells', *The Journal of infectious diseases*. J Infect Dis, 172(5), pp. 1397–1401. doi: 10.1093/INFDIS/172.5.1397.

Luck, S. N. *et al.* (2005) 'Invasion of Epithelial Cells by Locus of Enterocyte Effacement-Negative Enterohemorrhagic Escherichia coli', *Infection and Immunity*. American Society for Microbiology (ASM), 73(5), p. 3063. doi: 10.1128/IAI.73.5.3063-3071.2005.

Luna-Guevara, J. J. *et al.* (2019) 'The Role of Pathogenic E. coli in Fresh Vegetables: Behavior, Contamination Factors, and Preventive Measures', *International Journal of Microbiology*. Hindawi Limited. doi: 10.1155/2019/2894328.

Madhogaria, B., Bhowmik, P. and Kundu, A. (2022) 'Correlation between human gut microbiome and diseases', *Infectious Medicine*. Elsevier, 1(3), pp. 180–191. doi: 10.1016/J.IMJ.2022.08.004.

Maier, L. *et al.* (2018a) 'Extensive impact of non-antibiotic drugs on human gut bacteria', *Nature*. Nature, 555(7698), pp. 623–628. doi: 10.1038/NATURE25979.

Maier, L. *et al.* (2018b) 'Extensive impact of non-antibiotic drugs on human gut bacteria', *Nature*. Nature Publishing Group, 555(7698), pp. 623–628. doi: 10.1038/nature25979.

Mallick, E. M. *et al.* (2014) 'The ability of an attaching and effacing pathogen to trigger localized actin assembly contributes to virulence by promoting mucosal attachment', *Cellular microbiology*. NIH Public Access, 16(9), p. 1405. doi: 10.1111/CMI.12302.

Mamber, S. W., Brookshire, K. W. and Forenza, S. (1990) 'Induction of the SOS response in Escherichia coli by azidothymidine and dideoxynucleosides.', *Antimicrobial Agents and Chemotherapy*. American Society for Microbiology (ASM), 34(6), p. 1237. doi: 10.1128/AAC.34.6.1237.

Marković, K. G. *et al.* (2022) 'Colicins and Microcins Produced by Enterobacteriaceae: Characterization, Mode of Action, and Putative Applications', *International Journal of Environmental Research and Public Health*. Multidisciplinary Digital Publishing Institute (MDPI), 19(18), p. 11825. doi: 10.3390/IJERPH191811825.

Martins, F. H. *et al.* (2022a) 'Interactions between Enterohemorrhagic Escherichia coli (EHEC) and Gut Commensals at the Interface of Human Colonoids', *mBio*. American Society for Microbiology, 13(3), pp. 1–15. doi: 10.1128/mbio.01321-22.

Martins, F. H. *et al.* (2022b) 'Interactions between Enterohemorrhagic Escherichia coli (EHEC) and Gut Commensals at the Interface of Human Colonoids', *mBio*. mBio, 13(3). doi: 10.1128/MBIO.01321-22.

Maslowska, K. H., Makiela-Dzbenska, K. and Fijalkowska, I. J. (2019) 'The SOS system: A complex and tightly regulated response to DNA damage', *Environmental and Molecular Mutagenesis*. Wiley-Blackwell, 60(4), p. 368. doi: 10.1002/EM.22267.

Matussek, A. *et al.* (2023) 'Genome-wide association study of hemolytic uremic syndrome causing Shiga toxin-producing Escherichia coli from Sweden, 1994–2018', *European Journal of Clinical Microbiology and Infectious Diseases*. Springer Science and Business Media Deutschland GmbH, 42(6), pp. 771–779. doi: 10.1007/S10096-023-04600-1/FIGURES/2.

Mayer, C. L. *et al.* (2012) 'Shiga Toxins and the Pathophysiology of Hemolytic Uremic Syndrome in Humans and Animals', *Toxins*. Multidisciplinary Digital Publishing Institute (MDPI), 4(11), p. 1261. doi: 10.3390/TOXINS4111261.

McGannon, C. M., Fuller, C. A. and Weiss, A. A. (2010) 'Different classes of antibiotics differentially influence shiga toxin production', *Antimicrobial Agents and Chemotherapy*. American Society for Microbiology, 54(9), pp. 3790–3798. doi: 10.1128/AAC.01783-09/ASSET/451B80AF-1CE1-4D41-BDEF-110EEDB02281/ASSETS/GRAPHIC/ZAC9991092630006.JPEG.

McWilliams, B. D. and Torres, A. G. (2014) 'EHEC Adhesins', *Microbiology spectrum*. NIH Public Access, 2(2), p. EHEC-0003-2013. doi: 10.1128/MICROBIOLSPEC.EHEC-0003-2013.

Mejías, M. P. *et al.* (2016) 'Development of camelid single chain antibodies against Shiga toxin type 2 (Stx2) with therapeutic potential against Hemolytic Uremic Syndrome (HUS)', *Scientific Reports 2016 6:1*. Nature Publishing Group, 6(1), pp. 1–11. doi: 10.1038/srep24913.

Mellies, J. L. and Lorenzen, E. (2014) ' Enterohemorrhagic Escherichia coli Virulence Gene Regulation ', *Microbiology Spectrum*. American Society for Microbiology, 2(4). doi: 10.1128/MICROBIOLSPEC.EHEC-0004-2013/ASSET/6955822C-4FB2-4A1D-A150-8CF062344723/ASSETS/GRAPHIC/EHEC-0004-2013-FIG5.GIF.

Mellmann, A. *et al.* (2011) 'Prospective genomic characterization of the german enterohemorrhagic Escherichia coli O104:H4 outbreak by rapid next generation sequencing technology', *PLoS ONE*, 6(7). doi: 10.1371/JOURNAL.PONE.0022751.

Mengistu, D. Y. and Mengesha, Y. (2023) 'New approaches for severity intervention and rapid diagnosis of enterohemorrhagic Escherichia coli: a review', *All Life*. Taylor & Francis, 16(1). doi:

10.1080/26895293.2023.2218582.

Militello, K. T. *et al.* (2016) '5-azacytidine induces transcriptome changes in Escherichia coli via DNA methylation-dependent and DNA methylation-independent mechanisms', *BMC Microbiology*. BioMed Central Ltd., 16(1), pp. 1–12. doi: 10.1186/S12866-016-0741-4/TABLES/4.

Mo, C. Y. *et al.* (2018) 'Inhibitors of LexA Autoproteolysis and the Bacterial SOS Response Discovered by an Academic-Industry Partnership', *ACS Infectious Diseases*. American Chemical Society, 4(3), pp. 349–359. doi: 10.1021/ACSINFECDIS.7B00122/SUPPL_FILE/ID7B00122_SI_001.PDF.

Moreira de Gouveia, M. I., Bernalier-Donadille, A. and Jubelin, G. (2024) 'Enterobacteriaceae in the Human Gut: Dynamics and Ecological Roles in Health and Disease', *Biology 2024, Vol. 13, Page 142*. Multidisciplinary Digital Publishing Institute, 13(3), p. 142. doi: 10.3390/BIOLOGY13030142.

Mosso, H. M. *et al.* (2019) 'A Putative Microcin Amplifies Shiga Toxin 2a Production of Escherichia coli O157:H7', *Journal of bacteriology*. J Bacteriol, 202(1). doi: 10.1128/JB.00353-19.

Mousa, W. K. (2022) 'The microbiome-product colibactin hits unique cellular targets mediating host–microbe interaction', *Frontiers in Pharmacology*. Frontiers Media SA, 13. doi: 10.3389/FPHAR.2022.958012.

Moxley, R. A. *et al.* (2017) 'Efficacy of Urtoxazumab (TMA-15 Humanized Monoclonal Antibody Specific for Shiga Toxin 2) Against Post-Diarrheal Neurological Sequelae Caused by Escherichia coli O157:H7 Infection in the Neonatal Gnotobiotic Piglet Model', *Toxins 2017, Vol. 9, Page 49*. Multidisciplinary Digital Publishing Institute, 9(2), p. 49. doi: 10.3390/TOXINS9020049.

Mühlen, S. *et al.* (2020a) 'Identification of Antibiotics That Diminish Disease in a Murine Model of Enterohemorrhagic Escherichia coli Infection', *Antimicrobial Agents and Chemotherapy*. American Society for Microbiology (ASM), 64(4). doi: 10.1128/AAC.02159-19.

Mühlen, S. *et al.* (2020b) 'Identification of Antibiotics That Diminish Disease in a Murine Model of Enterohemorrhagic Escherichia coli Infection', *Antimicrobial agents and chemotherapy*. Antimicrob Agents Chemother, 64(4). doi: 10.1128/AAC.02159-19.

Mühlen, S. and Dersch, P. (2020) 'Treatment Strategies for Infections With Shiga Toxin-Producing Escherichia coli', *Frontiers in Cellular and Infection Microbiology*, 10(May), pp. 1–17. doi: 10.3389/fcimb.2020.00169.

Munns, K. D. *et al.* (2015) 'Perspectives on Super-Shedding of Escherichia coli O157:H7 by Cattle', *https://home.liebertpub.com/fpd*. Mary Ann Liebert, Inc. 140 Huguenot Street, 3rd Floor New Rochelle, NY 10801 USA , 12(2), pp. 89–103. doi: 10.1089/FPD.2014.1829.

Murakami, J. *et al.* (2000) 'Macrolides and clindamycin suppress the release of Shiga-like toxins from Escherichia coli O157:H7 in vitro', *International journal of antimicrobial agents*. Int J Antimicrob Agents, 15(2), pp. 103–109. doi: 10.1016/S0924-8579(00)00126-6.

Nagata, N. *et al.* (2022) 'Population-level Metagenomics Uncovers Distinct Effects of Multiple Medications on the Human Gut Microbiome', *Gastroenterology*. W.B. Saunders, 163(4), pp. 1038–1052. doi: 10.1053/j.gastro.2022.06.070.

Nakanishi, N. *et al.* (2009) 'Regulation of virulence by butyrate sensing in enterohaemorrhagic Escherichia coli', *Microbiology (Reading, England)*. Microbiology (Reading), 155(Pt 2), pp. 521–530. doi: 10.1099/MIC.0.023499-0.

Nakata, K. *et al.* (1997) '[Suppressive effect of clarithromycin on the production of verotoxin by E. coli O157]', *Kansenshogaku zasshi. The Journal of the Japanese Association for Infectious Diseases*. Kansenshogaku Zasshi, 71(5), pp. 437–442. doi: 10.11150/KANSENSHOGAKUZASSHI1970.71.437.

Nascimento, J. M. C., Silva, M. V. and Fernandes, S. A. (2008) 'Zidovudine: An Alternative Agent to Antimicrobials in the Treatment of Salmonellosis?', *International Journal of Infectious Diseases*. Elsevier BV, 12, pp. e217–e218. doi: 10.1016/j.ijid.2008.05.540.

Nataro, J. P. and Kaper, J. B. (1998) 'Diarrheagenic Escherichia coli', *Clinical Microbiology Reviews*. American Society for Microbiology (ASM), 11(1), p. 142. doi: 10.1128/CMR.11.1.142.

Naylor, S. W. *et al.* (2003) 'Lymphoid follicle-dense mucosa at the terminal rectum is the principal site of colonization of enterohemorrhagic Escherichia coli O157:H7 in the bovine host', *Infection and Immunity*. American Society for Microbiology, 71(3), pp. 1505–1512. doi: 10.1128/IAI.71.3.1505-1512.2003/ASSET/60FF837D-A455-4339-BBD3-ADABD52964EE/ASSETS/GRAPHIC/II0331339004.JPEG.

Neu, C. *et al.* (2023) 'Cardiovascular impairment in Shiga-toxin-2-induced experimental hemolytic–uremic syndrome: a pilot study', *Frontiers in Immunology*. Frontiers Media SA, 14. doi: 10.3389/FIMMU.2023.1252818/FULL.

Nguyen, Y. and Sperandio, V. (2012) 'Enterohemorrhagic E. coli (EHEC) pathogenesis', *Frontiers in Cellular and Infection Microbiology*. Frontiers Media SA, 2, p. 90. doi: 10.3389/FCIMB.2012.00090.

Nickolai, D. J. *et al.* (1985) 'Effects of storage temperature and pH on the stability of eleven beta-lactam antibiotics in MIC trays', *Journal of clinical microbiology*. J Clin Microbiol, 21(3), pp. 366–370. doi: 10.1128/JCM.21.3.366-370.1985.

Nishino, K. *et al.* (2021) 'Function and Inhibitory Mechanisms of Multidrug Efflux Pumps', *Frontiers in Microbiology*. Frontiers Media S.A., 12, p. 737288. doi: 10.3389/FMICB.2021.737288/BIBTEX.

Nowicki, D. *et al.* (2016) 'Isothiocyanates as effective agents against enterohemorrhagic Escherichia coli: Insight to the mode of action', *Scientific Reports*. Nature Publishing Group, 6(February), pp. 1–12. doi: 10.1038/srep22263.

O'Brien, A. D. *et al.* (1983) 'Escherichia coli O157:H7 strains associated with haemorrhagic colitis in the United States produce a Shigella dysenteriae 1 (SHIGA) like cytotoxin', *Lancet (London, England)*. Lancet, 1(8326 Pt 1), p. 702. doi: 10.1016/S0140-6736(83)91987-6.

O'Brien, A. D. *et al.* (1984) 'Shiga-like toxin-converting phages from Escherichia coli strains that cause hemorrhagic colitis or infantile diarrhea', *Science*, 226(4675), pp. 694–696. doi: 10.1126/SCIENCE.6387911.

O'Brien, A. D. and LaVeck, G. D. (1983) 'Purification and characterization of a Shigella dysenteriae 1-like toxin produced by Escherichia coli', *Infection and immunity*. Infect Immun, 40(2), pp. 675–683. doi: 10.1128/IAI.40.2.675-683.1983.

Obata, F. *et al.* (2008) 'Shiga Toxin 2 Affects the Central Nervous System Through Receptor Gb3 Localized to Neurons', *The Journal of infectious diseases*. NIH Public Access, 198(9), p. 1398. doi: 10.1086/591911.

Obrig, T. G. (2010) 'Escherichia coli Shiga Toxin Mechanisms of Action in Renal Disease', *Toxins*. Multidisciplinary Digital Publishing Institute (MDPI), 2(12), p. 2769. doi: 10.3390/TOXINS2122769.

Ogawa, M. *et al.* (2001) 'Protective effect of Lactobacillus casei strain Shirota on Shiga toxin-producing Escherichia coli O157:H7 infection in infant rabbits', *Infection and Immunity*. American Society for Microbiology, 69(2), pp. 1101–1108. doi: 10.1128/IAI.69.2.1101-1108.2001/ASSET/B10FBE74-8C2A-4B74-92C1-8903D69CFD71/ASSETS/GRAPHIC/II0211035004.JPEG.

Ogunrinola, G. A. *et al.* (2020) 'The Human Microbiome and Its Impacts on Health', *International Journal of Microbiology*. Hindawi Limited, 2020. doi: 10.1155/2020/8045646.

Ogura, Y. *et al.* (2015) 'The Shiga toxin 2 production level in enterohemorrhagic Escherichia coli O157:H7 is correlated with the subtypes of toxin-encoding phage', *Scientific Reports 2015 5:1*. Nature Publishing Group, 5(1), pp. 1–11. doi: 10.1038/srep16663.

Ohnishi, T. *et al.* (1986) 'An ovulation inducing agent containing clomiphene citrate causes DNA-strand breaks without SOS responses in Escherichia coli', *Mutation Research/DNA Repair Reports*. Elsevier, 165(2), pp. 57–61. doi: 10.1016/0167-8817(86)90060-X.

Olsen, S. J. *et al.* (2002) 'A waterborne outbreak of Escherichia coli O157:H7 infections and hemolytic uremic syndrome: Implications for rural water systems', *Emerging Infectious Diseases*, 8(4), pp. 370–375. doi: 10.3201/eid0804.000218.

Omisakin, F. *et al.* (2003) 'Concentration and prevalence of Escherichia coli O157 in cattle feces at slaughter', *Applied and Environmental Microbiology*. American Society for Microbiology, 69(5), pp. 2444–2447. doi: 10.1128/AEM.69.5.2444-2447.2003/ASSET/F04F7C68-8B80-40C9-8DCA-A3BE6A62637E/ASSETS/GRAPHIC/AM0531858002.JPEG.

Oren, A. and Garrity, G. M. (2021) 'Valid publication of the names of forty-two phyla of prokaryotes', *International Journal of Systematic and Evolutionary Microbiology*. Microbiology Society, 71(10), p. 005056. doi: 10.1099/IJSEM.0.005056/CITE/REFWORKS.

Orth, D. *et al.* (2008) 'Prevention and treatment of enterohemorrhagic Escherichia coli infections in humans', *Expert Review of Anti-infective Therapy*. Taylor & Francis, 6(1), pp. 101–108. doi: 10.1586/14787210.6.1.101.

Pacheco, A. R. *et al.* (2012) 'Fucose sensing regulates bacterial intestinal colonization', *Nature*, 492(7427), pp. 113–117. doi: 10.1038/NATURE11623.

Pacheco, A. R. and Sperandio, V. (2012) 'Shiga toxin in enterohemorrhagic E.coli: regulation and novel anti-virulence strategies.', *Frontiers in cellular and infection microbiology*, 2(June), p. 81. doi: 10.3389/fcimb.2012.00081.

Pakbin, B., Brück, W. M. and Rossen, J. W. A. (2021) 'Virulence Factors of Enteric Pathogenic Escherichia coli: A Review', *International Journal of Molecular Sciences*. Multidisciplinary Digital Publishing Institute (MDPI), 22(18). doi: 10.3390/IJMS22189922.

Palacios, N. *et al.* (2021) 'Effect of Levodopa Initiation on the Gut Microbiota in Parkinson's Disease', *Frontiers in Neurology*. Frontiers Media SA, 12, p. 574529. doi: 10.3389/FNEUR.2021.574529.

Park, D. S. and Park, J. H. (2021) 'Characteristics of Bacteriophage Isolates and Expression of Shiga Toxin Genes Transferred to Non Shiga Toxin-Producing E. coli by Transduction', *Journal of Microbiology and Biotechnology*. Korean Society for Microbiology and Biotechnology, 31(5), p. 710. doi: 10.4014/JMB.2102.02040.

Patangia, D. V. *et al.* (2022) 'Impact of antibiotics on the human microbiome and consequences for host health', *MicrobiologyOpen*. Wiley-Blackwell, 11(1). doi: 10.1002/MBO3.1260.

Paton, J. C. and Paton, A. W. (1998) 'Pathogenesis and Diagnosis of Shiga Toxin-Producing Escherichia coli Infections', *Clinical Microbiology Reviews*. American Society for Microbiology (ASM), 11(3), p. 450. doi: 10.1128/CMR.11.3.450.

Pennington, H. (2010) 'Escherichia coli O157', *Lancet (London, England)*. Lancet, 376(9750), pp. 1428–1435. doi: 10.1016/S0140-6736(10)60963-4.

Phillips, A. D. *et al.* (2000) 'Enterohaemorrhagic Escherichia coliO157:H7 target Peyer's patches in humans and cause attaching/effacing lesions in both human and bovine intestine', *Gut*. BMJ Publishing Group, 47(3), pp. 377–381. doi: 10.1136/GUT.47.3.377.

Pifer, R. *et al.* (2018) 'Redox, amino acid, and fatty acid metabolism intersect with bacterial virulence

in the gut', *Proceedings of the National Academy of Sciences of the United States of America*, 115(45), pp. E10712–E10719. doi: 10.1073/pnas.1813451115.

Pinto, A., Celi, A. B. and Goldstein, J. (2023) 'Shiga toxin and its effect on the central nervous system', *Trending Topics in Escherichia coli Research: The Latin American Perspective*. Springer International Publishing, pp. 177–204. doi: 10.1007/978-3-031-29882-0_8/COVER.

Pinto, G. *et al.* (2021) 'Insights into the genome architecture and evolution of Shiga toxin encoding bacteriophages of Escherichia coli', *BMC Genomics*. BMC, 22(1). doi: 10.1186/S12864-021-07685-0.

Pö, L. *et al.* (2023) 'Microbiota-derived genotoxin tilimycin generates colonic stem cell mutations ll Microbiota-derived genotoxin tilimycin generates colonic stem cell mutations', *CellReports*, 42, p. 112199. doi: 10.1016/j.celrep.2023.112199.

Podlesek, Z. and Žgur Bertok, D. (2020) 'The DNA Damage Inducible SOS Response Is a Key Player in the Generation of Bacterial Persister Cells and Population Wide Tolerance', *Frontiers in Microbiology*. Frontiers Media S.A., 11, p. 561210. doi: 10.3389/FMICB.2020.01785/BIBTEX.

Pokharel, P., Dhakal, S. and Dozois, C. M. (2023) 'The Diversity of Escherichia coli Pathotypes and Vaccination Strategies against This Versatile Bacterial Pathogen', *Microorganisms 2023, Vol. 11, Page 344*. Multidisciplinary Digital Publishing Institute, 11(2), p. 344. doi: 10.3390/MICROORGANISMS11020344.

Price, C. T. D., Lee, I. R. and Gustafson, J. E. (2000) 'The effects of salicylate on bacteria', *The International Journal of Biochemistry & Cell Biology*. Pergamon, 32(10), pp. 1029–1043. doi: 10.1016/S1357-2725(00)00042-X.

Pundziene, B. *et al.* (2015) 'Long-term follow-up of children with typical hemolytic uremic syndrome', *Medicina*. No longer published by Elsevier, 51(3), pp. 146–151. doi: 10.1016/J.MEDICI.2015.06.004.

Purdel, C. *et al.* (2023) 'Exploring the potential impact of probiotic use on drug metabolism and efficacy', *Biomedicine & Pharmacotherapy*. Elsevier Masson, 161, p. 114468. doi: 10.1016/J.BIOPHA.2023.114468.

Putze, J. *et al.* (2009) 'Genetic structure and distribution of the colibactin genomic island among members of the family Enterobacteriaceae', *Infection and Immunity*, 77(11), pp. 4696–4703. doi: 10.1128/IAI.00522-09.

Quiñones, B. *et al.* (2012) 'O-antigen and Virulence Profiling of Shiga Toxin-Producing Escherichia coli by a Rapid and Cost–Effective DNA Microarray Colorimetric Method', *Frontiers in Cellular and Infection Microbiology*. Frontiers Media SA, 2, p. 61. doi: 10.3389/FCIMB.2012.00061.

Rahal, E. A. *et al.* (2011) 'Role of rifampicin in limiting Escherichia coli O157:H7 Shiga-like toxin expression and enhancement of survival of infected BALB/c mice', *International journal of antimicrobial agents*. Int J Antimicrob Agents, 37(2), pp. 135–139. doi: 10.1016/J.IJANTIMICAG.2010.10.009.

Rahman, M. S., Pal, A. K. and Chatterjee, S. N. (1993) 'Induction of SOS like responses by nitrofurantoin in Vibrio cholerae el tor cells', *Archives of microbiology*. Arch Microbiol, 159(1), pp. 98–100. doi: 10.1007/BF00244270.

Ramatla, T. *et al.* (2024) 'Molecular detection of Shiga toxin and extended-spectrum beta-lactamase (ESBL)-producing Escherichia coli isolates from sheep and goats', *Molecular Biology Reports*. Springer Science and Business Media B.V., 51(1), pp. 1–12. doi: 10.1007/S11033-023-08987-0/FIGURES/2.

Ramstad, S. N. *et al.* (2021) 'Effects of antimicrobials on Shiga toxin production in high-virulent Shiga toxin-producing Escherichia coli', *Microbial Pathogenesis*. Academic Press, 152, p. 104636. doi: 10.1016/J.MICPATH.2020.104636.

Rangel, J. M. *et al.* (2005) 'Epidemiology of Escherichia coli O157:H7 Outbreaks, United States, 1982–2002', *Emerging Infectious Diseases*. Centers for Disease Control and Prevention, 11(4), p. 603. doi: 10.3201/EID1104.040739.

Rasko, D. A. *et al.* (2011) ' Origins of the E. coli Strain Causing an Outbreak of Hemolytic–Uremic Syndrome in Germany ', *New England Journal of Medicine*. Massachusetts Medical Society, 365(8), pp. 709–717. doi: 10.1056/NEJMOA1106920/SUPPL_FILE/NEJMOA1106920_DISCLOSURES.PDF.

Rasooly, R. *et al.* (2017) 'Low-Cost Charged-Coupled Device (CCD) Based Detectors for Shiga Toxins Activity Analysis', *Methods in molecular biology (Clifton, N.J.)*. Methods Mol Biol, 1571, pp. 233–249. doi: 10.1007/978-1-4939-6848-0_15.

Rebuffat, S. (2011) 'Bacteriocins from Gram-Negative Bacteria: A Classification?', *Prokaryotic Antimicrobial Peptides*. Springer, New York, NY, pp. 55–72. doi: 10.1007/978-1-4419-7692-5_4.

Revitt-Mills, S. A. *et al.* (2022) 'Defects in DNA double-strand break repair resensitize antibiotic-resistant Escherichia coli to multiple bactericidal antibiotics', *MicrobiologyOpen*. John Wiley & Sons, Ltd, 11(5), p. e1316. doi: 10.1002/MBO3.1316.

Reznikov, M. and McDonald, P. J. (1983) 'Effect of Metronidazole on Escherichia coli in the Presence of Bacteroides fragilis: An Investigation in Mice', *Chemotherapy*. S. Karger AG, 29(3), pp. 225–229. doi: 10.1159/000238201.

Rigottier-Gois, L. (2013) 'Dysbiosis in inflammatory bowel diseases: the oxygen hypothesis', *The ISME journal*. ISME J, 7(7), pp. 1256–1261. doi: 10.1038/ISMEJ.2013.80.

Rki (2011) 'Abschließende Darstellung und Bewertung der epidemiologischen Erkenntnisse im'. Available at: www.rki.de (Accessed: 17 January 2024).

Rodríguez-Rubio, L. *et al.* (2021) 'Bacteriophages of Shiga Toxin-Producing Escherichia coli and Their Contribution to Pathogenicity', *Pathogens*. Multidisciplinary Digital Publishing Institute (MDPI), 10(4). doi: 10.3390/PATHOGENS10040404.

Rohde, H. *et al.* (2011) 'Open-source genomic analysis of Shiga-toxin-producing E. coli O104:H4', *The New England journal of medicine*. N Engl J Med, 365(8), pp. 718–724. doi: 10.1056/NEJMOA1107643.

Rozanov, D. V., D'Ari, R. and Sineoky, S. P. (1998) 'RecA-independent pathways of lambdoid prophage induction in Escherichia coli', *Journal of Bacteriology*, 180(23), pp. 6306–6315. doi: 10.1128/.180.23.6306-6315.1998.

De Sablet, T. *et al.* (2009) 'Human Microbiota-Secreted Factors Inhibit Shiga Toxin Synthesis by Enterohemorrhagic Escherichia coli O157:H7', *Infection and Immunity*. American Society for Microbiology (ASM), 77(2), p. 783. doi: 10.1128/IAI.01048-08.

Safdar, N. *et al.* (2002) 'Risk of Hemolytic Uremic Syndrome After Antibiotic Treatment of Escherichia coli O157:H7 Enteritis: A Meta-analysis', *JAMA*. American Medical Association, 288(8), pp. 996–1001. doi: 10.1001/JAMA.288.8.996.

Salvadori, M. and Bertoni, E. (2013) 'Update on hemolytic uremic syndrome: Diagnostic and therapeutic recommendations', *World Journal of Nephrology*. Baishideng Publishing Group Inc, 2(3), p. 56. doi: 10.5527/WJN.V2.I3.56.

Sandvig, K. (2001) 'Shiga toxins', *Toxicon*. Pergamon, 39(11), pp. 1629–1635. doi: 10.1016/S0041-0101(01)00150-7.

Sandvig, K. *et al.* (2010) 'Endocytosis and retrograde transport of Shiga toxin', *Elsevier*. doi: 10.1016/j.toxicon.2009.11.021.

Santos, A. C. de M. *et al.* (2020) 'Diversity of Hybrid- and Hetero-Pathogenic Escherichia coli and Their Potential Implication in More Severe Diseases', *Frontiers in Cellular and Infection Microbiology*. Frontiers Media S.A., 10, p. 532570. doi: 10.3389/FCIMB.2020.00339/BIBTEX.

Sayin, S. *et al.* (2023) 'Evolved bacterial resistance to the chemotherapy gemcitabine modulates its efficacy in co-cultured cancer cells', *eLife*. eLife Sciences Publications, Ltd, 12, p. 83140. doi: 10.7554/ELIFE.83140.

Schamberger, G. P. and Diez-Gonzalez, F. (2002) 'Selection of Recently Isolated Colicinogenic Escherichia coli Strains Inhibitory to Escherichia coli O157:H7', *Journal of Food Protection*. Elsevier, 65(9), pp. 1381–1387. doi: 10.4315/0362-028X-65.9.1381.

Scheutz, F. *et al.* (2012) 'Multicenter evaluation of a sequence-based protocol for subtyping Shiga toxins and standardizing Stx nomenclature', *Journal of Clinical Microbiology*, 50(9), pp. 2951–2963. doi: 10.1128/JCM.00860-12.

Schiller, P. *et al.* (2021) 'The Superior Adherence Phenotype of E. coli O104:H4 is Directly Mediated by the Aggregative Adherence Fimbriae Type I', *Virulence*. Taylor & Francis, 12(1), p. 346. doi: 10.1080/21505594.2020.1868841.

Schink, S. J. *et al.* (2022) 'MetA is a "thermal fuse" that inhibits growth and protects Escherichia coli at elevated temperatures', *Cell reports*. Cell Rep, 40(9). doi: 10.1016/J.CELREP.2022.111290.

Schüller, S. (2011) 'Shiga Toxin Interaction with Human Intestinal Epithelium', *Toxins 2011, Vol. 3, Pages 626-639*. Molecular Diversity Preservation International, 3(6), pp. 626–639. doi: 10.3390/TOXINS3060626.

Schwartzman, G. *et al.* (1979) 'Chlortetracycline Hydrochloride', *Analytical Profiles of Drug Substances and Excipients*. Academic Press, 8(C), pp. 101–137. doi: 10.1016/S0099-5428(08)60115-X.

Schwidder, M., Heinisch, L. and Schmidt, H. (2019) 'Genetics, Toxicity, and Distribution of Enterohemorrhagic Escherichia coli Hemolysin', *Toxins 2019, Vol. 11, Page 502*. Multidisciplinary Digital Publishing Institute, 11(9), p. 502. doi: 10.3390/TOXINS11090502.

Secher, T. *et al.* (2015) 'Retrograde Trafficking Inhibitor of Shiga Toxins Reduces Morbidity and Mortality of Mice Infected with Enterohemorrhagic Escherichia coli', *Antimicrobial agents and chemotherapy*. Antimicrob Agents Chemother, 59(8), pp. 5010–5013. doi: 10.1128/AAC.00455-15.

Segata, N. *et al.* (2011) 'Metagenomic biomarker discovery and explanation', *Genome biology*. Genome Biol, 12(6). doi: 10.1186/GB-2011-12-6-R60.

Sekar, A. *et al.* (2024) 'Synergistic use of anti-inflammatory ketorolac and gentamicin to target staphylococcal biofilms', *Journal of Translational Medicine*. BioMed Central Ltd, 22(1), pp. 1–20. doi: 10.1186/S12967-024-04871-Y/FIGURES/5.

Selyunin, A. S. *et al.* (2019) 'Tamoxifen blocks retrograde trafficking of Shiga toxin 1 and 2 and protects against lethal toxicosis', *Life science alliance*. Life Sci Alliance, 2(3). doi: 10.26508/LSA.201900439.

Sexton, J. Z. *et al.* (2010) 'Novel Inhibitors of E. coli RecA ATPase Activity', *Current Chemical Genomics*. Bentham Science Publishers, 4(1), p. 34. doi: 10.2174/1875397301004010034.

Sheng, S. *et al.* (2023) 'Effects of levodopa on gut bacterial antibiotic resistance in Parkinson's disease rat', *Frontiers in Aging Neuroscience*. Frontiers Media S.A., 15, p. 1122712. doi: 10.3389/FNAGI.2023.1122712/BIBTEX.

Sherman, P. M. *et al.* (2005) 'Probiotics reduce enterohemorrhagic Escherichia coli O157:H7- and enteropathogenic E. coli O127:H6-induced changes in polarized T84 epithelial cell monolayers by

reducing bacterial adhesion and cytoskeletal rearrangements', *Infection and Immunity*. American Society for Microbiology, 73(8), pp. 5183–5188. doi: 10.1128/IAI.73.8.5183-5188.2005/ASSET/083B6CE8-D4FA-4D93-9033-6E5D005C055F/ASSETS/GRAPHIC/ZII0080550900004.JPEG.

Shimada, O. *et al.* (1999) 'Rearrangements of actin cytoskeleton during infection with Escherichia coli O157 in macrophages', *Cell structure and function*. Cell Struct Funct, 24(5), pp. 237–246. doi: 10.1247/CSF.24.237.

Shimizu, T. *et al.* (2011) 'Construction of a novel bioluminescent reporter system for investigating Shiga toxin expression of enterohemorrhagic Escherichia coli', *Gene*. Elsevier, 478(1–2), pp. 1–10. doi: 10.1016/J.GENE.2011.01.006.

Shimizu, T., Ohta, Y. and Noda, M. (2009) 'Shiga Toxin 2 Is Specifically Released from Bacterial Cells by Two Different Mechanisms', *Infection and Immunity*. American Society for Microbiology (ASM), 77(7), p. 2813. doi: 10.1128/IAI.00060-09.

Shun, T. Y. *et al.* (2011) 'Identifying actives from HTS data sets: Practical approaches for the selection of an appropriate HTS data-processing method and quality control review', *Journal of Biomolecular Screening*. SAGE PublicationsSage CA: Los Angeles, CA, 16(1), pp. 1–14. doi: 10.1177/1087057110389039/ASSET/IMAGES/LARGE/10.1177_1087057110389039-FIG6.JPEG.

Siegler, R. L. *et al.* (2003) 'Response to Shiga toxin 1 and 2 in a baboon model of hemolytic uremic syndrome', *Pediatric Nephrology*. Springer, 18(2), pp. 92–96. doi: 10.1007/S00467-002-1035-7/METRICS.

Silpe, J. E. *et al.* (2022) 'The bacterial toxin colibactin triggers prophage induction', *Nature 2022 603:7900*. Nature Publishing Group, 603(7900), pp. 315–320. doi: 10.1038/s41586-022-04444-3.

Smith, W. E. *et al.* (2003) 'Shiga toxin 1 triggers a ribotoxic stress response leading to p38 and JNK activation and induction of apoptosis in intestinal epithelial cells', *Infection and immunity*. Infect Immun, 71(3), pp. 1497–1504. doi: 10.1128/IAI.71.3.1497-1504.2003.

Ståhl, A. lie *et al.* (2015) 'A Novel Mechanism of Bacterial Toxin Transfer within Host Blood Cell-Derived Microvesicles', *PLOS Pathogens*. Public Library of Science, 11(2), p. e1004619. doi: 10.1371/JOURNAL.PPAT.1004619.

Stecher, B. *et al.* (2010) 'Like will to like: abundances of closely related species can predict susceptibility to intestinal colonization by pathogenic and commensal bacteria', *PLoS pathogens*. PLoS Pathog, 6(1). doi: 10.1371/JOURNAL.PPAT.1000711.

Stecher, B. (2015) 'The Roles of Inflammation, Nutrient Availability and the Commensal Microbiota in Enteric Pathogen Infection', *Microbiology Spectrum*. ASM PressWashington, DC, 3(3). doi: 10.1128/MICROBIOLSPEC.MBP-0008-2014.

Stigi, K. A. *et al.* (2012) 'Laboratory practices and incidence of non-O157 shiga toxin-producing Escherichia coli infections', *Emerging infectious diseases*. Emerg Infect Dis, 18(3), pp. 477–479. doi: 10.3201/EID1803.111358.

Storr, M. and Stengel, A. (2021) '[Systematic review: clinical evidence of probiotics in the prevention of antibiotic-associated diarrhoea]', *MMW Fortschritte der Medizin*. MMW Fortschr Med, 163(Suppl 4), pp. 19–26. doi: 10.1007/S15006-021-9762-5.

Sukumar, N. *et al.* (2014) 'Exploitation of Mycobacterium tuberculosis Reporter Strains to Probe the Impact of Vaccination at Sites of Infection', *PLOS Pathogens*. Public Library of Science, 10(9), p. e1004394. doi: 10.1371/JOURNAL.PPAT.1004394.

Sumabe, B. K. *et al.* (2021) 'Nucleoside Analogues Are Potent Inducers of Pol V-mediated Mutagenesis', *Biomolecules*. Multidisciplinary Digital Publishing Institute (MDPI), 11(6). doi:

10.3390/BIOM11060843.

Tahamtan, Y., Hayati, M. and Namavari, M. M. (2010) 'Prevalence and distribution of the stx1, stx2 genes in Shiga toxin producing E. coli (STEC) isolates from cattle', *Iranian Journal of Microbiology*. Tehran University of Medical Sciences, 2(1), p. 8. Available at: /pmc/articles/PMC3279763/ (Accessed: 15 November 2023).

Takahashi, M. *et al.* (2004a) 'The effect of probiotic treatment with Clostridium butyricum on enterohemorrhagic Escherichia coli O157:H7 infection in mice', *FEMS immunology and medical microbiology*. FEMS Immunol Med Microbiol, 41(3), pp. 219–226. doi: 10.1016/J.FEMSIM.2004.03.010.

Takahashi, M. *et al.* (2004b) 'The effect of probiotic treatment with Clostridium butyricum on enterohemorrhagic Escherichia coli O157:H7 infection in mice', *FEMS Immunology & Medical Microbiology*. Oxford Academic, 41(3), pp. 219–226. doi: 10.1016/J.FEMSIM.2004.03.010.

Tang, Y. *et al.* (2023) 'Antibacterial and Antibiofilm Activities of Sertindole and Its Antibacterial Mechanism against Staphylococcus aureus', *ACS Omega*. American Chemical Society, 8(6), pp. 5415–5425. doi: 10.1021/ACSOMEGA.2C06569/ASSET/IMAGES/LARGE/AO2C06569_0009.JPEG.

Tarr, P. I. and Freedman, S. B. (2022) 'Why antibiotics should not be used to treat Shiga toxin-producing Escherichia coli infections', *Current opinion in gastroenterology*. Curr Opin Gastroenterol, 38(1), pp. 30–38. doi: 10.1097/MOG.0000000000000798.

Terajima, J. *et al.* (2017) 'Shiga Toxin (Verotoxin)-producingEscherichia coli and Foodborne Disease:A Review', *Food Safety*. Food Safety Commission of Japan, 5(2), pp. 35–53. doi: 10.14252/foodsafetyfscj.2016029.

Tesh, V. L. (2010) 'Induction of apoptosis by Shiga toxins', *Future Microbiology*, 5(3), pp. 431–453. doi: 10.2217/FMB.10.4.

Thursby, E. and Juge, N. (2017) 'Introduction to the human gut microbiota', *Biochemical Journal*, 474(11), pp. 1823–1836. doi: 10.1042/BCJ20160510.

Toshima, H. *et al.* (2007) 'Enhancement of Shiga toxin production in enterohemorrhagic Escherichia coli serotype O157:H7 by DNase colicins', *Applied and environmental microbiology*. Appl Environ Microbiol, 73(23), pp. 7582–7588. doi: 10.1128/AEM.01326-07.

Trofa, A. F. *et al.* (1999) 'Dr. Kiyoshi Shiga: Discoverer of the dysentery bacillus', *Clinical Infectious Diseases*. Oxford Academic, 29(5), pp. 1303–1306. doi: 10.1086/313437/2/29-5-1303-FIG002.GIF.

Tronnet, S. *et al.* (2020) 'The Genotoxin Colibactin Shapes Gut Microbiota in Mice', *mSphere*, 5(4), pp. 1–11. doi: 10.1128/msphere.00589-20.

Ursell, L. K. *et al.* (2012) 'Defining the Human Microbiome', *Nutrition reviews*. NIH Public Access, 70(Suppl 1), p. S38. doi: 10.1111/J.1753-4887.2012.00493.X.

Vacca, M. *et al.* (2020) 'The Controversial Role of Human Gut Lachnospiraceae', *Microorganisms*. Multidisciplinary Digital Publishing Institute (MDPI), 8(4). doi: 10.3390/MICROORGANISMS8040573.

Valat, C. *et al.* (2012) 'CTX-M-15 Extended-Spectrum-Lactamase in a Shiga Toxin-Producing Escherichia coli Isolate of Serotype O111:H8'. doi: 10.1128/AEM.06997-11.

Vannini, A. *et al.* (2012) 'A convenient and robust in vivo reporter system to monitor gene expression in the human pathogen helicobacter pylori', *Applied and Environmental Microbiology*. American Society for Microbiology, 78(18), pp. 6524–6533. doi: 10.1128/AEM.01252-12/ASSET/6E314E46-0239-4046-8B97-3068D0AA22E7/ASSETS/GRAPHIC/ZAM9991036310005.JPEG.

Vaterodt, L. *et al.* (2018) 'Short- and Long-Term Renal Outcome of Hemolytic-Uremic Syndrome in

Childhood', *Frontiers in Pediatrics*. Frontiers Media SA, 6, p. 220. doi: 10.3389/FPED.2018.00220.

Vazquez-Gutierrez, P. *et al.* (2016) 'High iron-sequestrating bifidobacteria inhibit enteropathogen growth and adhesion to intestinal epithelial cells in vitro', *Frontiers in Microbiology*. Frontiers Media SA, 7(SEP), p. 218227. doi: 10.3389/FMICB.2016.01480/BIBTEX.

Ventola, C. L. (2015) 'The Antibiotic Resistance Crisis: Part 1: Causes and Threats', *Pharmacy and Therapeutics*. MediMedia, USA, 40(4), p. 277. doi: Article.

Verweyen, H. M. *et al.* (2000) 'Enterohemorrhagic Escherichia coli infections: Following transmission routes', *Pediatric Nephrology*. Springer Verlag, 14(1), pp. 73–83. doi: 10.1007/S004670050018/METRICS.

Vogt, S. L. *et al.* (2023) 'Enterohemorrhagic Escherichia coli responds to gut microbiota metabolites by altering metabolism and activating stress responses', *Gut Microbes*. Taylor & Francis, 15(1). doi: 10.1080/19490976.2023.2190303.

Walterspiel, J. N. *et al.* (1992) 'Effect of subinhibitory concentrations of antibiotics on extracellular Shiga-like toxin I', *Infection*. Infection, 20(1), pp. 25–29. doi: 10.1007/BF01704889.

Wang, T., El Meouche, I. and Dunlop, M. J. (2017) 'Bacterial persistence induced by salicylate via reactive oxygen species', *Scientific Reports*. Nature Publishing Group, 7. doi: 10.1038/SREP43839.

Wang, X. *et al.* (2024) 'A Comprehensive Review on Shiga Toxin Subtypes and Their Niche-Related Distribution Characteristics in Shiga-Toxin-Producing E. coli and Other Bacterial Hosts', *Microorganisms 2024, Vol. 12, Page 687*. Multidisciplinary Digital Publishing Institute, 12(4), p. 687. doi: 10.3390/MICROORGANISMS12040687.

Welinder-Olsson, C. and Kaijser, B. (2005) 'Enterohemorrhagic Escherichia coli (EHEC)', *Scandinavian Journal of Infectious Diseases*, 37(6–7), pp. 405–416. doi: 10.1080/00365540510038523.

Wen, S. X. *et al.* (2006) 'A plant-based oral vaccine to protect against systemic intoxication by Shiga toxin type 2', *Proceedings of the National Academy of Sciences of the United States of America*. National Academy of Sciences, 103(18), pp. 7082–7087. doi: 10.1073/PNAS.0510843103/SUPPL_FILE/INDEX.HTML.

Wigle, T. J. *et al.* (2009) 'Inhibitors of RecA Activity Discovered by High-Throughput Screening: Cell-Permeable Small Molecules Attenuate the SOS Response in Escherichia coli', *Journal of biomolecular screening*. NIH Public Access, 14(9), p. 1092. doi: 10.1177/1087057109342126.

Wong, C. S. *et al.* (2000) 'THE RISK OF THE HEMOLYTIC–UREMIC SYNDROME AFTER ANTIBIOTIC TREATMENT OF ESCHERICHIA COLI O157:H7 INFECTIONS', *The New England journal of medicine*. NIH Public Access, 342(26), p. 1930. doi: 10.1056/NEJM200006293422601.

Wong, C. S. *et al.* (2012) 'Risk Factors for the Hemolytic Uremic Syndrome in Children Infected With Escherichia coli O157:H7: A Multivariable Analysis', *Clinical Infectious Diseases: An Official Publication of the Infectious Diseases Society of America*. Oxford University Press, 55(1), p. 33. doi: 10.1093/CID/CIS299.

Woods, D. and Turchi, J. J. (2013) 'Chemotherapy induced DNA damage response: Convergence of drugs and pathways', *Cancer Biology & Therapy*. Taylor & Francis, 14(5), p. 379. doi: 10.4161/CBT.23761.

Woodward, M. J. *et al.* (1999) 'Infection of gnotobiotic calves with Escherichia coli 0157:H7 strain A84', *Veterinary Record*. John Wiley & Sons, Ltd, 144(17), pp. 466–470. doi: 10.1136/VR.144.17.466.

Wray, C. *et al.* (2000) 'Natural and experimental infection of normal caftle with Escherichia coli 0157', *Veterinary Record*. John Wiley & Sons, Ltd, 147(3), pp. 65–68. doi: 10.1136/VR.147.3.65.

Yakimov, A., Bakhlanova, I. and Baitin, D. (2021) 'Targeting evolution of antibiotic resistance by SOS response inhibition', *Computational and Structural Biotechnology Journal*. Research Network of Computational and Structural Biotechnology, 19, p. 777. doi: 10.1016/J.CSBJ.2021.01.003.

Yamanishi, Y. *et al.* (2022) 'Impact of Intestinal Bacteria on Levodopa Pharmacokinetics in LCIG Therapy', *Movement disorders clinical practice*. Mov Disord Clin Pract, 9(3), pp. 362–368. doi: 10.1002/MDC3.13417.

Yang, S. C. *et al.* (2014) 'Antibacterial activities of bacteriocins: application in foods and pharmaceuticals', *Frontiers in Microbiology*. Frontiers Media SA, 5(MAY). doi: 10.3389/FMICB.2014.00241.

Yang, W. *et al.* (2023) 'Enterohemorrhagic Escherichia coli senses microbiota-derived nicotinamide to increase its virulence and colonization in the large intestine', *CellReports*, 42, p. 112638. doi: 10.1016/j.celrep.2023.112638.

Yeo, W. S. *et al.* (2018) 'The FDA-approved anti-cancer drugs, streptozotocin and floxuridine, reduce the virulence of Staphylococcus aureus', *Scientific reports*. Sci Rep, 8(1). doi: 10.1038/S41598-018-20617-5.

Yoh, M., Frimpong, E. K. and Honda, T. (1997) ' Effect of antimicrobial agents, especially fosfomycin, on the production and release of Vero toxin by enterohaemorrhagic Escherichia coli O157:H7 ', *FEMS Immunology & Medical Microbiology*. Oxford University Press (OUP), 19(1), pp. 57–64. doi: 10.1111/J.1574-695X.1997.TB01072.X.

Yoshimura, K., Matsui, T. and Itoh, K. (2010) 'Prevention of Escherichia coli O157:H7 infection in gnotobiotic mice associated with Bifidobacterium strains', *Antonie van Leeuwenhoek*. Antonie Van Leeuwenhoek, 97(2), pp. 107–117. doi: 10.1007/S10482-009-9391-Y.

Zhang, J. *et al.* (2023) 'Meta-analysis of the effects of proton pump inhibitors on the human gut microbiota', *BMC Microbiology*. BioMed Central Ltd, 23(1), pp. 1–12. doi: 10.1186/S12866-023-02895-W/FIGURES/7.

Zhang, J. H., Chung, T. D. Y. and Oldenburg, K. R. (2000) 'Confirmation of primary active substances from high throughput screening of chemical and biological populations: A statistical approach and practical considerations', *Journal of Combinatorial Chemistry*. American Chemical Society, 2(3), pp. 258–265. doi: 10.1021/CC9900706.

Zhang, M. *et al.* (2022) 'The Life Cycle Transitions of Temperate Phages: Regulating Factors and Potential Ecological Implications', *Viruses 2022, Vol. 14, Page 1904*. Multidisciplinary Digital Publishing Institute, 14(9), p. 1904. doi: 10.3390/V14091904.

Zhang, Q. *et al.* (2009) 'Gnotobiotic piglet infection model for evaluating the safe use of antibiotics against Escherichia coli O157:H7 infection', *The Journal of Infectious Diseases*. Oxford Academic, 199(4), pp. 486–493. doi: 10.1086/596509.

Zhang, S. *et al.* (2020) 'Short Chain Fatty Acids Modulate the Growth and Virulence of Pathosymbiont Escherichia coli and Host Response', *Antibiotics*. Multidisciplinary Digital Publishing Institute (MDPI), 9(8), pp. 1–20. doi: 10.3390/ANTIBIOTICS9080462.

Zhang, X. *et al.* (2000) 'Quinolone antibiotics induce Shiga toxin-encoding bacteriophages, toxin production, and death in mice', *Journal of Infectious Diseases*, 181(2), pp. 664–670. doi: 10.1086/315239.

Zhijin Wu, Dongmei Liu and Yunxia Sui (2008) 'Quantitative assessment of hit detection and confirmation in single and duplicate high-throughput screenings', *Journal of Biomolecular Screening*, 13(2), pp. 159–167. doi: 10.1177/1087057107312628.

Zhu, T. *et al.* (2013) 'Hit Identification and Optimization in Virtual Screening: Practical

Recommendations Based Upon a Critical Literature Analysis', *Journal of medicinal chemistry*. NIH Public Access, 56(17), p. 6560. doi: 10.1021/JM301916B.

Zimmermann, P. and Curtis, N. (2019) 'The effect of antibiotics on the composition of the intestinal microbiota - a systematic review', *The Journal of infection*. J Infect, 79(6), pp. 471–489. doi: 10.1016/J.JINF.2019.10.008.

Zoufaly, A. *et al.* (2013) 'Risk Factors for Development of Hemolytic Uremic Syndrome in a Cohort of Adult Patients with STEC 0104:H4 Infection', *PLoS ONE*. PLOS, 8(3), p. 59209. doi: 10.1371/JOURNAL.PONE.0059209.

Zumbrun, S. D. *et al.* (2013) 'Dietary choice affects Shiga toxin-producing Escherichia coli (STEC) O157:H7 colonization and disease', *Proceedings of the National Academy of Sciences of the United States of America*. National Academy of Sciences, 110(23), pp. E2126–E2133. doi: 10.1073/PNAS.1222014110/SUPPL_FILE/SD01.XLSX.

Zuppi, M. *et al.* (2020) 'Investigation on the Evolution of Shiga Toxin-Converting Phages Based on Whole Genome Sequencing', *Frontiers in Microbiology*. Frontiers Media S.A., 11, p. 546143. doi: 10.3389/FMICB.2020.01472/BIBTEX.

7. Supplementary Materials

7.1 Supplemental Figure 1 (*stx2* inducing compounds)

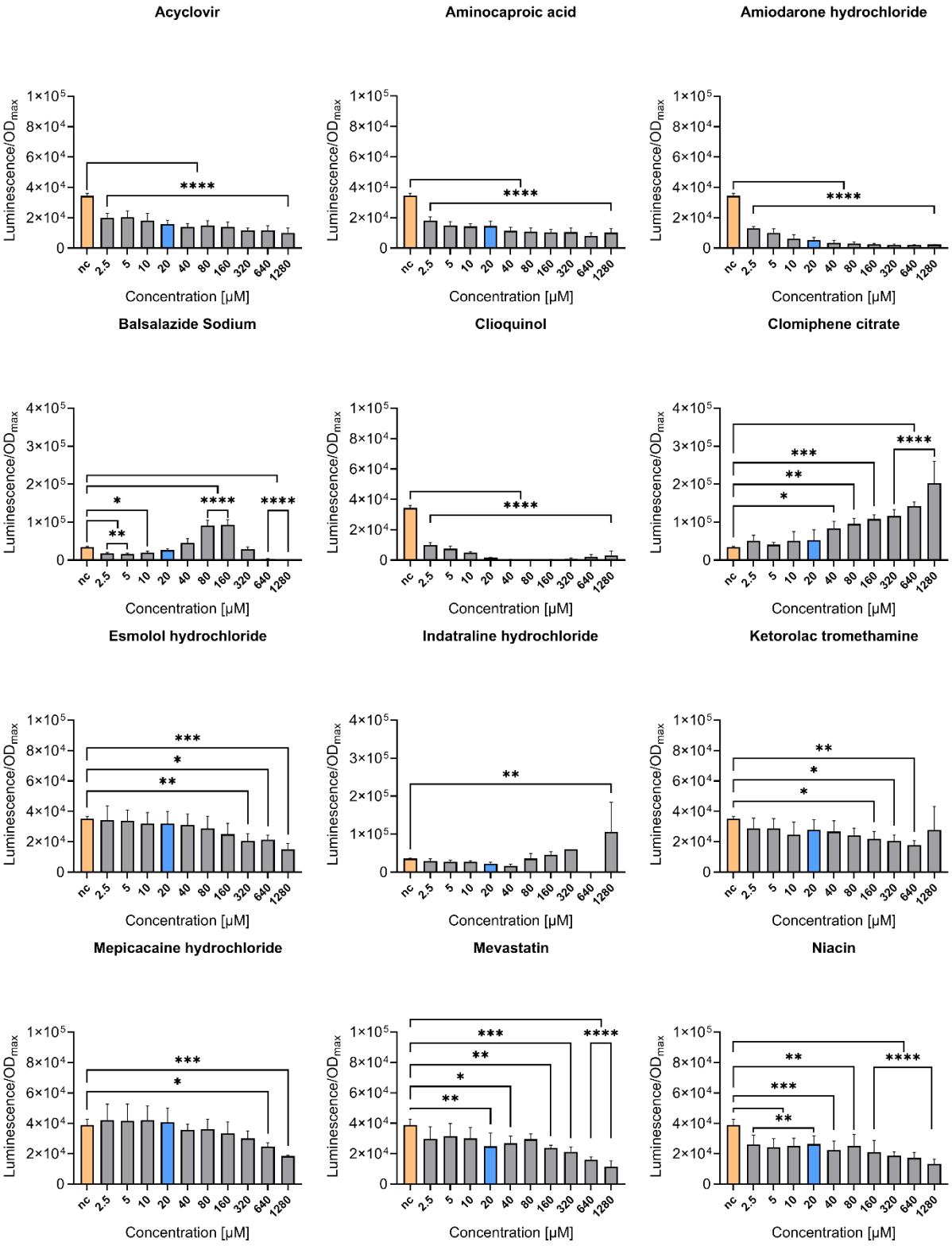

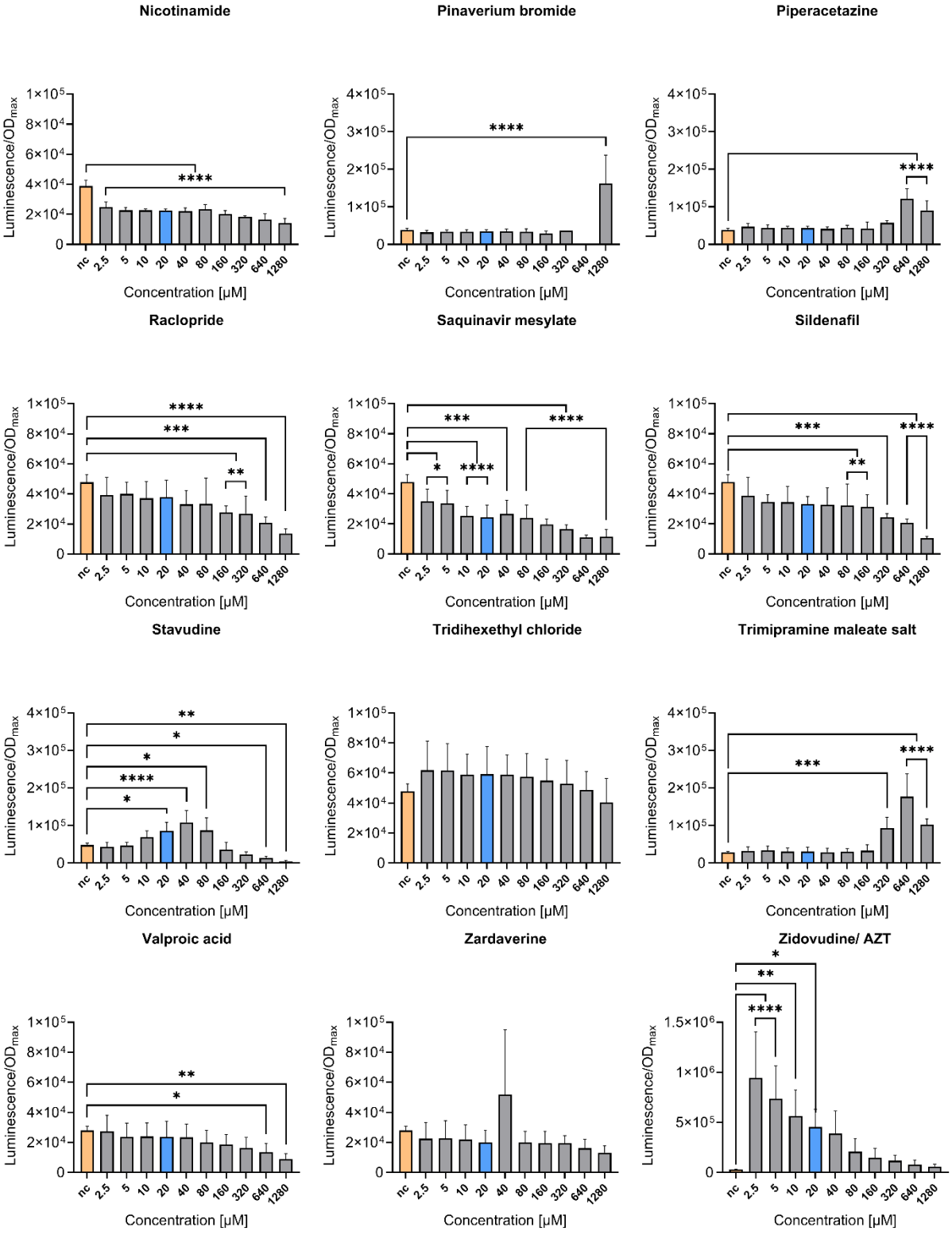

Supplemental Figure 1. Dose-dependent influence of *stx2*-inducing compounds on CW^{gluc}. Luminescence/OD$_{max}$ values of the reporter strain exposed to increasing concentrations (2.5 µM - 1.280 µM) of different compounds (acyclovir, aminocaproic acid, amiodarone hydrochloride, balsalazide sodium, clioquinol, clomiphene citrate, esmolol hydrochloride, indatraline hydrochloride, ketorolac tromethamine, mepicacaine hydrochloride, mevastatin, niacin, nicotinamide, pinaverium bromide, piperacetazine, raclopride, saquinavir mesylate, sildenafil, stavudine, tridihexethyl chloride, trimipramine maleate salt, valproic acid, zardaverine and zidovudine). The blue bar marks the concentration used in

the initial screen (20 µM). The orange bar indicates Luminescence/OD_{max} ratio of the negative control (no compound). Shown is the mean and StD of four independent experiments. Statistical analysis using one-way ANOVA followed by Dunnett multiple comparison test was performed (* $p < 0.05$, ** $p < 0.01$, *** $p < 0.001$, **** $p < 0.0001$).

7.2 Supplemental Table 1 (161 Shiga toxin 2 active compounds)

Supplemental Table 1			
Compound Name	**Therapeutic class**	**Therapeutic effect**	**Effect on Shiga toxin 2**
Etomidate	Central Nervous System	Anesthetic	inducing
Allantoin	Dermatology	Antipsoriatic	inducing
Tridihexethyl chloride	Neuromuscular	Antispastic	inducing
Idoxuridine	Infectiology	Antiviral	inducing
Chloramphenicol	Infectiology	Antibacterial	inhibiting
Penbutolol sulfate	Cardiovascular	Antianginal	inducing
Metronidazole	Infectiology	Antiamebic	inhibiting
Fulvestrant	Endocrinology	Antineoplastic	inducing
Edrophonium chloride	Diagnostic	Anti-fatigue	inducing
Prednicarbate	Metabolism	Anti-Inflammatory	inducing
R(-) Apomorphine hydrochloride hemihydrate	Central Nervous System	Antiparkinsonian	inducing
Danazol	Endocrinology	Anabolic	Gluc interacting
Ciprofloxacin hydrochloride monohydrate	Infectiology	Antibacterial	inhibiting*
Cefotaxime sodium salt	Infectiology	Antibacterial	inhibiting
Tetracycline hydrochloride	Infectiology	Antibacterial	inhibiting
Chlorhexidine	Infectiology	Antibacterial	inhibiting
Chlortetracycline hydrochloride	Infectiology	Antiamebic	inhibiting
Chloroxine	Dermatology	No information	Gluc interacting
Didanosine	Infectiology	Antiviral	inducing
Dihydrostreptomycin sulfate	Infectiology	Antibacterial	inhibiting
Saquinavir mesylate	Immunology	Antiviral	inducing**
Nitrofurantoin	Infectiology	Antibacterial	inducing
Repaglinide	Endocrinology	Antidiabetic	inducing
Trifluridine	Metabolism	Antiviral	inducing
Oxolinic acid	Metabolism	Antibacterial	inducing*
Tiratricol triiodothyroacetic acid	Endocrinology	Antihypothyroid	Gluc interacting

Flumequine	Infectiology	Antibacterial	inducing*
Verteporfin	Ophthalmology	No information	Gluc interacting
Norfloxacin	Infectiology	Antibacterial	inhibiting*
Antimycin A	Infectiology	Antibacterial	inhibiting
Ronidazole	Infectiology	Antibacterial	inducing
Ofloxacin	Infectiology	Antibacterial	inhibiting
Lomefloxacin hydrochloride	Infectiology	Antibacterial	inhibiting*
Dorzolamide hydrochloride	Cardiovascular	Antiglaucoma	inducing
Piperacetazine	Central Nervous System	Antipsychotic	inducing
Ticarcillin sodium	Infectiology	Antibacterial	inducing
Benzylpenicillin sodium	Infectiology	Antibacterial	inducing
Sarafloxacin	Infectiology	Antibacterial	inhibiting*
Oxytetracycline dihydrate	Infectiology	Antibacterial	inhibiting
Minocycline hydrochloride	Infectiology	Antibacterial	inhibiting
Cefepime hydrochloride	Infectiology	Antibacterial	inhibiting
Streptomycin sulfate	Infectiology	Antibacterial	inducing
Cefoperazone dihydrate	Infectiology	Antibacterial	inhibiting
Quinethazone	Cardiovascular	Antihypertensive	inducing
Zidovudine/ AZT	Infectiology	Antiviral	inducing
Dobutamine hydrochloride	Cardiovascular	Analeptic	inducing
Amoxicillin	Metabolism	Antibacterial	inducing*
Benzbromarone	Cardiovascular	Antianginal	Gluc interacting
Rifabutin	Infectiology	Antibacterial	inducing
Nicardipine hydrochloride	Cardiovascular	Antianginal	inducing
Amikacin hydrate	Infectiology	Antibacterial	inhibiting
Clomiphene citrate (Z/E)	Endocrinology	No information	inducing
Buspirone hydrochloride	Central Nervous System	No information	inducing
Amphotericin B	Infectiology	Antibacterial	inducing
Anastrozole	Oncology	Antineoplastic	inducing
Chicago sky blue 6B	Central Nervous System	No information	Gluc interacting
Pefloxacine	Infectiology	Antibacterial	inhibiting*
Calcipotriene	Dermatology	Antipsoriatic	inducing
Meclozine dihydrochloride	Allergology	Antiemetic	inducing
Gatifloxacin	Infectiology	Antibacterial	inhibiting
Cefixime	Infectiology	Antibacterial	inhibiting
Tosufloxacin hydrochloride	Infectiology	Antibacterial	inhibiting*
Rifapentine	Infectiology	Antibacterial	Gluc interacting
Niridazole	Infectiology	Antihelmintic	inducing
Ceforanide	Infectiology	Antibacterial	inhibiting
Imatinib	Oncology	Antineoplastic	inducing**

Cefotetan	Infectiology	Antibacterial	inhibiting
Raclopride	Central Nervous System	No information	inducing**
Closantel	Infectiology	Antihelmintic	Gluc interacting
Moxifloxacin	Infectiology	Antibacterial	inhibiting*
Doxycycline hydrochloride	Metabolism	Antibacterial	inhibiting
Cefotiam hydrochloride	Infectiology	Antibacterial	inhibiting
Cefaclor hydrate	Infectiology	Antibacterial	inducing
Daunorubicin hydrochloride	Infectiology	Antibacterial	Gluc interacting
Ceftazidime pentahydrate	Infectiology	Antibacterial	inhibiting
Sulbactam	Infectiology	Antibacterial	inducing
Nitrofural	Infectiology	Antibacterial	inducing
Cefdinir	Infectiology	Antibacterial	inhibiting
Rifampicin	Infectiology	Antibacterial	inducing
Azithromycin	Infectiology	Antibacterial	inhibiting
Tobramycin	Infectiology	Antibacterial	inhibiting
Formoterol fumarate	Respiratory	Antiasthmatic	inducing
Nifuroxazide	Infectiology	Antibacterial	inducing
Rufloxacin	Infectiology	Antibacterial	inducing*
Fleroxacin	Infectiology	Antibacterial	inhibiting*
Entacapone	Central Nervous System	Antiparkinsonian	Gluc interacting
Clavulanate potassium salt	Infectiology	Antibacterial	inducing
Mometasone furoate	Endocrinology	Anti-inflammatory	inducing
Dacarbazine	Oncology	Antineoplastic	inducing
Triclosan	Infectiology	Antibacterial	inhibiting
Enoxacin	Infectiology	Antibacterial	inhibiting*
Zafirlukast	Respiratory	Antiasthmatic	Gluc interacting
Carbadox	Infectiology	Antibacterial	inducing
Sparfloxacin	Infectiology	Antibacterial	inhibiting
Loracarbef	Infectiology	Antibacterial	inducing
Montelukast	Respiratory	Antiasthmatic	inducing
Sertindole	Central Nervous System	Antipsychotic	inducing
Sulmazole	Cardiovascular	Cardiotonic	inhibiting **
Flunisolide	Endocrinology	Anti-inflammatory	inducing
Nilvadipine	Cardiovascular	Antianginal	inducing
Pinaverium bromide	Neuromuscular	Antispastic	inducing**
Mepivacaine hydrochloride	Neuromuscular	Local anesthetic	inducing
Nalidixic acid sodium salt	Infectiology	Antibacterial	inducing*
Clarithromycin	Infectiology	Antibacterial	inhibiting
Hexestrol	Endocrinology	Antineoplastic	Gluc interacting
Cefmetazole sodium salt	Infectiology	Antibacterial	inducing
Benzocaine	Neuromuscular	Local anesthetic	inducing

Cephalothin sodium salt	Infectiology	Antibacterial	inducing
Sildenafil	Cardiovascular	Antihypertensive	inducing**
Sulfamethoxypyridazine	Infectiology	Antibacterial	inducing
Estradiol Valerate	Endocrinology	Contraceptive	inducing
Streptozotocin	Oncology	Antineoplastic	inducing
Isoetharine mesylate salt	Respiratory	Bronchodilator	inducing
Demeclocycline hydrochloride	Metabolism	Antibacterial	inhibiting
Piperacillin sodium salt	Metabolism	Antibacterial	inhibiting*
Furaltadone hydrochloride	Infectiology	Antibacterial	inducing
Ethoxyquin	Metabolism	Antifungal	inducing
Alexidine dihydrochloride	Infectiology	Antibacterial	Gluc interacting
Cinoxacin	Metabolism	Antibacterial	inducing
Merbromin	Infectiology	Antibacterial	Gluc interacting
Fosinopril	Cardiovascular	Antihypertensive	Gluc interacting
Hexachlorophene	Infectiology	Antiseptic	Gluc interacting
Trimipramine maleate salt	Central Nervous System	Antidepressant	inducing
Piromidic acid	Metabolism	Antibacterial	inducing
Furazolidone	Metabolism	No information	inducing
Cefsulodin sodium salt	Metabolism	Antibacterial	inducing
Moxalactam disodium salt	Metabolism	Antibacterial	inhibiting
Cefoxitin sodium salt	Metabolism	Antibacterial	inducing
Clinafloxacin	Infectiology	Antibacterial	inhibiting*
Liothyronine	Endocrinology	No information	Gluc interacting
Roxithromycin	Metabolism	Antibacterial	inhibiting
Beclomethasone dipropionate	Metabolism	Anti-inflammatory	inducing
Luteolin	Respiratory	Expectorant	Gluc interacting
Clioquinol	Metabolism	Antiamebic	inducing**
Pipemidic acid	Metabolism	Antibacterial	inducing
(+)-Isoproterenol (+)-bitartrate salt	Respiratory	Antiasthmatic	inducing
Lorglumide sodium salt	Metabolism	Antiulcer	inducing
Ketorolac tromethamine	Central Nervous System	Analgesic	inducing**
Benserazide hydrochloride	Central Nervous System	Antiparkinsonian	inducing
Stavudine	Infectiology	Antiviral	inducing
Florfenicol	Metabolism	Antibacterial	inhibiting
Sotalol hydrochloride	Cardiovascular	Antianginal	inducing
Methacycline hydrochloride	Metabolism	Antibacterial	inhibiting
Floxuridine	Oncology	Antineoplastic	inducing
Indatraline hydrochloride	Central Nervous System	Antidepressant	inducing
Zardaverine	Respiratory	Bronchodilator	inducing**

Guaiacol	Respiratory	Expectorant	inducing**
Norgestimate	Endocrinology	No information	inducing
Gliquidone	Endocrinology	Antidiabetic	Gluc interacting
Lymecycline	Metabolism	Antibacterial	inhibiting **
Apramycin	Metabolism	Antibacterial	inducing
Talampicillin hydrochloride	Metabolism	Antibacterial	inhibiting*
Tribenoside	Cardiovascular	No information	Gluc interacting
Colistin sulfate	Infectiology	Antibacterial	inhibiting
Cefazolin sodium salt	Metabolism	Antibacterial	inhibiting
Sisomicin sulfate	Infectiology	Antibacterial	inducing
Diethylstilbestrol	Endocrinology	No information	Gluc interacting
Thimerosal	Infectiology	Antiseptic	inhibiting
Clofazimine	Infectiology	Antibacterial	inducing
Meclocycline sulfosalicylate	Infectiology	Antibacterial	inhibiting
Efavirenz	Infectiology	Antiviral	inhibiting **

* At low concentrations show different effect

** No effect on concentration-dependent screen

7.3 (Supplemental Table 2 (Prestwick Chemical Library®)

Supplimental Table 2

Prestw numbe r	Plate Nb / Positio n Nb	Chemical name	Structure	fmla structure	Mol weight	Precautions	CAS numbe r	Therapeutic class	Therapeutic effect
Prestw-1	01A02	Azaguanine-8	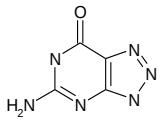	C4H4N6O	152.12	Store at room temperature	134-58-7	Oncology	Antineoplastic
Prestw-2	01A03	Allantoin	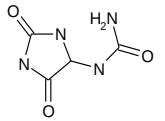	C4H6N4O3	158.12	Store at room temperature	97-59-6	Dermatology	Antipsoriatic
									Vulnerary
Prestw-3	01A04	Acetazolamide	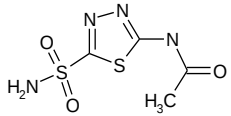	C4H6N4O3S2	222.25	Store at room temperature	59-66-5	Metabolism	Anticonvulsant
									Antiglaucoma
									Diuretic
Prestw-4	01A05	Metformin hydrochloride	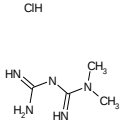	C4H12ClN5	165.63	Store at room temperature	1115-70-4	Endocrinology	Anorectic
									Antidiabetic
									Antilipemic

Prestw-5	01A06	Atracurium besylate	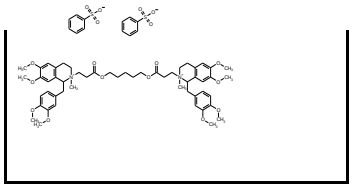	C65H82N2O18S2	1243.51	Store at -20°C	64228-81-5	Neuromuscular	Curarizing
Prestw-6	01A07	Isoflupredone acetate	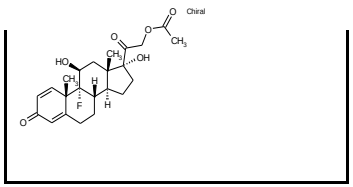	C23H29FO6	420.48	Store at room temperature	338-98-7	Endocrinology	Anti-inflammatory
Prestw-7	01A08	Amiloride hydrochloride dihydrate	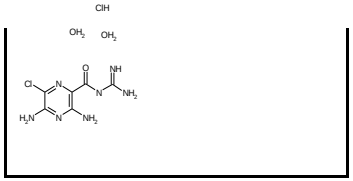	C6H13Cl2N7O3	302.12	Store at room temperature Toxic	17440-83-4	Metabolism	Antihypertensive
									Diuretic
Prestw-8	01A09	Amprolium hydrochloride	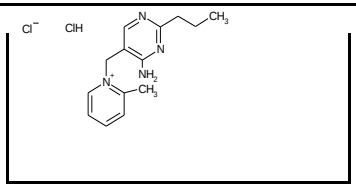	C14H20Cl2N4	315.25	Store at room temperature	137-88-2	Infectiology	Anticoccidial
								Metabolism	Antiparasitic
Prestw-9	01A10	Hydrochlorothiazide	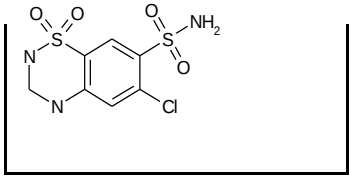	C7H8ClN3O4S2	297.74	Store at room temperature	58-93-5	Metabolism	Antihypertensive
									Diuretic
Prestw-10	01A11	Sulfaguanidine	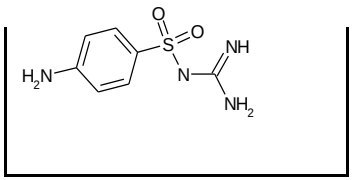	C7H10N4O2S	214.25	Store at room temperature	57-67-0	Infectiology	Antibacterial

								Metabolism	
Prestw-11	01B02	Meticrane	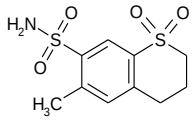	C10H13NO4S2	275.35	Store at room temperature	1084-65-7	Metabolism	Antihypertensive
									Diuretic
Prestw-12	01B03	Benzonatate	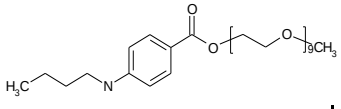	C30H53NO11	603.76	Store at room temperature	104-31-4	Neuromuscular	Antitussive
									Local anesthetic
Prestw-13	01B04	Hydroflumethiazide	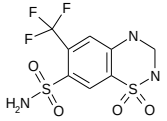	C8H8F3N3O4S2	331.29	Store at room temperature	135-09-1	Metabolism	Antihypertensive
									Diuretic
Prestw-14	01B05	Sulfacetamide sodic hydrate	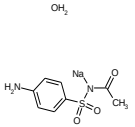	C8H11N2NaO4S	254.24	Store at room temperature	6209-17-2	Dermatology	Antibacterial
								Infectiology	Antipsoriatic
								Metabolism	
Prestw-15	01B06	Heptaminol hydrochloride	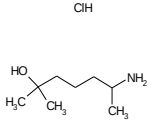	C8H20ClNO	181.71	Store at room temperature	543-15-7	Cardiovascular	Analeptic
									Positive inotropic
									Vasodilator

Prestw-16	01B07	Sulfathiazole	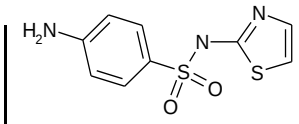	C9H9N3O2S2	255.32	Store at room temperature	72-14-0	Infectiology	Antibacterial
								Metabolism	
Prestw-17	01B08	Levodopa	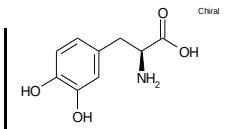	C9H11NO4	197.19	Store at room temperature Oxygen sensitive : rapide oxidation in aqueous solution Light sensitive	59-92-7	Central Nervous System	Antiparkinsonian
Prestw-18	01B09	Idoxuridine	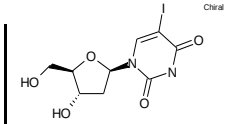	C9H11IN2O5	354.10	Store at room temperature	54-42-2	Infectiology	Antiviral
Prestw-19	01B10	Captopril	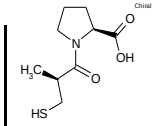	C9H15NO3S	217.29	Store at room temperature Toxic	62571-86-2	Cardiovascular	Antihypertensive
									Vasodilator
Prestw-20	01B11	Minoxidil	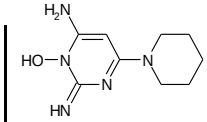	C9H15N5O	209.25	Store at room temperature	38304-91-5	Cardiovascular	Anti-alopecia
									Antihypertensive
									Vasodilator

Prestw-21	01C02	Sulfaphenazole	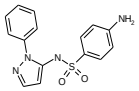	C15H14N4O2S	314.37	Store at room temperature	526-08-9	Infectiology	Antibacterial
								Metabolism	
Prestw-22	01C03	Panthenol (D)	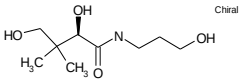	C9H19NO4	205.26	Store at room temperature	81-13-0	Metabolism	Anti-alopecia
Prestw-23	01C04	Sulfadiazine	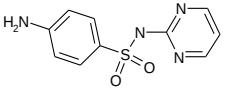	C10H10N4O2S	250.28	Store at room temperature	68-35-9	Infectiology	Antibacterial
								Metabolism	
Prestw-24	01C05	Norethynodrel	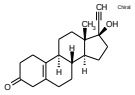	C20H26O2	298.43	Store at room temperature	68-23-5	Endocrinology	Contraceptive
Prestw-25	01C06	Thiamphenicol	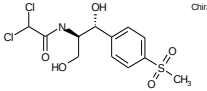	C12H15Cl2NO5S	356.23	Store at room temperature	15318-45-3	Infectiology	Antibacterial
								Metabolism	
Prestw-26	01C07	Cimetidine	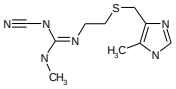	C10H16N6S	252.34	Light sensitive Store at +4°C	51481-61-9	Gastroenterology	Antiulcer
Prestw-27	01C08	Doxylamine succinate		C21H28N2O5	388.47	Store at room temperature	562-10-7	Allergology	Anti-anorectic
								Central Nervous System	Antiemetic

									Antihistaminic
									Antitussive
									Sedative
Prestw-28	01C09	Ethambutol dihydrochloride	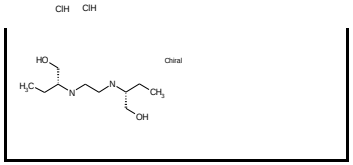	C10H26Cl2N2O2	277.24	Store at room temperature	1070-11-7	Infectiology	Antibacterial
Prestw-29	01C10	Antipyrine	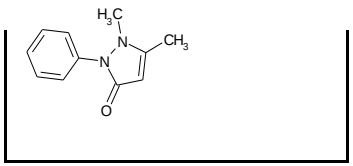	C11H12N2O	188.23	Store at room temperature	60-80-0	Central Nervous System	Analgesic
								Metabolism	Anti-inflammatory
									Antipyretic
Prestw-30	01C11	Antipyrine, 4-hydroxy	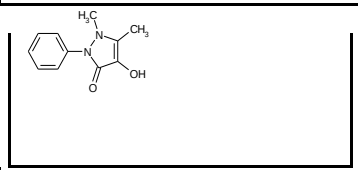	C11H12N2O2	204.23	Store at room temperature	1672-63-5	Metabolism	
Prestw-31	01D02	Chloramphenicol	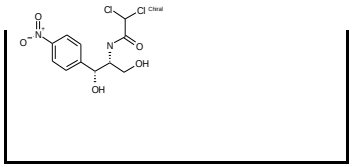	C11H12Cl2N2O5	323.13	Store at room temperature	56-75-7	Infectiology	Antibacterial
								Metabolism	
Prestw-32	01D03	Epirizole	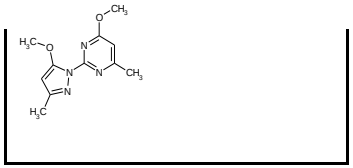	C11H14N4O2	234.26	Store at +4°C	18694-40-1	Central Nervous System	Analgesic
									Anti-inflammatory
									Antipyretic

Prestw-33	01D04	Diprophylline	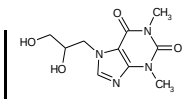	C10H14N4O4	254.25	Store at room temperature	479-18-5	Cardiovascular	Analeptic
								Respiratory	Antispastic
									Bronchodilator
									Diuretic
Prestw-34	01D05	Triamterene	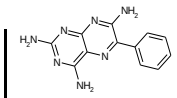	C12H11N7	253.27	Store at room temperature	396-01-0	Metabolism	Antihypertensive
									Diuretic
Prestw-35	01D06	Dapsone	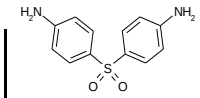	C12H12N2O2S	248.31	Store at room temperature	80-08-0	Infectiology	Antibacterial
									Antimalarial
Prestw-36	01D07	Troleandomycin	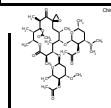	C41H67NO15	813.99	Store at room temperature	2751-09-9	Infectiology	Antibacterial
								Metabolism	
Prestw-37	01D08	Pyrimethamine	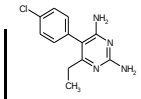	C12H13ClN4	248.72	Store at room temperature	58-14-0	Infectiology	Antimalarial
									Antiprotozoal
Prestw-38	01D09	Hexamethonium dibromide dihydrate	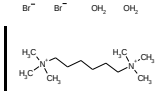	C12H34Br2N2O2	398.22	Store at room temperature	55-97-0	Cardiovascular	Antihypertensive

								Neuromuscular	
Prestw-39	01D10	Diflunisal	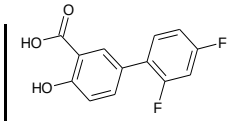	C13H8F2O3	250.20	Store at room temperature	22494-42-4	Central Nervous System	Analgesic
								Metabolism	Anti-inflammatory
									Antipyretic
									Uricosuric
Prestw-40	01D11	Niclosamide	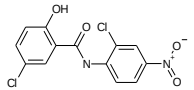	C13H8Cl2N2O4	327.13	Store at room temperature	50-65-7	Infectiology	Antihelmintic
Prestw-41	01E02	Procaine hydrochloride	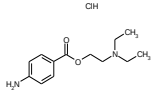	C13H21ClN2O2	272.78	Store at room temperature	51-05-8	Neuromuscular	Local anesthetic
Prestw-42	01E03	Moxisylyte hydrochoride	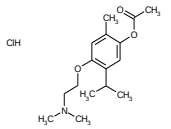	C16H26ClNO3	315.84	Store at room temperature	964-52-3	Cardiovascular	Erectile dysfunction treatment
									Vasodilator
Prestw-43	01E04	Betazole hydrochloride		C5H11Cl2N3	184.07	Store at room temperature	138-92-1	Gastroenterology	Diagnostic
Prestw-44	01E05	Isoxicam	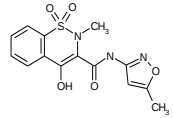	C14H13N3O5S	335.34	Store at room temperature	34552-84-6	Central Nervous System	Analgesic

								Metabolism	Anti-inflammatory
									Antipyretic
Prestw-45	01E06	Naproxen	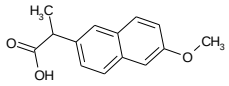	C14H14O3	230.27	Store at room temperature	22204-53-1	Central Nervous System	Analgesic
								Metabolism	Anti-inflammatory
									Antipyretic
Prestw-46	01E07	Naphazoline hydrochloride	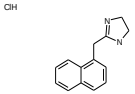	C14H15ClN2	246.74	Store at room temperature	550-99-2	Cardiovascular	Nasal Decongestant
									Vasoconstrictor
Prestw-47	01E08	Ticlopidine hydrochloride	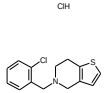	C14H15Cl2NS	300.25	Store at room temperature	53885-35-1	Hematology	Anticoagulant
									Antiplatelet
Prestw-48	01E09	Dicyclomine hydrochloride		C19H36ClNO2	345.96	Store at room temperature	67-92-5	Gastroenterology	Antispastic
Prestw-49	01E10	Amyleine hydrochloride		C14H22ClNO2	271.79	Store at room temperature	532-59-2	Neuromuscular	Local anesthetic

Prestw-50	01E11	Lidocaine hydrochloride	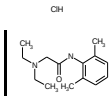	C14H23ClN2O	270.81	Store at room temperature	73-78-9	Cardiovascular	Antiarrhythmic
								Neuromuscular	Local anesthetic
Prestw-51	01F02	Trichlorfon	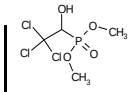	C4H8Cl3O4P	257.44	Store at room temperature	52-68-6	Infectiology	Antiparasitic
Prestw-52	01F03	Carbamazepine	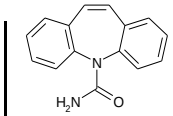	C15H12N2O	236.28	Store at room temperature	298-46-4	Central Nervous System	Analgesic
									Anticonvulsant
									Antidiuretic
									Muscle relaxant
Prestw-53	01F04	Triflupromazine hydrochloride	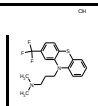	C18H20ClF3N2S	388.89	Store at room temperature	1098-60-8	Central Nervous System	Antiemetic
									Antipsychotic
									Anxiolytic
Prestw-54	01F05	Mefenamic acid	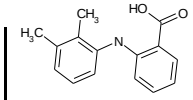	C15H15NO2	241.29	Store at room temperature	61-68-7	Central Nervous System	Analgesic
								Metabolism	Anti-inflammatory
									Antipyretic
Prestw-55	01F06	Acetohexamide	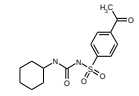	C15H20N2O4S	324.40	Store at room temperature	968-81-0	Endocrinology	Antidiabetic

Prestw-56	01F07	Sulpiride	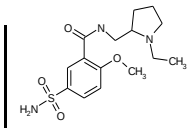	C15H23N3O4S	341.43	Store at room temperature	15676-16-1	Central Nervous System	Antidepressant
									Antiemetic
									Antipsychotic
Prestw-57	01F08	Benoxinate hydrochloride	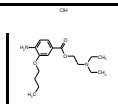	C17H29ClN2O3	344.89	Store at room temperature	5987-82-6	Neuromuscular	Local anesthetic
Prestw-58	01F09	Oxethazaine	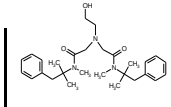	C28H41N3O3	467.66	Store at room temperature	126-27-2	Neuromuscular	Local anesthetic
Prestw-59	01F10	Pheniramine maleate	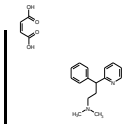	C20H24N2O4	356.43	Light sensitive Store at room temperature	132-20-7	Allergology	Antihistaminic
								Central Nervous System	Antitussive
									Sedative
Prestw-60	01F11	Tolazoline hydrochloride	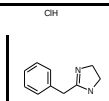	C10H13ClN2	196.68	Store at room temperature	59-97-2	Cardiovascular	Vasodilator
Prestw-61	01G02	Morantel tartrate	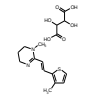	C16H22N2O6S	370.43	Store at room temperature	26155-31-7	Infectiology	Antihelmintic

Prestw-62	01G03	Homatropine hydrobromide (R,S)	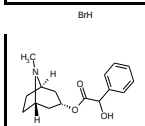	C16H22BrNO3	356.26	Store at room temperature Light sensitive	51-56-9	Diagnostic	Antispastic
								Ophthalmology	Mydriatic
Prestw-63	01G04	Nifedipine	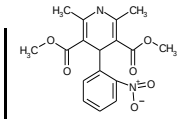	C17H18N2O6	346.34	Store at room temperature Very light sensitive	21829-25-4	Cardiovascular	Antianginal
									Antihypertensive
									Vasodilator
Prestw-64	01G05	Chlorpromazine hydrochloride	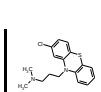	C17H20Cl2N2S	355.33	Store at room temperature	69-09-0	Cardiovascular	Antiemetic
								Central Nervous System	Antihypertensive
									Antipsychotic
Prestw-65	01G06	Diphenhydramine hydrochloride	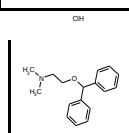	C17H22ClNO	291.82	Store at room temperature Light sensitive	147-24-0	Allergology	Antiemetic
								Central Nervous System	Antihistaminic

									Antitussive
									Sedative
Prestw-66	01G07	Minaprine dihydrochloride	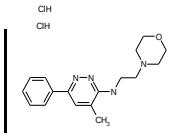	C17H24Cl2N4O	371.31	Store at room temperature	25953-17-7	Central Nervous System	Anti-Alzheimer
									Antidepressant
Prestw-67	01G08	Miconazole		C18H14Cl4N2O	416.14	Store at room temperature	22916-47-8	Infectiology	Antifungal
								Metabolism	
Prestw-68	01G09	Isoxsuprine hydrochloride	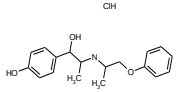	C18H24ClNO3	337.85	Store at room temperature	579-56-6	Cardiovascular	Vasodilator
Prestw-69	01G10	Acebutolol hydrochloride	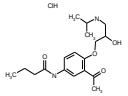	C18H29ClN2O4	372.90	Store at +4°C	34381-68-5	Cardiovascular	Antianginal
									Antiarrhythmic
									Antihypertensive
Prestw-70	01G11	Tolnaftate	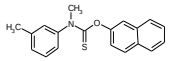	C19H17NOS	307.42	Store at +4°C	2398-96-1	Infectiology	Antifungal
Prestw-71	01H02	Todralazine hydrochloride	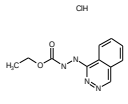	C11H13ClN4O2	268.70	Store at room temperature	3778-76-5	Cardiovascular	Antihypertensive

Prestw-72	01H03	Imipramine hydrochloride	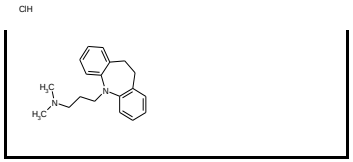	C19H25ClN2	316.88	Store at room temperature	113-52-0	Central Nervous System	Antidepressant
Prestw-73	01H04	Sulindac	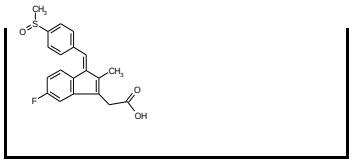	C20H17FO3S	356.42	Store at room temperature	38194-50-2	Central Nervous System	Analgesic
									Anti-inflammatory
									Antipyretic
Prestw-74	01H05	Amitryptiline hydrochloride	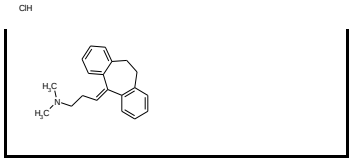	C20H24ClN	313.87	Store at room temperature	549-18-8	Central Nervous System	Antidepressant
Prestw-75	01H06	Adiphenine hydrochloride		C20H26ClNO2	347.89	Store at room temperature	50-42-0	Neuromuscular	Antispastic
Prestw-76	01H07	Dibucaine	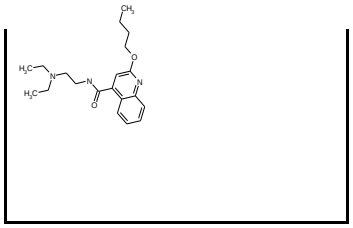	C20H29N3O2	343.47	Store at room temperature Desiccate Light sensitive	85-79-0	Neuromuscular	Local anesthetic
Prestw-77	01H08	Prednisone	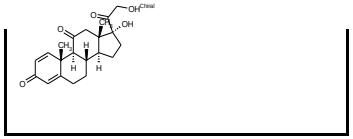	C21H26O5	358.44	Store at room temperature	53-03-2	Dermatology	Anti-inflammatory
								Endocrinology	Antipruritic

								Immunology	Immunosuppressant
Prestw-78	01H09	Thioridazine hydrochloride	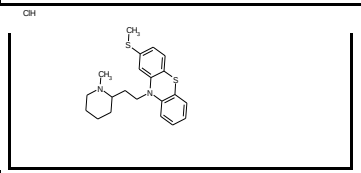	C21H27ClN2S2	407.04	Store at room temperature	130-61-0	Central Nervous System	Antipsychotic
Prestw-79	01H10	Diphemanil methylsulfate	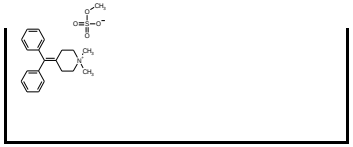	C21H27NO4S	389.52	Store at room temperature	62-97-5	Gastroenterology	Antispastic
									Antiulcer
Prestw-80	01H11	Trimethobenzamide hydrochloride	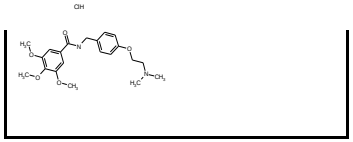	C21H29ClN2O5	424.93	Store at room temperature	554-92-7	Central Nervous System	Antiemetic
Prestw-81	02A02	Metronidazole	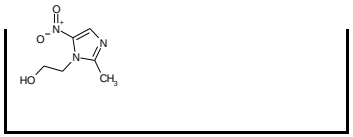	C6H9N3O3	171.16	Store at +4°C Light sensitive	443-48-1	Infectiology	Antiamebic
								Metabolism	Antibacterial
									Antiprotozoal
Prestw-1424	02A03	Fulvestrant	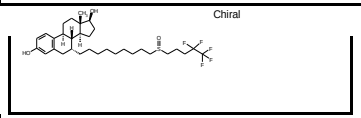	C32H47F5O3S	606.79	Store at room temperature	129453-61-8	Endocrinology	Antineoplastic
								Oncology	
Prestw-83	02A04	Edrophonium chloride		C10H16ClNO	201.70	Store at room temperature	116-38-1	Diagnostic	Anti-fatigue
								Neuromuscular	

Prestw-84	02A05	Moroxidine hydrochloride	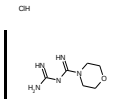	C6H14ClN5O	207.66	Store at room temperature	3160-91-6	Infectiology	Antiviral
Prestw-85	02A06	Baclofen (R,S)	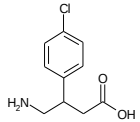	C10H12ClNO2	213.67	Store at room temperature	1134-47-0	Central Nervous System	Antispastic
									Muscle relaxant
Prestw-86	02A07	Acyclovir	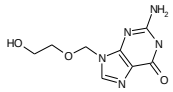	C8H11N5O3	225.21	Store at room temperature	59277-89-3	Metabolism	Antiviral
Prestw-87	02A08	Diazoxide	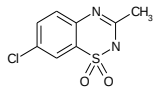	C8H7ClN2O2S	230.67	Store at room temperature	364-98-7	Cardiovascular	Antidiuretic
								Metabolism	Antihypertensive
									Vasodilator
Prestw-88	02A09	Amidopyrine	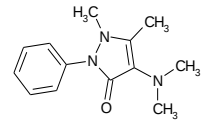	C13H17N3O	231.30	Store at room temperature Light sensitive Oxidation in presence of water	58-15-1	Central Nervous System	Analgesic
								Metabolism	Anti-inflammatory
									Antipyretic

Prestw-1179	02A10	Busulfan	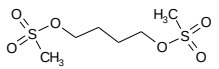	C6H14O6S2	246.30	Store at +4°C	55-98-1	Oncology	Antineoplastic
Prestw-90	02A11	Pindolol		C14H20N2O2	248.33	Store at +4°C Light sensitive	13523-86-9	Cardiovascular	Antianginal
								Ophthalmology	Antiarrhythmic
									Antiglaucoma
									Antihypertensive
Prestw-91	02B02	Khellin	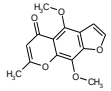	C14H12O5	260.25	Store at room temperature	82-02-0	Cardiovascular	Antispastic
								Gastroenterology	Antitussive
								Respiratory	Vasodilator
Prestw-92	02B03	Zimelidine dihydrochloride monohydrate	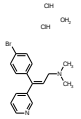	C16H21BrCl2N2O	408.17	Store at room temperature	61129-30-4	Central Nervous System	Antidepressant
Prestw-93	02B04	Azacyclonol	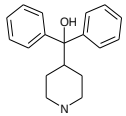	C18H21NO	267.37	Store at room temperature	115-46-8	Central Nervous System	Antipsychotic
Prestw-94	02B05	Azathioprine		C9H7N7O2S	277.27	Store at 0°C	446-86-6	Oncology	Antineoplastic

									Immunosuppressant
Prestw-95	02B06	Lynestrenol	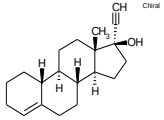	C20H28O	284.45	Store at -20°C	52-76-6	Endocrinology	Contraceptive
Prestw-96	02B07	Guanabenz acetate	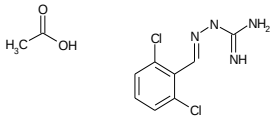	C10H12Cl2N4O2	291.14	Store at room temperature	23256-50-0	Central Nervous System	Antihypertensive
Prestw-97	02B08	Disulfiram	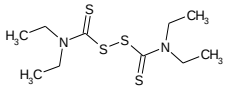	C10H20N2S4	296.54	Store at room temperature	97-77-8	Metabolism	Antabuse effect
Prestw-98	02B09	Acetylsalicylsalicylic acid	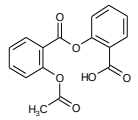	C16H12O6	300.27	Store at room temperature	530-75-6	Central Nervous System	Analgesic
								Metabolism	Anticoagulant
									Anti-inflammatory
									Antipyretic
Prestw-99	02B10	Mianserine hydrochloride		C18H21ClN2	300.83	Store at +4°C	21535-47-7	Cardiovascular	Antidepressant
									Anxiolytic

Prestw-100	02B11	Nocodazole	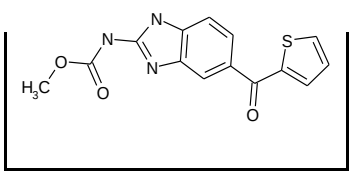	C14H11N3O3S	301.33	Store at +4°C	31430-18-9	Oncology	Antineoplastic
Prestw-101	02C02	R(-) Apomorphine hydrochloride hemihydrate	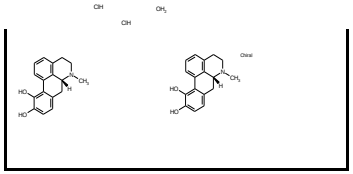	C34H38Cl2N2O5	625.60	Store at +4°C Light sensitive Desiccate	41372-20-7	Central Nervous System	Antiparkinsonian
									Emetic
Prestw-102	02C03	Amoxapine	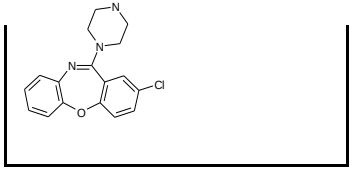	C17H16ClN3O	313.79	Store at room temperature	14028-44-5	Central Nervous System	Antidepressant
									Antipsychotic
Prestw-103	02C04	Cyproheptadine hydrochloride		C21H22ClN	323.87	Store at room temperature	969-33-5	Allergology	Antihistaminic
								Central Nervous System	Antipruritic
									Sedative
Prestw-104	02C05	Famotidine	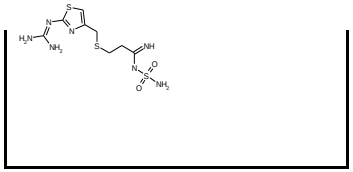	C8H15N7O2S3	337.45	Store at room temperature	76824-35-6	Gastroenterology	Antiulcer
Prestw-105	02C06	Danazol	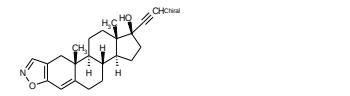	C22H27NO2	337.47	Store at room temperature	17230-88-5	Endocrinology	Anabolic

									Antigonadotropin
Prestw-106	02C07	Nicorandil	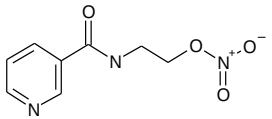	C8H9N3O4	211.18	Store -20°C	65141-46-0	Cardiovascular	Antianginal
									Vasodilator
Prestw-1314	02C08	Pioglitazone	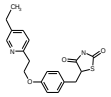	C19H20N2O3S	356.45	Store at room temperature	111025-46-8	Endocrinology	
								Metabolism	
Prestw-108	02C09	Nomifensine maleate	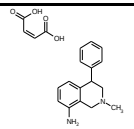	C20H22N2O4	354.41	Store at room temperature	32795-47-4	Central Nervous System	Antidepressant
Prestw-109	02C10	Dizocilpine maleate	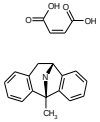	C20H19NO4	337.38	Store at room temperature	77086-22-7	Central Nervous System	Anticonvulsant
Prestw-1192	02C11	Oxandrolone	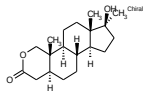	C19H30O3	306.45	Store at room temperature	53-39-4	Endocrinology	

Prestw-111	02D02	Naloxone hydrochloride	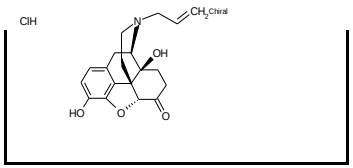	C19H22ClNO4	363.84	Store at +4°C desiccate	357-08-4	Central Nervous System	Opioate antidote
Prestw-112	02D03	Metolazone	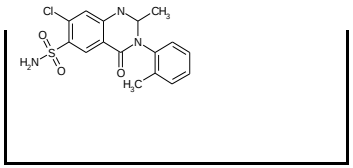	C16H16ClN3O3S	365.84	Store at room temperature	17560-51-9	Cardiovascular	Antihypertensive
									Diuretic
Prestw-113	02D04	Ciprofloxacin hydrochloride monohydrate		C17H21ClFN3O4	385.83	Store at -20	93107-08-5	Infectiology	Antibacterial
								Metabolism	Antiprotozoal
Prestw-114	02D05	Ampicillin trihydrate	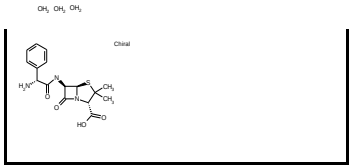	C16H25N3O7S	403.46	Store at 2°C	7177-48-2	Infectiology	Antibacterial
								Metabolism	
Prestw-115	02D06	Haloperidol	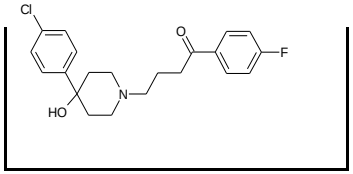	C21H23ClFNO2	375.87	Store at room temperature	52-86-8	Central Nervous System	Antiemetic
									Antipsychotic
Prestw-116	02D07	Naltrexone hydrochloride dihydrate	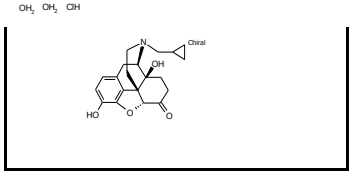	C20H28ClNO6	413.90	Store at +4°C	16676-29-2	Central Nervous System	Analgesic

Prestw-117	02D08	Chlorpheniramine maleate	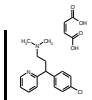	C20H23ClN2O4	390.87	Store at room temperature	113-92-8	Allergology	Antihistaminic
								Central Nervous System	Antitussive
									Sedative
Prestw-118	02D09	Nalbuphine hydrochloride	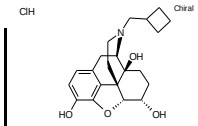	C21H28ClNO4	393.91	Store at room temperature	23277-43-2	Central Nervous System	Analgesic
Prestw-119	02D10	Picotamide monohydrate	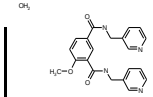	C21H22N4O4	394.43	Store at -20	80530-63-8	Hematology	Anticoagulant
									Antiplatelet
									Thrombolytic
Prestw-120	02D11	Triamcinolone	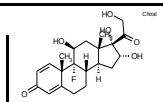	C21H27FO6	394.44	Store at room temperature	124-94-7	Endocrinology	Anti-inflammatory
								Immunology	Immunosuppressant
Prestw-121	02E02	Bromocryptine mesylate	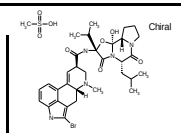	C33H44BrN5O8S	750.72	Store at +4°C	22260-51-1	Central Nervous System	Antiparkinsonian

Prestw-1471	02E03	Amfepramone hydrochloride	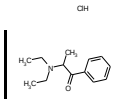	C13H20ClNO	241.76	Store at room temperature	90-84-6	Central Nervous System	
Prestw-123	02E04	Dehydrocholic acid	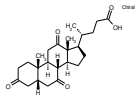	C24H34O5	402.54	Store at room temperature	81-23-2	Gastroenterology	Choleretic
								Metabolism	
Prestw-1184	02E05	Tioconazole	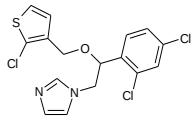	C16H13Cl3N2OS	387.72	Store at +4°C	65899-73-2	Infectiology	Antifungal
								Metabolism	
Prestw-125	02E06	Perphenazine	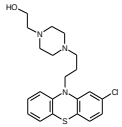	C21H26ClN3OS	403.98	Store at -20°C	58-39-9	Central Nervous System	Antiemetic
									Antipsychotic
Prestw-126	02E07	Mefloquine hydrochloride	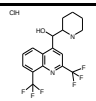	C17H17ClF6N2O	414.78	Store at -20°C	51773-92-3	Infectiology	Antimalarial
Prestw-127	02E08	Isoconazole	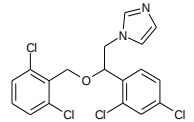	C18H14Cl4N2O	416.14	Store at -20°C	27523-40-6	Infectiology	Antibacterial
								Metabolism	Antifungal
Prestw-128	02E09	Spironolactone	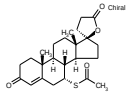	C24H32O4S	416.58	Store at room temperature	52-01-7	Endocrinology	Diuretic

Prestw-129	02E10	Pirenzepine dihydrochloride	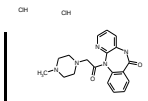	C19H23Cl2N5O2	424.33	Store at room temperature Desiccate	29868-97-1	Gastroenterology	Antiulcer
Prestw-130	02E11	Dexamethasone acetate	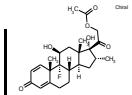	C24H31FO6	434.51	Store at room temperature	1177-87-3	Endocrinology	Anti-inflammatory
								Metabolism	Immunosuppressant
Prestw-131	02F02	Glipizide	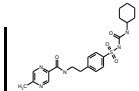	C21H27N5O4S	445.54	Store at room temperature	29094-61-9	Endocrinology	Antidiabetic
Prestw-132	02F03	Loxapine succinate	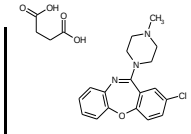	C22H24ClN3O5	445.91	Store at room temperature	27833-64-3	Central Nervous System	Antipsychotic
									Anxiolytic
Prestw-133	02F04	Hydroxyzine dihydrochloride	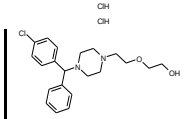	C21H29Cl3N2O2	447.84	Store at room temperature UV sensitive in solution	2192-20-3	Allergology	Antiemetic
								Central Nervous System	Antihistaminic
									Antipruritic
									Anxiolytic
									Sedative
Prestw-134	02F05	Diltiazem hydrochloride	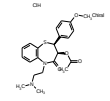	C22H27ClN2O4S	450.99	Store at +4°C	33286-22-5	Cardiovascular	Antianginal

								Hematology	Antiarrhythmic
								Metabolism	Antihypertensive
									Antiplatelet
									Diuretic
									Vasodilator
Prestw-135	02F06	Methotrexate	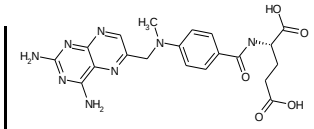	C20H22N8O5	454.45	Store at -20°C Alkaline solutions : decomposition	59-05-2	Oncology	Antineoplastic
Prestw-136	02F07	Astemizole	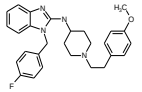	C28H31FN4O	458.58	Store at room temperature	68844-77-9	Allergology	Antihistaminic
Prestw-137	02F08	Clindamycin hydrochloride	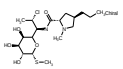	C18H34Cl2N2O5S	461.45	Store at room temperature	21462-39-5	Infectiology	Antibacterial
								Metabolism	
Prestw-138	02F09	Terfenadine	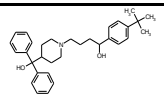	C32H41NO2	471.69	Store at +4°C Light sensitive	50679-08-8	Allergology	Antihistaminic
									Antipruritic
Prestw-139	02F10	Cefotaxime sodium salt	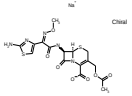	C16H16N5NaO7S2	477.45	Store at +4°C	64485-93-4	Infectiology	Antibacterial
								Metabolism	

Prestw-140	02F11	Tetracycline hydrochloride	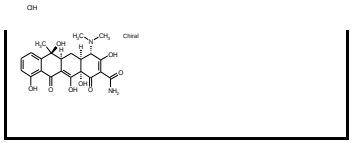	C22H25ClN2O8	480.91	Store below 0°C	64-75-5	Infectiology	Antibacterial
								Metabolism	
Prestw-141	02G02	Verapamil hydrochloride		C27H39ClN2O4	491.08	Store at room temperature	152-11-4	Cardiovascular	Antihypertensive
Prestw-142	02G03	Dipyridamole	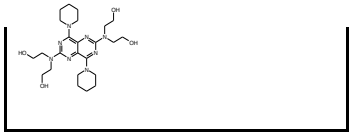	C24H40N8O4	504.64	Store at room temperature	58-32-2	Cardiovascular	Anticoagulant
								Hematology	Antiplatelet
									Vasodilator
Prestw-143	02G04	Chlorhexidine	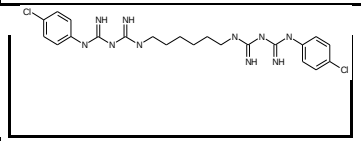	C22H30Cl2N10	505.46	Store at +4°C	55-56-1	Infectiology	Antibacterial
									Antiseptic
Prestw-144	02G05	Loperamide hydrochloride		C29H34Cl2N2O2	513.51	Store at room temperature	34552-83-5	Gastroenterology	Antidiarrheal
Prestw-145	02G06	Chlortetracycline hydrochloride		C22H24Cl2N2O8	515.35	Store below 0°C	64-72-2	Infectiology	Antiamebic
								Metabolism	Antibacterial
Prestw-146	02G07	Tamoxifen citrate	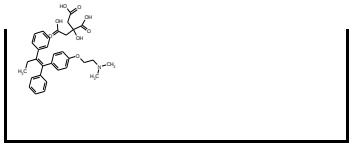	C32H37NO8	563.65	Store at +4°C Desiccate	54965-24-1	Endocrinology	Antineoplastic
								Oncology	

Prestw-147	02G08	Nicergoline	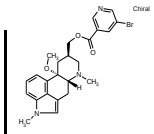	C24H26BrN3O3	484.40	Store at +4°C	not availabl e	Cardiovascular	Anti-ischemic
									Vasodilator
Prestw-148	02G09	Canrenoic acid potassium salt	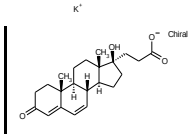	C22H29KO4	396.58	Store at room temperature	2181-04-6	Endocrinology	Antihypertensive
									Diuretic
Prestw-149	02G10	Thioproperazine dimesylate	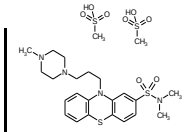	C24H38N4O8S4	638.85	Store below 0°C	2347-80-0	Central Nervous System	Antiemetic
									Antipsychotic
Prestw-150	02G11	Dihydroergotamine tartrate	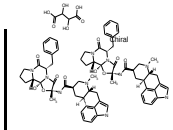	C70H80N10O16	1317.48	Store at room temperature	5989-77-5	Central Nervous System	Antimigraine
Prestw-151	02H02	Erythromycin	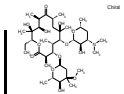	C37H67NO13	733.95	Store at room temperature	114-07-8	Infectiology	Antibacterial
								Metabolism	Anti-inflammatory
Prestw-1474	02H03	Chloroxine	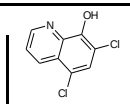	C9H5Cl2NO	214.05	Store at room temperature	773-76-2	Dermatology	

								Metabolism	
Prestw-153	02H04	Didanosine	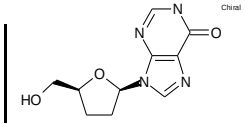	C10H12N4O3	236.23	store at -20°C	69655-05-6	Infectiology	Antiviral
								Metabolism	
Prestw-154	02H05	Josamycin	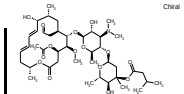	C42H69NO15	828.02	Store at +4°C Toxic	16846-24-5	Infectiology	Antibacterial
								Metabolism	
Prestw-155	02H06	Paclitaxel	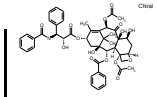	C47H51NO14	853.93	Store at room temperature	33069-62-4	Oncology	Antineoplastic
Prestw-156	02H07	Ivermectin	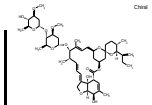	C48H74O14	875.12	Store at +4°C	70288-86-7	Infectiology	Antihelmintic
								Metabolism	Antiparasitic
Prestw-157	02H08	Gallamine triethiodide	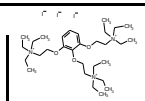	C30H60I3N3O3	891.54	Store at +4°C	65-29-2	Neuromuscular	Muscle relaxant
Prestw-158	02H09	Neomycin sulfate	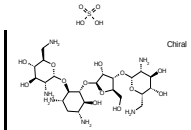	C23H48N6O17S	712.73	Store at room temperature Desiccate Light sensitive	1405-10-3	Infectiology	Antibacterial
								Metabolism	

Prestw-159	02H10	Dihydrostreptomycin sulfate	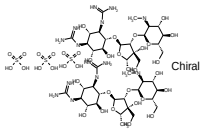	C42H88N14O36S3	1461.43	Store at +4°C	5490-27-7	Infectiology	Antibacterial
								Metabolism	
Prestw-160	02H11	Gentamicine sulfate	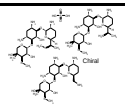	C60H125N15O25S	1488.81	Store at +4°C Dessiccate	1405-41-0	Infectiology	Antibacterial
								Metabolism	
Prestw-161	03A02	Isoniazid	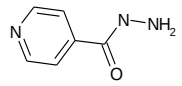	C6H7N3O	137.14	Store at room temperature	54-85-3	Infectiology	Antibacterial
								Metabolism	
Prestw-162	03A03	Pentylenetetrazole	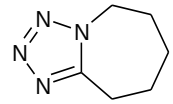	C6H10N4	138.17	Store at room temperature Hygroscopic !!! POISON !!!	54-95-5	Central Nervous System	Analeptic
								Respiratory	CNS Stimulant
Prestw-163	03A04	Chlorzoxazone	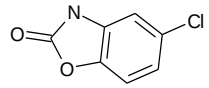	C7H4ClNO2	169.57	Store at room temperature	95-25-0	Central Nervous System	Anticonvulsant
									Muscle relaxant
Prestw-164	03A05	Ornidazole	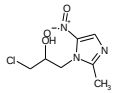	C7H10ClN3O3	219.63	Store at room temperature	16773-42-5	Infectiology	Antibacterial

								Metabolism	Antiparasitic
									Antiprotozoal
									Antitrichomonal
Prestw-165	03A06	Ethosuximide	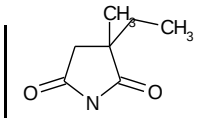	C7H11NO2	141.17	Store at room temperature	77-67-8	Central Nervous System	Anticonvulsant
Prestw-166	03A07	Mafenide hydrochloride	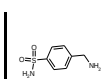	C7H11ClN2O2S	222.69	Store at room temperature	138-37-4	Infectiology	Antibacterial
								Metabolism	Antiseptic
Prestw-167	03A08	Riluzole hydrochloride	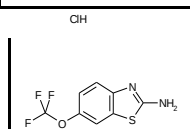	C8H6ClF3N2OS	270.66	Store at room temperature	not available	Central Nervous System	Antispastic
									Neuroprotectant
Prestw-168	03A09	Nitrofurantoin	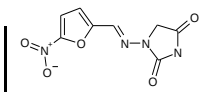	C8H6N4O5	238.16	Store at room temperature	67-20-9	Infectiology	Antibacterial
Prestw-169	03A10	Hydralazine hydrochloride	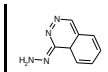	C8H9ClN4	196.64	Store at room temperature	304-20-1	Cardiovascular	Antihypertensive
Prestw-170	03A11	Phenelzine sulfate	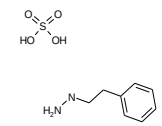	C8H14N2O4S	234.28	Store at room temperature	156-51-4	Central Nervous System	Antidepressant

Prestw-171	03B02	Tranexamic acid	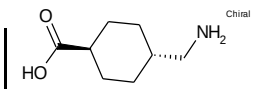	C8H15NO2	157.21	Store at room temperature	1197-18-8	Hematology	Hemostatic
Prestw-172	03B03	Etofylline	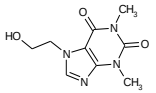	C9H12N4O3	224.22	Store at room temperature	519-37-9	Cardiovascular	Antispastic
								Respiratory	Bronchodilator
									Cardiotonic
									Diuretic
Prestw-173	03B04	Tranylcypromine hydrochloride		C9H12ClN	169.66	Store at +4°C	1986-47-6	Central Nervous System	Antidepressant
Prestw-174	03B05	Alverine citrate salt	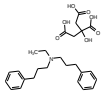	C26H35NO7	473.57	Store at room temperature	5560-59-8	Neuromuscular	Antispastic
Prestw-175	03B06	Aceclofenac	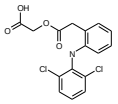	C16H13Cl2NO4	354.19	Store at room temperature	89796-99-6	Central Nervous System	Analgesic
								Metabolism	Anti-inflammatory
Prestw-176	03B07	Iproniazide phosphate	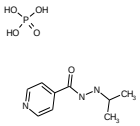	C9H16N3O5P	277.22	Store at 2°C	305-33-9	Cardiovascular	Antidepressant

								Central Nervous System	Antihypertensive
Prestw-177	03B08	Sulfamethoxazole	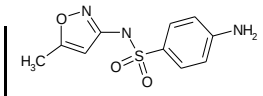	C10H11N3O3S	253.28	Store at room temperature	723-46-6	Infectiology	Antibacterial
								Metabolism	
Prestw-178	03B09	Mephenesin	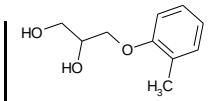	C10H14O3	182.22	Store at room temperature	59-47-2	Central Nervous System	Anticonvulsant
								Neuromuscular	Local anesthetic
									Muscle relaxant
Prestw-179	03B10	Phenformin hydrochloride	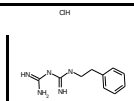	C10H16ClN5	241.73	Store at room temperature	834-28-6	Endocrinology	Antidiabetic
Prestw-180	03B11	Flutamide	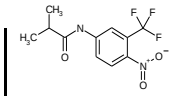	C11H11F3N2O3	276.22	Store at room temperature	13311-84-7	Oncology	Antineoplastic
Prestw-181	03C02	Ampyrone	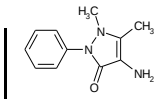	C11H13N3O	203.25	Store at room temperature	83-07-8	Central Nervous System	Analgesic
								Metabolism	Anticoagulant
									Anti-inflammatory

									Antipyretic
Prestw-182	03C03	Levamisole hydrochloride	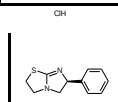	C11H13ClN2S	240.76	Store at room temperature	16595-80-5	Immunology	Antihelmintic
								Infectiology	Immunomodulator
								Metabolism	
Prestw-183	03C04	Pargyline hydrochloride	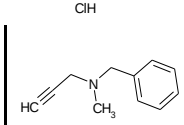	C11H14ClN	195.69	Store at -20°C Aqueous solutions instable	306-07-0	Cardiovascular	Antidepressant
								Central Nervous System	Antihypertensive
Prestw-184	03C05	Methocarbamol	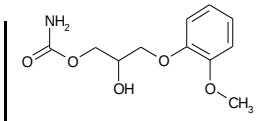	C11H15NO5	241.25	Store at room temperature	532-03-6	Central Nervous System	Analgesic
									Muscle relaxant
Prestw-185	03C06	Aztreonam	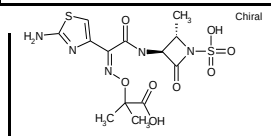	C13H17N5O8S2	435.44	Store at +4°C	78110-38-0	Infectiology	Antibacterial
								Metabolism	
Prestw-186	03C07	Cloxacillin sodium salt	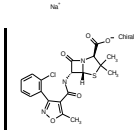	C19H17ClN3NaO5S	457.87	Store at -20°C	642-78-4	Infectiology	Antibacterial
								Metabolism	

Prestw-187	03C08	Catharanthine	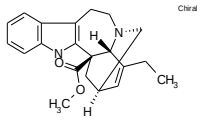	C21H24N2O2	336.44	store at -20°C	2468-21-5	Oncology	Antineoplastic
Prestw-188	03C09	Pentolinium bitartrate	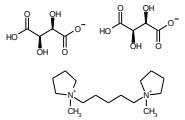	C23H42N2O12	538.60	Store at +4°C	52-62-0	Cardiovascular	Antihypertensive
Prestw-189	03C10	Aminopurine, 6-benzyl	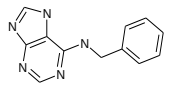	C12H11N5	225.25	Store at room temperature	1214-39-7	Endocrinology	
Prestw-190	03C11	Tolbutamide	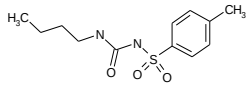	C12H18N2O3S	270.35	Store at room temperature	64-77-7	Endocrinology	Antidiabetic
Prestw-191	03D02	Midodrine hydrochloride	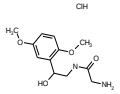	C12H19ClN2O4	290.75	Store at room temperature	3092-17-9	Cardiovascular	Antihypertensive
Prestw-192	03D03	Thalidomide	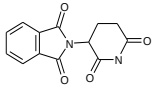	C13H10N2O4	258.24	Store at room temperature Teratogenic	50-35-1	Central Nervous System	Hypnotic
								Immunology	Immunosuppressant
Prestw-193	03D04	Oxolinic acid	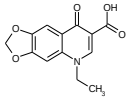	C13H11NO5	261.24	Store at +4°C	14698-29-4	Metabolism	Antibacterial
								Infectiology	

Prestw-194	03D05	Nimesulide	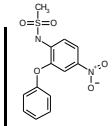	C13H12N2O5S	308.31	Store at +4°C	51803-78-2	Metabolism	Anti-inflammatory
Prestw-1231	03D06	Asenapine maleate	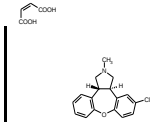	C21H20ClNO5	401.85	Store at room temperature	85650-56-2	Central Nervous System	Antipsychotic
Prestw-196	03D07	Pentoxifylline	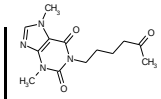	C13H18N4O3	278.31	Store at room temperature	6493-05-6	Cardiovascular	Bronchodilator
								Respiratory	Vasodilator
Prestw-197	03D08	Metaraminol bitartrate	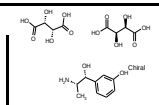	C17H25NO14	467.39	Store at room temperature	33402-03-8	Cardiovascular	Antihypotensive
									Vasoconstrictor
Prestw-198	03D09	Salbutamol	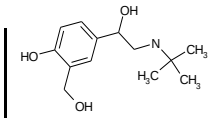	C13H21NO3	239.32	Store at room temperature Light sensitive	18559-94-9	Neuromuscular	Bronchodilator
								Respiratory	Tocolytic
Prestw-199	03D10	Prilocaine hydrochloride	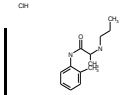	C13H21ClN2O	256.78	Store at room temperature	1786-81-8	Neuromuscular	Local anesthetic
Prestw-200	03D11	Camptothecine (S,+)	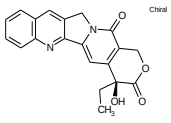	C20H16N2O4	348.36	Store at +4°C	7689-03-4	Oncology	Antineoplastic

Prestw-201	03E02	Ranitidine hydrochloride	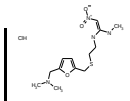	C13H23ClN4O3S	350.87	Store at room temperature	66357-59-3	Gastroenterology	Antiulcer
Prestw-202	03E03	Tiratricol, 3,3',5-triiodothyroacetic acid	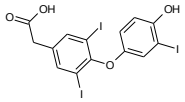	C14H9I3O4	621.94	Store at -20°C	51-24-1	Endocrinology	Antihypothyroid
									Hypocholesterolemic
Prestw-203	03E04	Flufenamic acid	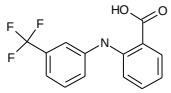	C14H10F3NO2	281.24	Store at room temperature	530-78-9	Central Nervous System	Analgesic
									Anti-inflammatory
									Antipyretic
Prestw-204	03E05	Flumequine	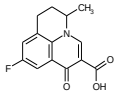	C14H12FNO3	261.26	Store at room temperature	42835-25-6	Infectiology	Antibacterial
								Metabolism	
Prestw-205	03E06	Tolfenamic acid	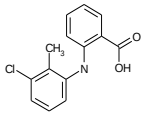	C14H12ClNO2	261.71	Store at room temperature	13710-19-5	Central Nervous System	Analgesic
								Metabolism	Anti-inflammatory

Prestw-206	03E07	Meclofenamic acid sodium salt monohydrate	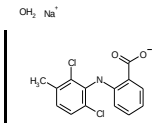	C14H12Cl2NNaO3	336.15	Store at room temperature	6385-02-0	Central Nervous System	Anti-inflammatory
									Antipyretic
Prestw-1181	03E08	Tibolone	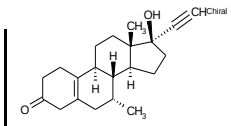	C21H28O2	312.46	Store at +4°C	5630-53-5	Endocrinology	
Prestw-208	03E09	Trimethoprim	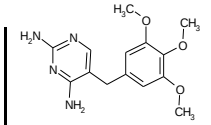	C14H18N4O3	290.32	Store at +4°C	738-70-5	Infectiology	Antibacterial
								Metabolism	Antimalarial
Prestw-209	03E10	Metoclopramide monohydrochloride	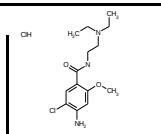	C14H23Cl2N3O2	336.26	Store at room temperature	7232-21-5	Central Nervous System	Antiemetic
Prestw-210	03E11	Fenbendazole	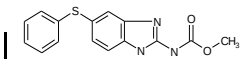	C15H13N3O2S	299.35	Store at room temperature	43210-67-9	Infectiology	Antihelmintic
								Metabolism	
Prestw-211	03F02	Piroxicam	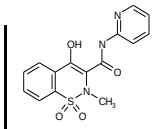	C15H13N3O4S	331.35	Store at +4°C	36322-90-4	Central Nervous System	Analgesic
								Hematology	Anticoagulant

								Metabolism	Anti-inflammatory
									Antiplatelet
									Antipyretic
									Uricosuric
Prestw-212	03F03	Pyrantel tartrate	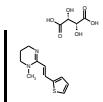	C15H20N2O6S	356.40	Store at room temperature	33401-94-4	Infectiology	Antihelmintic
Prestw-213	03F04	Fenspiride hydrochloride	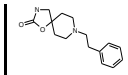	C15H21ClN2O2	296.80	Store at room temperature	5053-08-7	Respiratory	Antitussive
									Bronchodilator
Prestw-214	03F05	Gemfibrozil	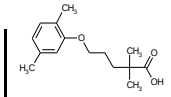	C15H22O3	250.34	Store at room temperature	25812-30-0	Metabolism	Hypocholesterolemic
									Lipid-lowering
Prestw-215	03F06	Mefexamide hydrochloride	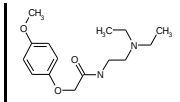	C15H25ClN2O3	316.83	Store at room temperature	3413-64-7	Central Nervous System	CNS Stimulant
Prestw-216	03F07	Tiapride hydrochloride	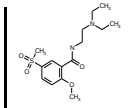	C15H25ClN2O4S	364.89	Store at room temperature	51012-33-0	Central Nervous System	Antiemetic
									Antipsychotic
									Anxiolytic
									Sedative

Prestw-217	03F08	Mebendazole	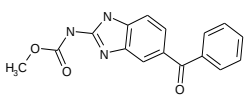	C16H13N3O3	295.30	Store at room temperature	31431-39-7	Infectiology	Antihelmintic
								Metabolism	
Prestw-218	03F09	Fenbufen	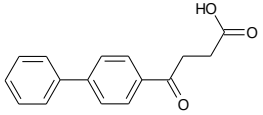	C16H14O3	254.29	Store at room temperature	36330-85-5	Central Nervous System	Analgesic
								Metabolism	Anti-inflammatory
									Antipyretic
Prestw-219	03F10	Ketoprofen	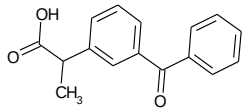	C16H14O3	254.29	Store at room temperature	22071-15-4	Central Nervous System	Analgesic
								Metabolism	Anti-inflammatory
									Antipyretic
Prestw-220	03F11	Indapamide		C16H16ClN3O3S	365.84	Store at room temperature	26807-65-8	Metabolism	Antihypertensive
									Diuretic
Prestw-221	03G02	Norfloxacin	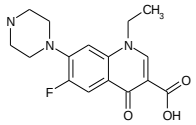	C16H18FN3O3	319.34	Store at +4°C	70458-96-7	Infectiology	Antibacterial
								Metabolism	

Prestw-222	03G03	Antimycin A	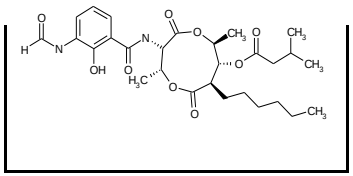	C28H40N2O9	548.64	Store at -20°C	1397-94-0	Infectiology	Antibacterial
								Metabolism	Antifungal
Prestw-223	03G04	Xylometazoline hydrochloride	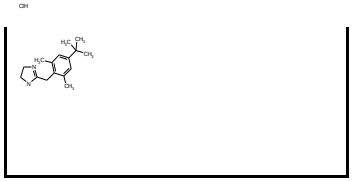	C16H25ClN2	280.84	Store at room temperature	1218-35-5	Cardiovascular	Nasal Decongestant
									Vasoconstrictor
Prestw-224	03G05	Oxymetazoline hydrochloride	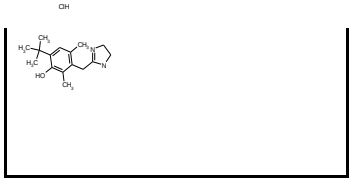	C16H25ClN2O	296.84	Store at room temperature	2315-02-8	Respiratory	Nasal Decongestant
									Vasoconstrictor
Prestw-225	03G06	Nifenazone	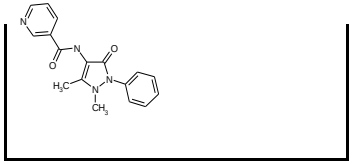	C17H16N4O2	308.34	Store at +4°C	2139-47-1	Central Nervous System	Analgesic
								Metabolism	Anti-inflammatory
									Antipyretic
Prestw-226	03G07	Griseofulvin	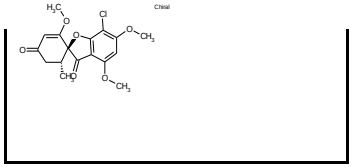	C17H17ClO6	352.77	Store at -20°C	126-07-8	Infectiology	Antifungal
								Metabolism	Anti-inflammatory

Prestw-227	03G08	Clemizole hydrochloride	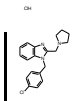	C19H21Cl2N3	362.31	Store at room temperature	1163-36-6	Allergology	Antibacterial
								Dermatology	Antifungal
								Infectiology	Antihistaminic
									Antipruritic
Prestw-228	03G09	Tropicamide	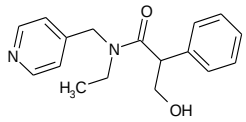	C17H20N2O2	284.36	Store at +4°C	1508-75-4	Neuromuscular	Mydriatic
Prestw-229	03G10	Nefopam hydrochloride	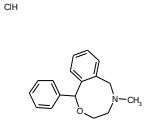	C17H20ClNO	289.81	Store at room temperature	23327-57-3	Central Nervous System	Analgesic
Prestw-230	03G11	Phentolamine hydrochloride		C17H20ClN3O	317.82	Store at room temperature	73-05-2	Cardiovascular	Antihypertensive
									Vasodilator
Prestw-231	03H02	Etodolac	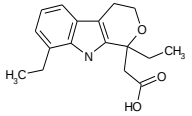	C17H21NO3	287.36	Store at +4°C	41340-25-4	Central Nervous System	Analgesic
								Hematology	Anti-inflammatory
									Antiplatelet
									Antipyretic

Prestw-232	03H03	Scopolamin-N-oxide hydrobromide	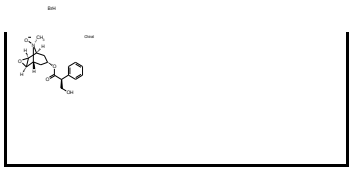	C17H22BrNO5	400.27	Store at room temperature	6106-81-6	Neuromuscular	Antispastic
									Mydriatic
Prestw-233	03H04	Hyoscyamine (L)	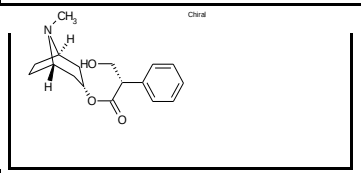	C17H23NO3	289.38	Store at 2 to 8°C	101-31-5	Central Nervous System	Antiemetic
								Ophthalmology	Antispastic
									Mydriatic
Prestw-234	03H05	Chlorphensin carbamate	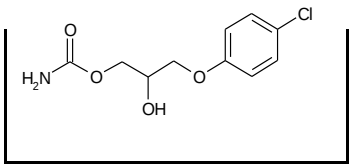	C10H12ClNO4	245.66	Store at room temperature	886-74-8	Central Nervous System	Muscle relaxant
Prestw-1515	03H06	Fadrozole hydrochloride	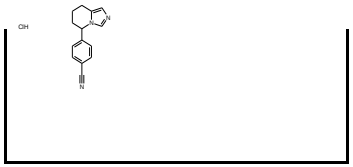	C14H14ClN3	259.74	Store at room temperature	102676-31-3	Oncology	Antineoplastic
Prestw-236	03H07	Dilazep dihydrochloride	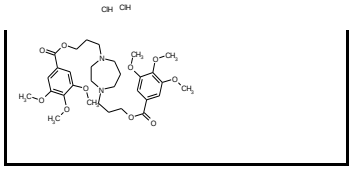	C31H46Cl2N2O10	677.63	Store at +4°C	20153-98-4	Cardiovascular	Antiplatelet
								Hematology	Vasodilator
Prestw-237	03H08	Ofloxacin	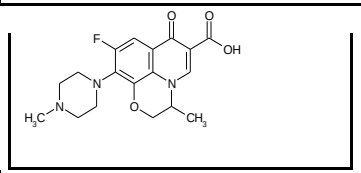	C18H20FN3O4	361.38	Store at +4°C	82419-36-1	Infectiology	Antibacterial
								Metabolism	

Prestw-238	03H09	Lomefloxacin hydrochloride	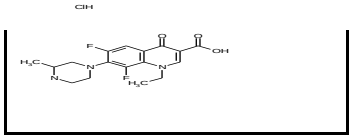	C17H20ClF2N3O3	387.82	Store at -20°C	98079-52-8	Infectiology	Antibacterial
								Metabolism	
Prestw-239	03H10	Orphenadrine hydrochloride	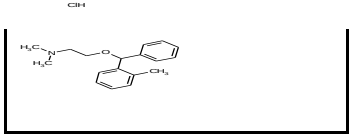	C18H24ClNO	305.85	Store at RT	341-69-5	Allergology	Antihistaminic
								Central Nervous System	Antiparkinsonian
Prestw-240	03H11	Proglumide		C18H26N2O4	334.42	Store at room temperature	6620-60-6	Gastroenterology	Antiulcer
Prestw-241	04A02	Mexiletine hydrochloride		C11H18ClNO	215.73	Store at +4°C	5370-01-4	Cardiovascular	Antiarrhythmic
								Neuromuscular	Local anesthetic
Prestw-242	04A03	Flavoxate hydrochloride		C24H26ClNO4	427.93	Store at room temperature	3717-88-2	Metabolism	Antispastic
Prestw-243	04A04	Bufexamac	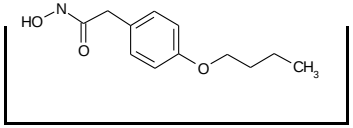	C12H17NO3	223.27	Store at room temperature	2438-72-4	Central Nervous System	Analgesic
								Metabolism	Anti-inflammatory
									Antipyretic

Prestw-244	04A05	Glutethimide, para-amino	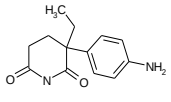	C13H16N2O2	232.28	Store at room temperature	125-84-8	Oncology	Antineoplastic
Prestw-245	04A06	Dropropizine (R,S)	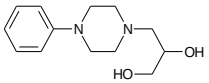	C13H20N2O2	236.32	Store at room temperature	17692-31-8	Respiratory	Antitussive
Prestw-246	04A07	Pinacidil		C13H19N5	245.33	Store at room temperature	85371-64-8	Cardiovascular	Antihypertensive
									Vasodilator
Prestw-247	04A08	Albendazole	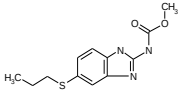	C12H15N3O2S	265.34	Store at room temperature	54965-21-8	Metabolism	Antihelmintic
									Antiparasitic
Prestw-248	04A09	Clonidine hydrochloride		C9H10Cl3N3	266.56	Store at +4°C Light sensitive	4205-91-8	Cardiovascular	Analgesic
								Central Nervous System	Antihypotensive
									Sedative
Prestw-249	04A10	Bupropion hydrochloride	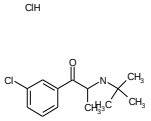	C13H19Cl2NO	276.21	Store at room temperature	31677-93-7	Central Nervous System	Antidepressant

Prestw-250	04A11	Alprenololhydrochloride	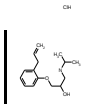	C15H24ClNO2	285.82	Store at room temperature	13707-88-5	Cardiovascular	Antianginal
									Antiarrhythmic
									Antihypertensive
Prestw-251	04B02	Chlorothiazide	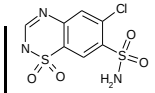	C7H6ClN3O4S2	295.72	Store at room temperature	58-94-6	Metabolism	Antihypertensive
									Diuretic
Prestw-252	04B03	Diphenidolhydrochloride	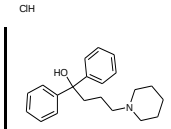	C21H28ClNO	345.92	Store at room temperature	3254-89-5	Central Nervous System	Antiemetic
									Antivertigo
Prestw-253	04B04	Norethindrone	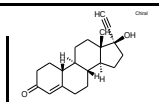	C20H26O2	298.43	Store at room temperature	68-22-4	Endocrinology	Contraceptive
Prestw-254	04B05	Nortriptyline hydrochloride	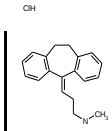	C19H22ClN	299.85	Store at room temperature	894-71-3	Central Nervous System	Antidepressant
									CNS Stimulant
Prestw-255	04B06	Niflumic acid	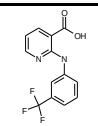	C13H9F3N2O2	282.22	Store at room temperature	4394-00-7	Central Nervous System	Analgesic

								Metabolism	Anti-inflammatory
									Antipyretic
Prestw-256	04B07	Isotretinoin	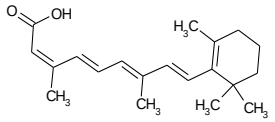	C20H28O2	300.44	Store at -20°C Light sensitive	4759-48-2	Dermatology	Keratolytic
Prestw-257	04B08	Retinoic acid	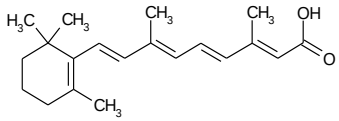	C20H28O2	300.44	Store at -20°C Light sensitive Store under nitrogen	302-79-4	Dermatology	Keratolytic
Prestw-258	04B09	Antazoline hydrochloride		C17H20ClN3	301.82	Store at room temperature	2508-72-7	Allergology	Antihistaminic
								Central Nervous System	Sedative
Prestw-259	04B10	Ethacrynic acid	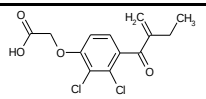	C13H12Cl2O4	303.14	Store at room temperature	58-54-8	Metabolism	Diuretic
Prestw-260	04B11	Praziquantel	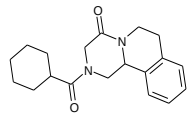	C19H24N2O2	312.42	Store at -20°C	55268-74-1	Infectiology	Antihelmintic

Prestw-261	04C02	Ethisterone	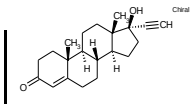	C21H28O2	312.46	Store at room temperature	434-03-7	Endocrinology	Contraceptive
Prestw-262	04C03	Triprolidine hydrochloride	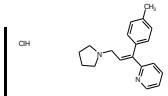	C19H23ClN2	314.86	Store at +4°C	550-70-9	Allergology	Antihistaminic
								Central Nervous System	Sedative
Prestw-263	04C04	Doxepin hydrochloride	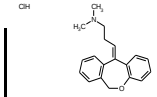	C19H22ClNO	315.85	Store at room temperature	1229-29-4	Allergology	Anticonvulsant
								Central Nervous System	Antidepressant
									Antipruritic
									Antispastic
									Muscle relaxant
Prestw-264	04C05	Dyclonine hydrochloride	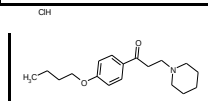	C18H28ClNO2	325.88	Store at room temperature	536-43-6	Neuromuscular	Local anesthetic
Prestw-265	04C06	Dimenhydrinate	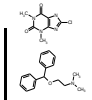	C24H28ClN5O3	469.98	Store at room temperature	523-87-5	Allergology	Antiemetic
								Central Nervous System	Antihistaminic
									Antivertigo

Prestw-266	04C07	Disopyramide		C21H29N3O	339.48	Store at room temperature	3737-09-5	Cardiovascular	Antiarrhythmic
Prestw-267	04C08	Clotrimazole		C22H17ClN2	344.85	Store at room temperature	23593-75-1	Infectiology	Antibacterial
									Antifungal
Prestw-268	04C09	Vinpocetine	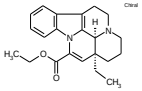	C22H26N2O2	350.46	Store at room temperature	42971-09-5	Cardiovascular	CNS Stimulant
								Central Nervous System	Neuroprotectant
									Vasodilator
Prestw-269	04C10	Clomipramine hydrochloride		C19H24Cl2N2	351.32	Store at room temperature	17321-77-6	Central Nervous System	Antidepressant
Prestw-270	04C11	Fendiline hydrochloride		C23H26ClN	351.92	Store at room temperature	13636-18-5	Cardiovascular	Antianginal
Prestw-271	04D02	Vincamine	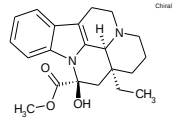	C21H26N2O3	354.45	Store at room temperature	1617-90-9	Central Nervous System	CNS Stimulant
									Vasodilator

Prestw-272	04D03	Indomethacin	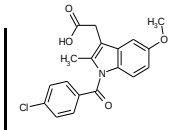	C19H16ClNO4	357.80	Store at room temperature	53-86-1	Central Nervous System	Analgesic
								Metabolism	Anti-inflammatory
									Antipyretic
									Uricosuric
Prestw-273	04D04	Cortisone	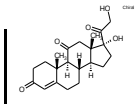	C21H28O5	360.45	Store at room temperature	53-06-5	Endocrinology	Anti-inflammatory
								Metabolism	Immunosuppressant
Prestw-274	04D05	Prednisolone	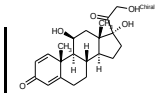	C21H28O5	360.45	Store at room temperature	50-24-8	Endocrinology	Anti-inflammatory
								Immunology	Immunosuppressant
Prestw-275	04D06	Fenofibrate	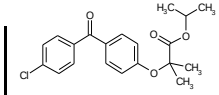	C20H21ClO4	360.84	Store at room temperature	49562-28-9	Metabolism	Hypocholesterolemic
									Lipid-lowering
									Uricosuric
Prestw-276	04D07	Bumetanide	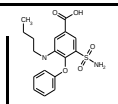	C17H20N2O5S	364.42	Store at room temperature	28395-03-1	Metabolism	Diuretic

Prestw-277	04D08	Labetalol hydrochloride	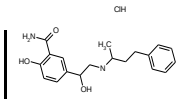	C19H25ClN2O3	364.88	Store at room temperature	32780-64-6	Cardiovascular	Antihypotensive
Prestw-278	04D09	Cinnarizine	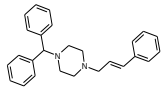	C26H28N2	368.53	Store at room temperature	298-57-7	Allergology	Antihistaminic
								Central Nervous System	Antivertigo
									Sedative
									Vasodilator
Prestw-279	04D10	Methylprednisolone, 6-alpha	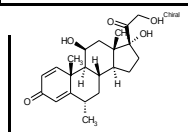	C22H30O5	374.48	Store at room temperature	83-43-2	Endocrinology	Anti-inflammatory
									Immunosuppressant
Prestw-280	04D11	Quinidine hydrochloride monohydrate	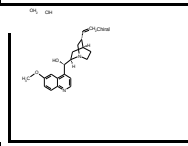	C20H27ClN2O3	378.90	Store at room temperature	6151-40-2	Cardiovascular	Antiarrhythmic
								Infectiology	Antimalarial
Prestw-281	04E02	Fludrocortisone acetate	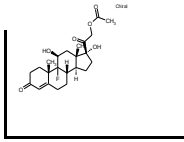	C23H31FO6	422.50	Store at room temperature	514-36-3	Dermatology	Anti-inflammatory
								Endocrinology	Antipruritic
Prestw-282	04E03	Fenoterol hydrobromide	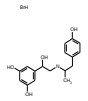	C17H22BrNO4	384.27	Store at room temperature	1944-12-3	Neuromuscular	Bronchodilator

								Respiratory	Tocolytic
Prestw-283	04E04	Homochlorcyclizine dihydrochloride	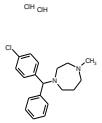	C19H25Cl3N2	387.78	Store at room temperature	1982-36-1	Allergology	Antihistaminic
								Central Nervous System	Sedative
Prestw-284	04E05	Diethylcarbamazine citrate	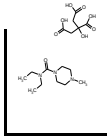	C16H29N3O8	391.42	Store at room temperature	1642-54-2	Infectiology	Antihelmintic
								Metabolism	
Prestw-285	04E06	Chenodiol	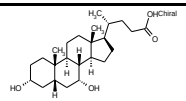	C24H40O4	392.58	Store at room temperature	474-25-9	Gastroenterology	Cholagogue
									Choleretic
Prestw-286	04E07	Perhexiline maleate		C23H39NO4	393.57	Store at room temperature	6724-53-4	Cardiovascular	Antianginal
Prestw-287	04E08	Oxybutynin chloride	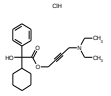	C22H32ClNO3	393.96	Store at room temperature	1508-65-2	Neuromuscular	Antispastic
Prestw-288	04E09	Spiperone	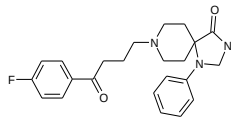	C23H26FN3O2	395.48	Store at room temperature	749-02-0	Central Nervous System	Antipsychotic

Prestw-289	04E10	Pyrilamine maleate	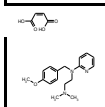	C21H27N3O5	401.47	Store at room temperature	59-33-6	Allergology	Antihistaminic
								Central Nervous System	Antipruritic
								Respiratory	Antitussive
									Sedative
Prestw-290	04E11	Sulfinpyrazone	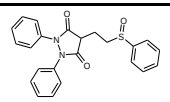	C23H20N2O3S	404.49	Store at room temperature	57-96-5	Hematology	Antiplatelet
								Metabolism	Uricosuric
Prestw-291	04F02	Dantrolene sodium salt	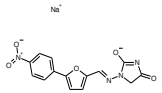	C14H9N4NaO5	336.24	Store at room temperature	14663-23-1	Neuromuscular	Muscle relaxant
Prestw-292	04F03	Trazodone hydrochloride	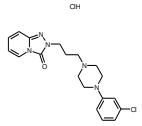	C19H23Cl2N5O	408.33	Store at room temperature	25332-39-2	Central Nervous System	Antidepressant
Prestw-293	04F04	Glafenine hydrochloride	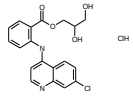	C19H18Cl2N2O4	409.27	Store at room temperature	65513-72-6	Metabolism	Analgesic
Prestw-294	04F05	Pimethixene maleate		C23H23NO4S	409.51	Store at room temperature	13187-06-9	Allergology	Antihistaminic

								Central Nervous System	Antitussive
								Respiratory	Bronchodilator
									Sedative
Prestw-295	04F06	Pergolide mesylate	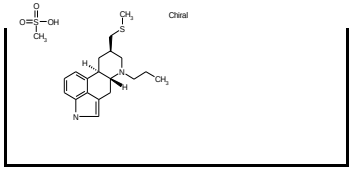	C20H30N2O3S2	410.60	Store at -20°C	66104-23-2	Central Nervous System	Antiparkinsonian
Prestw-296	04F07	Acemetacin	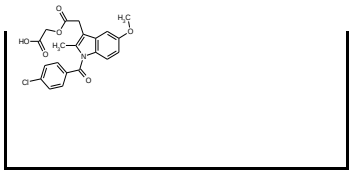	C21H18ClNO6	415.83	Store at room temperature	53164-05-9	Metabolism	Anti-inflammatory
Prestw-297	04F08	Benzydamine hydrochloride	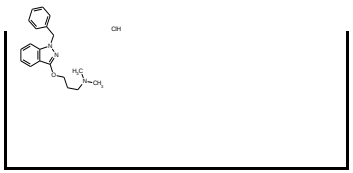	C19H24ClN3O	345.88	Store at +4°C	132-69-4	Central Nervous System	Analgesic
								Metabolism	Anti-inflammatory
									Antipyretic
Prestw-298	04F09	Fipexide hydrochloride	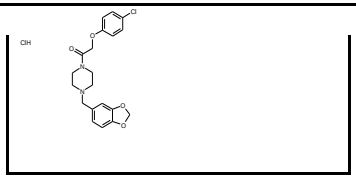	C20H22Cl2N2O4	425.32	Store at room temperature	34161-23-4	Central Nervous System	Anti-fatigue
									CNS Stimulant

Prestw-299	04F10	Mifepristone	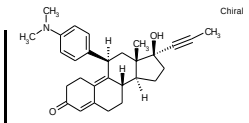	C29H35NO2	429.61	Store at +4°C	84371-65-3	Endocrinology	Abortifacient
Prestw-300	04F11	Diperodon hydrochloride	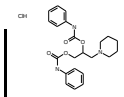	C22H28ClN3O4	433.94	Store at room temperature	537-12-2	Neuromuscular	Local anesthetic
Prestw-301	04G02	Lisinopril	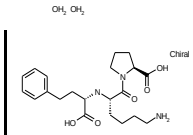	C21H35N3O7	441.53	Store at -20°C	83915-83-7	Cardiovascular	Antihypertensive
									Vasodilator
Prestw-302	04G03	Lincomycin hydrochloride	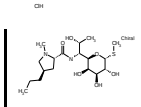	C18H35ClN2O6S	443.01	Store at +4°C	859-18-7	Infectiology	Antibacterial
								Metabolism	
Prestw-303	04G04	Telenzepine dihydrochloride	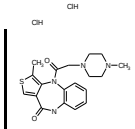	C19H24Cl2N4O2S	443.40	Store at room temperature	147416-96-4	Gastroenterology	Antiulcer
Prestw-304	04G05	Econazole nitrate	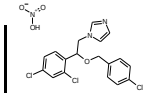	C18H16Cl3N3O4	444.70	Store at room temperature	24169-02-6	Infectiology	Antifungal
								Metabolism	
Prestw-305	04G06	Bupivacaine hydrochloride	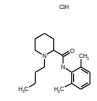	C18H29ClN2O	324.90	Store at room temperature	18010-40-7	Neuromuscular	Local anesthetic

Prestw-306	04G07	Clemastine fumarate	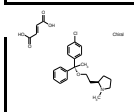	C25H30ClNO5	459.97	Store at room temperature	14976-57-9	Allergology	Antiemetic
								Central Nervous System	Antihistaminic
									Sedative
Prestw-307	04G08	Oxytetracycline dihydrate	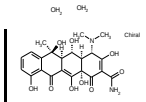	C22H28N2O11	496.48	Store at room temperature	6153-64-6	Infectiology	Antibacterial
								Metabolism	
Prestw-308	04G09	Pimozide	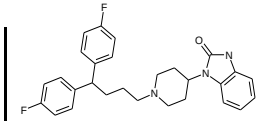	C28H29F2N3O	461.56	Store +4°C	2062-78-4	Central Nervous System	Antipsychotic
Prestw-309	04G10	Amodiaquin dihydrochloride dihydrate	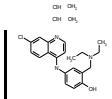	C20H28Cl3N3O3	464.82	Store at room temperature	6398-98-7	Infectiology	Anti-inflammatory
								Metabolism	Antimalarial
Prestw-310	04G11	Mebeverine hydrochloride	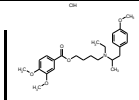	C25H36ClNO5	466.02	Store at +4°C Light sensitive	2753-45-9	Neuromuscular	Antispastic
Prestw-311	04H02	Ifenprodil tartrate	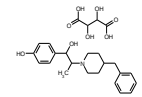	C25H33NO8	475.54	Store at room temperature	23210-58-4	Cardiovascular	Vasodilator

Prestw-312	04H03	Flunarizine dihydrochloride	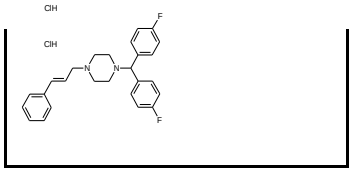	C26H28Cl2F2N2	477.43	Store at +4°C	30484-77-6	Central Nervous System	Anticonvulsant
									Vasodilator
Prestw-313	04H04	Trifluoperazine dihydrochloride	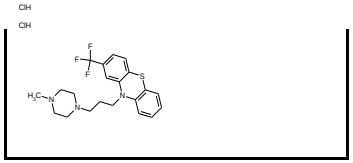	C21H26Cl2F3N3S	480.43	Store at room temperature	440-17-5	Central Nervous System	Antiemetic
									Antipsychotic
Prestw-314	04H05	Enalapril maleate		C24H32N2O9	492.53	Store at room temperature	76095-16-4	Cardiovascular	Antihypertensive
Prestw-315	04H06	Minocycline hydrochloride	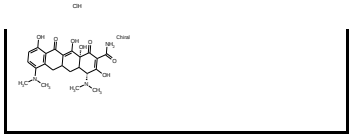	C23H28ClN3O7	493.95	Store at +4°C	13614-98-7	Infectiology	Antibacterial
								Metabolism	
Prestw-316	04H07	Glibenclamide	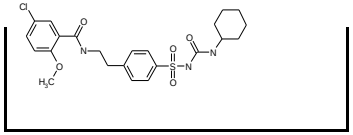	C23H28ClN3O5S	494.01	Store at room temperature	10238-21-8	Endocrinology	Antidiabetic
Prestw-317	04H08	Guanethidine sulfate	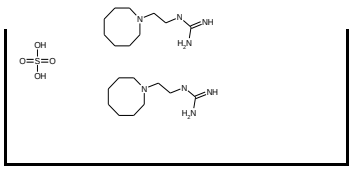	C20H46N8O4S	494.70	Store at room temperature	60-02-6	Central Nervous System	Antihypertensive
								Diagnostic	Local anesthetic

Prestw-318	04H09	Quinacrine dihydrochloride dihydrate	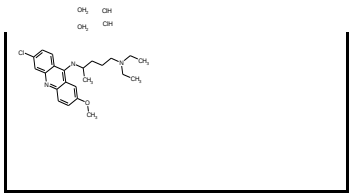	C23H36Cl3N3O3	508.92	Store at room temperature Light sensitive	6151-30-0	Infectiology	Antihelmintic
								Metabolism	Antileishmanial
									Antimalarial
									Antiparasitic
									Antiprotozoal
									Antitrichomonal
Prestw-319	04H10	Clofilium tosylate	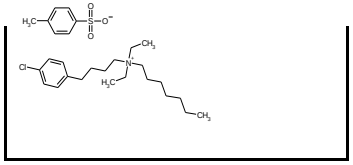	C28H44ClNO3S	510.18	Store at RT	92953-10-1	Cardiovascular	Antiarrhythmic
Prestw-320	04H11	Fluphenazine dihydrochloride	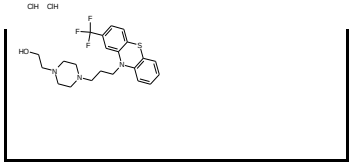	C22H28Cl2F3N3OS	510.45	Store at room temperature	146-56-5	Central Nervous System	Antipsychotic
Prestw-321	05A02	Streptomycin sulfate	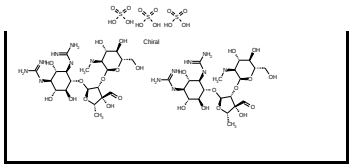	C42H84N14O36S3	1457.40	Store at +4°C	3810-74-0	Infectiology	Antibacterial
								Metabolism	
Prestw-322	05A03	Alfuzosin hydrochloride	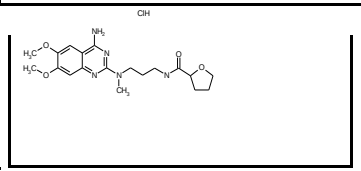	C19H28ClN5O4	425.92	Store at -20	81403-68-1	Cardiovascular	Vasodilator
Prestw-323	05A04	Chlorpropamide	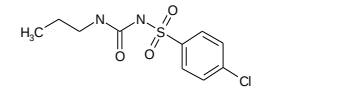	C10H13ClN2O3S	276.74	Store at room temperature	94-20-2	Endocrinology	Antidiabetic

Prestw-324	05A05	Phenylpropanolamine hydrochloride	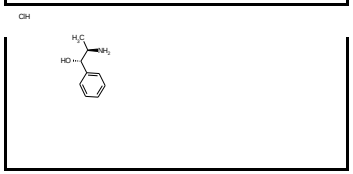	C9H14ClNO	187.67	Store at room temperature	154-41-6	Respiratory	Antihypotensive
									Nasal Decongestant
									Vasoconstrictor
Prestw-325	05A06	Ascorbic acid	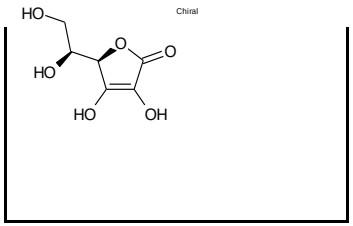	C6H8O6	176.13	Store at room temperature Rapide oxidation in solution	50-81-7	Metabolism	Anti-oxidant
									CNS Stimulant
									Hemostatic
Prestw-326	05A07	Methyldopa (L,-)		C10H13NO4	211.22	Store at room temperature	555-30-6	Cardiovascular	Antihypertensive
								Central Nervous System	
Prestw-327	05A08	Cefoperazone dihydrate	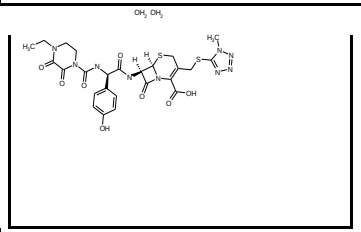	C25H31N9O10S2	681.71	Store at -20°C Highly unstable in alkaline solution	not availabl e	Infectiology	Antibacterial
								Metabolism	

Prestw-328	05A09	Zoxazolamine	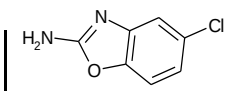	C7H5ClN2O	168.58	Store at +4°C	61-80-3	Metabolism	Antigout
								Neuromuscular	Muscle relaxant
									Uricosuric
Prestw-329	05A10	Tacrine hydrochloride	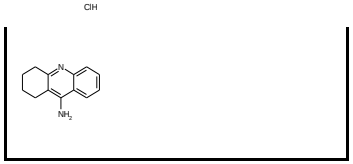	C13H15ClN2	234.73	Store at +4°C	1684-40-8	Central Nervous System	CNS Stimulant
Prestw-330	05A11	Bisoprolol fumarate	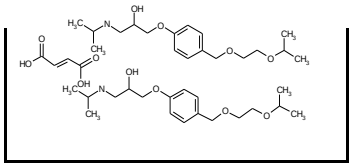	C40H66N2O12	766.98	Store at -20°C	104344-23-2	Cardiovascular	Antianginal
									Antiarrhythmic
									Antihypertensive
Prestw-331	05B02	Tremorine dihydrochloride	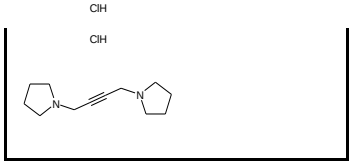	C12H22Cl2N2	265.23	Store at -20°C	51-73-0	Central Nervous System	CNS Stimulant
Prestw-332	05B03	Practolol	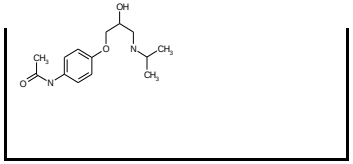	C14H22N2O3	266.34	Store at room temperature	6673-35-4	Cardiovascular	Antianginal
									Antihypertensive
Prestw-333	05B04	Zidovudine, AZT	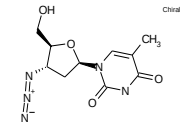	C10H13N5O4	267.25	Store at -20°C	30516-87-1	Infectiology	Antiviral

								Metabolism	
Prestw-334	05B05	Sulfisoxazole	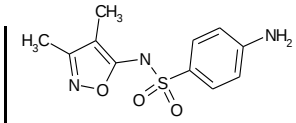	C11H13N3O3S	267.31	Store at +4°C	127-69-5	Infectiology	Antibacterial
								Metabolism	
Prestw-335	05B06	Zaprinast	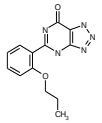	C13H13N5O2	271.28	Store at room temperature	37762-06-4	Cardiovascular	Erectile dysfunction treatment
Prestw-336	05B07	Chlormezanone	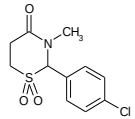	C11H12ClNO3S	273.74	Store at room temperature	80-77-3	Central Nervous System	Anxiolytic
								Neuromuscular	Muscle relaxant
Prestw-337	05B08	Procainamide hydrochloride	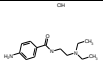	C13H22ClN3O	271.79	Store at room temperature	614-39-1	Cardiovascular	Antiarrhythmic
								Neuromuscular	Local anesthetic
									Vasodilator

Prestw-338	05B09	N6-methyladenosine	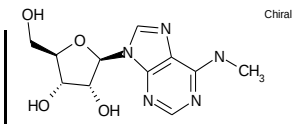	C11H15N5O4	281.27	Store at -20°C	1867-73-8	Oncology	Antineoplastic
Prestw-339	05B10	Guanfacine hydrochloride	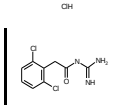	C9H10Cl3N3O	282.56	Store at room temperature	29110-48-3	Cardiovascular	Antihypertensive
								Central Nervous System	
Prestw-340	05B11	Domperidone	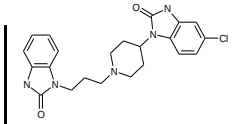	C22H24ClN5O2	425.92	Store at -20°C	57808-66-9	Central Nervous System	Antiemetic
Prestw-341	05C02	Furosemide	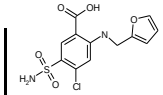	C12H11ClN2O5S	330.75	Store at room temperature	54-31-9	Metabolism	Antihypertensive
									Diuretic
Prestw-342	05C03	Methapyrilene hydrochloride	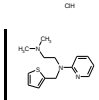	C14H20ClN3S	297.85	Store at room temperature	135-23-9	Allergology	Antihistaminic
								Central Nervous System	Sedative
Prestw-343	05C04	Desipramine hydrochloride	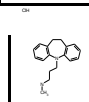	C18H23ClN2	302.85	Store at +4°C	58-28-6	Central Nervous System	Antidepressant
									CNS Stimulant

Prestw-344	05C05	Clorgyline hydrochloride	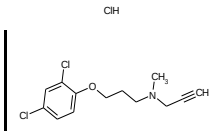	C13H16Cl3NO	308.64	Store at +4°C	17780-75-5	Central Nervous System	Antidepressant
Prestw-345	05C06	Clenbuterol hydrochloride	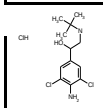	C12H19Cl3N2O	313.66	Store at +4°C	21898-19-1	Neuromuscular	Antiasthmatic
								Respiratory	Bronchodilator
									Tocolytic
Prestw-346	05C07	Maprotiline hydrochloride	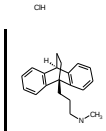	C20H24ClN	313.87	Store at room temperature	10347-81-6	Central Nervous System	Antidepressant
									Anxiolytic
Prestw-347	05C08	Thioguanosine	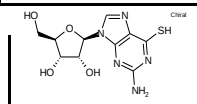	C10H13N5O4S	299.31	Store at room temperature	85-31-4	Metabolism	Antineoplastic
								Oncology	
Prestw-348	05C09	Chlorprothixene hydrochloride	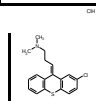	C18H19Cl2NS	352.33	Store at +4°C Light sensitive	6469-93-8	Central Nervous System	Antiemetic
									Antipsychotic
Prestw-349	05C10	Ritodrine hydrochloride	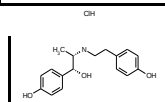	C17H22ClNO3	323.82	Store at room temperature	23239-51-2	Neuromuscular	Tocolytic

Prestw-350	05C11	Clozapine	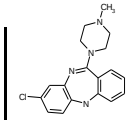	C18H19ClN4	326.83	Store at room temperature Light sensitive	5786-21-0	Central Nervous System	Antiparkinsonian
									Antipsychotic
Prestw-351	05D02	Chlorthalidone	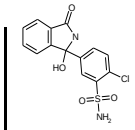	C14H11ClN2O4S	338.77	Store at +4°C	77-36-1	Metabolism	Antihypertensive
									Diuretic
Prestw-352	05D03	Dobutamine hydrochloride	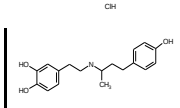	C18H24ClNO3	337.85	Store at +2°C	49745-95-1	Cardiovascular	Analeptic
									Cardiotonic
									Positive inotropic
Prestw-353	05D04	Moclobemide	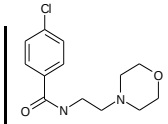	C13H17ClN2O2	268.75	store at -20°C	71320-77-9	Central Nervous System	Antidepressant
Prestw-354	05D05	Clopamide	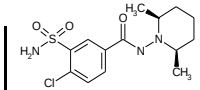	C14H20ClN3O3S	345.85	Store at room temperature	636-54-4	Metabolism	Antihypertensive
									Diuretic

Prestw-355	05D06	Hycanthone	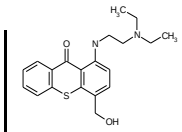	C20H24N2O2S	356.49	Store at -20°C	3105-97-3	Infectiology	Antihelmintic
									Antiparasitic
Prestw-356	05D07	Adenosine 5'-monophosphate monohydrate	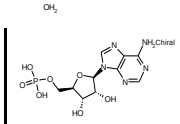	C10H16N5O8P	365.24	Store at +4°C	18422-05-4	Cardiovascular	Antiarrhythmic
								Metabolism	
Prestw-357	05D08	Amoxicillin	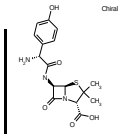	C16H19N3O5S	365.41	Store at +4°C	26787-78-0	Metabolism	Antibacterial
								Infectiology	
Prestw-1603	05D09	Pemirolast potassium	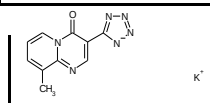	C10H7KN6O	266.31	Store at room temperature	100299-08-9	Ophthalmology	
Prestw-359	05D10	Dextromethorphan hydrobromide monohydrate	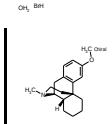	C18H28BrNO2	370.33	Store at room temperature	6700-34-1	Central Nervous System	Antitussive
Prestw-360	05D11	Droperidol	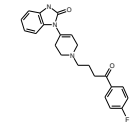	C22H22FN3O2	379.44	Store at +4°C	548-73-2	Central Nervous System	Antipsychotic

Prestw-361	05E02	Bambuterol hydrochloride		C18H30ClN3O5	403.91	Store at -20°C	81732-46-9	Neuromuscular	Bronchodilator
								Respiratory	Tocolytic
Prestw-362	05E03	Betamethasone	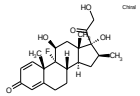	C22H29FO5	392.47	Store at room temperature	378-44-9	Endocrinology	Anti-inflammatory
									Antipruritic
									Immunosuppressant
Prestw-363	05E04	Colchicine	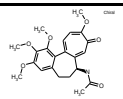	C22H25NO6	399.45	Store at room temperature	64-86-8	Metabolism	Antigout
									Anti-inflammatory
Prestw-364	05E05	Metergoline	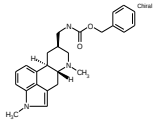	C25H29N3O2	403.53	Store at -20°C	17692-51-2	Central Nervous System	Antiprolactin
Prestw-365	05E06	Brinzolamide	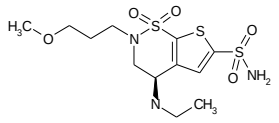	C12H21N3O5S3	383.51	Store at -20°C	138890-62-7	Metabolism	Antiglaucoma
									Diuretic

Prestw-366	05E07	Ambroxol hydrochloride	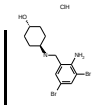	C13H19Br2ClN2O	414.57	Store at +4°C	23828-92-4	Respiratory	Expectorant
									Mucolytic
Prestw-367	05E08	Benfluorex hydrochloride	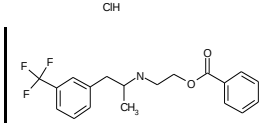	C19H21ClF3NO2	387.83	Store at room temperature	23642-66-2	Central Nervous System	Anorectic
									Antidiabetic
									CNS Stimulant
Prestw-368	05E09	Bepridil hydrochloride	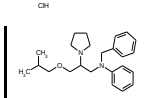	C24H35ClN2O	403.01	Store at room temperature	74764-40-2	Cardiovascular	Antianginal
									Antiarrhythmic
									Antihypotensive
									Vasodilator
Prestw-369	05E10	Meloxicam	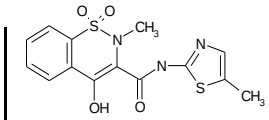	C14H13N3O4S2	351.41	store at -20°C	71125-38-7	Metabolism	Anti-inflammatory
Prestw-370	05E11	Benzbromarone	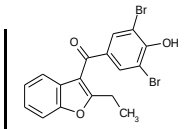	C17H12Br2O3	424.09	Store at +4°C	3562-84-3	Cardiovascular	Antianginal
									Antigout
									Antispastic
									Uricosuric
									Vasodilator

Prestw-371	05F02	Ketotifen fumarate	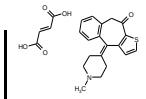	C23H23NO5S	425.51	Store at room temperature	34580-14-8	Allergology	Antihistaminic
Prestw-372	05F03	Debrisoquin sulfate	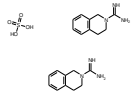	C20H28N6O4S	448.55	Store at room temperature	581-88-4	Cardiovascular	Antihypertensive
Prestw-373	05F04	Amethopterin (R,S)	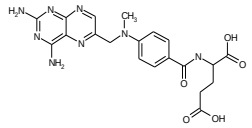	C20H22N8O5	454.45	Store at -20°C	60388-53-6	Immunology	Anti-inflammatory
								Metabolism	Antineoplastic
								Oxytocic	
Prestw-374	05F05	Methylergometrine maleate	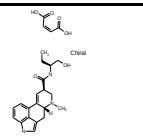	C24H29N3O6	455.52	Store at room temperature	57432-61-8	Neuromuscular	Hemostatic
Prestw-375	05F06	Methiothepin maleate	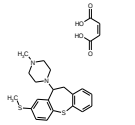	C24H28N2O4S2	472.63	Store at room temperature	19728-88-2	Central Nervous System	Antipsychotic
Prestw-376	05F07	Clofazimine	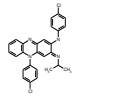	C27H22Cl2N4	473.41	Store at room temperature	2030-63-9	Infectiology	Antibacterial
Prestw-377	05F08	Nafronyl oxalate	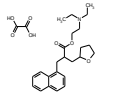	C26H35NO7	473.57	Store at room temperature	3200-06-4	Cardiovascular	Anti-ischemic

								Neuromuscular	Antispastic
									Vasodilator
Prestw-378	05F09	Bezafibrate	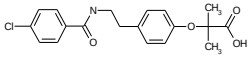	C19H20ClNO4	361.83	Store at room temperature	41859-67-0	Metabolism	Antilipemic
									Hypocholesterolemic
									Lipid-lowering
Prestw-1152	05F10	Nefazodone HCl	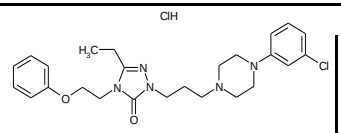	C25H33Cl2N5O2	506.48	Store at +4°C	82752-99-6	Central Nervous System	Antidepressant
Prestw-380	05F11	Clebopride maleate	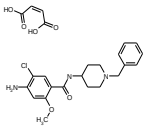	C24H28ClN3O6	489.96	Store at +4°C	84370-95-6	Central Nervous System	Antiemetic
									Antispastic
Prestw-381	05G02	Lidoflazine	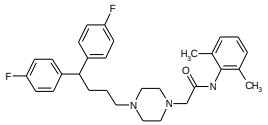	C30H35F2N3O	491.63	Store at +4°C	3416-26-0	Cardiovascular	Antianginal
									Antiarrhythmic
									Vasodilator
Prestw-382	05G03	Betaxolol hydrochloride	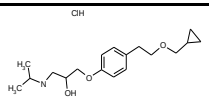	C18H30ClNO3	343.90	Store at -20	63659-19-8	Cardiovascular	Antiglaucoma
								Ophthalmology	Antihypertensive

Prestw-383	05G04	Nicardipine hydrochloride	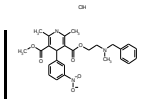	C26H30ClN3O6	516.00	Store at +4°C	54527-84-3	Cardiovascular	Antianginal
									Antihypertensive
Prestw-384	05G05	Probucol	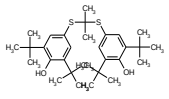	C31H48O2S2	516.86	Store at room temperature	23288-49-5	Metabolism	Antilipemic
									Hypocholesterolemic
Prestw-385	05G06	Mitoxantrone dihydrochloride	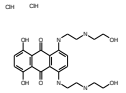	C22H30Cl2N4O6	517.41	Store at room temperature Hygroscopic	70476-82-3	Oncology	Antineoplastic
Prestw-386	05G07	GBR 12909 dihydrochloride	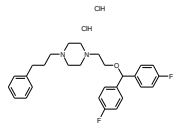	C28H34Cl2F2N2O	523.50	Store at room temperature	67469-78-7	Central Nervous System	Antidepressant
Prestw-387	05G08	Carbetapentane citrate	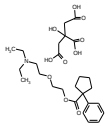	C26H39NO10	525.60	Store at room temperature	23142-01-0	Central Nervous System	Antispastic
								Neuromuscular	Antitussive
									Local anesthetic
Prestw-388	05G09	Dequalinium dichloride	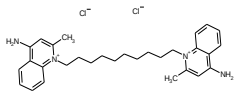	C30H40Cl2N4	527.59	Store at room temperature	522-51-0	Infectiology	Antibacterial

									Antiseptic
Prestw-389	05G10	Ketoconazole	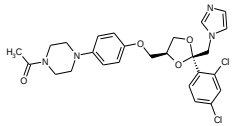	C26H28Cl2N4O4	531.44	Store at +4°C	65277-42-1	Infectiology	Antifungal
								Metabolism	
Prestw-390	05G11	Fusidic acid sodium salt	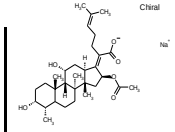	C31H47NaO6	538.71	+ 4°C	751-94-0	Infectiology	Antibacterial
								Metabolism	
Prestw-391	05H02	Terbutaline hemisulfate	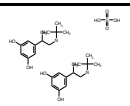	C24H40N2O10S	548.66	Store at room temperature	23031-32-5	Respiratory	Antiasthmatic
									Bronchodilator
									Muscle relaxant
Prestw-392	05H03	Ketanserin tartrate hydrate	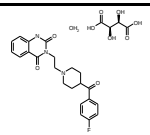	C26H30FN3O10	563.54	Store at room temperature	83846-83-7	Cardiovascular	Antihypertensive
									Vasodilator
Prestw-393	05H04	Hemicholinium bromide	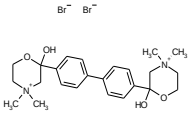	C24H34Br2N2O4	574.36	Store at room temperature !!! POISON !!!	312-45-8	Neuromuscular	Curarizing

Prestw-394	05H05	Kanamycin A sulfate	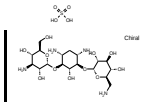	C18H38N4O15S	582.59	Store at room temperature	25389-94-0	Infectiology	Antibacterial
								Metabolism	
Prestw-395	05H06	Amikacin hydrate	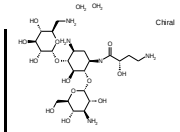	C22H47N5O15	621.64	Store at +4°C	37517-28-5	Infectiology	Antibacterial
								Metabolism	
Prestw-396	05H07	Etoposide	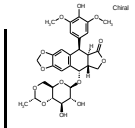	C29H32O13	588.57	Store at room temperature Light sensitive	33419-42-0	Oncology	Antineoplastic
Prestw-397	05H08	Clomiphene citrate (Z,E)	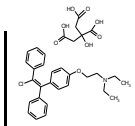	C32H36ClNO8	598.10	Store at +4°C	50-41-9	Endocrinology	
Prestw-398	05H09	Oxantel pamoate	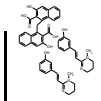	C49H48N4O8	820.95	Store at room temperature	68813-55-8	Infectiology	Antihelmintic

Prestw-399	05H10	Prochlorperazine dimaleate	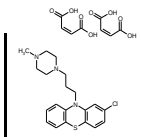	C28H32ClN3O8S	606.10	Store at room temperature	84-02-6	Central Nervous System	Antiemetic
									Antipsychotic
Prestw-400	05H11	Hesperidin	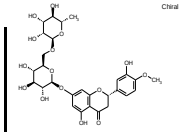	C28H34O15	610.57	Store at +4°C	520-26-3	Oncology	Anti-haemorrhoids
									Antineoplastic
									Anti-oxidant
Prestw-401	06A02	Testosterone propionate	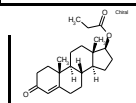	C22H32O3	344.50	Store at room temperature	57-85-2	Endocrinology	Anabolic
Prestw-1269	06A03	Haloprogin	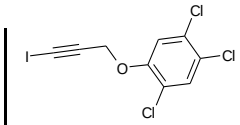	C9H4Cl3IO	361.40	Store at room temperature	777-11-7	Central Nervous System	Anesthetic
									Antifungal
Prestw-403	06A04	Thyroxine (L)	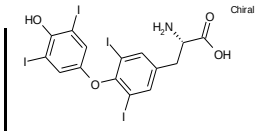	C15H11I4NO4	776.88	Store at RT	51-48-9	Endocrinology	Antihypothyroid
								Metabolism	Antilipemic
									Hypocholesterolemic
									Lipid-lowering

Prestw-1288	06A05	Idebenone	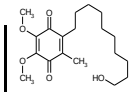	C19H30O5	338.45	Store at room temperature	58186-27-9	Oncology	Antineoplastic
Prestw-405	06A06	Pepstatin A	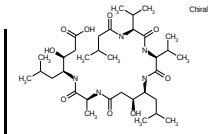	C34H63N5O9	685.91	Store at -20°C	26305-03-3	Infectiology	Antiviral
								Metabolism	
Prestw-406	06A07	Morpholinoethylamino-3-benzocyclohepta-(5,6-c)-pyridazine dihydrochloride	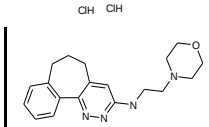	C19H26Cl2N4O	397.35	Store at room temperature	115767-94-7		
Prestw-407	06A08	Adamantamine fumarate	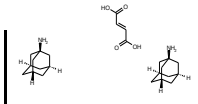	C24H38N2O4	418.58	Store at room temperature	80789-67-9	Infectiology	Antiviral
Prestw-408	06A09	Butoconazole nitrate	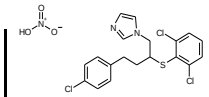	C19H18Cl3N3O3S	474.80	Store at room temperature	32872-77-1	Infectiology	Antibacterial
								Metabolism	Antifungal
Prestw-409	06A10	Amiodarone hydrochloride	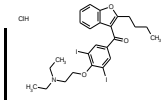	C25H30ClI2NO3	681.78	Store at +4°C	19774-82-4	Cardiovascular	Antianginal
									Antiarrhythmic
Prestw-410	06A11	Amphotericin B	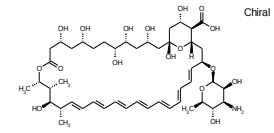	C47H73NO17	924.10	Store at +4°C	1397-89-3	Infectiology	Antibacterial

									Antifungal
Prestw-411	06B02	Androsterone	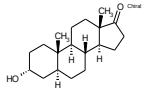	C19H30O2	290.45	Store at room temperature	53-41-8	Endocrinology	Anabolic
Prestw-1489	06B03	Amifostine	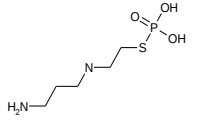	C5H15N2O3PS	214.22	Store at +4°C	20537-88-6	Diagnostic	
Prestw-413	06B04	Carbarsone	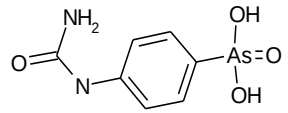	C7H9AsN2O4	260.08	Store at -20°C	121-59-5	Infectiology	Antiamebic
									Antiprotozoal
Prestw-1219	06B05	Amlodipine	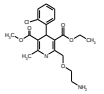	C20H25ClN2O5	408.89	Store at room temperature	88150-42-9	Cardiovascular	Antihypertensive
Prestw-1147	06B06	Modafinil	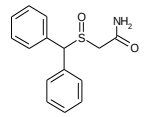	C15H15NO2S	273.36	Store at +4°C	68693-11-8	Central Nervous System	CNS Stimulant
Prestw-416	06B07	Bacampicillin hydrochloride		C21H28ClN3O7S	501.99	Store at -20°C	37661-08-8	Infectiology	Antibacterial
								Metabolism	

Prestw-1298	06B08	Lamivudine	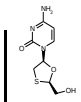	C8H11N3O3S	229.26	Store at room temperature	134678-17-4	Infectiology	Antiviral
								Metabolism	
Prestw-418	06B09	Biotin	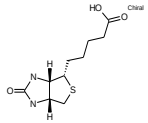	C10H16N2O3S	244.31	Store at +4°C	58-85-5	Metabolism	
Prestw-419	06B10	Bisacodyl	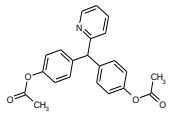	C22H19NO4	361.40	Store at +4°C	603-50-9	Gastroenterology	Laxative
Prestw-1242	06B11	Erlotinib	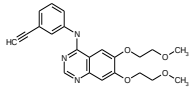	C22H23N3O4	393.45	Store at room temperature	183321-74-6	Oncology	Antineoplastic
Prestw-421	06C02	Suloctidil	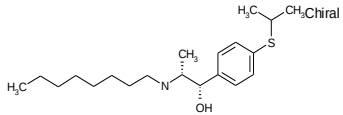	C20H35NOS	337.57	Store at +4°C	54063-56-8	Neuromuscular	Antiplatelet
									Vasodilator
Prestw-1368	06C03	Zotepine	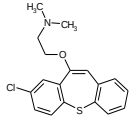	C18H18ClNOS	331.87	Store at room temperature	26615-21-4	Central Nervous System	Antipsychotic
Prestw-423	06C04	Carisoprodol	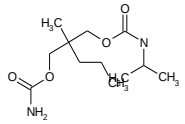	C12H24N2O4	260.34	Store at room temperature	78-44-4	Central Nervous System	Analgesic

									Antipyretic
									Muscle relaxant
									Sedative
Prestw-424	06C05	Cephalosporanic acid, 7-amino	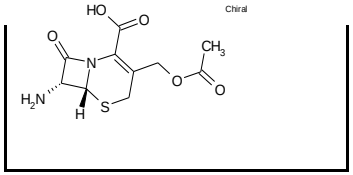	C10H12N2O5S	272.28	Store at +4°C	957-68-6	Infectiology	Antibacterial
								Metabolism	
Prestw-425	06C06	Chicago sky blue 6B	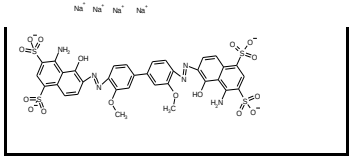	C34H24N6Na4O16S4	992.82	Store at room temperature	2610-05-1	Central Nervous System	
Prestw-426	06C07	Buflomedil hydrochloride	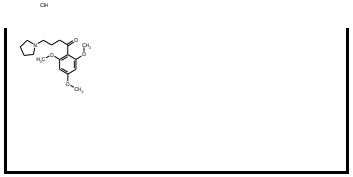	C17H26ClNO4	343.85	Store at room temperature	35543-24-9	Cardiovascular	Vasodilator
Prestw-1393	06C08	Dibenzepine hydrochloride	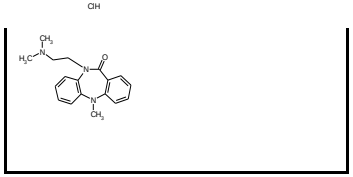	C18H22ClN3O	331.85	Store at room temperature	315-80-0	Central Nervous System	Antidepressant
Prestw-428	06C09	Roxatidine Acetate HCl	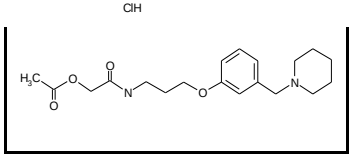	C19H29ClN2O4	384.91	store at -20°C	93793-83-0	Gastroenterology	Antiulcer

Prestw-1505	06C10	Valacyclovir hydrochloride	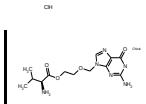	C13H21ClN6O4	360.80	Store at room temperature	124832-27-5	Infectiology	Antiviral
								Metabolism	
Prestw-430	06C11	Cisapride	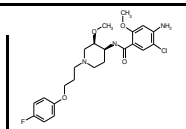	C23H29ClFN3O4	465.96	Store at -20°C	81098-60-4	Gastroenterology	Gastroprokinetic
Prestw-1303	06D02	Pefloxacine	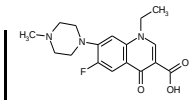	C17H20FN3O3	333.37	Store at room temperature	70458-92-3	Infectiology	Antibacterial
								Metabolism	
Prestw-432	06D03	Corticosterone	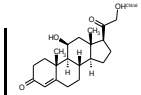	C21H30O4	346.47	Store at room temperature	50-22-6	Endocrinology	Anti-inflammatory
									Immunosuppressant
Prestw-433	06D04	Cyanocobalamin	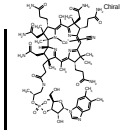	C63H88CoN14O14P	1355.40	Store at -20°C	68-19-9	Metabolism	Analgesic
Prestw-434	06D05	Cefadroxil	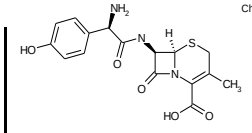	C16H17N3O5S	363.39	Store at +4°C	50370-12-2	Infectiology	Antibacterial
								Metabolism	

Prestw-435	06D06	Cyclosporin A	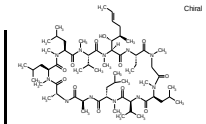	C62H111N11O12	1202.64	Store at -20°C	59865-13-3	Immunology	Immunosuppressant
Prestw-436	06D07	Digitoxigenin	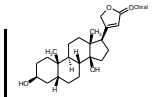	C23H34O4	374.53	Store at room temperature	143-62-4	Cardiovascular	Cardiotonic
Prestw-437	06D08	Digoxin	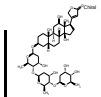	C41H64O14	780.96	Store at room temperature	20830-75-5	Cardiovascular	Cardiotonic
Prestw-438	06D09	Doxorubicin hydrochloride	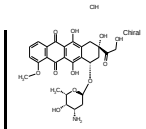	C27H30ClNO11	579.99	Store at -20°C !!! POISON !!!	25316-40-9	Infectiology	Antibacterial
								Oncology	Antineoplastic
									Immunosuppressant
Prestw-439	06D10	Carbimazole	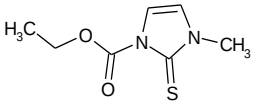	C7H10N2O2S	186.23	Store at -20°C	22232-54-8	Metabolism	Antihyperthyroid
Prestw-440	06D11	Epiandrosterone	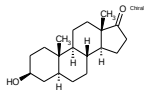	C19H30O2	290.45	Store at room temperature	481-29-8	Endocrinology	Anabolic

Prestw-441	06E02	Estradiol-17 beta	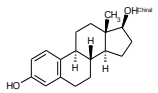	C18H24O2	272.39	Store at room temperature	50-28-2	Endocrinology	Antigonadotropin
Prestw-1380	06E03	Clobutinol hydrochloride	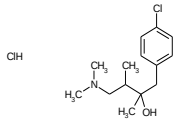	C14H23Cl2NO	292.25	Store at room temperature	1215-83-4	Central Nervous System	Antitussive
Prestw-443	06E04	Gabazine bromide	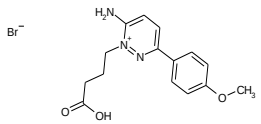	C15H18BrN3O3	368.23	Store at room temperature	105538-73-6	Central Nervous System	CNS Stimulant
Prestw-1156	06E05	Oxcarbazepine	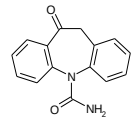	C15H12N2O2	252.28	Store at +4°C	28721-07-5	Central Nervous System	Anticonvulsant
Prestw-445	06E06	Cyclobenzaprine hydrochloride		C20H22ClN	311.86	Store at room temperature	6202-23-9	Neuromuscular	Muscle relaxant
Prestw-446	06E07	Carteolol hydrochloride	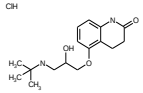	C16H25ClN2O3	328.84	Store at -20°C	51781-21-6	Cardiovascular	Antiglaucoma
								Ophthalmology	Antihypertensive
Prestw-447	06E08	Hydrocortisone base	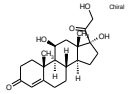	C21H30O5	362.47	Store at room temperature	50-23-7	Endocrinology	Anti-inflammatory

Prestw-448	06E09	Hydroxytacrine maleate (R,S)	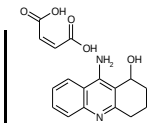	C17H18N2O5	330.34	Store at room temperature	118909-22-1	Central Nervous System	Anti-Alzheimer
Prestw-449	06E10	Pilocarpine nitrate	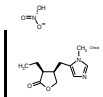	C11H17N3O5	271.28	Store at room temperature Poison!	148-72-1	Ophthalmology	Antiglaucoma
Prestw-450	06E11	Dicloxacillin sodium salt hydrate	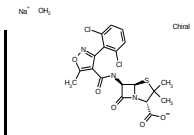	C19H18Cl2N3NaO6S	510.33	Store at +4°C	13412-64-1	Infectiology	Antibacterial
								Metabolism	
Prestw-451	06F02	Alizapride HCl	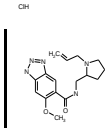	C16H22ClN5O2	351.84	store at -20°C	59338-87-3	Central Nervous System	Antiemetic
Prestw-1161	06F03	Stanozolol	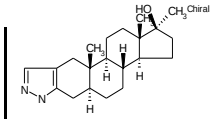	C21H32N2O	328.50	Store at +4°C	10418-03-8	Endocrinology	
Prestw-1257	06F04	Calcipotriene	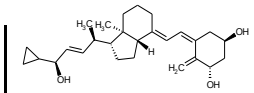	C27H40O3	412.62	Store at room temperature	112965-21-6	Dermatology	Antipsoriatic
								Metabolism	
Prestw-1429	06F05	Linezolid	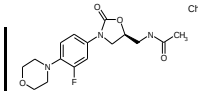	C16H20FN3O4	337.35	Store at room temperature	165800-03-3	Infectiology	Antibacterial

								Metabolism	
Prestw-455	06F06	Mebhydroline 1,5-naphtalenedisulfonate	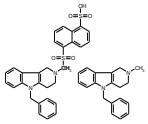	C48H48N4O6S2	841.07	Store at room temperature	6153-33-9	Allergology	Antihistaminic
Prestw-456	06F07	Meclocycline sulfosalicylate	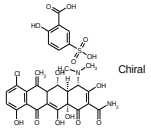	C29H27ClN2O14S	695.06	Store at room temperature	73816-42-9	Infectiology	Antibacterial
								Metabolism	
Prestw-457	06F08	Meclozine dihydrochloride	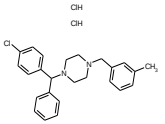	C25H29Cl3N2	463.88	Store at +4°C	1104-22-9	Allergology	Antiemetic
								Central Nervous System	Antihistaminic
									Sedative
Prestw-458	06F09	Melatonin	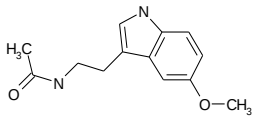	C13H16N2O2	232.28	Store at -20°C	73-31-4	Central Nervous System	Anticonvulsant
								Endocrinology	Anti-oxidant
								Immunology	Immunostimulant
Prestw-1251	06F10	Butalbital	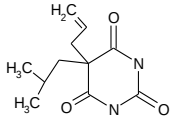	C11H16N2O3	224.26	Store at room temperature	77-26-9	Central Nervous System	Hypnotic

									Sedative
Prestw-460	06F11	Dinoprost trometamol	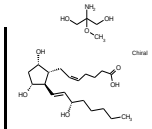	C24H45NO8	475.63	Store at -20°C	38362-01-5	Endocrinology	Oxytocic
Prestw-461	06G02	Tropisetron HCl	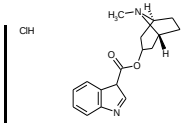	C17H21ClN2O2	320.82	Store at room temperature	105826-92-4	Central Nervous System	Antiemetic
Prestw-462	06G03	Cefixime	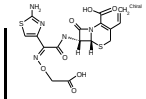	C16H15N5O7S2	453.46	Store at room temperature	79350-37-1	Infectiology	Antibacterial
								Metabolism	
Prestw-463	06G04	Metrizamide	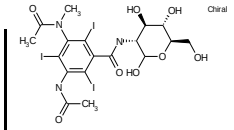	C18H22I3N3O8	789.10	Store at -20°C Light sensitive Dessicate	31112-62-6	Diagnostic	Contrastant
Prestw-1323	06G05	Quetiapine hemifumarate	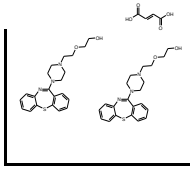	C46H54N6O8S2	883.11	Store at room temperature	111974-72-2	Central Nervous System	Antipsychotic
Prestw-1464	06G06	Tosufloxacin hydrochloride	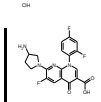	C19H16ClF3N4O3	440.81	Store at room temperature	100490-36-6	Infectiology	Antibacterial
								Metabolism	

Prestw-1400	06G07	Efavirenz	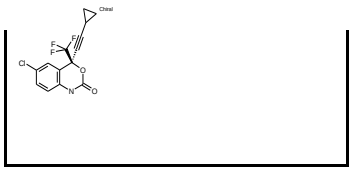	C14H9ClF3NO2	315.68	Store at room temperature	154598-52-4	Infectiology	Antiviral
								Metabolism	
Prestw-1157	06G08	Rifapentine	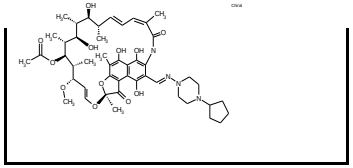	C47H64N4O12	877.05	Store at +4°C	61379-65-5	Infectiology	Antibacterial
								Metabolism	
Prestw-468	06G09	Neostigmine bromide	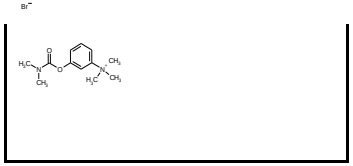	C12H19BrN2O2	303.20	Store at room temperature	114-80-7	Diagnostic	Anti-fatigue
Prestw-469	06G10	Niridazole	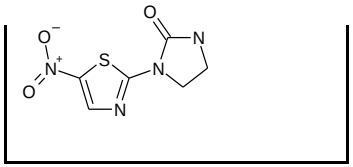	C6H6N4O3S	214.20	Store below 0°C	61-57-4	Infectiology	Antihelmintic
								Metabolism	Antiparasitic
									Antiprotozoal
Prestw-470	06G11	Ceforanide	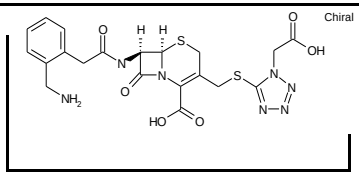	C20H21N7O6S2	519.56	Store below 0°C	60925-61-3	Infectiology	Antibacterial
								Metabolism	
Prestw-1358	06H02	Vatalanib		C20H15ClN4	346.82	Store at room temperature	212141-54-3	Oncology	Antineoplastic

Prestw-1295	06H03	Itopride	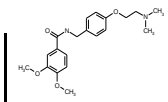	C20H26N2O4	358.44	Store at room temperature	122898-67-3	Metabolism	
Prestw-473	06H04	Cefotetan	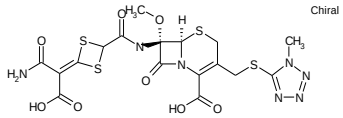	C17H17N7O8S4	575.62	Store at -20°C	69712-56-7	Infectiology	Antibacterial
								Metabolism	
Prestw-1254	06H05	Fentiazac	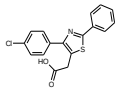	C17H12ClNO2S	329.81	Store at room temperature	18046-21-4	Metabolism	Anti-inflammatory
Prestw-475	06H06	Brompheniramine maleate	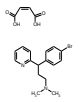	C20H23BrN2O4	435.32	Store at room temperature	980-71-2	Allergology	Antihistaminic
									Antipruritic
									Antitussive
									Sedative
Prestw-476	06H07	Primaquine diphosphate	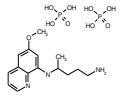	C15H27N3O9P2	455.34	Store at room temperature	63-45-6	Infectiology	Antimalarial
Prestw-477	06H08	Progesterone	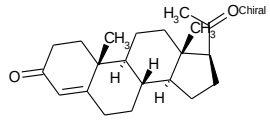	C21H30O2	314.47	Store at room temperature Mutagen Light sensitive	57-83-0	Endocrinology	Progestogen

Prestw-478	06H09	Felodipine		C18H19Cl2NO4	384.26	Store at -20°C	72509-76-3	Neuromuscular	Antianginal
									Antihypertensive
Prestw-1325	06H10	Raclopride	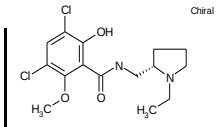	C15H20Cl2N2O3	347.24	Store at room temperature	84225-95-6	Central Nervous System	
Prestw-1385	06H11	Closantel	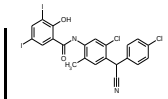	C22H14Cl2I2N2O2	663.08	Store at room temperature	57808-65-8	Infectiology	Antihelmintic
								Metabolism	Antiparasitic
Prestw-481	07A02	Serotonin hydrochloride	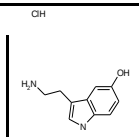	C10H13ClN2O	212.68	Store at -20°C Store under nitrogen Light sensitive	153-98-0	Central Nervous System	CNS Stimulant
								Endocrinology	
Prestw-482	07A03	Cefotiam hydrochloride	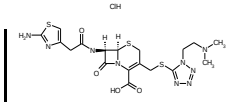	C18H24ClN9O4S3	562.09	Store at -20°C	61622-34-2	Infectiology	Antibacterial
								Metabolism	
Prestw-1336	07A04	Rofecoxib	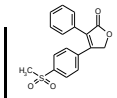	C17H14O4S	314.36	Store at room temperature	162011-90-7	Metabolism	Anti-inflammatory

Prestw-484	07A05	Benperidol	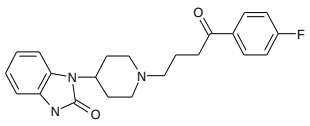	C22H24FN3O2	381.45	Store below 0°C	2062-84-2	Central Nervous System	Antipsychotic
Prestw-485	07A06	Cefaclor hydrate		C15H16ClN3O5S	385.83	Store at room temperature	70356-03-5	Infectiology	Antibacterial
								Metabolism	
Prestw-486	07A07	Colistin sulfate	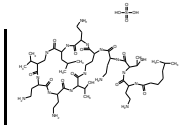	C52H100N16O17S	1253.54	Store at +4°C	1264-72-8	Infectiology	Antibacterial
Prestw-487	07A08	Daunorubicin hydrochloride		C27H30ClNO10	563.99	Store at -20°C	23541-50-6	Infectiology	Antibacterial
								Oncology	Antineoplastic
Prestw-488	07A09	Dosulepin hydrochloride	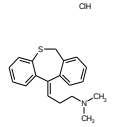	C19H22ClNS	331.91	Store below 0°C	897-15-4	Central Nervous System	Antidepressant
									CNS Stimulant
Prestw-489	07A10	Ceftazidime pentahydrate	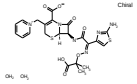	C22H32N6O12S2	636.66	Store at -20°C	78439-06-2	Infectiology	Antibacterial
								Metabolism	

Prestw-490	07A11	Iobenguane sulfate	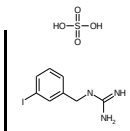	C8H12IN3O4S	373.17	Store at -20°C	103346-16-3	Oncology	Antineoplastic
Prestw-491	07B02	Metixene hydrochloride	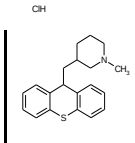	C20H24ClNS	345.94	Store below 0°C	1553-34-0	Central Nervous System	Antiparkinsonian
								Neuromuscular	Antispastic
Prestw-492	07B03	Nitrofural	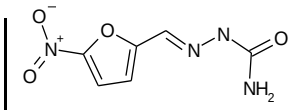	C6H6N4O4	198.14	Store at -20°C	59-87-0	Infectiology	Antibacterial
Prestw-493	07B04	Omeprazole	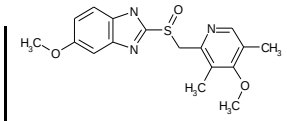	C17H19N3O3S	345.42	Store at -20°C	73590-58-6	Gastroenterology	Antiulcer
Prestw-494	07B05	Propylthiouracil	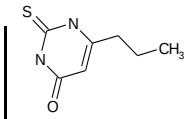	C7H10N2OS	170.23	Store at -20°C	51-52-5	Metabolism	Antihyperthyroid
Prestw-495	07B06	Terconazole	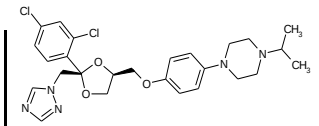	C26H31Cl2N5O3	532.47	Store at -20°C	67915-31-5	Infectiology	Antifungal
								Metabolism	

Prestw-496	07B07	Tiaprofenic acid	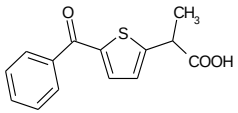	C14H12O3S	260.31	Store at -20°C	33005-95-7	Central Nervous System	Analgesic
								Metabolism	Anti-inflammatory
									Antipyretic
Prestw-497	07B08	Vancomycin hydrochloride	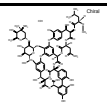	C66H76Cl3N9O24	1485.75	Store at -20°C	1404-93-9	Infectiology	Antibacterial
								Metabolism	
Prestw-498	07B09	Artemisinin	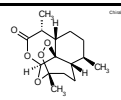	C15H22O5	282.34	Store at room temperature	63968-64-9	Infectiology	Antimalarial
Prestw-499	07B10	Propafenone hydrochloride	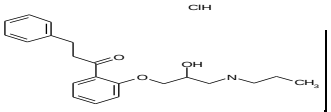	C21H28ClNO3	377.92	Store at +4°C	34183-22-7	Cardiovascular	Antiarrhythmic
Prestw-500	07B11	Ethamivan	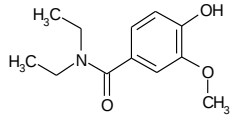	C12H17NO3	223.27	Store at room temperature	304-84-7	Central Nervous System	Analeptic
									CNS stimulant
Prestw-501	07C02	Vigabatrin	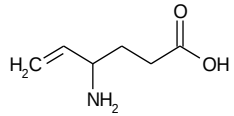	C6H11NO2	129.16	Store at room temperature	60643-86-9	Central Nervous System	Anticonvulsant
									Antiepileptic

Prestw-502	07C03	Biperiden hydrochloride	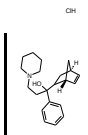	C21H30ClNO	347.93	Store below 0°C	1235-82-1	Central Nervous System	Antiparkinsonian
Prestw-503	07C04	Cetirizine dihydrochloride	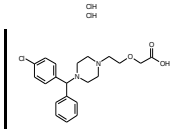	C21H27Cl3N2O3	461.82	Store at -20°C	83881-52-1	Allergology	Antihistaminic
									Antipruritic
Prestw-504	07C05	Etifenin	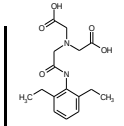	C16H22N2O5	322.36	Store at -20°C	63245-28-3	Diagnostic	Chemosensitizer
Prestw-505	07C06	Metaproterenol sulfate, orciprenaline sulfate	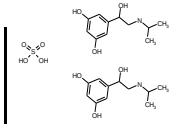	C22H36N2O10S	520.60	Store at -20°C	5874-97-5	Respiratory	Bronchodilator
Prestw-506	07C07	Sisomicin sulfate	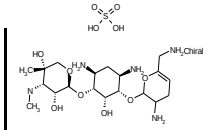	C19H39N5O11S	545.61	Store at -20°C	53179-09-2	Infectiology	Antibacterial
								Metabolism	
Prestw-1159	07C08	Sibutramine HCl	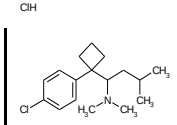	C17H27Cl2N	316.32	Store at +4°C	125494-59-9	Central Nervous System	

Prestw-110	07C09	Acenocoumarol	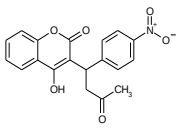	C19H15NO6	353.33	Store at -20°C	152-72-7	Hematology	Anticoagulant
Prestw-509	07C10	Bromperidol	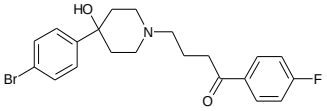	C21H23BrFNO2	420.33	Store below 0°C	10457-90-6	Central Nervous System	Antipsychotic
Prestw-510	07C11	Cyclizine hydrochloride	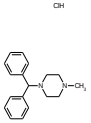	C18H23ClN2	302.85	Store below 0°C Light sensitive	303-25-3	Allergology	Antiemetic
								Central Nervous System	Antihistaminic
									Antivertigo
									Sedative
Prestw-511	07D02	Fluoxetine hydrochloride	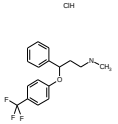	C17H19ClF3NO	345.80	Store at -20°C	59333-67-4	Central Nervous System	Antidepressant
Prestw-512	07D03	Iohexol	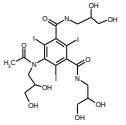	C19H26I3N3O9	821.15	Store at -20°C	66108-95-0	Diagnostic	Contrastant
Prestw-513	07D04	Norcyclobenzaprine	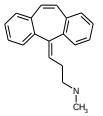	C19H19N	261.37	Store at +4°C	303-50-4	Gastroenterology	Antiulcer

Prestw-514	07D05	Pyrazinamide	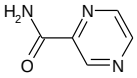	C5H5N3O	123.12	Store at room temperature	98-96-4	Infectiology	Antibacterial
								Metabolism	
Prestw-515	07D06	Trimethadione	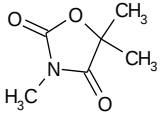	C6H9NO3	143.14	Store at room temperature	127-48-0	Central Nervous System	Anticonvulsant
									Antiepileptic
Prestw-516	07D07	Lovastatin	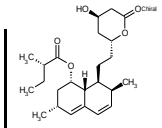	C24H36O5	404.55	Store at +4°C	75330-75-5	Metabolism	Hypocholesterolemic
Prestw-517	07D08	Nystatine	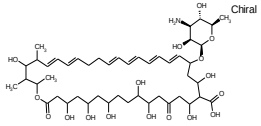	C47H75NO17	926.12	Store below 0°C	1400-61-9	Infectiology	Antifungal
Prestw-518	07D09	Budesonide	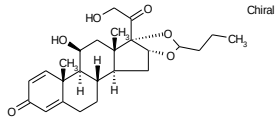	C25H34O6	430.55	Store at -20°C	51333-22-3	Endocrinology	Anti-inflammatory
Prestw-519	07D10	Imipenem	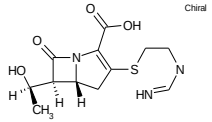	C12H17N3O4S	299.35	Store at -20°C	74431-23-5	Infectiology	Antibacterial
								Metabolism	
Prestw-520	07D11	Sulfasalazine	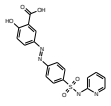	C18H14N4O5S	398.40	Store at -20°C	599-79-1	Infectiology	Antibacterial

								Metabolism	Anti-inflammatory
Prestw-1430	07E02	Lofexidine	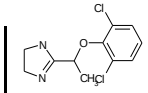	C11H12Cl2N2O	259.14	Store at room temperature	31036-80-3	Cardiovascular	Antihypertensive
Prestw-522	07E03	Thiostrepton	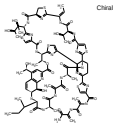	C72H85N19O18S5	1664.92	Store at -20°C	1393-48-2	Infectiology	Antibacterial
Prestw-1169	07E04	Miglitol	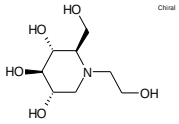	C8H17NO5	207.23	Store at +4°C	72432-03-2	Endocrinology	Antidiabetic
								Metabolism	
Prestw-524	07E05	Tiabendazole	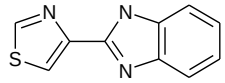	C10H7N3S	201.25	Store at -20	148-79-8	Infectiology	Antifungal
								Metabolism	Antihelmintic
									Antiparasitic
Prestw-525	07E06	Rifampicin	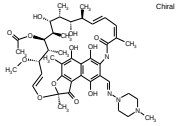	C43H58N4O12	822.96	Store at +4°C	13292-46-1	Infectiology	Antibacterial
								Metabolism	

Prestw-526	07E07	Ethionamide	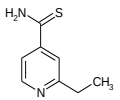	C8H10N2S	166.25	Store at +4°C	536-33-4	Infectiology	Antibacterial
								Metabolism	
Prestw-527	07E08	Tenoxicam	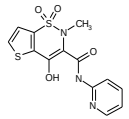	C13H11N3O4S2	337.38	Store at room temperature	59804-37-4	Central Nervous System	Analgesic
								Metabolism	Anti-inflammatory
									Antipyretic
Prestw-528	07E09	Triflusal	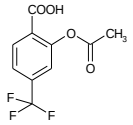	C10H7F3O4	248.16	Store at -20	322-79-2	Hematology	Anticoagulant
									Antiplatelet
Prestw-529	07E10	Mesoridazine besylate	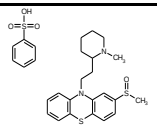	C27H32N2O4S3	544.76	Store at room temperature	32672-69-8	Central Nervous System	Antipsychotic
Prestw-530	07E11	Trolox	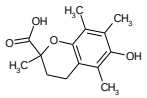	C14H18O4	250.30	Store at +4°C	53188-07-1	Metabolism	Anti-oxidant
Prestw-531	07F02	Pirenperone	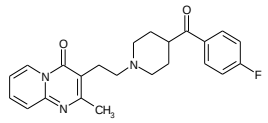	C23H24FN3O2	393.47	Store at room temperature	75444-65-4	Central Nervous System	

Prestw-532	07F03	Isoquinoline, 6,7-dimethoxy-1-methyl-1,2,3,4-tetrahydro, hydrochloride	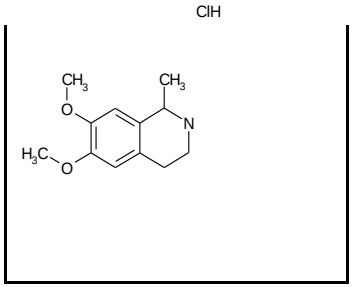	C12H18ClNO2	243.74	Store at room temperature	2984-97-0		
Prestw-533	07F04	Phenacetin	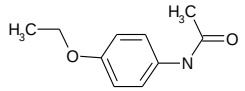	C10H13NO2	179.22	Store at room temperature	62-44-2	Central Nervous System	Analgesic
								Metabolism	Antipyretic
Prestw-534	07F05	Atovaquone	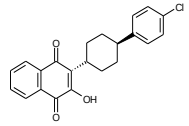	C22H19ClO3	366.85	Store at -20°C	95233-18-4	Infectiology	Antimalarial
									Antiprotozoal
Prestw-535	07F06	Methoxamine hydrochloride	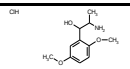	C11H18ClNO3	247.72	Store at +4°C	61-16-5	Cardiovascular	Antihypotensive
									Vasoconstrictor
Prestw-953	07F07	(S)-(-)-Atenolol	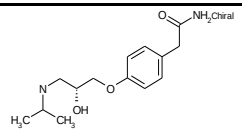	C14H22N2O3	266.34	Store below 0°C	93379-54-5	Cardiovascular	Antianginal
									Antiarrhythmic

									Antihypertensive
Prestw-537	07F08	Piracetam	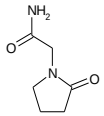	C6H10N2O2	142.16	Store at room temperature	7491-74-9	Central Nervous System	CNS Stimulant
Prestw-538	07F09	Phenindione	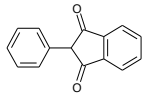	C15H10O2	222.25	Store at +4°C	83-12-5	Hematology	Anticoagulant
Prestw-539	07F10	Thiocolchicoside	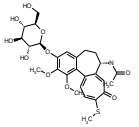	C27H33NO10S	563.63	Store at -20°C	602-41-5	Central Nervous System	Antispastic
									Muscle relaxant
Prestw-540	07F11	Clorsulon	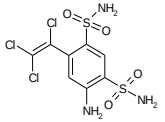	C8H8Cl3N3O4S2	380.66	Store at -20°C	60200-06-8	Infectiology	Antihelmintic
								Metabolism	
Prestw-541	07G02	Ciclopirox ethanolamine		C14H24N2O3	268.36	Store at room temperature	41621-49-2	Infectiology	Antibacterial
								Metabolism	Antifungal
Prestw-542	07G03	Probenecid	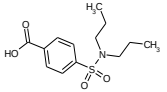	C13H19NO4S	285.36	Store at room temperature	57-66-9	Metabolism	Antigout

									Uricosuric
Prestw-543	07G04	Betahistine mesylate	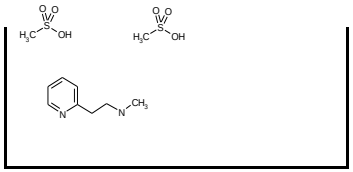	C10H20N2O6S2	328.41	Store at -20°C	54856-23-4	Allergology	Vasodilator
Prestw-544	07G05	Tobramycin	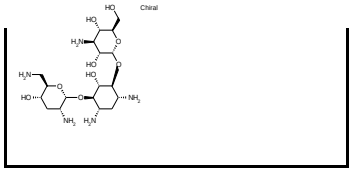	C18H37N5O9	467.52	Store at -20°C	32986-56-4	Infectiology	Antibacterial
								Metabolism	
Prestw-545	07G06	Tetramisole hydrochloride	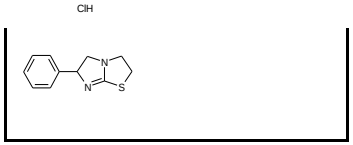	C11H13ClN2S	240.76	Store at room temperature	5086-74-8	Immunology	Antihelmintic
								Infectiology	Antiparasitic
									Immunomodulator
Prestw-546	07G07	Pregnenolone	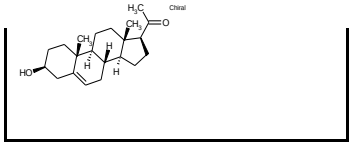	C21H32O2	316.49	Store at room temperature	145-13-1	Endocrinology	Anabolic
									Anti-inflammatory
Prestw-547	07G08	Molsidomine	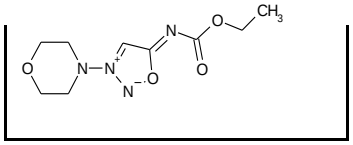	C9H14N4O4	242.24	Store at +4°C	25717-80-0	Cardiovascular	Antianginal
								Hematology	Anticoagulant
									Antiplatelet
									Vasodilator

Prestw-548	07G09	Chloroquine diphosphate	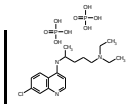	C18H32ClN3O8P2	515.87	Store at room temperature	50-63-5	Metabolism	Anti-inflammatory
									Antimalarial
									Antiprotozoal
Prestw-549	07G10	Trimetazidine dihydrochloride	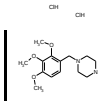	C14H24Cl2N2O3	339.26	Store at room temperature	13171-25-0	Cardiovascular	Antianginal
									Anti-ischemic
									Vasodilator
Prestw-550	07G11	Parthenolide	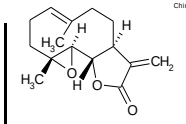	C15H20O3	248.32	Store at -20°C Desiccate	20554-84-1	Metabolism	Anti-inflammatory
									Antispastic
Prestw-551	07H02	Hexetidine	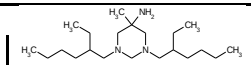	C21H45N3	339.61	Store at room temperature	141-94-6	Infectiology	Antifungal
									Antiseptic
Prestw-552	07H03	Selegiline hydrochloride	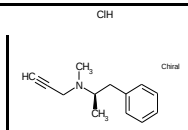	C13H18ClN	223.75	Store at -20°c	14611-52-0	Central Nervous System	Antiparkinsonian
Prestw-553	07H04	Pentamidine isethionate	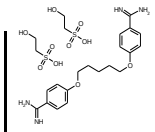	C23H36N4O10S2	592.69	Store at -20°C Light sensitive	140-64-7	Infectiology	Antifungal
									Antiparasitic

									Antiprotozoal
Prestw-554	07H05	Tolazamide	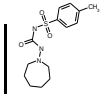	C14H21N3O3S	311.41	Store at room temperature	1156-19-0	Metabolism	Antidiabetic
Prestw-555	07H06	Nifuroxazide	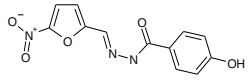	C12H9N3O5	275.22	Store at room temperature	965-52-6	Infectiology	Antibacterial
								Metabolism	
Prestw-1144	07H07	Mirtazapine	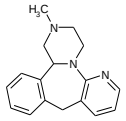	C17H19N3	265.36	Store at +4°C	61337-67-5	Central Nervous System	Antidepressant
Prestw-557	07H08	Dirithromycin	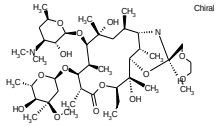	C42H78N2O14	835.09	Store at -20°C	62013-04-1	Infectiology	Antibacterial
								Metabolism	
Prestw-558	07H09	Gliclazide	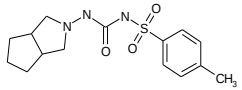	C15H21N3O3S	323.42	Store at room temperature	21187-98-4	Metabolism	Anticoagulant
									Antidiabetic
Prestw-559	07H10	DO 897/99	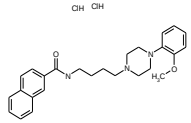	C26H33Cl2N3O2	490.48	Store at room temperature	not available	Central Nervous System	Antidepressant

Prestw-560	07H11	Prenylamine lactate	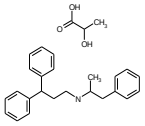	C27H33NO3	419.57	Store at +4°C	69-43-2	Cardiovascular	Antianginal
								Central Nervous System	Anxiolytic
									Vasodilator
Prestw-1188	08A02	Ziprasidone Hydrochloride	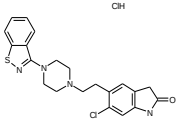	C21H22Cl2N4OS	449.41	Store at room temperature	138982-67-9	Central Nervous System	Antipsychotic
Prestw-1441	08A03	Mevastatin	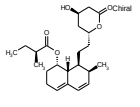	C23H34O5	390.52	Store at room temperature	73573-88-3	Cardiovascular	Hypocholesterolemic
Prestw-1322	08A04	Pyridostigmine iodide		C9H13IN2O2	308.12	Store at room temperature	4685-03-4	Central Nervous System	
Prestw-1491	08A05	Pentobarbital	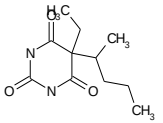	C11H18N2O3	226.28	Store at room temperature	76-74-4	Central Nervous System	Anesthetic
									Hypnotic
									Sedative
Prestw-565	08A06	Atropine sulfate monohydrate	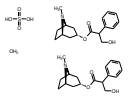	C34H50N2O11S	694.85	Store at room temperature	5908-99-6	Ophthalmology	Antispastic

									Mydriatic
Prestw-566	08A07	Eserine hemisulfate salt	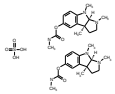	C30H44N6O8S	648.78	Store at +4°C Light sensitive	64-47-1	Central Nervous System	Antiglaucoma
								Neuromuscular	
								Ophthalmology	
Prestw-1139	08A08	Itraconazole	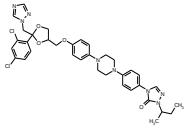	C35H38Cl2N8O4	705.65	Store at +4°C	84625-61-6	Infectiology	Antifungal
								Metabolism	
Prestw-1174	08A09	Acarbose	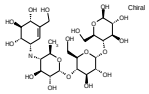	C25H43NO18	645.62	Store at room temperature	56180-94-0	Endocrinology	Antidiabetic
Prestw-1403	08A10	Entacapone	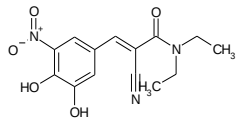	C14H15N3O5	305.29	Store at room temperature	130929-57-6	Central Nervous System	Antiparkinsonian
Prestw-1449	08A11	Nicotinamide	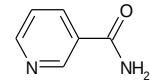	C6H6N2O	122.13	Store at room temperature	98-92-0	Dermatology	

Prestw-571	08B02	Tetracaïne hydrochloride	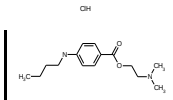	C15H25ClN2O2	300.83	Store at room temperature	136-47-0	Neuromuscular	
Prestw-572	08B03	Mometasone furoate	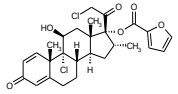	C27H30Cl2O6	521.44	Store at room temperature	83919-23-7	Endocrinology	Anti-inflammatory
Prestw-1467	08B04	Troglitazone	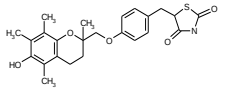	C24H27NO5S	441.55	Store at room temperature	97322-87-7	Metabolism	Antidiabetic
									Anti-inflammatory
Prestw-574	08B05	Dacarbazine	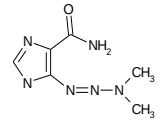	C6H10N6O	182.19	Store at +4°C Light sensitive in solution Toxic	4342-03-4	Oncology	Antineoplastic
Prestw-1351	08B06	Tenatoprazole	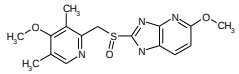	C16H18N4O3S	346.41	Store at room temperature	113712-98-4	Metabolism	Antiulcer
Prestw-576	08B07	Acetopromazine maleate salt	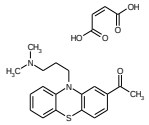	C23H26N2O5S	442.54	Store at -20°C	3598-37-6	Central Nervous System	Antiemetic
									Antipsychotic
									Antitussive
									Sedative

Prestw-1271	08B08	Escitalopram	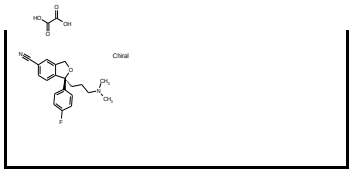	C22H23FN2O5	414.44	Store at room temperature	128196-01-0	Central Nervous System	Antidepressant
Prestw-1158	08B09	Ropinirole HCl	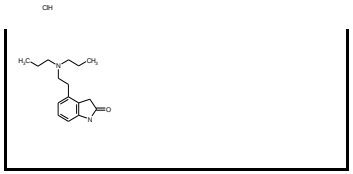	C16H25ClN2O	296.84	Store at +4°C	91374-20-8	Central Nervous System	Antiparkinsonian
Prestw-1297	08B10	Lacidipine	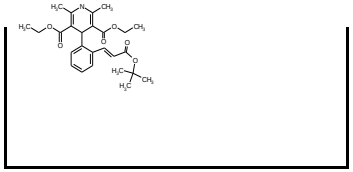	C26H33NO6	455.56	Store at room temperature	103890-78-4	Cardiovascular	Antihypertensive
Prestw-1228	08B11	Argatroban	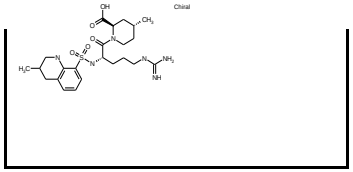	C23H36N6O5S	508.64	Store at room temperature	74863-84-6	Hematology	Anticoagulant
Prestw-1328	08C02	Reboxetine mesylate		C20H27NO6S	409.51	Store at room temperature	98769-81-4	Central Nervous System	Antidepressant
Prestw-1498	08C03	Camylofine chlorhydrate		C19H34Cl2N2O2	393.40	Store at room temperature	54-30-8		
Prestw-583	08C04	Papaverine hydrochloride	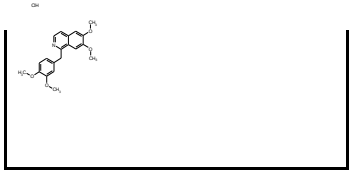	C20H22ClNO4	375.86	Store at room temperature	61-25-6	Cardiovascular	Antispastic

								Gastroenterology	Antitussive
								Respiratory	Erectile dysfunction treatment
									Vasodilator
Prestw-584	08C05	Yohimbine hydrochloride	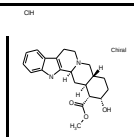	C21H27ClN2O3	390.91	Store at room temperature	65-19-0	Cardiovascular	Erectile dysfunction treatment
									Vasodilator
Prestw-1500	08C06	Voriconazole	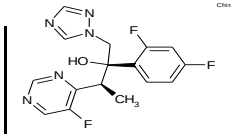	C16H14F3N5O	349.32	Store at room temperature	137234-62-9	Infectiology	Antifungal
								Metabolism	
Prestw-1211	08C07	Alfacalcidol	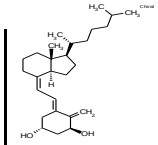	C27H44O2	400.65	Store at room temperature	41294-56-8	Metabolism	Antiosteoporetic
Prestw-587	08C08	Cilostazol	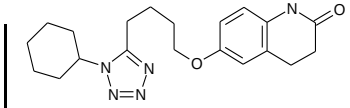	C20H27N5O2	369.47	store at -20°C	73963-72-1	Hematology	Anticoagulant
Prestw-588	08C09	Galanthamine hydrobromide	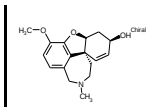	C17H22BrNO3	368.27	Store at -20°C Toxic Light sensitive	1953-04-4	Central Nervous System	Analgesic

									Anti-Alzheimer
									Anti-fatigue
Prestw-1130	08C10	Azelastine HCl	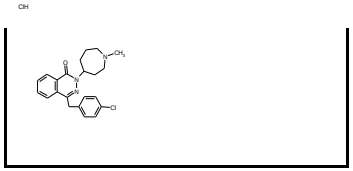	C22H25Cl2N3O	418.37	Store at +4°C	79307-93-0	Immunology	Antihistaminic
Prestw-1409	08C11	Etretinate	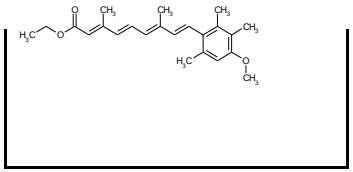	C23H30O3	354.49	Store at room temperature	54350-48-0	Dermatology	Antipsoriatic
Prestw-1274	08D02	Emedastine	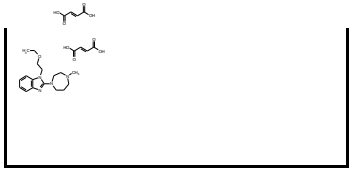	C25H34N4O9	534.57	Store at room temperature	87233-61-2	Allergology	Antihistaminic
Prestw-1407	08D03	Etofenamate	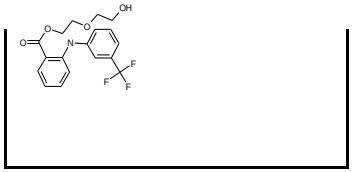	C18H18F3NO4	369.34	Store at room temperature	30544-47-9	Metabolism	Anti-inflammatory
Prestw-1369	08D04	Zaleplon	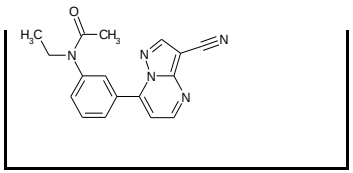	C17H15N5O	305.34	Store at room temperature	151319-34-5	Central Nervous System	Hypnotic
									Sedative
Prestw-594	08D05	Diclofenac sodium	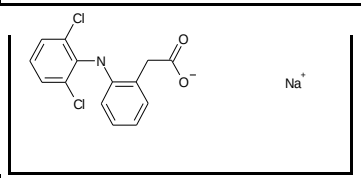	C14H10Cl2NNaO2	318.14	Store at room temperature	15307-79-6	Central Nervous System	Anti-inflammatory
								Metabolism	

Prestw-1410	08D06	Exemestane	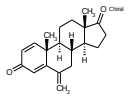	C20H24O2	296.41	Store at room temperature	107868-30-4	Endocrinology	Antineoplastic
								Oncology	
Prestw-1499	08D07	Fomepizole	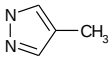	C4H6N2	82.11	Store at room temperature	7554-65-6	Metabolism	
Prestw-1183	08D08	Temozolomide	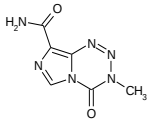	C6H6N6O2	194.15	Store at +4°C	85622-93-1	Oncology	Antineoplastic
Prestw-598	08D09	Xylazine	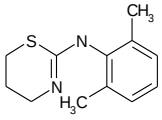	C12H16N2S	220.34	Store at -20	7361-61-7	Central Nervous System	Analgesic
									Sedative
Prestw-1132	08D10	Celiprolol HCl	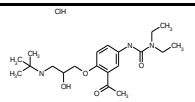	C20H34ClN3O4	415.96	Store at +4°C	57470-78-7	Cardiovascular	Antianginal
									Antihypertensive
Prestw-1367	08D11	Zopiclone	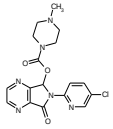	C17H17ClN6O3	388.82	Store at room temperature	43200-80-2	Central Nervous System	Hypnotic
									Sedative

Prestw-1198	08E02	Tranilast	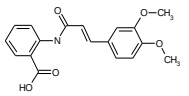	C18H17NO5	327.34	Store at room temperature	53902-12-8	Allergology	Antiallergic
Prestw-1182	08E03	Tizanidine HCl	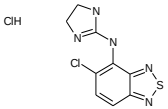	C9H9Cl2N5S	290.18	Store at +4°C	51322-75-9	Metabolism	Muscle relaxant
Prestw-1364	08E04	Zafirlukast	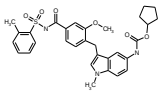	C31H33N3O6S	575.69	Store at room temperature	107753-78-6	Respiratory	Antiasthmatic
Prestw-1252	08E05	Butenafine Hydrochloride	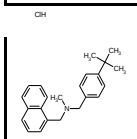	C23H28ClN	353.94	Store at room temperature	101828-21-1	Infectiology	Antifungal
								Metabolism	
Prestw-1121	08E06	Carbadox	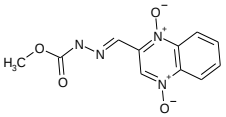	C11H10N4O4	262.23	Store at +4°C	6804-07-5	Infectiology	Antibacterial
Prestw-1331	08E07	Rimantadine Hydrochloride	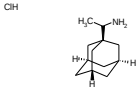	C12H22ClN	215.77	Store at room temperature	13392-28-4	Infectiology	Antiviral
Prestw-607	08E08	Eburnamonine (-)	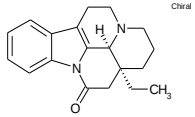	C19H22N2O	294.40	Store at room temperature	4880-88-0	Central Nervous System	Vasodilator

Prestw-1460	08E09	Oxibendazol	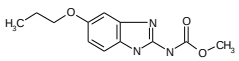	C12H15N3O3	249.27	Store at room temperature	20559-55-1	Metabolism	
Prestw-1292	08E10	Ipsapirone	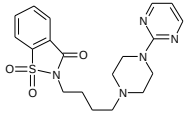	C19H23N5O3S	401.49	Store at room temperature	95847-70-4	Central Nervous System	
Prestw-1284	08E11	Hydroxychloroquine sulfate	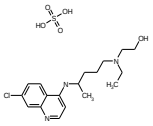	C18H28ClN3O5S	433.96	Store at room temperature	747-36-4	Metabolism	Antimalarial
Prestw-1431	08F02	Loracarbef	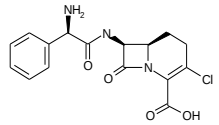	C16H16ClN3O4	349.78	Store at -20°C	121961-22-6	Infectiology	Antibacterial
								Metabolism	
Prestw-1501	08F03	Fenipentol	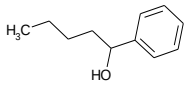	C11H16O	164.25	Store at room temperature	583-03-9	Metabolism	Choleretic
Prestw-1503	08F04	Diosmin	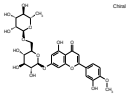	C28H32O15	608.56	Store at room temperature	520-27-4	Cardiovascular	
Prestw-1177	08F05	Carbidopa	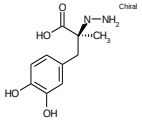	C10H14N2O4	226.23	Store at +4°C	28860-95-9	Central Nervous System	Antiparkinsonian

Prestw-1604	08F06	(-)-Emtricitabine		C8H10FN3O3S	247.25	Store at room temperature	143491-57-0	Infectiology	Antiviral
Prestw-616	08F07	Demecarium bromide	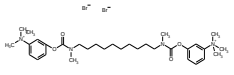	C32H52Br2N4O4	716.60	Store at room temperature	56-94-0	Ophthalmology	Antiglaucoma
Prestw-617	08F08	Quipazine dimaleate salt	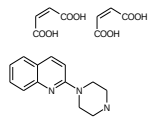	C21H23N3O8	445.43	Store at -20°C Light sensitive	150323-78-7	Central Nervous System	Antiemetic
Prestw-1127	08F09	Acipimox	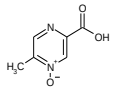	C6H6N2O3	154.13	Store at +4°C	51037-30-0	Metabolism	Antilipemic
Prestw-619	08F10	Diflorasone Diacetate	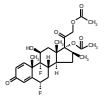	C26H32F2O7	494.54	Store at room temperature	33564-31-7	Endocrinology	Anti-inflammatory
									Antipruritic
									Antipsoriatic
Prestw-1502	08F11	Acamprosate calcium	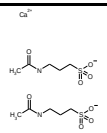	C10H20CaN2O8S2	400.49	Store at room temperature	77337-73-6	Central Nervous System	
								Metabolism	

Prestw-1506	08G02	Mizolastine	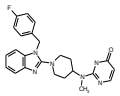	C24H25FN6O	432.50	Store at room temperature	108612-45-9	Allergology	
Prestw-1217	08G03	Amisulpride	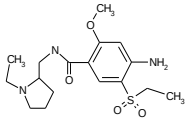	C17H27N3O4S	369.49	Store at room temperature	71675-85-9	Central Nervous System	Antipsychotic
Prestw-623	08G04	Pyridoxine hydrochloride		C8H12ClNO3	205.64	Store at +4°C	58-56-0	Metabolism	
Prestw-1469	08G05	Mercaptopurine	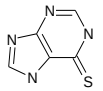	C5H4N4S	152.18	Store at room temperature	50-44-2	Immunology	Immunosuppressant
								Oncology	
Prestw-1134	08G06	Cytarabine	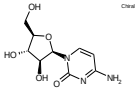	C9H13N3O5	243.22	Store at +4°C	147-94-4	Oncology	Antineoplastic
Prestw-626	08G07	Racecadotril	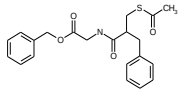	C21H23NO4S	385.49	Store at room temperature	81110-73-8	Gastroenterology	Antidiarrheal

Prestw-627	08G08	Folic acid	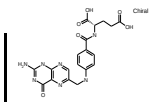	C19H19N7O6	441.41	Store at room temperature	59-30-3	Metabolism	
Prestw-1129	08G09	Benazepril HCl	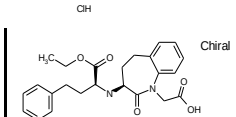	C24H29ClN2O5	460.96	Store at +4°C	86541-74-4	Cardiovascular	Antihypertensive
Prestw-1178	08G10	Aniracetam	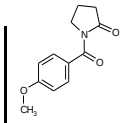	C12H13NO3	219.24	Store at +4°C	72432-10-1	Central Nervous System	Anti-Alzheimer
Prestw-630	08G11	Dimethisoquin hydrochloride	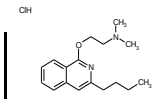	C17H25ClN2O	308.85	Store at room temperature	2773-92-4	Neuromuscular	Antipruritic
									Local anesthetic
Prestw-1210	08H02	Alendronate sodium	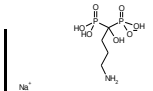	C4H12NNaO7P2	271.08	Store at room temperature	121268-17-5	Metabolism	Antiosteoporetic
Prestw-632	08H03	Dipivefrin hydrochloride	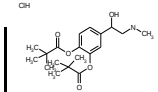	C19H30ClNO5	387.91	Store at room temperature	64019-93-8	Ophthalmology	Antiglaucoma

Prestw-633	08H04	Thiorphan	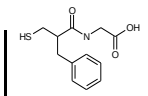	C12H15NO3S	253.32	Store at room temperature	76721-89-6	Gastroenterology	Antidiarrheal
Prestw-1463	08H05	Tomoxetine hydrochloride	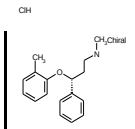	C17H22ClNO	291.82	Store at room temperature	82248-59-7	Central Nervous System	
Prestw-1511	08H06	Aceclidine Hydrochloride	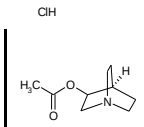	C9H16ClNO2	205.69	Store at -20°C	6109-70-2	Ophthalmology	Antiglaucoma
Prestw-1488	08H07	Penciclovir	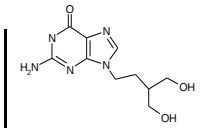	C10H15N5O3	253.26	Store at +4°C	39809-25-1	Infectiology	Antiviral
								Metabolism	
Prestw-1427	08H08	Levetiracetam	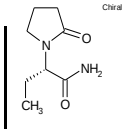	C8H14N2O2	170.21	Store at room temperature	102767-28-2	Central Nervous System	Anticonvulsant
Prestw-1392	08H09	Dexfenfluramine hydrochloride	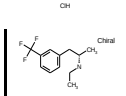	C12H17ClF3N	267.72	Store at room temperature	3239-45-0	Central Nervous System	Anorectic
Prestw-1408	08H10	Etoricoxib	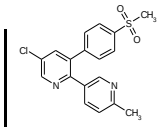	C18H15ClN2O2S	358.85	Store at room temperature	202409-33-4	Central Nervous System	Analgesic

								Metabolism	Anti-inflammatory
Prestw-1341	08H11	Sertindole	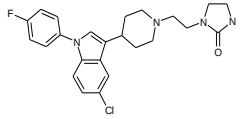	C24H26ClFN4O	440.95	Store at room temperature	106516-24-9	Central Nervous System	Antipsychotic
Prestw-641	09A02	Sulmazole	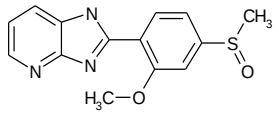	C14H13N3O2S	287.34	Store at 2°C	73384-60-8	Cardiovascular	Cardiotonic
								Metabolism	
Prestw-1270	09A03	Gefitinib	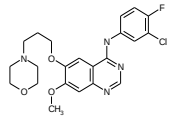	C22H24ClFN4O3	446.91	Store at +4°C	184475-35-2	Oncology	Antineoplastic
Prestw-643	09A04	Flunisolide	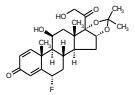	C24H31FO6	434.51	Store at room temperarure	3385-03-3	Endocrinology	Anti-inflammatory
Prestw-644	09A05	N-Acetyl-DL-homocysteine Thiolactone		C6H9NO2S	159.21	Store below 0°C	1195-16-0	Respiratory	Expectorant
Prestw-645	09A06	Flurandrenolide	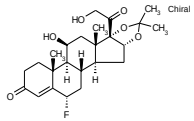	C24H33FO6	436.53	Store at RT	1524-88-5	Dermatology	Anti-inflammatory
								Endocrinology	Antipruritic

Prestw-1125	09A07	Oxiconazole Nitrate	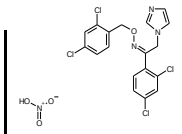	C18H14Cl4N4O4	492.15	Store at +4°C	64211-46-7	Infectiology	Antifungal
								Metabolism	
Prestw-1166	09A08	Rebamipide	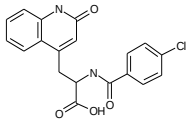	C19H15ClN2O4	370.80	Store at +4°C	90098-04-7	Metabolism	Antiulcer
Prestw-1154	09A09	Nilvadipine	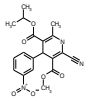	C19H19N3O6	385.38	Store at +4°C	75530-68-6	Cardiovascular	Antianginal
									Antihypertensive
Prestw-649	09A10	Etanidazole		C7H10N4O4	214.18	Store at 2°C	22668-01-5	Oncology	Antineoplastic
									Chemosensitizer
Prestw-1601	09A11	Pinaverium bromide	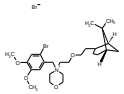	C26H41Br2NO4	591.43	Store at room temperature	53251-94-8	Neuromuscular	Antispastic
Prestw-651	09B02	Glimepiride	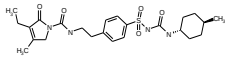	C24H34N4O5S	490.63	Store at room temperature	93479-97-1	Endocrinology	Antidiabetic

Prestw-652	09B03	Picrotoxinin	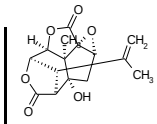	C15H16O6	292.29	Store at room temperature	17617-45-7	Central Nervous System	Analeptic
Prestw-653	09B04	Mepenzolate bromide		C21H26BrNO3	420.35	Store at room temperature	76-90-4	Neuromuscular	Antispastic
									Antiulcer
Prestw-654	09B05	Benfotiamine	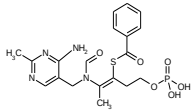	C19H23N4O6PS	466.46	Store at 2°C	22457-89-2	Metabolism	
Prestw-655	09B06	Halcinonide	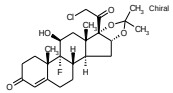	C24H32ClFO5	454.97	Store at room temperature	3093-35-4	Dermatology	Anti-inflammatory
								Endocrinology	Antipruritic
Prestw-656	09B07	Lanatoside C	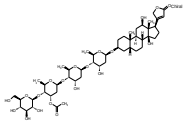	C49H76O20	985.14	Store below 0°C	17575-22-3	Cardiovascular	Cardiotonic
Prestw-657	09B08	Benzamil hydrochloride	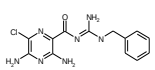	C13H15Cl2N7O	356.22	Store at 2°C	2898-76-2	Metabolism	Antihypertensive
									Diuretic

Prestw-658	09B09	Suxibuzone	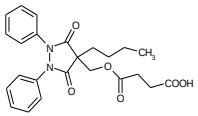	C24H26N2O6	438.48	Store at room temperature	27470-51-5	Central Nervous System	Analgesic
								Metabolism	Anti-inflammatory
									Antipyretic
Prestw-659	09B10	6-Furfurylaminopurine	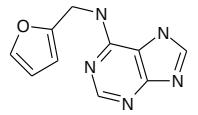	C10H9N5O	215.22	Store below 0°C	525-79-1	Dermatology	
								Metabolism	
Prestw-660	09B11	Avermectin B1a	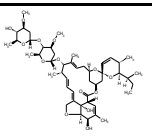	C48H72O14	873.10	Store at -20°C Toxic	71751-41-2	Infectiology	Antihelmintic
Prestw-1317	09C02	Pranlukast	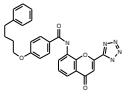	C27H23N5O4	481.52	Store at room temperature	103177-37-3	Respiratory	Antiasthmatic
Prestw-1477	09C03	Penicillamine	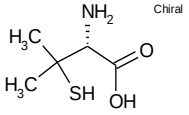	C5H11NO2S	149.21	Store at +4°C	52-66-4	Central Nervous System	Analgesic
Prestw-1365	09C04	Zileuton	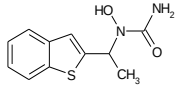	C11H12N2O2S	236.29	Store at room temperature	111406-87-2	Respiratory	Antiasthmatic

Prestw-1432	09C05	Loratadine	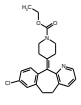	C22H23ClN2O2	382.89	Store at room temperature	79794-75-5	Allergology	Antihistaminic
Prestw-1387	09C06	Tetraethylenepentamine pentahydrochloride	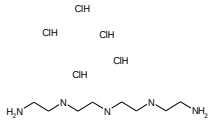	C8H28Cl5N5	371.61	Store at room temperature	4961-41-5	Metabolism	Antilipemic
Prestw-666	09C07	Nisoldipine	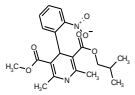	C20H24N2O6	388.42	store at -20°C	63675-72-9	Cardiovascular	Antianginal
									Antihypertensive
Prestw-1507	09C08	Acefylline	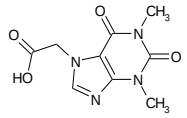	C9H10N4O4	238.20	Store at room temperature	652-37-9	Central Nervous System	CNS Stimulant
Prestw-1165	09C09	Acitretin	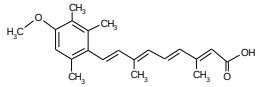	C21H26O3	326.44	Store at +4°C	55079-83-9	Dermatology	Antipsoriatic
Prestw-1162	09C10	Zonisamide	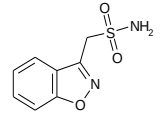	C8H8N2O3S	212.23	Store at +4°C	68291-97-4	Central Nervous System	Anticonvulsant
Prestw-1173	09C11	Irsogladine maleate	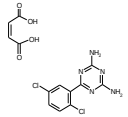	C13H11Cl2N5O4	372.17	Store at +4°C	84504-69-8	Metabolism	Antiulcer

Prestw-671	09D02	Dydrogesterone	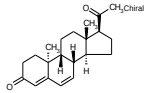	C21H28O2	312.46	Store at room temperature	152-62-5	Endocrinology	Progestogen
Prestw-1346	09D03	Sumatriptan succinate	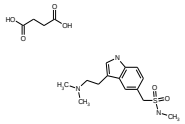	C18H27N3O6S	413.50	Store at room temperature	103628-48-4	Central Nervous System	Antimigraine
Prestw-1456	09D04	Opipramol dihydrochloride	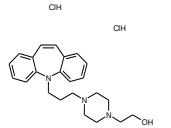	C23H31Cl2N3O	436.43	Store at room temperature	909-39-7	Central Nervous System	Antidepressant
									Antipsychotic
Prestw-1447	09D05	Nalidixic acid sodium salt		C12H11N2NaO3	254.22	Store at room temperature	3374-05-8	Infectiology	Antibacterial
								Metabolism	
Prestw-1475	09D06	Oxacillin sodium	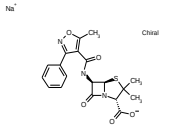	C19H18N3NaO5S	423.43	Store at +4°C	1173-88-2	Infectiology	Antibacterial
								Metabolism	

Prestw-676	09D07	Beta-Escin	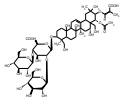	C54H84O25	1133.26	Store at room temperature	11072-93-8	Metabolism	Antineoplastic
								Oncology	Diuretic
Prestw-631	09D08	Thiamine hydrochloride		C12H18Cl2N4OS	337.27	Store at -20°C	67-03-8	Immunology	Immunostimulant
								Metabolism	
Prestw-1349	09D09	Tazobactam	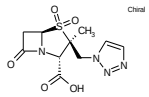	C10H12N4O5S	300.29	Store at room temperature	89786-04-9	Infectiology	Antibacterial
								Metabolism	
Prestw-1285	09D10	Ibandronate sodium	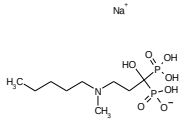	C9H22NNaO7P2	341.22	Store at -20°C	114084-78-5	Metabolism	Antiosteoporetic
Prestw-1363	09D11	Warfarin	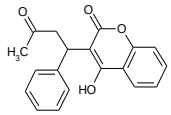	C19H16O4	308.34	Store at -20°C	81-81-2	Hematology	Anticoagulant
Prestw-1318	09E02	Pranoprofen	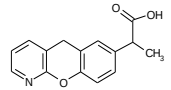	C15H13NO3	255.28	Store at room temperature	52549-17-4	Metabolism	Anti-inflammatory
Prestw-1340	09E03	Secnidazole		C7H11N3O3	185.18	Store at room temperature	3366-95-8	Infectiology	Antiamebic

								Metabolism	
Prestw-683	09E04	Pempidine tartrate	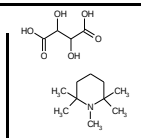	C14H27NO6	305.37	Store at 2°C	546-48-5	Cardiovascular	Antihypotensive
									Vasodilator
Prestw-1381	09E05	Clodronate	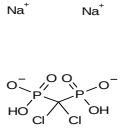	CH2Cl2Na2O6P2	288.86	Store at room temperature	22560-50-5	Metabolism	
Prestw-1508	09E06	Ibutilide fumarate	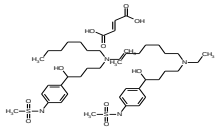	C44H76N4O10S2	885.25	Store at room temperature	122647-32-9	Cardiovascular	Antiarrhythmic
Prestw-1194	09E07	Thimerosal	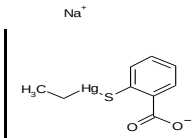	C9H9HgNaO2S	404.81	Store at room temperature	54-64-8	Infectiology	Antiseptic
Prestw-1465	09E08	Tramadol hydrochloride	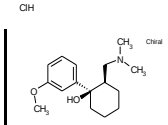	C16H26ClNO2	299.84	Store at room temperature	27203-92-5	Central Nervous System	Analgesic
Prestw-688	09E09	Estropipate	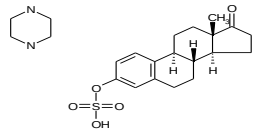	C22H32N2O5S	436.57	Store at room temperature	7280-37-7	Endocrinology	

Prestw-1253	09E10	Butylscopolammonium (n-) bromide	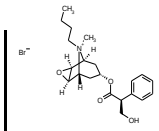	C21H30BrNO4	440.38	Store at room temperature	149-64-4	Central Nervous System	Antispastic
Prestw-1494	09E11	Irinotecan hydrochloride trihydrate	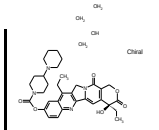	C33H45ClN4O9	677.20	Store at room temperature	136572-09-3	Oncology	Antineoplastic
Prestw-1353	09F02	Tylosin	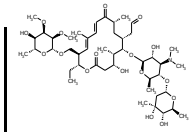	C46H77NO17	916.12	Store at +4°C	1401-69-0	Infectiology	Antibacterial
								Metabolism	
Prestw-692	09F03	Citalopram Hydrobromide	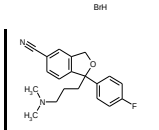	C20H22BrFN2O	405.31	-20°C	59729-32-7	Central Nervous System	Antidepressant
Prestw-693	09F04	Promazine hydrochloride	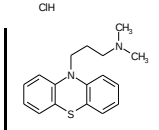	C17H21ClN2S	320.89	Store at room temperature	53-60-1	Central Nervous System	Antipsychotic
Prestw-694	09F05	Sulfamerazine	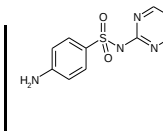	C11H12N4O2S	264.31	Store at room temperature	127-79-7	Infectiology	Antibacterial
								Metabolism	

Prestw-1170	09F06	Venlafaxine	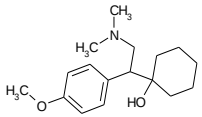	C17H27NO2	277.41	Store at +4°C	93413-69-5	Central Nervous System	Antidepressant
Prestw-696	09F07	Ethotoin	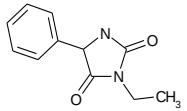	C11H12N2O2	204.23	Store at room temperature	86-35-1	Central Nervous System	Anticonvulsant
Prestw-697	09F08	3-alpha-Hydroxy-5-beta-androstan-17-one	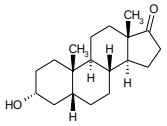	C19H30O2	290.45	Store at -20°C	53-42-9	Endocrinology	
Prestw-698	09F09	Tetrahydrozoline hydrochloride	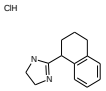	C13H17ClN2	236.75	Store at room temperature	522-48-5	Cardiovascular	Nasal Decongestant
									Vasoconstrictor
Prestw-699	09F10	Hexestrol	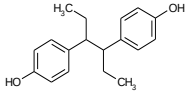	C18H22O2	270.37	Store at room temperature	84-16-2	Endocrinology	Antineoplastic
								Oncology	
Prestw-700	09F11	Cefmetazole sodium salt	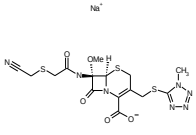	C15H16N7NaO5S3	493.52	Store at 2°C	56796-39-5	Infectiology	Antibacterial
								Metabolism	

Prestw-701	09G02	Trihexyphenidyl-D,L Hydrochloride	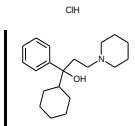	C20H32ClNO	337.94	Store at room temperature	58947-95-8	Central Nervous System	Antiparkinsonian
Prestw-702	09G03	Succinylsulfathiazole	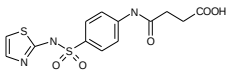	C13H13N3O5S2	355.39	Store at room temperature	116-43-8	Infectiology	Antibacterial
								Metabolism	
Prestw-703	09G04	Famprofazone	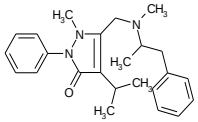	C24H31N3O	377.53	Store at room temperature	22881-35-2	Central Nervous System	Analgesic
								Metabolism	Antipyretic
Prestw-704	09G05	Bromopride	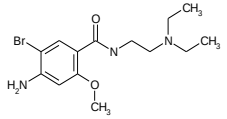	C14H22BrN3O2	344.25	Store at 2°C	4093-35-0	Central Nervous System	Antiemetic
Prestw-705	09G06	Methyl benzethonium chloride	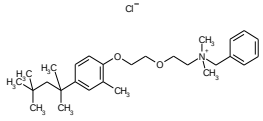	C28H44ClNO2	462.12	Store at room temperature	25155-18-4	Infectiology	Antibacterial
Prestw-706	09G07	Chlorcyclizine hydrochloride		C18H22Cl2N2	337.30	Store at +4°C	1620-21-9	Allergology	Antiemetic
								Central Nervous System	Antihistaminic
									Sedative

Prestw-707	09G08	Diphenylpyraline hydrochloride	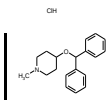	C19H24ClNO	317.86	Store at room temperature	132-18-3	Allergology	Antihistaminic
								Central Nervous System	Antipruritic
									Sedative
Prestw-708	09G09	Benzethonium chloride	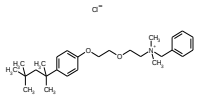	C27H42ClNO2	448.09	Store at room temperature	121-54-0	Infectiology	Antibacterial
									Antiseptic
Prestw-709	09G10	Trioxsalen	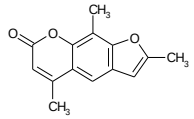	C14H12O3	228.25	Store below 0°C	3902-71-4	Dermatology	
Prestw-1136	09G11	Doxofylline	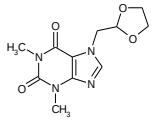	C11H14N4O4	266.26	Store at +4°C	69975-86-6	Respiratory	Bronchodilator
Prestw-711	09H02	Sulfabenzamide	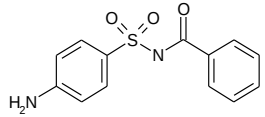	C13H12N2O3S	276.32	Store at 2°C	127-71-9	Infectiology	Antibacterial
								Metabolism	
Prestw-712	09H03	Benzocaine	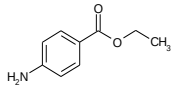	C9H11NO2	165.19	Store at room temperature	94-09-7	Neuromuscular	Local anesthetic

Prestw-713	09H04	Dipyrone	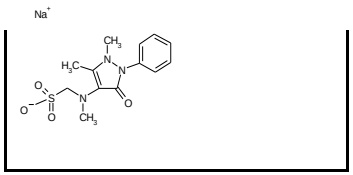	C13H16N3NaO4S	333.34	Store at 2°C	5907-38-0	Central Nervous System	Analgesic
								Metabolism	Antiasthmatic
									Antipyretic
									Bronchodilator
Prestw-714	09H05	Isosorbide dinitrate		C6H8N2O8	236.14	Store at room temperature	87-33-2	Cardiovascular	Antianginal
Prestw-715	09H06	Sulfachloropyridazine	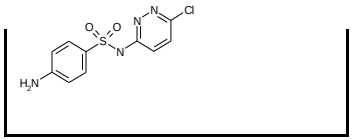	C10H9ClN4O2S	284.73	Store at room temperature	80-32-0	Infectiology	Antibacterial
								Metabolism	
Prestw-716	09H07	Pramoxine hydrochloride	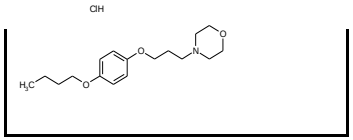	C17H28ClNO3	329.87	Store at room temperature	637-58-1	Neuromuscular	Local anesthetic
Prestw-717	09H08	Finasteride	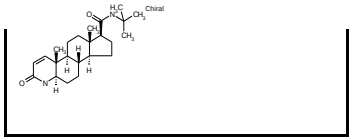	C23H36N2O2	372.56	Store at room temperature	98319-26-7	Endocrinology	Anti-alopecia
									Antineoplastic
Prestw-718	09H09	Fluorometholone	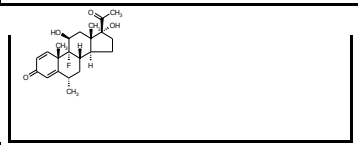	C22H29FO4	376.47	Store at room temperature	426-13-1	Endocrinology	Anti-inflammatory
Prestw-719	09H10	Cephalothin sodium salt	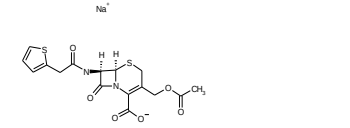	C16H15N2NaO6S2	418.43	Store at 2°C	58-71-9	Infectiology	Antibacterial

								Metabolism	
Prestw-720	09H11	Cefuroxime sodium salt	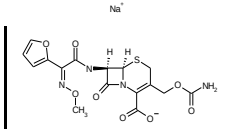	C16H15N4NaO8S	446.37	Store at 2°C	56238-63-2	Infectiology	Antibacterial
								Metabolism	
Prestw-721	10A02	Althiazide	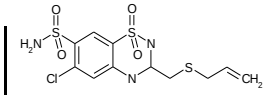	C11H14ClN3O4S3	383.90	Store at room temperature	5588-16-9	Metabolism	Antihypertensive
									Diuretic
Prestw-722	10A03	Isopyrin hydrochloride	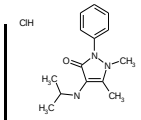	C14H20ClN3O	281.79	Store at 2°C	18342-39-7	Central Nervous System	Analgesic
								Metabolism	Anti-inflammatory
									Antipyretic
Prestw-723	10A04	Phenethicillin potassium salt	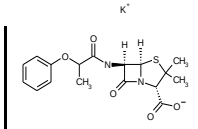	C17H19KN2O5S	402.52	Store at room temperature	132-93-4	Infectiology	Antibacterial
								Metabolism	

Prestw-724	10A05	Sulfamethoxypyridazine	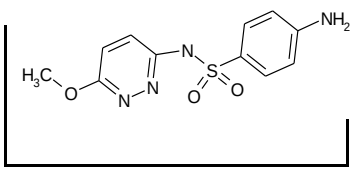	C11H12N4O3S	280.31	Store at 2°C	80-35-3	Infectiology	Antibacterial
								Metabolism	
Prestw-725	10A06	Deferoxamine mesylate	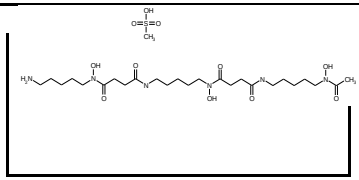	C26H52N6O11S	656.80	Store below 0°C	138-14-7	Diagnostic	Chelating
								Hematology	
Prestw-726	10A07	Mephentermine hemisulfate	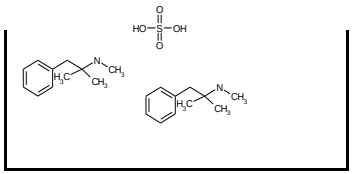	C22H36N2O4S	424.61	Store at room temperature	1212-72-2	Cardiovascular	Antihypotensive
									Vasoconstrictor
Prestw-1140	10A08	Liranaftate	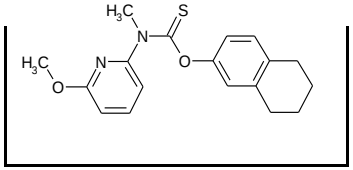	C18H20N2O2S	328.44	Store at +4°C	88678-31-3	Infectiology	Antifungal
								Metabolism	
Prestw-728	10A09	Sulfadimethoxine	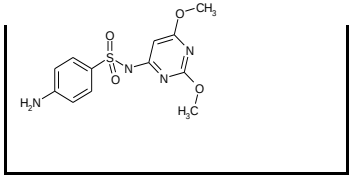	C12H14N4O4S	310.33	Store at 4°C	122-11-2	Infectiology	Antibacterial
								Metabolism	
Prestw-729	10A10	Sulfanilamide	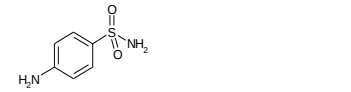	C6H8N2O2S	172.21	Store at room temperature	63-74-1	Infectiology	Antibacterial

								Metabolism	
Prestw-730	10A11	Balsalazide Sodium	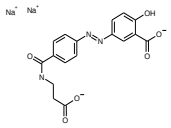	C17H13N3Na2O6	401.29	store at -20°C	80573-04-2	Gastroenterology	Anti-inflammatory
Prestw-731	10B02	Sulfaquinoxaline sodium salt	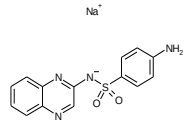	C14H11N4NaO2S	322.32	Store at room temperature	967-80-6	Infectiology	Antibacterial
								Metabolism	
Prestw-732	10B03	Streptozotocin	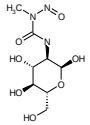	C8H15N3O7	265.22	Store below 0°C	18883-66-4	Oncology	Antineoplastic
Prestw-733	10B04	Metoprolol-(+,-) (+)-tartrate salt	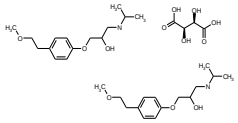	C34H56N2O12	684.83	Store at room temperature	56392-17-7	Cardiovascular	Antiarrhythmic
									Antihypertensive
Prestw-734	10B05	Flumethasone	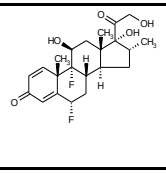	C22H28F2O5	410.46	Store at 2°C	2135-17-3	Metabolism	Anti-inflammatory

Prestw-735	10B06	Flecainide acetate	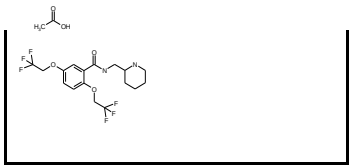	C19H24F6N2O5	474.40	Store at -20°C	54143-56-5	Cardiovascular	Antiarrhythmic
Prestw-736	10B07	Cefazolin sodium salt	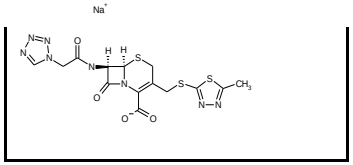	C14H13N8NaO4S3	476.49	Store at 2°C	27164-46-1	Metabolism	Antibacterial
								Infectiology	
Prestw-737	10B08	Atractyloside potassium salt	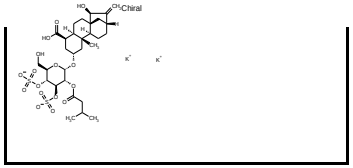	C30H44K2O16S2	803.01	Store at room temperature	102130-43-8	Oncology	Antineoplastic
Prestw-738	10B09	Folinic acid calcium salt	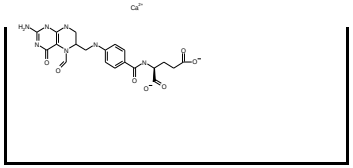	C20H21CaN7O7	511.51	Store at room temperature	6035-45-6	Hematology	Antianemic
Prestw-739	10B10	Levonordefrin	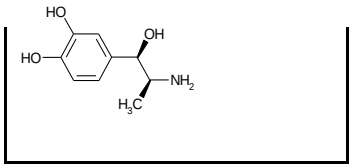	C9H13NO3	183.21	Store below 0°C	829-74-3	Cardiovascular	Vasoconstrictor
Prestw-740	10B11	Ebselen	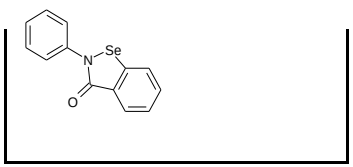	C13H9NOSe	274.18	Store at 2-8°C	60940-34-3	Metabolism	Anti-inflammatory
Prestw-741	10C02	Nadide	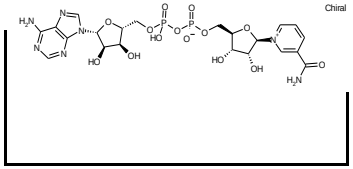	C21H27N7O14P2	663.44	Store below 0°C	53-84-9	Metabolism	

Prestw-742	10C03	Sulfamethizole	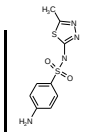	C9H10N4O2S2	270.33	Store at 2°C	144-82-1	Metabolism	Antibacterial
								Infectiology	
Prestw-743	10C04	Medrysone	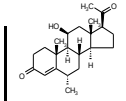	C22H32O3	344.50	Store at 2°C	2668-66-8	Metabolism	Anti-inflammatory
Prestw-744	10C05	Flunixin meglumine	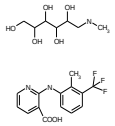	C21H28F3N3O7	491.47	Store at -20°C	42461-84-7	Central Nervous System	Analgesic
								Metabolism	Anti-inflammatory
									Antipyretic
Prestw-745	10C06	Spiramycin	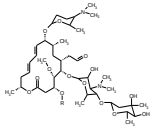	C43H73N2O14R	842.07	Store at 2°C	8025-81-8	Metabolism	Antibacterial
								Infectiology	
Prestw-746	10C07	Glycopyrrolate	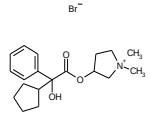	C19H28BrNO3	398.34	Store below 0°C	596-51-0	Gastroenterology	Antispastic
								Neuromuscular	

Prestw-1600	10C08	Aprepitant	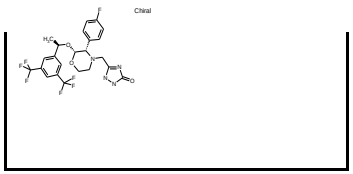	C23H21F7N4O3	534.44	Store at room temperature	170729-80-3	Metabolism	Antiemetic
Prestw-748	10C09	Monensin sodium salt	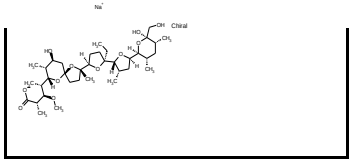	C36H61NaO11	692.87	Store at 2°C	22373-78-0	Infectiology	Antibacterial
Prestw-749	10C10	Isoetharine mesylate salt	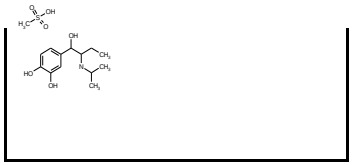	C14H25NO6S	335.42	Store at 2°C	7279-75-6	Respiratory	Bronchodilator
Prestw-750	10C11	Mevalonic-D, L acid lactone	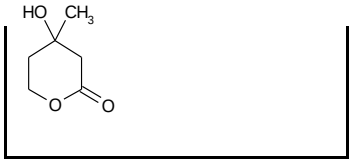	C6H10O3	130.14	Store below 0°C	674-26-0	Cardiovascular	Antilipemic
Prestw-751	10D02	Terazosin hydrochloride	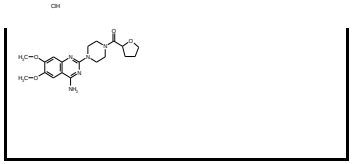	C19H26ClN5O4	423.90	Store at room temperature	63590-64-7	Cardiovascular	Antihypertensive
Prestw-752	10D03	Phenazopyridine hydrochloride	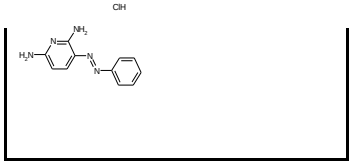	C11H12ClN5	249.70	Store at room temperature	136-40-3	Central Nervous System	Analgesic
Prestw-753	10D04	Demeclocycline hydrochloride	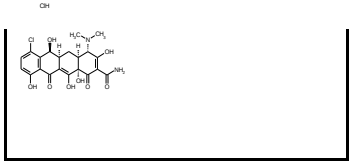	C21H22Cl2N2O8	501.32	Store below O°C	64-73-3	Metabolism	Antibacterial
								Infectiology	

Prestw-754	10D05	Fenoprofen calcium salt dihydrate	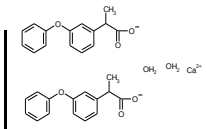	C30H30CaO8	558.65	Store at room temperature	53746-45-5	Metabolism	Anti-inflammatory
Prestw-755	10D06	Piperacillin sodium salt	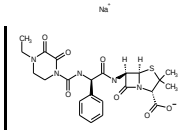	C23H26N5NaO7S	539.55	Store at 2°C	59703-84-3	Metabolism	Antibacterial
								Infectiology	
Prestw-756	10D07	Diethylstilbestrol	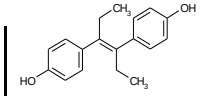	C18H20O2	268.36	Store at room temperature	56-53-1	Endocrinology	
								Oncology	
Prestw-757	10D08	Chlorotrianisene	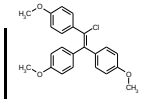	C23H21ClO3	380.88	Store at room temperature	569-57-3	Endocrinology	Antineoplastic
								Oncology	
Prestw-758	10D09	Ribostamycin sulfate salt	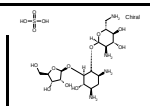	C17H36N4O14S	552.56	Store at 2°C	53797-35-6	Metabolism	Antibacterial
								Infectiology	
Prestw-759	10D10	Methacholine chloride	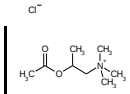	C8H18ClNO2	195.69	Store at room temperature	62-51-1	Diagnostic	
								Respiratory	

Prestw-760	10D11	Pipenzolate bromide		C22H28BrNO3	434.38	Store at room temperature	125-51-9	Gastroenterology	Antispastic
								Neuromuscular	
Prestw-761	10E02	Butamben	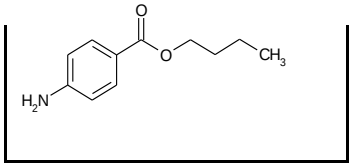	C11H15NO2	193.25	Store at room temperature	94-25-7	Central Nervous System	Anesthetic
Prestw-762	10E03	Sulfapyridine	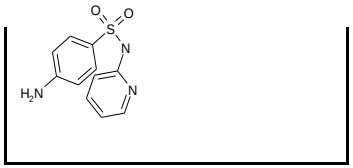	C11H11N3O2S	249.29	Store at 2°C	144-83-2	Metabolism	Antibacterial
								Infectiology	
Prestw-763	10E04	Meclofenoxate hydrochloride	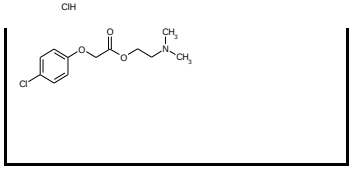	C12H17Cl2NO3	294.18	Store below 0°C	3685-84-5	Central Nervous System	CNS Stimulant
Prestw-764	10E05	Furaltadone hydrochloride	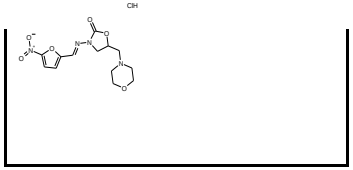	C13H17ClN4O6	360.76	Store at 2°C	3759-92-0	Infectiology	Antibacterial
Prestw-765	10E06	Ethoxyquin	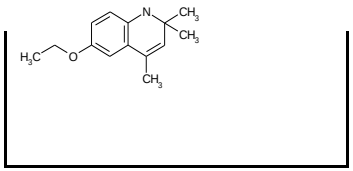	C14H19NO	217.31	Store at room temperature	91-53-2	Metabolism	Antifungal

Prestw-766	10E07	Tinidazole	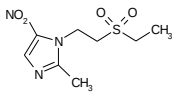	C8H13N3O4S	247.27	Store at room temperature	19387-91-8	Infectiology	Antiamebic
									Antibacterial
Prestw-767	10E08	Guanadrel sulfate	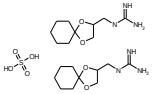	C20H40N6O8S	524.64	Store at room temperature	22195-34-2	Cardiovascular	Antihypertensive
Prestw-768	10E09	Vidarabine	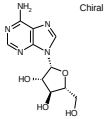	C10H13N5O4	267.25	Store at below 0°C	5536-17-4	Metabolism	Antiviral
Prestw-769	10E10	Sulfameter	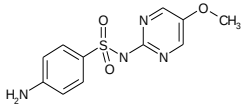	C11H12N4O3S	280.31	Store at 2°C	651-06-9	Metabolism	Antibacterial
								Infectiology	
Prestw-770	10E11	Isopropamide iodide	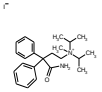	C23H33IN2O	480.44	Store at room temperature	71-81-8	Metabolism	Antiulcer
Prestw-771	10F02	Alclometasone dipropionate	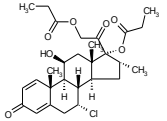	C28H37ClO7	521.06	Store at room temperature	66734-13-2	Metabolism	Anti-inflammatory
Prestw-772	10F03	Leflunomide	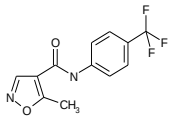	C12H9F3N2O2	270.21	Store at 2°C	75706-12-6	Immunology	Immunosuppressant

Prestw-773	10F04	Norgestrel-(-)-D	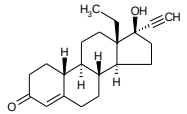	C21H28O2	312.46	Store at 2°C	797-63-7	Endocrinology	Contraceptive
Prestw-774	10F05	Fluocinonide	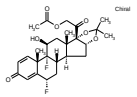	C26H32F2O7	494.54	Store at room temperature	356-12-7	Metabolism	Anti-inflammatory
Prestw-775	10F06	Sulfamethazine sodium salt	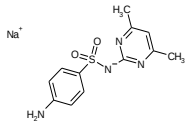	C12H13N4NaO2S	300.32	Store at 2°C	1981-58-4	Metabolism	Antibacterial
								Infectiology	
Prestw-776	10F07	Guaifenesin	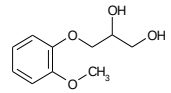	C10H14O4	198.22	Store at room temperature	93-14-1	Respiratory	Bronchodilator
									Expectorant
Prestw-777	10F08	Alexidine dihydrochloride	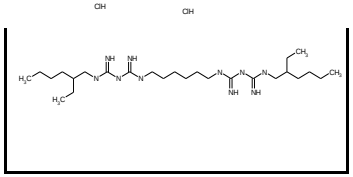	C26H58Cl2N10	581.73	Store at room temperature	22573-93-9	Infectiology	Antibacterial
Prestw-778	10F09	Proadifen hydrochloride		C23H32ClNO2	389.97	Store below 0°C	62-68-0	Neuromuscular	Local anesthetic

Prestw-779	10F10	Zomepirac sodium salt	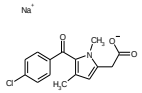	C15H13ClNNaO3	313.72	Store at room temperature	64092-48-4	Metabolism	Anti-inflammatory
Prestw-780	10F11	Cinoxacin	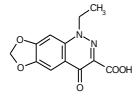	C12H10N2O5	262.22	Store at room temperature	28657-80-9	Metabolism	Antibacterial
								Infectiology	
Prestw-781	10G02	Clobetasol propionate	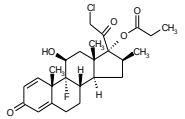	C25H32ClFO5	466.98	Store at 2°C	25122-46-7	Metabolism	Anti-inflammatory
Prestw-782	10G03	Podophyllotoxin	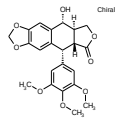	C22H22O8	414.42	Store at +4°C	518-28-5	Metabolism	Antiviral
Prestw-783	10G04	Clofibric acid	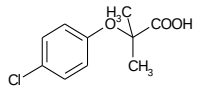	C10H11ClO3	214.65	Store at room temperature	882-09-7	Metabolism	Antilipemic
Prestw-784	10G05	Bendroflumethiazide	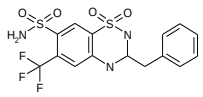	C15H14F3N3O4S2	421.42	Store at room temperature	73-48-3	Cardiovascular	Antihypertensive

									Diuretic
Prestw-785	10G06	Dicumarol	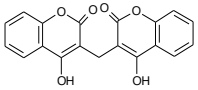	C19H12O6	336.30	Store at room temperature	66-76-2	Hematology	Anticoagulant
Prestw-786	10G07	Methimazole		C4H6N2S	114.17	Store at room temperature	60-56-0	Endocrinology	
Prestw-787	10G08	Merbromin		C20H8Br2HgNa2O6	750.66	Store at room temperature	129-16-8	Infectiology	Antibacterial
Prestw-788	10G09	Hexylcaine hydrochloride	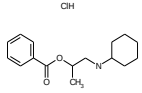	C16H24ClNO2	297.83	Store at room temperature	532-76-3	Dermatology	Anesthetic
Prestw-789	10G10	Drofenine hydrochloride	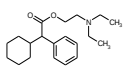	C20H32ClNO2	353.94	Store at 2°C	548-66-3	Neuromuscular	Antispastic
Prestw-790	10G11	Cycloheximide	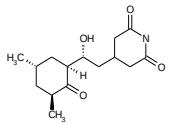	C15H23NO4	281.35	Store at 2°C	66-81-9	Infectiology	Antibacterial

Prestw-791	10H02	(R) -Naproxen sodium salt	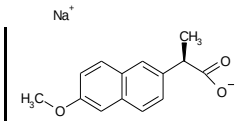	C14H13NaO3	252.25	Store at 2°C	23979-41-1	Metabolism	Anti-inflammatory
Prestw-792	10H03	Propidium iodide	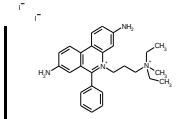	C27H34I2N4	668.41	Store at 2°C	25535-16-4	Infectiology	Antibacterial
Prestw-793	10H04	Cloperastine hydrochloride		C20H25Cl2NO	366.33	Store at room temperature	14984-68-0	Respiratory	Antitussive
Prestw-794	10H05	Eucatropine hydrochloride	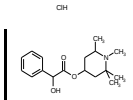	C17H26ClNO3	327.85	Store at room temperature	536-93-6	Neuromuscular	Antiglaucoma
								Ophthalmology	
Prestw-795	10H06	Isocarboxazid	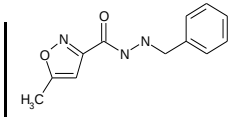	C12H13N3O2	231.26	Store at room temperature	59-63-2	Central Nervous System	Antidepressant
Prestw-796	10H07	Lithocholic acid	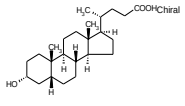	C24H40O3	376.58	Store at room temperature	434-13-9	Metabolism	Cholagogue

									Choleretic
Prestw-797	10H08	Methotrimeprazine maleat salt	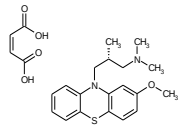	C23H28N2O5S	444.55	Store at room temperature	7104-38-3	Central Nervous System	Analgesic
									Antiemetic
									Sedative
Prestw-798	10H09	Dienestrol	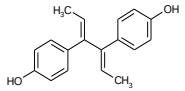	C18H18O2	266.34	Store at room temperature	84-17-3	Endocrinology	
Prestw-799	10H10	Pridinol methanesulfonate salt	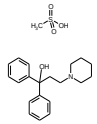	C21H29NO4S	391.53	Store at 2°C	6856-31-1	Central Nervous System	Antiparkinsonian
Prestw-800	10H11	Amrinone	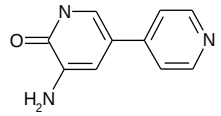	C10H9N3O	187.20	Store at 2°C	60719-84-8	Cardiovascular	
Prestw-801	11A02	Carbinoxamine maleate salt	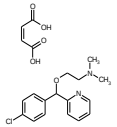	C20H23ClN2O5	406.87	Store at room temperature	3505-38-2	Allergology	Antihistaminic
								Metabolism	

Prestw-802	11A03	Methazolamide	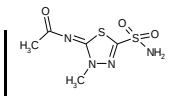	C5H8N4O3S2	236.27	Store at room temperature	554-57-4	Metabolism	Antiglaucoma
								Ophthalmology	Diuretic
Prestw-803	11A04	Pyrithyldione	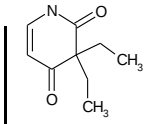	C9H13NO2	167.21	Store at room temperature	77-04-3	Central Nervous System	Hypnotic
									Sedative
Prestw-804	11A05	Spectinomycin dihydrochloride	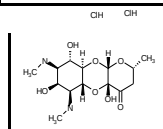	C14H26Cl2N2O7	405.28	Store at 2°C	21736-83-4	Metabolism	Antibacterial
								Infectiology	
Prestw-805	11A06	Piromidic acid	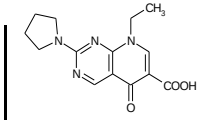	C14H16N4O3	288.31	Store at 4°C	19562-30-2	Metabolism	Antibacterial
								Infectiology	
Prestw-806	11A07	Trimipramine maleate salt	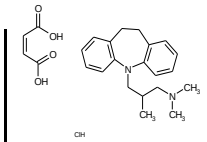	C24H30N2O4	410.52	Store at 2°C	521-78-8	Central Nervous System	Antidepressant
Prestw-807	11A08	Chloropyramine hydrochloride	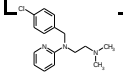	C16H21Cl2N3	326.27	Store at room temperature	6170-42-9	Allergology	Antihistaminic

Prestw-808	11A09	Furazolidone	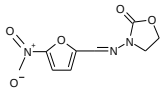	C8H7N3O5	225.16	Store at room temperature	67-45-8	Metabolism	
Prestw-809	11A10	Dichlorphenamide	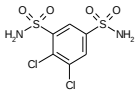	C6H6Cl2N2O4S2	305.16	Store at room temperature	120-97-8	Ophthalmology	Antiglaucoma
Prestw-810	11A11	Sulconazole nitrate		C18H16Cl3N3O3S	460.77	Store at room temperature	61318-91-0	Metabolism	Antifungal
Prestw-1233	11B02	Auranofin	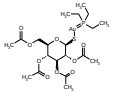	C20H34AuO9PS	678.49	Store at room temperature	34031-32-8	Metabolism	Analgesic
Prestw-812	11B03	Cromolyn disodium salt	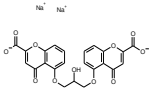	C23H14Na2O11	512.34	Store at room temperature	15826-37-6	Allergology	Antiasthmatic
								Metabolism	Anti-inflammatory
								Respiratory	
Prestw-813	11B04	Bucladesine sodium salt	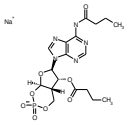	C18H23N5NaO8P	491.38	Store below 0°C	16980-89-5	Cardiovascular	

Prestw-814	11B05	Cefsulodin sodium salt	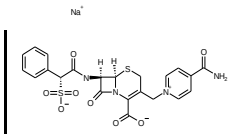	C22H19N4NaO8S2	554.54	Store at 2°C	52152-93-9	Metabolism	Antibacterial
								Infectiology	
Prestw-815	11B06	Fosfosal	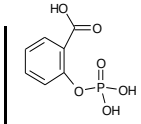	C7H7O6P	218.10	Store below 0°C	6064-83-1	Central Nervous System	Analgesic
Prestw-816	11B07	Suprofen	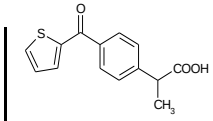	C14H12O3S	260.31	Store at room temperature	40828-46-4	Central Nervous System	Analgesic
								Metabolism	Anti-inflammatory
Prestw-1509	11B08	Deflazacort	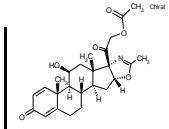	C25H31NO6	441.53	Store at romm temperature	14484-47-0	Immunology	Anti-inflammatory
								Metabolism	Immunosuppressant
Prestw-818	11B09	Nadolol	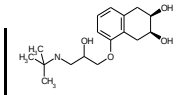	C17H27NO4	309.41	Store at room temperature	42200-33-9	Cardiovascular	Antianginal
									Antihypertensive
Prestw-819	11B10	Moxalactam disodium salt	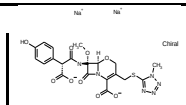	C20H18N6Na2O9S	564.44	Store at 4°C	64953-12-4	Metabolism	Antibacterial

								Infectiology	
Prestw-820	11B11	Aminophylline	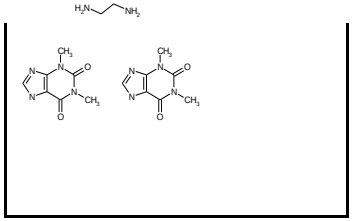	C16H24N10O4	420.43	!!! POISON !!! Store at room temperature Toxic	317-34-0	Cardiovascular	Bronchodilator
								Central Nervous System	CNS Stimulant
								Metabolism	Diuretic
								Respiratory	Muscle relaxant
									Vasodilator
Prestw-821	11C02	Azlocillin sodium salt	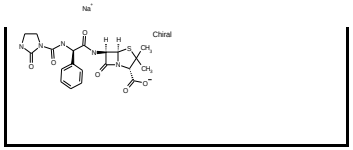	C20H22N5NaO6S	483.48	Store at room temperature	37091-65-9	Metabolism	Antibacterial
								Infectiology	
Prestw-822	11C03	Clidinium bromide		C22H26BrNO3	432.36	Store at room temperature	3485-62-9	Neuromuscular	Antispastic
Prestw-823	11C04	Sulfamonomethoxine	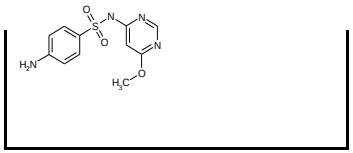	C11H12N4O3S	280.31	Store at room temperature	1220-83-3	Metabolism	Antibacterial
Prestw-824	11C05	Benzthiazide	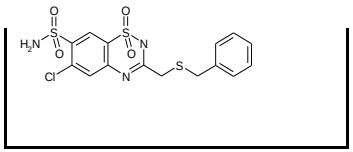	C15H14ClN3O4S3	431.94	Store at room temperature	91-33-8	Cardiovascular	Antihypertensive
									Diuretic

Prestw-825	11C06	Trichlormethiazide	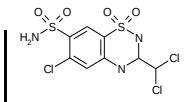	C8H8Cl3N3O4S2	380.66	Store at room temperature	133-67-5	Cardiovascular	Antihypertensive
									Diuretic
Prestw-826	11C07	Oxalamine citrate salt	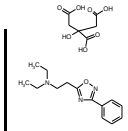	C20H27N3O8	437.45	Store at -20°C	1949-20-8	Central Nervous System	Anti-inflammatory
								Metabolism	Antispastic
								Respiratory	Antitussive
Prestw-827	11C08	Propantheline bromide	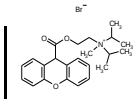	C23H30BrNO3	448.40	Store at room temperature	50-34-0	Neuromuscular	Antispastic
Prestw-1361	11C09	Viloxazine hydrochloride	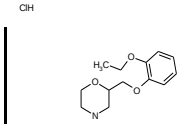	C13H20ClNO3	273.76	Store at room temperature	35604-67-2	Central Nervous System	Antidepressant
Prestw-829	11C10	Dimethadione	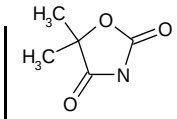	C5H7NO3	129.12	Store at 2°C	695-53-4	Central Nervous System	Anticonvulsant
Prestw-830	11C11	Ethaverine hydrochloride	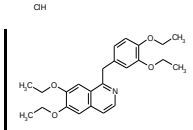	C24H30ClNO4	431.96	Store at 2°C	985-13-7	Central Nervous System	Antispastic

Prestw-831	11D02	Butacaine	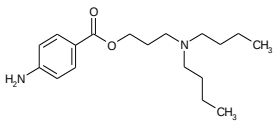	C18H30N2O2	306.45	Store below 0°C	149-16-6	Dermatology	Anesthetic
Prestw-832	11D03	Cefoxitin sodium salt	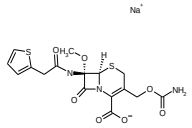	C16H16N3NaO7S2	449.44	Store at 2°C	33564-30-6	Metabolism	Antibacterial
								Infectiology	
Prestw-833	11D04	Ifosfamide	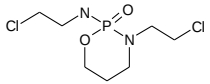	C7H15Cl2N2O2P	261.09	Store at room temperature	3778-73-2	Oncology	Antineoplastic
Prestw-834	11D05	Novobiocin sodium salt	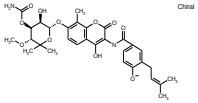	C31H35N2NaO11	634.62	Store at 2°C	1476-53-5	Metabolism	Antibacterial
								Infectiology	
Prestw-835	11D06	Tetrahydroxy-1,4-quinone monohydrate	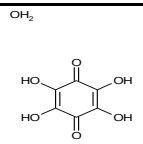	C6H6O7	190.11	Store at room temperature	319-89-1	Dermatology	Keratolytic
Prestw-836	11D07	Indoprofen	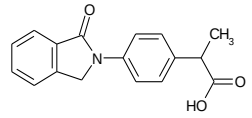	C17H15NO3	281.31	Store at room temperature	31842-01-0	Central Nervous System	Analgesic
								Metabolism	Anti-inflammatory

Prestw-837	11D08	Carbenoxolone disodium salt	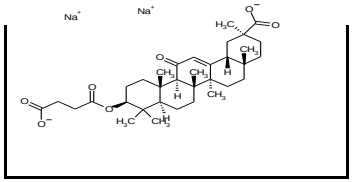	C34H48Na2O7	614.74	Store at 2°C	7421-40-1	Metabolism	Antiulcer
Prestw-838	11D09	Iocetamic acid	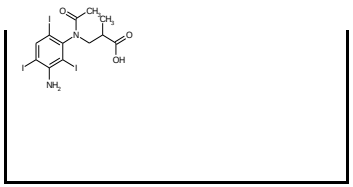	C12H13I3N2O3	613.96	Store at room temperature	16034-77-8	Diagnostic	Contrastant
Prestw-839	11D10	Ganciclovir	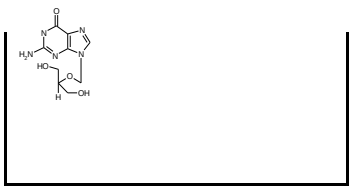	C9H13N5O4	255.24	Store at 2°C	82410-32-0	Metabolism	Antiviral
Prestw-840	11D11	Ethopropazine hydrochloride	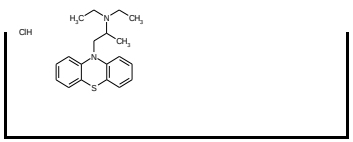	C19H25ClN2S	348.94	Store at 2°C	1094-08-2	Central Nervous System	Antiparkinsonian
Prestw-1455	11E02	Olanzapine	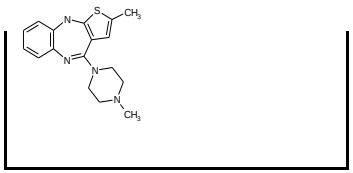	C17H20N4S	312.44	Store at room temperature	132539-06-1	Central Nervous System	Antipsychotic
Prestw-842	11E03	Trimeprazine tartrate	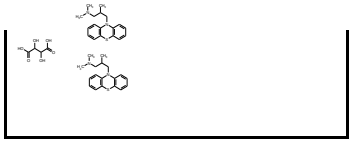	C40H50N4O6S2	747.00	Store at room temperature	4330-99-8	Allergology	Antihistaminic
								Central Nervous System	Antipruritic
								Dermatology	Sedative

Prestw-843	11E04	Nafcillin sodium salt monohydrate	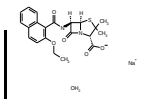	C21H23N2NaO6S	454.48	Store at 2°C	7177-50-6	Metabolism	Antibacterial
								Infectiology	
Prestw-844	11E05	Procyclidine hydrochloride	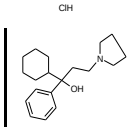	C19H30ClNO	323.91	Store at 2°C	1508-76-5	Central Nervous System	Antiparkinsonian
									Muscle relaxant
Prestw-845	11E06	Amiprilose hydrochloride	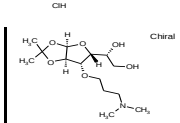	C14H28ClNO6	341.84	Store at 2°C	60414-06-4	Immunology	Immunomodulator
Prestw-846	11E07	Ethynylestradiol 3-methyl ether	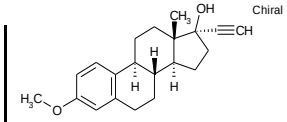	C21H26O2	310.44	Store at room temperature	72-33-3	Endocrinology	
Prestw-847	11E08	(-) -Levobunolol hydrochloride	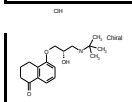	C17H26ClNO3	327.85	Store at -20°C	27912-14-7	Ophthalmology	Antiglaucoma
Prestw-848	11E09	Iodixanol	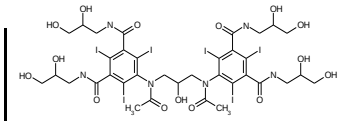	C35H44I6N6O15	1550.20	Store at -20°C	92339-11-2	Diagnostic	Contrastant

Prestw-1379	11E10	Clinafloxacin	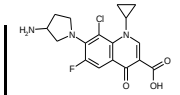	C17H17ClFN3O3	365.79	Store at room temperature	105956-97-6	Infectiology	Antibacterial
								Metabolism	
Prestw-850	11E11	Equilin	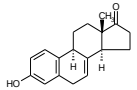	C18H20O2	268.36	Store at room temperature	474-86-2	Endocrinology	
Prestw-851	11F02	Paroxetine Hydrochloride	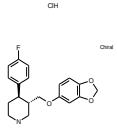	C19H21ClFNO3	365.84	-20°C	110429-35-1	Central Nervous System	Antidepressant
									CNS Stimulant
Prestw-1454	11F03	Nylidrin	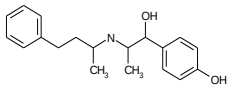	C19H25NO2	299.42	Store at room temperature	447-41-6	Cardiovascular	Vasodilator
Prestw-853	11F04	Liothyronine	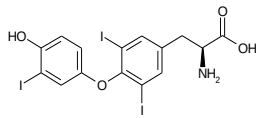	C15H12I3NO4	650.98	Store below 0°C	6893-02-3	Endocrinology	
Prestw-854	11F05	Roxithromycin	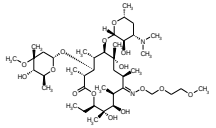	C41H76N2O15	837.07	Store below 0°C	80214-83-1	Metabolism	Antibacterial
								Infectiology	
Prestw-855	11F06	Beclomethasone dipropionate	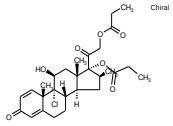	C28H37ClO7	521.06	Store at 2°C	5534-09-8	Metabolism	Anti-inflammatory

Prestw-856	11F07	Tolmetin sodium salt dihydrate	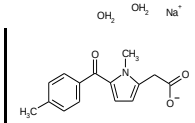	C15H18NNaO5	315.30	Store at room temperature	64490-92-2	Metabolism	Anti-inflammatory
Prestw-857	11F08	(+) -Levobunolol hydrochloride	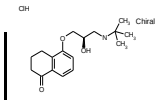	C17H26ClNO3	327.85	Store at -20°C	47141-41-3	Ophthalmology	Antiglaucoma
Prestw-858	11F09	Doxazosin mesylate	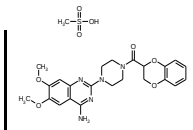	C24H29N5O8S	547.59	Store below 0°C Protect from light	77883-43-3	Cardiovascular	Antihypertensive
Prestw-859	11F10	Fluvastatin sodium salt	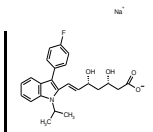	C24H25FNNaO4	433.46	Store at -20°C	93957-55-2	Cardiovascular	Antilipemic
Prestw-860	11F11	Methylhydantoin-5-(L)	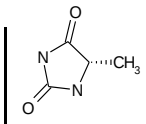	C4H6N2O2	114.10	Store at -20°C	40856-73-3	Central Nervous System	Anticonvulsant
Prestw-861	11G02	Gabapentin	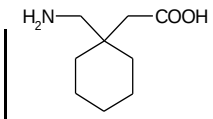	C9H17NO2	171.24	Store below 0°C	60142-96-3	Central Nervous System	Anticonvulsant

Prestw-862	11G03	Raloxifene hydrochloride	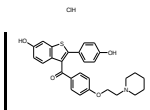	C28H28ClNO4S	510.06	Store at -20°C	82640-04-8	Endocrinology	
								Oncology	
Prestw-863	11G04	Etidronic acid, disodium salt		C2H6Na2O7P2	249.99	Store at -20	7414-83-7	Metabolism	Antiosteoporetic
									Chelating
Prestw-864	11G05	Methylhydantoin-5-(D)	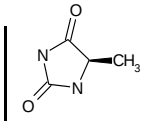	C4H6N2O2	114.10	Store at -20°C	55147-68-7		
Prestw-865	11G06	Simvastatin	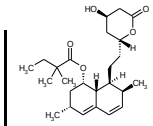	C25H38O5	418.58	Store at room - 20°C	79902-63-9	Cardiovascular	Antilipemic
Prestw-866	11G07	Azacytidine-5	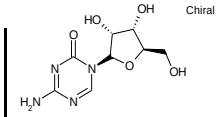	C8H12N4O5	244.21	Toxic Store at 4°C	320-67-2	Oncology	Antineoplastic
Prestw-867	11G08	Paromomycin sulfate	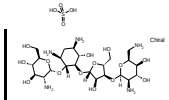	C23H47N5O18S	713.72	Store at room temperature	1263-89-4	Metabolism	Antiamebic
								Infectiology	Antibacterial
Prestw-868	11G09	Acetaminophen	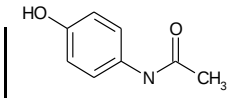	C8H9NO2	151.17	Store at room temperature	103-90-2	Central Nervous System	Analgesic
									Antipyretic

Prestw-869	11G10	Phthalylsulfathiazole	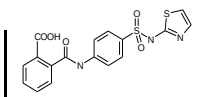	C17H13N3O5S2	403.44	Store at room temperature	85-73-4	Metabolism	Antibacterial
								Infectiology	
Prestw-870	11G11	Luteolin	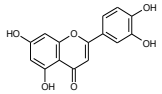	C15H10O6	286.24	Store at 2°C	491-70-3	Respiratory	Expectorant
Prestw-871	11H02	Iopamidol	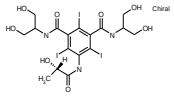	C17H22I3N3O8	777.09	Store at room temperature	60166-93-0	Diagnostic	Contrastant
Prestw-872	11H03	Iopromide	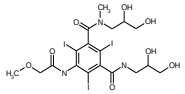	C18H24I3N3O8	791.12	Store at room temperature	73334-07-3	Diagnostic	Contrastant
Prestw-873	11H04	Theophylline monohydrate		C7H10N4O3	198.18	Store at room temperature	5967-84-0	Cardiovascular	Bronchodilator
								Central Nervous System	CNS Stimulant
								Respiratory	Diuretic
									Vasodilator
Prestw-874	11H05	Theobromine	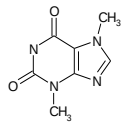	C7H8N4O2	180.17	Store at +4°C	83-67-0	Cardiovascular	Bronchodilator
								Respiratory	Diuretic

Prestw-875	11H06	Reserpine	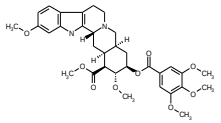	C33H40N2O9	608.69	RT	50-55-5	Central Nervous System	Antipsychotic
Prestw-1239	11H07	Bicalutamide	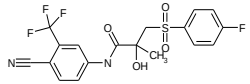	C18H14F4N2O4S	430.38	Store at room temperature	90357-06-5	Endocrinology	Antineoplastic
								Oncology	
Prestw-877	11H08	Scopolamine hydrochloride	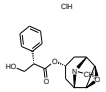	C17H22ClNO4	339.82	Store at 2°C	55-16-3	Central Nervous System	Antiemetic
Prestw-878	11H09	Ioversol	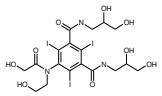	C18H24I3N3O9	807.12	Store at room temperature	87771-40-2	Diagnostic	Contrastant
Prestw-1495	11H10	Rabeprazole Sodium salt	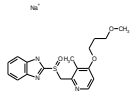	C18H21N3NaO3S	382.44	Store at room temperature	117976-89-3	Metabolism	Antiulcer
Prestw-880	11H11	Carbachol	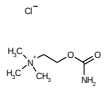	C6H15ClN2O2	182.65	Store at room temperature Hygroscopic	51-83-2	Cardiovascular	Antihypertensive
									Vasodilator
Prestw-881	12A02	Niacin	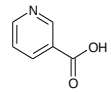	C6H5NO2	123.11	Store at room temperature	59-67-6	Cardiovascular	Antilipemic
									Vasodilator

Prestw-882	12A03	Bemegride	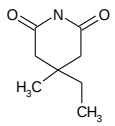	C8H13NO2	155.20	Store at room temperature	64-65-3	Central Nervous System	CNS stimulant
								Respiratory	
Prestw-883	12A04	Digoxigenin	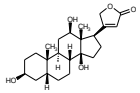	C23H34O5	390.52	Store at room temperature	1672-46-4	Diagnostic	
Prestw-884	12A05	Meglumine	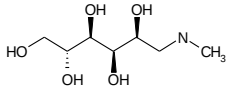	C7H17NO5	195.22	Store at room temperature	6284-40-8	Metabolism	Antileishmanial
								Respiratory	Antiseptic
									Expectorant
Prestw-1510	12A06	Dolasetron mesilate	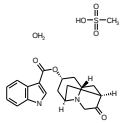	C20H26N2O7S	438.50	Store at room temperature	115956-13-3	Central Nervous System	Antiemetic
Prestw-886	12A07	Clioquinol		C9H5ClINO	305.50	Store at room temperature	130-26-7	Metabolism	Antiamebic
									Antifungal
									Antiseptic
Prestw-887	12A08	Oxybenzone	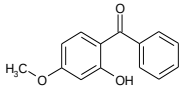	C14H12O3	228.25	Store at room temperature	131-57-7	Dermatology	

Prestw-888	12A09	Promethazine hydrochloride	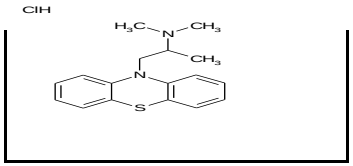	C17H21ClN2S	320.89	Store at room temperature	58-33-3	Allergology	Antihistaminic
								Central Nervous System	Sedative
Prestw-1167	12A10	Diacerein	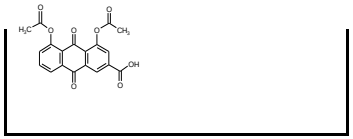	C19H12O8	368.30	Store at +4°C	13739-02-1	Immunology	Antiarthritic
Prestw-1137	12A11	Esmolol hydrochloride		C16H26ClNO4	331.84	Store at +4°C	81161-17-3	Cardiovascular	Antiarrhythmic
Prestw-1486	12B02	Cortisol acetate	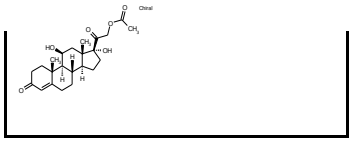	C23H32O6	404.51	Store at room temperature	50-03-3	Metabolism	Anti-inflammatory
Prestw-1416	12B03	Flubendazol	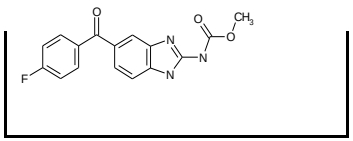	C16H12FN3O3	313.29	Store at room temperature	31430-15-6	Metabolism	
Prestw-893	12B04	Felbinac	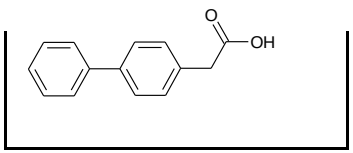	C14H12O2	212.25	Store at room temperature	5728-52-9	Central Nervous System	Analgesic
								Metabolism	Anti-inflammatory
Prestw-894	12B05	Butylparaben	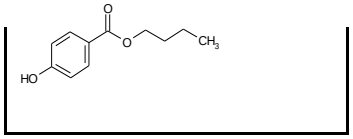	C11H14O3	194.23	Store at room temperature	94-26-8	Metabolism	Antifungal

Prestw-895	12B06	Aminohippuric acid	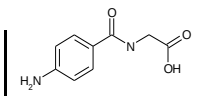	C9H10N2O3	194.19	Store at room temperature	61-78-9	Diagnostic	
Prestw-896	12B07	N-Acetyl-L-leucine	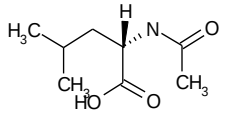	C8H15NO3	173.21	Store at room temperature	1188-21-2	Central Nervous System	Antivertigo
Prestw-897	12B08	Pipemidic acid	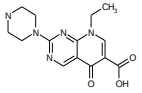	C14H17N5O3	303.32	Store at room temperature Hydroscopic	51940-44-4	Metabolism	Antibacterial
								Infectiology	
Prestw-898	12B09	Dioxybenzone	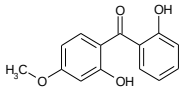	C14H12O4	244.25	Store at room temperature	131-53-3	Dermatology	
Prestw-899	12B10	Adrenosterone	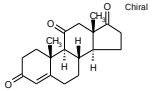	C19H24O3	300.40	Store at room temperature	382-45-6	Endocrinology	
Prestw-900	12B11	Methylatropine nitrate		C18H26N2O6	366.42	Store at room temperature	52-88-0	Neuromuscular	Antispastic
								Ophthalmology	Mydriatic
Prestw-901	12C02	Hymecromone	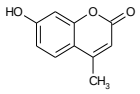	C10H8O3	176.17	Store at room temperature	90-33-5	Metabolism	Muscle relaxant

Prestw-1512	12C03	Abacavir Sulfate	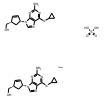	C28H38N12O6S	670.76	Store at room temperature	188062-50-2	Infectiology	Antiviral
Prestw-903	12C04	Diloxanide furoate	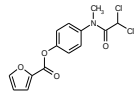	C14H11Cl2NO4	328.15	Store at room temperature	3736-81-0	Metabolism	Antiamebic
Prestw-904	12C05	Metyrapone	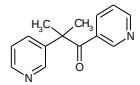	C14H14N2O	226.28	Store at room temperature	54-36-4	Endocrinology	
Prestw-905	12C06	Urapidil hydrochloride	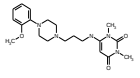	C20H30ClN5O3	423.95	Store at room temperature	64887-14-5	Cardiovascular	Antihypertensive
Prestw-906	12C07	Fluspirilen	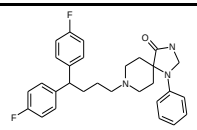	C29H31F2N3O	475.59	Store at room temperature	1841-19-6	Central Nervous System	Antipsychotic
Prestw-907	12C08	S-(+)-ibuprofen	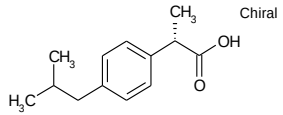	C13H18O2	206.29	Store at room temperature	51146-56-6	Central Nervous System	Analgesic
								Metabolism	Anti-inflammatory

Prestw-908	12C09	Ethynodiol diacetate	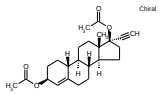	C24H32O4	384.52	Store at room temperature	297-76-7	Endocrinology	Contraceptive
Prestw-909	12C10	Nabumetone	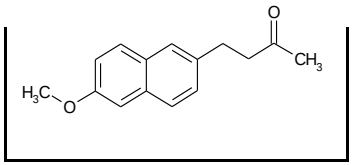	C15H16O2	228.29	Store at room temperature	42924-53-8	Central Nervous System	Analgesic
								Metabolism	Anti-inflammatory
Prestw-910	12C11	Nisoxetine hydrochloride	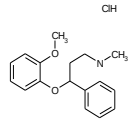	C17H22ClNO2	307.82	Store at room temperature	57754-86-6	Central Nervous System	Antidepressant
Prestw-911	12D02	(+)-Isoproterenol (+)-bitartrate salt	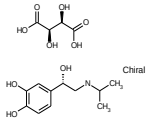	C15H23NO9	361.35	Store at room temperature	14638-70-1	Respiratory	Antiasthmatic
									Bronchodilator
									Vasodilator
Prestw-912	12D03	Monobenzone		C13H12O2	200.24	Store at room temperature	103-16-2	Dermatology	
Prestw-913	12D04	2-Aminobenzenesulfonamide	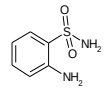	C6H8N2O2S	172.21	Store at room temperature	3306-62-5	Metabolism	Diuretic

Prestw-914	12D05	Estrone	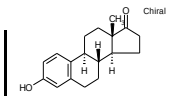	C18H22O2	270.37	Store at room temperature	53-16-7	Endocrinology	
Prestw-915	12D06	Lorglumide sodium salt	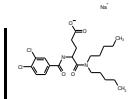	C22H31Cl2N2NaO4	481.40	Store at room temperature	97964-56-2	Metabolism	Antiulcer
Prestw-916	12D07	Nitrendipine	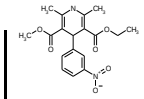	C18H20N2O6	360.37	Store at room temperature	39562-70-4	Cardiovascular	Antihypertensive
Prestw-917	12D08	Flurbiprofen	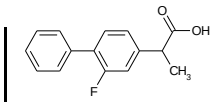	C15H13FO2	244.27	Store at room temperature	5104-49-4	Central Nervous System	Analgesic
								Metabolism	Anti-inflammatory
Prestw-918	12D09	Nimodipine	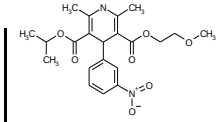	C21H26N2O7	418.45	Store at room temperature Photosensitive	66085-59-4	Cardiovascular	Vasodilator
Prestw-919	12D10	Bacitracin		C66H103N17O16S	1422.73	Store at 2°C	1405-87-4	Metabolism	Antibacterial
Prestw-920	12D11	L(-)-vesamicol hydrochloride	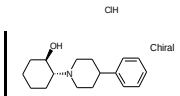	C17H26ClNO	295.86	Store at room temperature	112709-59-8	Neuromuscular	

Prestw-921	12E02	Nizatidine	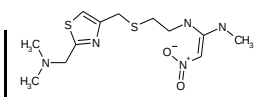	C12H21N5O2S2	331.46	Store at room temperature	76963-41-2	Metabolism	Antiulcer
Prestw-922	12E03	Thioperamide maleate	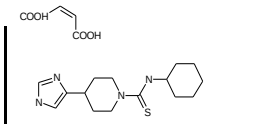	C19H28N4O4S	408.52	Store at RT	106243-16-7	Central Nervous System	Antiemetic
Prestw-923	12E04	Xamoterol hemifumarate	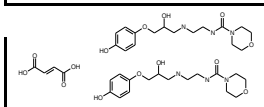	C36H54N6O14	794.86	Store at room temperature	73210-73-8	Cardiovascular	
Prestw-924	12E05	Rolipram	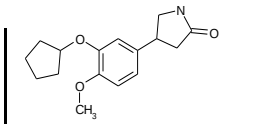	C16H21NO3	275.35	Store at room temperature	61413-54-5	Central Nervous System	Antidepressant
									Antipsychotic
									Antipsychotic
Prestw-925	12E06	Thonzonium bromide	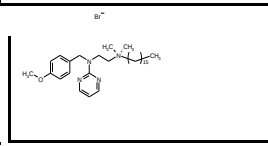	C32H55BrN4O	591.73	Store at room temperature	553-08-2	Dermatology	Antiseptic
Prestw-926	12E07	Idazoxan hydrochloride	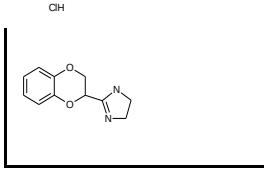	C11H13ClN2O2	240.69	Store at room temperature	79944-56-2	Central Nervous System	Antiparkinsonian
									Antipsychotic
Prestw-927	12E08	Quinapril HCl	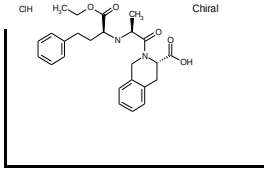	C25H31ClN2O5	474.99	Store at +4°C	82586-55-8	Cardiovascular	Antihypertensive

Prestw-928	12E09	Nilutamide	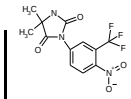	C12H10F3N3O4	317.23	Store at room temperature	63612-50-0	Oncology	Antineoplastic
Prestw-929	12E10	Ketorolac tromethamine	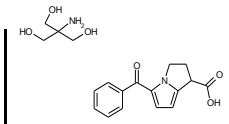	C19H24N2O6	376.41	Store at room temperature	74103-07-4	Central Nervous System	Analgesic
								Metabolism	Anti-inflammatory
									Antipyretic
Prestw-930	12E11	Protriptyline hydrochloride	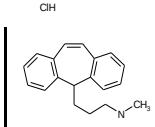	C19H22ClN	299.85	Store at room temperature	1225-55-4	Central Nervous System	Antidepressant
Prestw-931	12F02	Propofol	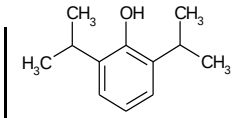	C12H18O	178.28	Store at room temperature	2078-54-8	Central Nervous System	Anesthetic
									Sedative
Prestw-932	12F03	S(-)Eticlopride hydrochloride	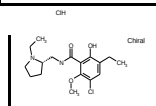	C17H26Cl2N2O3	377.31	Store at room temperature	97612-24-3	Central Nervous System	
Prestw-933	12F04	Primidone	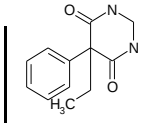	C12H14N2O2	218.26	Store at room temperature	125-33-7	Central Nervous System	Anticonvulsant

Prestw-934	12F05	Flucytosine		C4H4FN3O	129.09	Store at room temperature	2022-85-7	Metabolism	Antifungal
Prestw-935	12F06	(-)-MK 801 hydrogen maleate	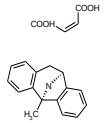	C20H19NO4	337.38	Store at room temperature	77086-19-2	Central Nervous System	Anticonvulsant
Prestw-936	12F07	Bephenium hydroxynaphthoate	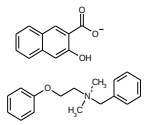	C28H29NO4	443.55	Store at room temperature	3818-50-6	Metabolism	
Prestw-937	12F08	Dehydroisoandosterone 3-acetate	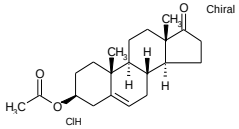	C21H30O3	330.47	Store at room temperature	853-23-6	Endocrinology	
Prestw-938	12F09	Benserazide hydrochloride	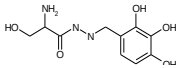	C10H16ClN3O5	293.71	Store at room temperature	14919-77-8	Central Nervous System	Antiparkinsonian
Prestw-939	12F10	Iodipamide	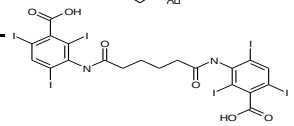	C20H14I6N2O6	1139.77	Store at room temperature	606-17-7	Diagnostic	Contrastant
Prestw-1213	12F11	Allopurinol	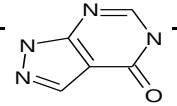	C5H4N4O	136.11	Store at room temperature	315-30-0	Metabolism	
Prestw-941	12G02	Pentetic acid	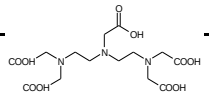	C14H23N3O10	393.35	Store at room temperature	67-43-6	Oncology	Chelating
									Radioprotectant

Prestw-942	12G03	Bretylium tosylate	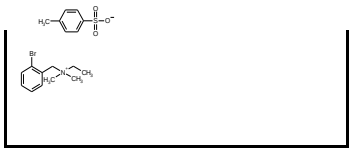	C18H24BrNO3S	414.36	Store at room temperature	61-75-6	Cardiovascular	Anesthetic
								Central Nervous System	Antiarrhythmic
									Antihypertensive
Prestw-943	12G04	Pralidoxime chloride	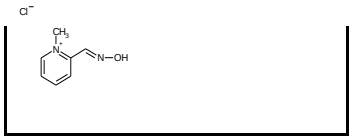	C7H9ClN2O	172.62	Store at room temperature	51-15-0	Neuromuscular	
Prestw-944	12G05	Phenoxybenzamine hydrochloride	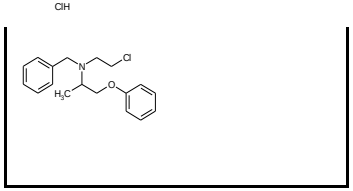	C18H23Cl2NO	340.30	Store at 2-8°C HUMAN CARCINOGEN	63-92-3	Cardiovascular	Antihypertensive
Prestw-945	12G06	Salmeterol	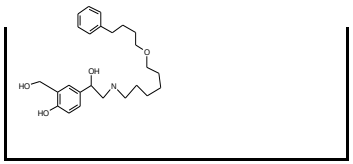	C25H37NO4	415.58	Store at -20°C	89365-50-4	Respiratory	Bronchodilator
Prestw-946	12G07	Altretamine	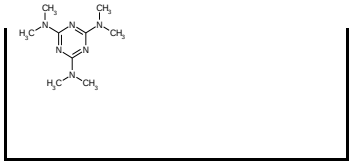	C9H18N6	210.28	Store at room temperature	645-05-6	Oncology	Antineoplastic
Prestw-947	12G08	Prazosin hydrochloride	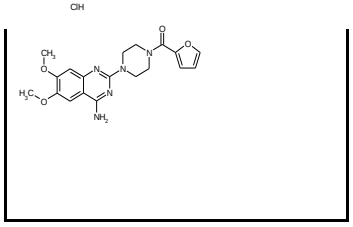	C19H22ClN5O4	419.87	Store at room temperature Hygroscopic Light sensitive	19237-84-4	Cardiovascular	Antihypertensive

Prestw-948	12G09	Timolol maleate salt		C17H28N4O7S	432.50	Store at room temperature	26921-17-5	Cardiovascular	Antianginal
								Ophthalmology	Antiarrhythmic
									Antiglaucoma
									Antihypertensive
Prestw-949	12G10	(+,-)-Octopamine hydrochloride	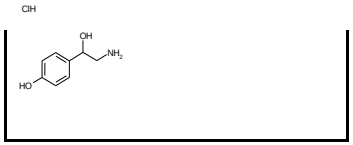	C8H12ClNO2	189.64	Store at room temperature	770-05-8	Cardiovascular	
Prestw-1279	12G11	Stavudine		C10H12N2O4	224.22	Store at room temperature	3056-17-5	Infectiology	Antiviral
								Metabolism	
Prestw-951	12H02	Crotamiton	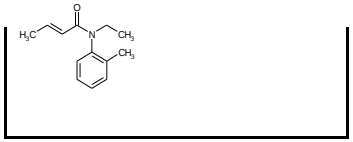	C13H17NO	203.29	Store at room temperature	483-63-6	Dermatology	Antipruritic
								Metabolism	
Prestw-1197	12H03	Toremifene		C26H28ClNO	405.97	Store at room temperature	89778-26-7	Endocrinology	Antineoplastic
								Oncology	
Prestw-536	12H04	(R)-(+)-Atenolol	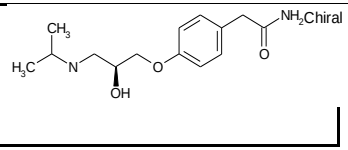	C14H22N2O3	266.34	Store below 0°C	56715-13-0	Cardiovascular	Antianginal
									Antiarrhythmic

									Antihypertensive
									Antimigraine
Prestw-954	12H05	Tyloxapol		C59H96O12	997.42	Store at room temperature	25301-02-4	Respiratory	Mucolytic
Prestw-955	12H06	Florfenicol	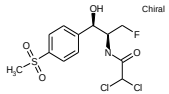	C12H14Cl2FNO4S	358.22	Store at room temperature	73231-34-2	Metabolism	Antibacterial
								Infectiology	
Prestw-956	12H07	Megestrol acetate	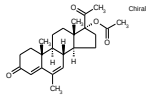	C24H32O4	384.52	Store at room temperature	595-33-5	Endocrinology	Antineoplastic
								Oncology	Contraceptive
Prestw-957	12H08	Deoxycorticosterone	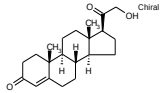	C21H30O3	330.47	Store at room temperature	64-85-7	Endocrinology	Anti-inflammatory
								Metabolism	
Prestw-958	12H09	Urosiol	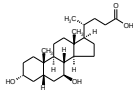	C24H40O4	392.58	Store at room temperature	128-13-2	Metabolism	
Prestw-959	12H10	Proparacaine hydrochloride	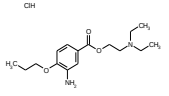	C16H27ClN2O3	330.86	Store at room temperature	5875-06-9	Central Nervous System	Anesthetic
Prestw-960	12H11	Aminocaproic acid	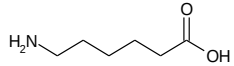	C6H13NO2	131.18	Store at room temperature	60-32-2	Allergology	Antifibrinolytic

								Hematology	Hemostatic
Prestw-961	13A02	Denatonium benzoate	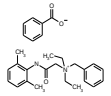	C28H34N2O3	446.59	Store at room temperature	3734-33-6	Neuromuscular	
Prestw-1259	13A03	Canrenone	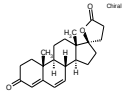	C22H28O3	340.47	Store at room temperature	976-71-6	Endocrinology	Diuretic
Prestw-963	13A04	Enilconazole	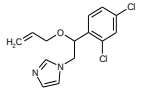	C14H14Cl2N2O	297.19	Store at room temperature	35554-44-0	Metabolism	Antifungal
Prestw-964	13A05	Methacycline hydrochloride	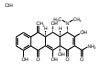	C22H23ClN2O8	478.89	Store at room temperature	3963-95-9	Metabolism	Antibacterial
								Infectiology	
Prestw-1415	13A06	Floxuridine	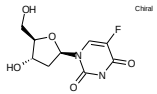	C9H11FN2O5	246.20	Store at room temperature	50-91-9	Oncology	Antineoplastic
									Antiviral
Prestw-966	13A07	Sotalol hydrochloride	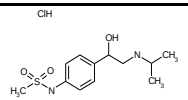	C12H21ClN2O3S	308.83	Store at room temperature	959-24-0	Cardiovascular	Antianginal
									Antiarrhythmic
									Antihypertensive
Prestw-1267	13A08	Gestrinone	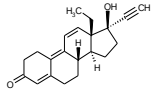	C21H24O2	308.42	Store at room temperature	16320-04-0	Endocrinology	Contraceptive

Prestw-968	13A09	Decamethonium bromide	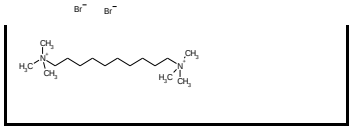	C16H38Br2N2	418.30	Store at room temperature	541-22-0	Neuromuscular	Muscle relaxant
Prestw-1514	13A10	Darifenacin hydrobromide	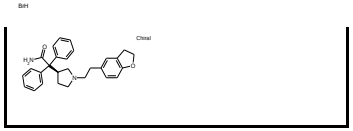	C28H31BrN2O2	507.48	Store at room temperature	133099-07-7	Neuromuscular	
Prestw-1602	13A11	Indatraline hydrochloride	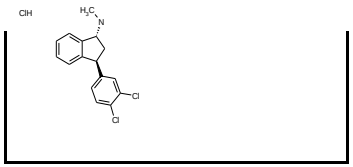	C16H16Cl3N	328.67	Store at room temperature	86939-10-8	Central Nervous System	Antidepressant
Prestw-971	13B02	Remoxipride Hydrochloride	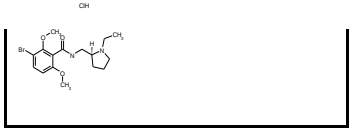	C16H24BrClN2O3	407.74	Store at room temperature	73220-03-8	Central Nervous System	Antipsychotic
Prestw-972	13B03	THIP Hydrochloride	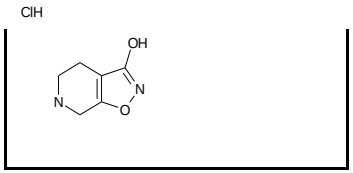	C6H9ClN2O2	176.60	Store at room temperature	85118-33-8	Central Nervous System	Sedative
Prestw-973	13B04	Pirlindole mesylate	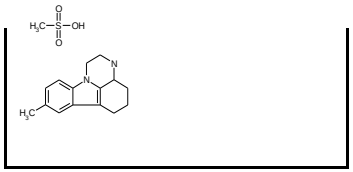	C16H22N2O3S	322.43	Store at room temperature	60762-57-4	Central Nervous System	Antidepressant
Prestw-974	13B05	Pronethalol hydrochloride	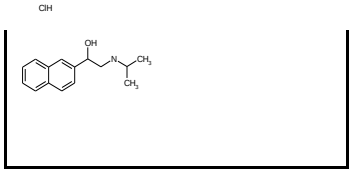	C15H20ClNO	265.79	Store at room temperature	51-02-5	Cardiovascular	Antianginal
									Antiarrhythmic
									Antihypertensive

Prestw-975	13B06	Naftopidil dihydrochloride	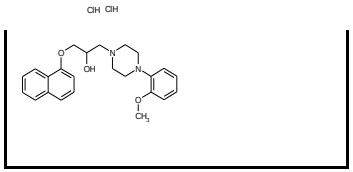	C24H30Cl2N2O3	465.42	Store at room temperature	57149-08-3	Cardiovascular	Antihypertensive
Prestw-976	13B07	Tracazolate hydrochloride	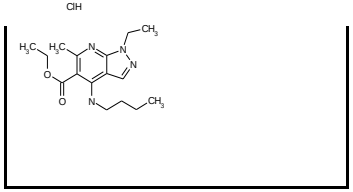	C16H25ClN4O2	340.86	Store at room temperature Photosensitive	41094-88-6	Central Nervous System	Anticonvulsant
									Sedative
Prestw-977	13B08	Zardaverine	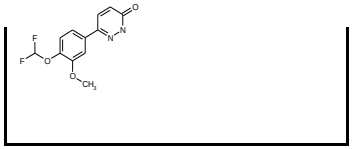	C12H10F2N2O3	268.22	Store at room temperature	101975-10-4	Respiratory	Bronchodilator
Prestw-978	13B09	Memantine Hydrochloride	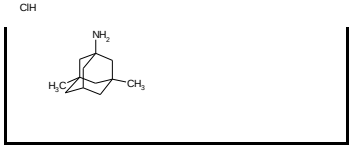	C12H22ClN	215.77	Store at room temperature	41100-52-1	Central Nervous System	Anti-Alzheimer
								Metabolism	Antiparkinsonian
									Antispastic
Prestw-979	13B10	Ozagrel hydrochloride	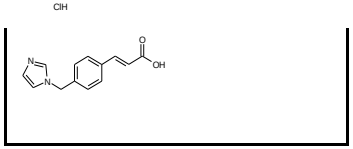	C13H13ClN2O2	264.71	Store at room temperature	78712-43-3	Cardiovascular	Antianginal
								Hematology	
Prestw-980	13B11	Piribedil hydrochloride	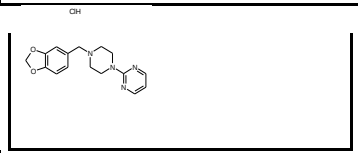	C16H19ClN4O2	334.81	Store at room temperature	78213-63-5	Cardiovascular	Antiparkinsonian

								Central Nervous System	Vasodilator
Prestw-981	13C02	Nitrocaramiphen hydrochloride	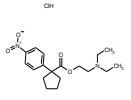	C18H27ClN2O4	370.88	Store at room temperature		Central Nervous System	
Prestw-982	13C03	Nandrolone	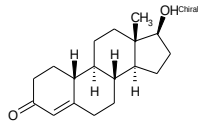	C18H26O2	274.41	store at -20°C	434-22-0	Endocrinology	Antianemic
								Hematology	
Prestw-983	13C04	Dimaprit dihydrochloride	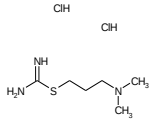	C6H17Cl2N3S	234.19	Store at room temperature	23256-33-9	Metabolism	
Prestw-1459	13C05	Oxfendazol	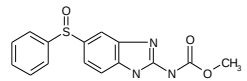	C15H13N3O3S	315.35	Store at room temperature	53716-50-0	Metabolism	
Prestw-1268	13C06	Guaiacol	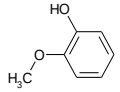	C7H8O2	124.14	Store at +4°C	90-05-1	Respiratory	Expectorant
Prestw-986	13C07	Proscillaridin A	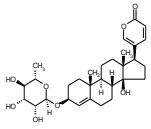	C30H42O8	530.66	Store at 2°C	466-06-8	Cardiovascular	

Prestw-1316	13C08	Pramipexole	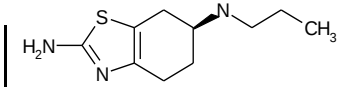	C10H17N3S	211.33	Store at room temperature	104632-26-0	Central Nervous System	Antiparkinsonian
Prestw-1452	13C09	Norgestimate	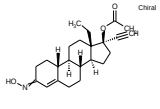	C23H31NO3	369.51	Store at room temperature	35189-28-7	Endocrinology	
Prestw-1374	13C10	Chlormadinone acetate	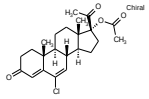	C23H29ClO4	404.94	Store at room temperature	302-22-7	Endocrinology	Antineoplastic
								Oncology	
Prestw-1310	13C11	Phenylbutazone	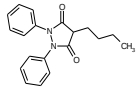	C19H20N2O2	308.38	Store at room temperature	50-33-9	Metabolism	Anti-inflammatory
Prestw-991	13D02	Gliquidone	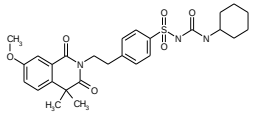	C27H33N3O6S	527.64	Store at +4°C	33342-05-1	Endocrinology	Antidiabetic
Prestw-992	13D03	Pizotifen malate		C23H27NO5S	429.54	Store at room temperature	5189-11-7	Allergology	Antihistaminic
								Cardiovascular	Antimigraine
								Central Nervous System	Sedative

Prestw-993	13D04	Ribavirin	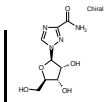	C8H12N4O5	244.21	Store at room temperature	36791-04-5	Metabolism	Antiviral
Prestw-994	13D05	Cyclopenthiazide	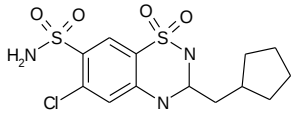	C13H18ClN3O4S2	379.89	Store at +4°C	742-20-1	Cardiovascular	Antihypertensive
									Diuretic
Prestw-995	13D06	Fluvoxamine maleate	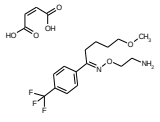	C19H25F3N2O6	434.42	Store at 2 - 8°C	61718-82-9	Central Nervous System	Antidepressant
									CNS Stimulant
Prestw-1321	13D07	Prothionamide		C9H12N2S	180.27	Store at room temperature	14222-60-7	Infectiology	Antibacterial
								Metabolism	
Prestw-997	13D08	Fluticasone propionate	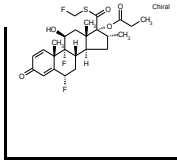	C25H31F3O5S	500.58	Store at room temperature	80474-14-2	Cardiovascular	Anti-inflammatory
								Metabolism	Vasodilator
Prestw-998	13D09	Zuclopenthixol dihydrochloride	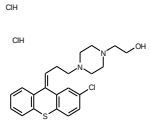	C22H27Cl3N2OS	473.90	Store at +4°C	633-59-0	Central Nervous System	Antipsychotic
									Antiviral
									Sedative

Prestw-999	13D10	Proguanil hydrochloride	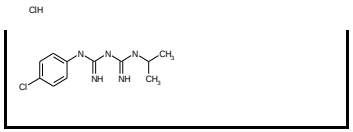	C11H17Cl2N5	290.20	Store at +4°C	637-32-1	Metabolism	Antimalarial
Prestw-1000	13D11	Lymecycline	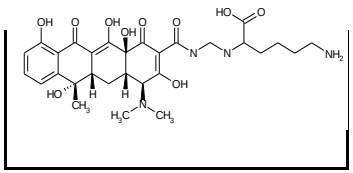	C29H38N4O10	602.65	Store at +4°C	992-21-2	Metabolism	Antibacterial
Prestw-1001	13E02	Alfadolone acetate	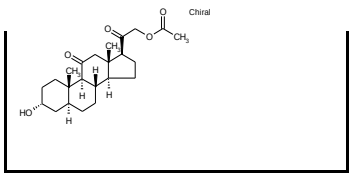	C23H34O5	390.52	Store at +4°C	23930-37-2	Central Nervous System	Anesthetic
Prestw-1002	13E03	Alfaxalone	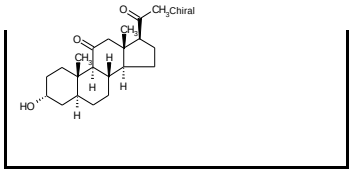	C21H32O3	332.49	Store at room temperature	23930-19-0	Central Nervous System	Anesthetic
Prestw-1003	13E04	Azapropazone	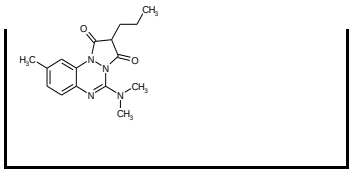	C16H20N4O2	300.36	Store at +4°C	13539-59-8	Central Nervous System	Analgesic
								Metabolism	Anti-inflammatory
Prestw-1004	13E05	Meptazinol hydrochloride	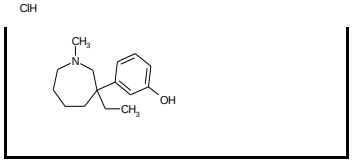	C15H24ClNO	269.82	Store at +4°C	59263-76-2	Central Nervous System	Analgesic
Prestw-1005	13E06	Apramycin	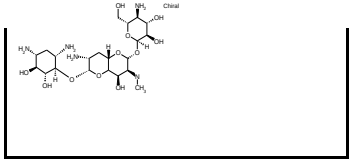	C21H41N5O11	539.59	Store at room temperature	37321-09-8	Metabolism	Antibacterial

								Infectiology	
Prestw-1006	13E07	Epitiostanol	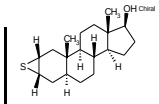	C19H30OS	306.51	Store at +4°C	2363-58-8	Oncology	Antineoplastic
Prestw-1007	13E08	Fursultiamine Hydrochloride	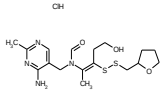	C17H27ClN4O3S2	435.01	Store at room temperature	2105-43-3	Metabolism	Anti-Alzheimer
Prestw-1008	13E09	Gabexate mesilate	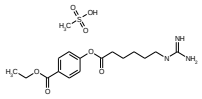	C17H27N3O7S	417.48	Store at room temperature	56974-61-9	Hematology	Anticoagulant
								Metabolism	
Prestw-1009	13E10	Pivampicillin	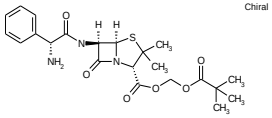	C22H29N3O6S	463.56	Store at +4°C	33817-20-8	Metabolism	Antibacterial
								Infectiology	
Prestw-1010	13E11	Talampicillin hydrochloride	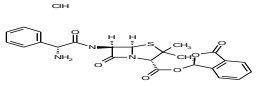	C24H24ClN3O6S	517.99	Store at room temperature	39878-70-1	Metabolism	Antibacterial
								Infectiology	
Prestw-1011	13F02	Flucloxacillin sodium	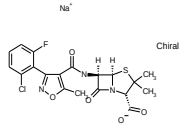	C19H16ClFN3NaO5S	475.86	Store at -20°C	1847-24-1	Metabolism	Antibacterial
								Infectiology	

Prestw-1012	13F03	Trapidil	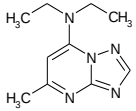	C10H15N5	205.26	Store at +4°C	15421-84-8	Cardiovascular	Vasodilator
Prestw-1013	13F04	Deptropine citrate	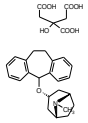	C29H35NO8	525.60	Store at +4°C	2169-75-7	Allergology	Antihistaminic
								Cardiovascular	Bronchodilator
								Respiratory	Vasodilator
Prestw-1014	13F05	Sertraline	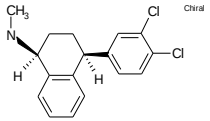	C17H17Cl2N	306.24	Store at -20°C	79617-96-2	Central Nervous System	Antidepressant
									CNS Stimulant
Prestw-1015	13F06	Ethamsylate	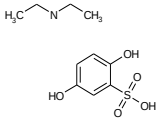	C10H17NO5S	263.31	Store at +4°C	2624-44-4	Cardiovascular	Antiplatelet
								Hematology	Hemostatic
Prestw-1016	13F07	Moxonidine	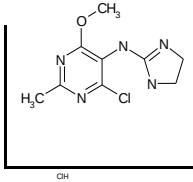	C9H12ClN5O	241.68	Store at +4°C	75438-57-2	Cardiovascular	Antihypertensive
Prestw-1017	13F08	Etilefrine hydrochloride	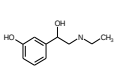	C10H16ClNO2	217.70	Store at +4°C	534-87-2	Cardiovascular	Vasoconstrictor

Prestw-1018	13F09	Alprostadil	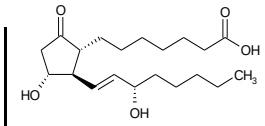	C20H34O5	354.49	Store at -20°C	745-65-3	Cardiovascular	Erectile dysfunction treatment
									Vasodilator
Prestw-1019	13F10	Tribenoside	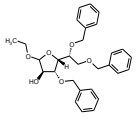	C29H34O6	478.59	Store at -20°C	10310-32-4	Cardiovascular	
Prestw-1020	13F11	Rimexolone	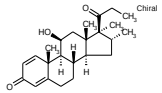	C24H34O3	370.54	Store at room temperature	49697-38-3	Metabolism	Anti-inflammatory
Prestw-1021	13G02	Isradipine	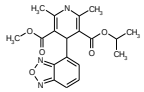	C19H21N3O5	371.40	Store at room temperature	75695-93-1	Cardiovascular	Antianginal
									Antihypertensive
Prestw-1022	13G03	Tiletamine hydrochloride	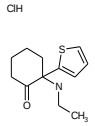	C12H18ClNOS	259.80	Store at room temperature	14176-50-2	Central Nervous System	Anesthetic
									Anticonvulsant
Prestw-1023	13G04	Isometheptene mucate	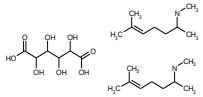	C24H48N2O8	492.66	Store at room temperature	7492-31-1	Cardiovascular	Antimigraine
									Vasoconstrictor

Prestw-1024	13G05	Nifurtimox	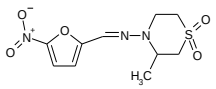	C10H13N3O5S	287.30	Store at room temperature	23256-30-6	Metabolism	
Prestw-1025	13G06	Letrozole	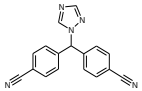	C17H11N5	285.31	Store at room temperature	112809-51-5	Oncology	Antineoplastic
Prestw-1026	13G07	Arbutin	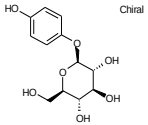	C12H16O7	272.26	Store at -20°C	497-76-7	Metabolism	Antibacterial
								Infectiology	
Prestw-1027	13G08	Tocainide hydrochloride	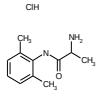	C11H17ClN2O	228.72	Store at RT	71395-14-7	Cardiovascular	Anesthetic
								Central Nervous System	Antiarrhythmic
Prestw-1028	13G09	Benzathine benzylpenicillin	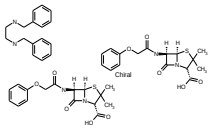	C48H56N6O10S2	941.14	Store at +4°C	5928-84-7	Metabolism	Antibacterial
								Infectiology	
Prestw-1029	13G10	Risperidone	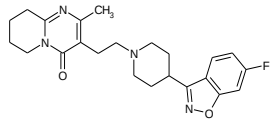	C23H27FN4O2	410.50	Store at +4°C	106266-06-2	Central Nervous System	Antipsychotic

Prestw-1030	13G11	Torsemide	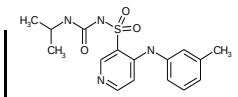	C16H20N4O3S	348.43	Store at room temperature	56211-40-6	Cardiovascular	Antihypertensive
									Diuretic
Prestw-1031	13H02	Halofantrine hydrochloride	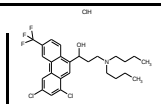	C26H31Cl3F3NO	536.90	Store at room temperature	36167-63-2	Metabolism	Antimalarial
Prestw-1032	13H03	Articaine hydrochloride	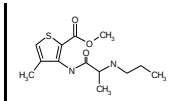	C13H21ClN2O3S	320.84	Store at +4°C	23964-57-0	Central Nervous System	Anesthetic
Prestw-1033	13H04	Nomegestrol acetate	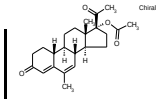	C23H30O4	370.49	Store at room temperature	58652-20-3	Endocrinology	Contraceptive
Prestw-1034	13H05	Pancuronium bromide	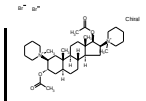	C35H60Br2N2O4	732.69	Store at room temperature	15500-66-0	Neuromuscular	Muscle relaxant
Prestw-1035	13H06	Molindone hydrochloride	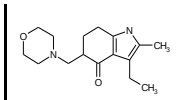	C16H25ClN2O2	312.84	Store at room temperature	15622-65-8	Central Nervous System	Antipsychotic

Prestw-1036	13H07	Alcuronium chloride	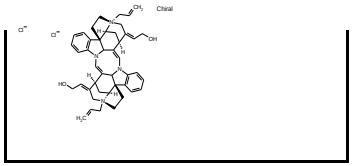	C44H50Cl2N4O2	737.82	Store at -20°C	15180-03-7	Neuromuscular	Muscle relaxant
Prestw-1037	13H08	Zalcitabine	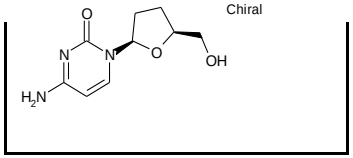	C9H13N3O3	211.22	Store at -20°C	7481-89-2	Metabolism	Antiviral
Prestw-1038	13H09	Methyldopate hydrochloride		C12H18ClNO4	275.73	Store at room temperature	2508-79-4	Cardiovascular	Antihypertensive
Prestw-1039	13H10	Levocabastine hydrochloride	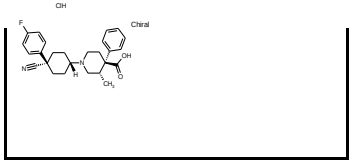	C26H30ClFN2O2	456.99	Store at +4°C	79547-78-7	Allergology	Antihistaminic
Prestw-1040	13H11	Pyrvinium pamoate	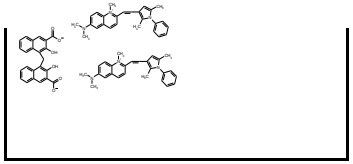	C75H70N6O6	1151.43	Store at room temperature	3546-41-6	Metabolism	
Prestw-1041	14A02	Etomidate	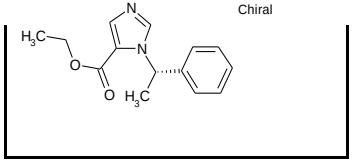	C14H16N2O2	244.30	Store at room temperature	33125-97-2	Central Nervous System	Anesthetic
									Hypnotic
Prestw-1042	14A03	Tridihexethyl chloride		C21H36ClNO	353.98	Store at room temperature	4310-35-4	Neuromuscular	Antispastic

Prestw-1043	14A04	Penbutolol sulfate	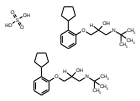	C36H60N2O8S	680.95	Store at room temperature	38363-32-5	Cardiovascular	Antianginal
									Antiarrhythmic
									Antihypertensive
Prestw-1044	14A05	Prednicarbate	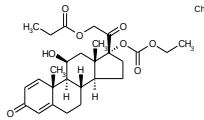	C27H36O8	488.58	Store at +4°C	73771-04-7	Metabolism	Anti-Inflammatory
Prestw-1045	14A06	Sertaconazole nitrate	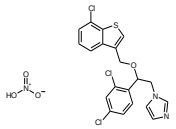	C20H16Cl3N3O4S	500.79	Store at +4°C	99592-39-9	Metabolism	Antibacterial
								Infectiology	Antifungal
Prestw-1046	14A07	Repaglinide	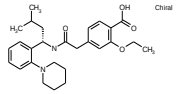	C27H36N2O4	452.60	Store at room temperature	135062-02-1	Endocrinology	Antidiabetic
Prestw-1047	14A08	Piretanide	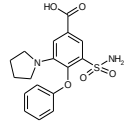	C17H18N2O5S	362.41	Store at +4°C	55837-27-9	Cardiovascular	Antihypertensive
									Diuretic
Prestw-1048	14A09	Piperacetazine	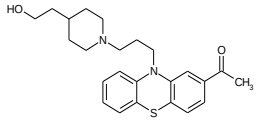	C24H30N2O2S	410.58	Store at room temperature	3819-00-9	Central Nervous System	Antipsychotic

Prestw-1049	14A10	Oxyphenbutazone	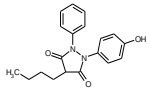	C19H20N2O3	324.38	Store at room temperature	129-20-4	Metabolism	Anti-inflammatory
Prestw-1050	14A11	Quinethazone	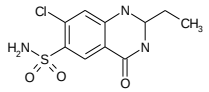	C10H12ClN3O3S	289.74	Store at room temperature	73-49-4	Cardiovascular	Antihypertensive
									Diuretic
Prestw-1051	14B02	Moricizine hydrochloride	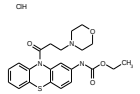	C22H26ClN3O4S	463.99	Store at room temperature	31883-05-3	Cardiovascular	Antiarrhythmic
Prestw-1052	14B03	Iopanoic acid	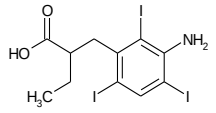	C11H12I3NO2	570.94	Store at +4°C	96-83-3	Diagnostic	Contrastant
Prestw-1053	14B04	Pivmecillinam hydrochloride	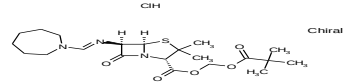	C21H34ClN3O5S	476.04	Store at -20°C	32887-03-9	Metabolism	Antibacterial
								Infectiology	
Prestw-1054	14B05	Levopropoxyphene napsylate	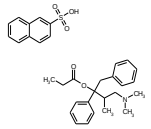	C32H37NO5S	547.72	Store at room temperature	5714-90-9	Central Nervous System	Analgesic
								Respiratory	Antitussive

Prestw-1055	14B06	Piperidolate hydrochloride	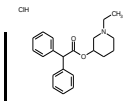	C21H26ClNO2	359.90	Store at room temperature	129-77-1	Neuromuscular	Antispastic
Prestw-1056	14B07	Trifluridine	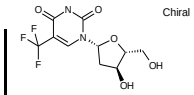	C10H11F3N2O5	296.20	Store at room temperature	70-00-8	Metabolism	Antiviral
Prestw-1057	14B08	Oxprenolol hydrochloride	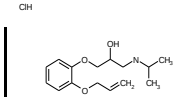	C15H24ClNO3	301.82	Store at room temperature	6452-73-9	Cardiovascular	Antianginal
									Antiarrhythmic
									Antihypertensive
Prestw-1058	14B09	Ondansetron Hydrochloride	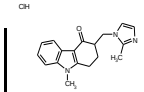	C18H20ClN3O	329.83	Store at room temperature	103639-04-9	Central Nervous System	Antianemic
Prestw-1059	14B10	Propoxycaine hydrochloride		C16H27ClN2O3	330.86	Store at room temperature	550-83-4	Central Nervous System	Anesthetic
Prestw-1060	14B11	Oxaprozin	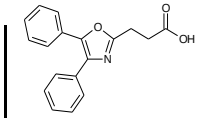	C18H15NO3	293.33	Store at room temperature	21256-18-8	Central Nervous System	Analgesic
								Metabolism	Anti-inflammatory

Prestw-1061	14C02	Phensuximide	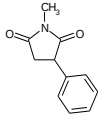	C11H11NO2	189.22	Store at room temperature	86-34-0	Central Nervous System	Anticonvulsant
Prestw-1062	14C03	Ioxaglic acid	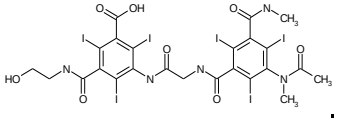	C24H21I6N5O8	1268.89	Store at +4°C	59017-64-0	Diagnostic	Contrastant
Prestw-1063	14C04	Naftifine hydrochloride	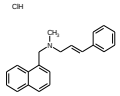	C21H22ClN	323.87	Store at -20°C	65473-14-5	Infectiology	Antifungal
								Metabolism	
Prestw-1064	14C05	Meprylcaine hydrochloride	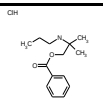	C14H22ClNO2	271.79	Store at room temperature	956-03-6	Neuromuscular	Local anesthetic
Prestw-1065	14C06	Milrinone	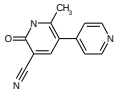	C12H9N3O	211.23	Store at room temperature	78415-72-2	Cardiovascular	Vasodilator
Prestw-1066	14C07	Methantheline bromide	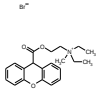	C21H26BrNO3	420.35	Store at room temperature Hydroscopic	53-46-3	Neuromuscular	Antispastic
Prestw-1067	14C08	Ticarcillin sodium	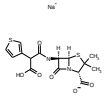	C15H15N2NaO6S2	406.41	Store at +2°C Hygroscopic	74682-62-5	Infectiology	Antibacterial

								Metabolism	
Prestw-1068	14C09	Thiethylperazine dimalate	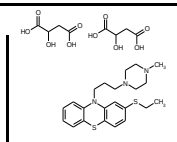	C30H41N3O10S2	667.80	Store at room temperature	52239-63-1	Central Nervous System	Antiemetic
									Antivertigo
Prestw-1069	14C10	Mesalamine	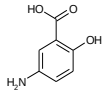	C7H7NO3	153.14	Store at 2°C	89-57-6	Metabolism	Anti-inflammatory
Prestw-1362	14C11	Vorinostat	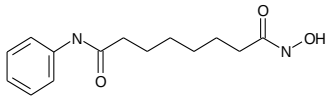	C14H20N2O3	264.33	Store at -20°C	149647-78-9	Oncology	Antineoplastic
Prestw-1071	14D02	Imidurea	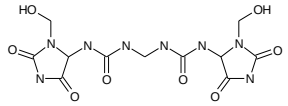	C11H16N8O8	388.30	Store at 2°C Polar,Hydrophilic	39236-46-9	Infectiology	Antifungal
Prestw-1072	14D03	Lansoprazole	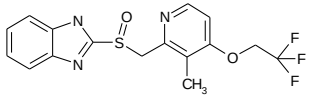	C16H14F3N3O2S	369.37	Store at 2°C	103577-45-3	Metabolism	Antiulcer
Prestw-1073	14D04	Bethanechol chloride	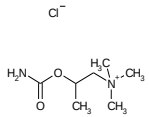	C7H17ClN2O2	196.68	Store at 2°C	590-63-6	Metabolism	

Prestw-1074	14D05	Cyproterone acetate	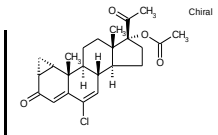	C24H29ClO4	416.95	Store at 2°C	427-51-0	Endocrinology	Antineoplastic
									Contraceptive
Prestw-1075	14D06	(R)-Propranolol hydrochloride	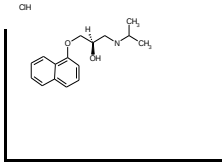	C16H22ClNO2	295.81	Store at 2°C	13071-11-9	Cardiovascular	Antianginal
									Antiarrhythmic
									Antihypertensive
									Antimigraine
Prestw-1076	14D07	Ciprofibrate	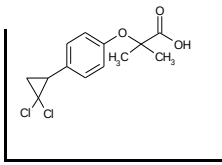	C13H14Cl2O3	289.16	Store at 2°C	52214-84-3	Metabolism	Hypocholesterolemic
Prestw-1420	14D08	Formestane	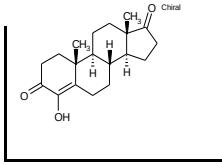	C19H26O3	302.42	Store at -20°C	566-48-3	Endocrinology	Antineoplastic
								Oncology	
Prestw-1078	14D09	Benzylpenicillin sodium	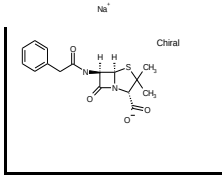	C16H17N2NaO4S	356.38	Store at 2°C	69-57-8	Infectiology	Antibacterial
								Metabolism	

Prestw-1079	14D10	Chlorambucil	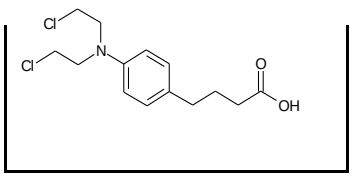	C14H19Cl2NO2	304.22	Store at 2°C HUMAN CARCINOGEN	305-03-3	Oncology	Antineoplastic
Prestw-1080	14D11	Methiazole	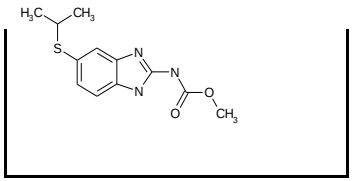	C12H15N3O2S	265.34	Store at 2°C	108579-67-5	Infectiology	Antihelmintic
								Metabolism	
Prestw-1081	14E02	(S)-propranolol hydrochloride	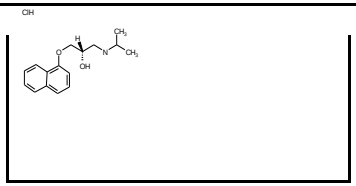	C16H22ClNO2	295.81	Store at 2°C	4199-10-4	Cardiovascular	Antianginal
									Antiarrhythmic
									Antihypertensive
Prestw-1082	14E03	(-)-Eseroline fumarate salt	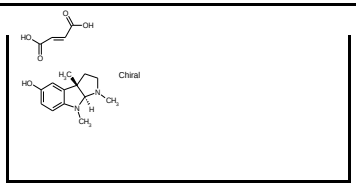	C17H22N2O5	334.38	Store at 2°C	104015-29-4	Central Nervous System	Analgesic
Prestw-1294	14E04	Isosorbide mononitrate	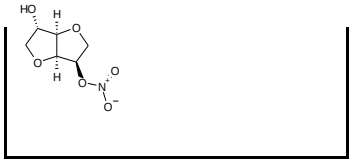	C6H9NO6	191.14	Store at -20°C	16051-77-7	Cardiovascular	Antianginal
Prestw-1516	14E05	Levalbuterol hydrochloride	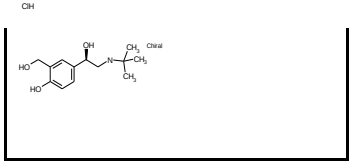	C13H22ClNO3	275.78	Store at room temperature	50293-90-8	Respiratory	Antiasthmatic
									Bronchodilator

Prestw-1493	14E06	Topiramate	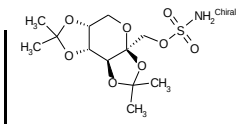	C12H21NO8S	339.37	Store at room temperature	97240-79-4	Central Nervous System	Anticonvulsant
									Antimigraine
Prestw-1086	14E07	D-cycloserine	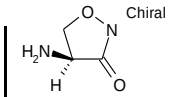	C3H6N2O2	102.09	Store at 2°C	68-41-7	Infectiology	Antibacterial
								Metabolism	
Prestw-1087	14E08	2-Chloropyrazine	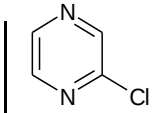	C4H3ClN2	114.53	Store at 4°C	14508-49-7	Cardiovascular	
Prestw-1088	14E09	(+,-)-Synephrine	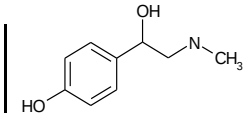	C9H13NO2	167.21	Store at 2°C	94-07-5	Cardiovascular	Vasoconstrictor
Prestw-1089	14E10	(S)-(-)-Cycloserine	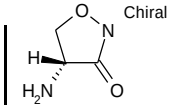	C3H6N2O2	102.09	Store at - 20°C	339-72-0	Infectiology	Antibacterial
								Metabolism	
Prestw-1090	14E11	Homosalate	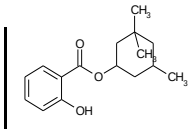	C16H22O3	262.35	Store at -20°C	118-56-9	Dermatology	Radioprotectant
Prestw-1091	14F02	Spaglumic acid	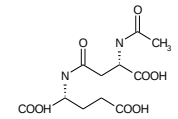	C11H16N2O8	304.26	Store at RT	4910-46-7	Allergology	Antiallergic

								Cardiovascular	Vasodilator
Prestw-1092	14F03	Ranolazine	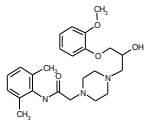	C24H33N3O4	427.55	store at -20°C	95635-55-5	Cardiovascular	Antianginal
Prestw-1443	14F04	Misoprostol	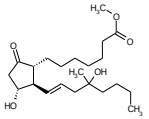	C22H38O5	382.55	Store at -20°C	59122-46-2	Metabolism	Antiulcer
Prestw-1094	14F05	Sulfadoxine	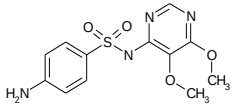	C12H14N4O4S	310.33	Store at -20°C	2447-57-6	Infectiology	Antibacterial
								Metabolism	
Prestw-1095	14F06	Cyclopentolate hydrochloride	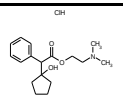	C17H26ClNO3	327.85	Store at -20°C	5870-29-1	Metabolism	
Prestw-1096	14F07	Estriol	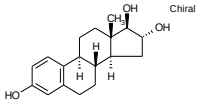	C18H24O3	288.39	Store at -20°C	50-27-1	Endocrinology	
Prestw-1097	14F08	(-)-Isoproterenol hydrochloride	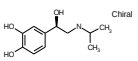	C11H18ClNO3	247.72	Store below 0°C	5984-95-2	Cardiovascular	Bronchodilator
								Respiratory	Vasodilator

Prestw-1339	14F09	Sarafloxacin	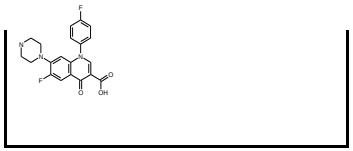	C20H17F2N3O3	385.37	Store at room temperature	98105-99-8	Infectiology	Antibacterial
								Metabolism	
Prestw-1099	14F10	Nialamide	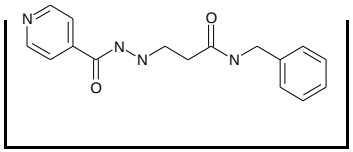	C16H18N4O2	298.35	Store at -20°C	51-12-7	Central Nervous System	Antidepressant
Prestw-1195	14F11	Toltrazuril	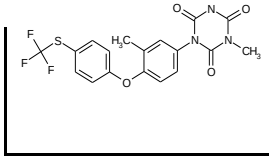	C18H14F3N3O4S	425.39	Store at room temperature	69004-03-1	Infectiology	Anticoccidial
Prestw-1101	14G02	Perindopril	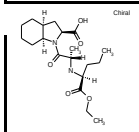	C19H32N2O5	368.48	store at -20°C	82834-16-0	Cardiovascular	Antihypertensive
Prestw-1102	14G03	Fexofenadine HCl	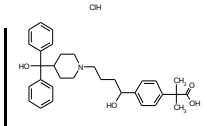	C32H40ClNO4	538.13	store at -20°C	153439-40-8	Allergology	Antihistaminic
Prestw-1202	14G04	4-aminosalicylic acid	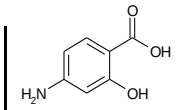	C7H7NO3	153.14	Store at room temperature	65-49-6	Infectiology	Antibacterial
								Metabolism	Antifungal
Prestw-1104	14G05	Clonixin Lysinate	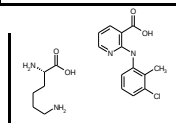	C19H25ClN4O4	408.89	store at -20°C	55837-30-4	Central Nervous System	Analgesic
								Infectiology	Antifungal

Prestw-1105	14G06	Verteporfin	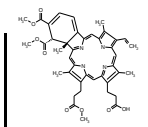	C41H42N4O8	718.81	Store at -20°C	129497-78-5	Ophthalmology	
Prestw-1106	14G07	Meropenem	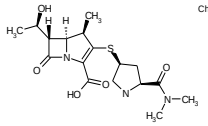	C17H25N3O5S	383.47	Store at -20°C	96036-03-2	Infectiology	Antibacterial
								Metabolism	
Prestw-1107	14G08	Ramipril	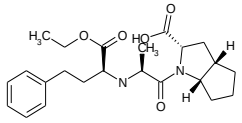	C23H32N2O5	416.52	Store at -20°C	87333-19-5	Cardiovascular	Antihypertensive
								Metabolism	
Prestw-1108	14G09	Mephenytoin	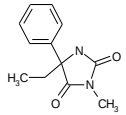	C12H14N2O2	218.26	Store at -20°C	50-12-4	Central Nervous System	Anticonvulsant
Prestw-1109	14G10	Rifabutin	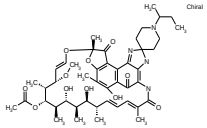	C46H62N4O11	847.03	Store at -20°C	72559-06-9	Infectiology	Antibacterial
								Metabolism	
Prestw-1110	14G11	Parbendazole	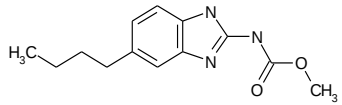	C13H17N3O2	247.30	Store at -20°C	14255-87-9	Infectiology	

								Metabolism	
Prestw-1111	14H02	Mecamylamine hydrochloride	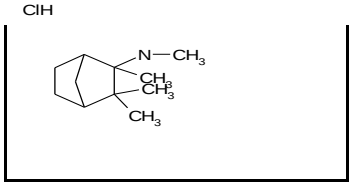	C11H22ClN	203.76	Store at -20°C	826-39-1	Cardiovascular	Antihypertensive
Prestw-1112	14H03	Procarbazine hydrochloride	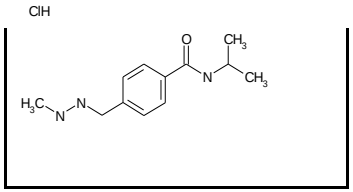	C12H20ClN3O	257.77	Store at -20°C HUMAN CARCINOGEN	366-70-1	Oncology	Antineoplastic
Prestw-1113	14H04	Viomycin sulfate	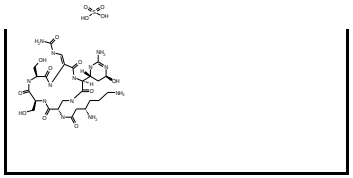	C25H45N13O14S	783.78	Store at -20°C Hygroscopic	37883-00-4	Infectiology	Antibacterial
								Metabolism	
Prestw-1114	14H05	Saquinavir mesylate	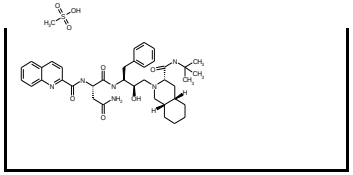	C39H54N6O8S	766.96	Store at +4°C	149845-06-7	Immunology	Antiviral
								Infectiology	
								Metabolism	
Prestw-1115	14H06	Ronidazole	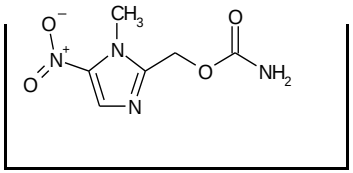	C6H8N4O4	200.16	Store below 0°C	7681-76-7	Infectiology	Antibacterial
								Metabolism	Antiprotozoal
									Antitrichomonal

Prestw-1116	14H07	Dorzolamide hydrochloride	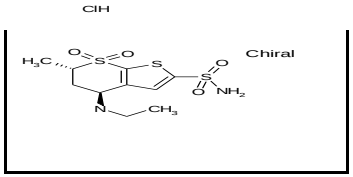	C10H17ClN2O4S3	360.90	Store at room temperature	130693-82-2	Cardiovascular	Antiglaucoma
									Antihypertensive
Prestw-1117	14H08	Azaperone	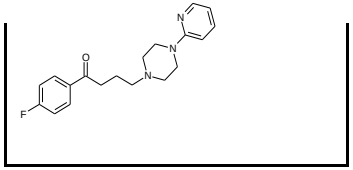	C19H22FN3O	327.41	Store at room temperature	1649-18-9	Central Nervous System	Antipsychotic
									Sedative
Prestw-1118	14H09	Cefepime hydrochloride	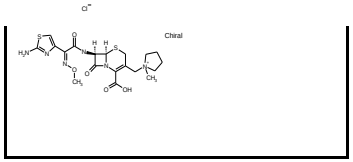	C19H25ClN6O5S2	517.03	Store at +4°C	123171-59-5	Infectiology	Antibacterial
								Metabolism	
Prestw-1119	14H10	Clocortolone pivalate	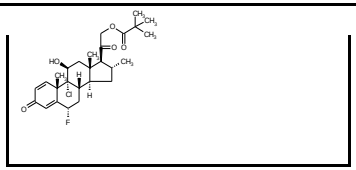	C27H36ClFO5	495.04	Store at +4°C	34097-16-0	Endocrinology	Anti-inflammatory
Prestw-1120	14H11	Nadifloxacin	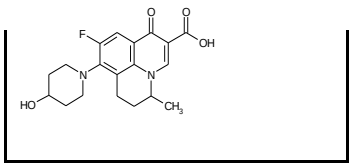	C19H21FN2O4	360.39	store at -20°C	124858-35-1	Infectiology	Antibacterial
								Metabolism	
Prestw-1283	15A02	Buspirone hydrochloride	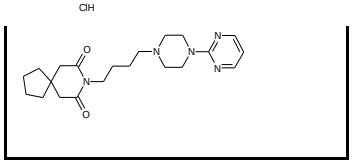	C21H32ClN5O2	421.97	Store at -20°C	33386-08-2	Central Nervous System	

Prestw-1222	15A03	Anastrozole	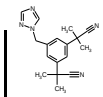	C17H19N5	293.37	Store at room temperature	120511-73-1	Oncology	Antineoplastic
Prestw-1399	15A04	Doxycycline hydrochloride	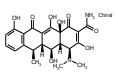	C22H25ClN2O8	480.91	Store at room temperature	10592-13-9	Metabolism	Antibacterial
Prestw-1345	15A05	Sulbactam	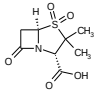	C8H11NO5S	233.24	Store at room temperature	68373-14-8	Infectiology	Antibacterial
								Metabolism	
Prestw-1414	15A06	Fleroxacin	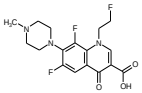	C17H18F3N3O3	369.35	Store at room temperature	79660-72-3	Infectiology	Antibacterial
Prestw-1315	15A07	Clavulanate potassium salt		C8H8KNO5	237.26	Store at - 20°C	58001-44-8	Infectiology	Antibacterial
								Metabolism	
Prestw-1482	15A08	Valproic acid	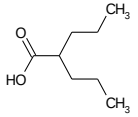	C8H16O2	144.22	Store at room temperature	99-66-1	Central Nervous System	Anticonvulsant
Prestw-1280	15A09	Mepivacaine hydrochloride		C15H23ClN2O	282.82	Store at room temperature	1722-62-9	Neuromuscular	Local anesthetic

Prestw-1478	15A10	Rifaximin	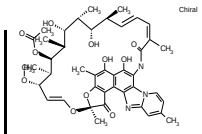	C43H51N3O11	785.90	Store at -20°C	80621-81-4	Infectiology	Antibacterial
								Metabolism	
Prestw-1473	15A11	Estradiol Valerate	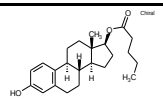	C23H32O3	356.51	Store at room temperature	979-32-8	Endocrinology	Contraceptive
Prestw-1206	15B02	Acetylcysteine	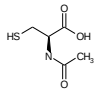	C5H9NO3S	163.20	Store at room temperature	616-91-1	Metabolism	Mucolytic
Prestw-1435	15B03	Melengestrol acetate	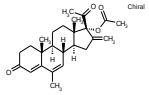	C25H32O4	396.53	Store at room temperature	2919-66-6	Endocrinology	
Prestw-1246	15B04	Bromhexine hydrochloride		C14H21Br2ClN2	412.60	Store at room temperature	611-75-6	Respiratory	Expectorant
Prestw-1223	15B05	Anethole-trithione	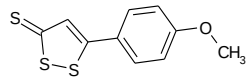	C10H8OS3	240.37	Store at room temperature	532-11-6	Metabolism	Choleretic
Prestw-1476	15B06	Amcinonide	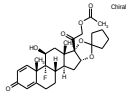	C28H35FO7	502.59	Store at room temperature	51022-69-6	Metabolism	Anti-inflammatory
Prestw-1256	15B07	Caffeine	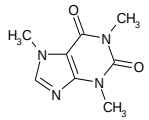	C8H10N4O2	194.19	Store at room temperature	58-08-2	Central Nervous System	CNS Stimulant
			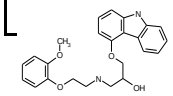						

Prestw-1262	15B08	Carvedilol		C24H26N2O4	406.49	Store at room temperature	72956-09-3	Cardiovascular	Antihypertensive
Prestw-1282	15B09	Methenamine		C6H12N4	140.19	Store at +4°C	100-97-0	Infectiology	Antibacterial
Prestw-1308	15B10	Phentermine hydrochloride	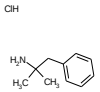	C10H16ClN	185.70	Store at room temperature	1197-21-3	Central Nervous System	
Prestw-1394	15B11	Diclazuril	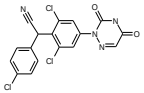	C17H9Cl3N4O2	407.65	Store at room temperature	101831-37-2	Metabolism	
Prestw-1249	15C02	Famciclovir	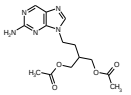	C14H19N5O4	321.34	Store at room temperature	104227-87-4	Infectiology	Antiviral
								Metabolism	
Prestw-1398	15C03	Dopamine hydrochloride	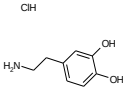	C8H12ClNO2	189.64	Store at room temperature	62-31-7	Cardiovascular	Antihypertensive
Prestw-1263	15C04	Cefdinir	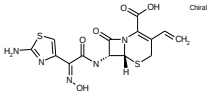	C14H13N5O5S2	395.42	Store at room temperature	91832-40-5	Infectiology	Antibacterial
								Metabolism	
Prestw-1261	15C05	Carprofen	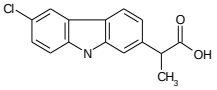	C15H12ClNO2	273.72	Store at room temperature	53716-49-7	Metabolism	Anti-inflammatory

Prestw-1371	15C06	Celecoxib	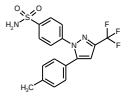	C17H14F3N3O2S	381.38	Store at room temperature	169590-42-5	Metabolism	Anti-inflammatory
Prestw-1258	15C07	Candesartan	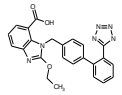	C24H20N6O3	440.47	Store at room temperature	139481-59-7	Cardiovascular	Antihypertensive
Prestw-1483	15C08	Fludarabine	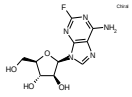	C10H12FN5O4	285.24	Store at room temperature	21679-14-1	Oncology	Antineoplastic
Prestw-1484	15C09	Cladribine	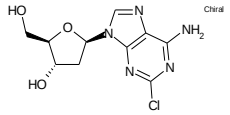	C10H12ClN5O3	285.69	Store at -20°C	4291-63-8	Oncology	Antineoplastic
Prestw-1356	15C10	Vardenafil	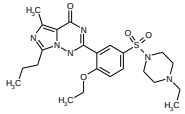	C23H32N6O4S	488.61	Store at room temperature	224785-90-4	Cardiovascular	Erectile dysfunction treatment
Prestw-1417	15C11	Fluconazole		C13H12F2N6O	306.28	Store at room temperature	86386-73-4	Metabolism	Antifungal
Prestw-1203	15D02	5-fluorouracil	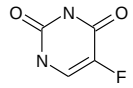	C4H3FN2O2	130.08	Store at room temperature	51-21-8	Oncology	Antineoplastic
Prestw-1487	15D03	Mesna	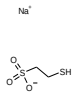	C2H5NaO3S2	164.18	Store at room temperature	19767-45-4	Oncology	Chemoprotectant

Prestw-1444	15D04	Mitotane	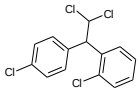	C14H10Cl4	320.05	Store at room temperature	53-19-0	Endocrinology	Antineoplastic
								Oncology	
Prestw-1497	15D05	Ambrisentan	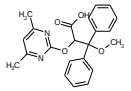	C22H22N2O4	378.43	Store at room temperature	177036-94-1	Cardiovascular	Antihypertensive
Prestw-1479	15D06	Triclosan	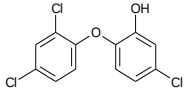	C12H7Cl3O2	289.55	Store at room temperature	3380-34-5	Infectiology	Antibacterial
									Antifungal
									Antiseptic
Prestw-1401	15D07	Enoxacin	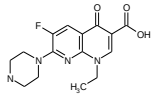	C15H17FN4O3	320.33	Store at room temperature	84294-96-2	Infectiology	Antibacterial
								Metabolism	
Prestw-1307	15D08	Olopatadine hydrochloride	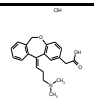	C21H24ClNO3	373.88	Store at room temperature	140462-76-6	Allergology	Antihistaminic
Prestw-1187	15D09	Granisetron	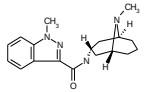	C18H24N4O	312.42	Store at room temperature	109889-09-0	Endocrinology	Antiemetic

Prestw-1224	15D10	Anthralin	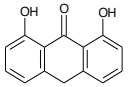	C14H10O3	226.23	Store at room temperature	1143-38-0	Dermatology	Antipsoriatic
Prestw-1492	15D11	Lamotrigine	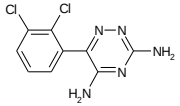	C9H7Cl2N5	256.10	Store at room temperature	84057-84-1	Central Nervous System	Anticonvulsant
Prestw-1383	15E02	Clofibrate	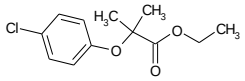	C12H15ClO3	242.70	Store at room temperature	637-07-0	Metabolism	Antilipemic
Prestw-1481	15E03	Cyclophosphamide	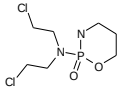	C7H15Cl2N2O2P	261.09	Store at room temperature	50-18-0	Immunology	Antineoplastic
								Oncology	Immunosuppressant
Prestw-1229	15E04	Aripiprazole	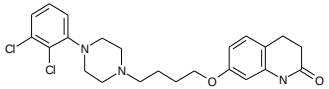	C23H27Cl2N3O2	448.40	Store at room temperature	129722-12-9	Central Nervous System	Antipsychotic
Prestw-1405	15E05	Ethinylestradiol	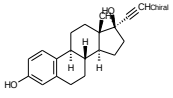	C20H24O2	296.41	Store at room temperature	57-63-6	Endocrinology	Contraceptive
Prestw-1419	15E06	Fluocinolone acetonide	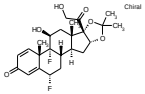	C24H30F2O6	452.50	Store at room temperature	67-73-2	Metabolism	Anti-inflammatory
Prestw-1343	15E07	Sparfloxacin	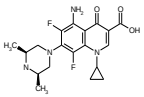	C19H22F2N4O3	392.41	Store at room temperature	110871-86-8	Infectiology	Antibacterial

								Metabolism	
Prestw-1390	15E08	Desloratadine	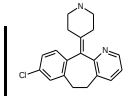	C19H19ClN2	310.83	Store at room temperature	100643-71-8	Allergology	Antihistaminic
Prestw-1378	15E09	Clarithromycin	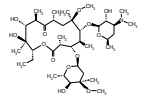	C38H69NO13	747.97	Store at room temperature	81103-11-9	Infectiology	Antibacterial
								Metabolism	
Prestw-1199	15E10	Tripelennamine hydrochloride		C16H22ClN3	291.83	Store at room temperature	154-69-8	Allergology	Antihistaminic
Prestw-1352	15E11	Tulobuterol	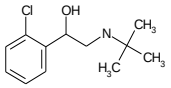	C12H18ClNO	227.74	Store at room temperature	41570-61-0	Respiratory	Bronchodilator
Prestw-1196	15F02	Topotecan	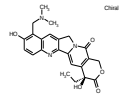	C23H23N3O5	421.46	Store at room temperature	123948-87-8	Oncology	Antineoplastic
Prestw-1232	15F03	Atorvastatin	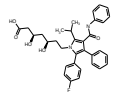	C33H35FN2O5	558.66	Store at room temperature	134523-00-5	Metabolism	
Prestw-1234	15F04	Azithromycin	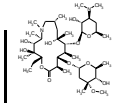	C38H72N2O12	749.00	Store at room temperature	83905-01-5	Infectiology	Antibacterial

								Metabolism	
Prestw-1286	15F05	Ibudilast	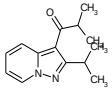	C14H18N2O	230.31	Store at room temperature	50847-11-5	Metabolism	Anti-inflammatory
Prestw-1433	15F06	Losartan	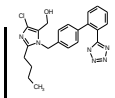	C22H23ClN6O	422.92	Store at room temperature	114798-26-4	Cardiovascular	Antihypertensive
Prestw-1236	15F07	Benztropine mesylate	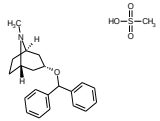	C22H29NO4S	403.54	Store at room temperature	132-17-2	Central Nervous System	Antiparkinsonian
Prestw-1359	15F08	Vecuronium bromide	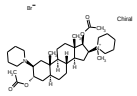	C34H57BrN2O4	637.75	Store at room temperature	50700-72-6	Metabolism	Muscle relaxant
Prestw-1350	15F09	Telmisartan	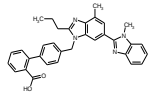	C33H30N4O2	514.63	Store at room temperature	144701-48-4	Cardiovascular	Antihypertensive
Prestw-1490	15F10	Nalmefene hydrochloride	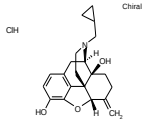	C21H26ClNO3	375.90	Store at room temperature	58895-64-0	Central Nervous System	
Prestw-1241	15F11	Bifonazole	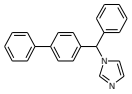	C22H18N2	310.40	Store at room temperature	60628-96-8	Infectiology	Antifungal
								Metabolism	

Prestw-1265	15G02	Gatifloxacin	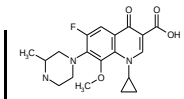	C19H22FN3O4	375.40	Store at room temperature	112811-59-3	Infectiology	Antibacterial
								Metabolism	
Prestw-1244	15G03	Bosentan	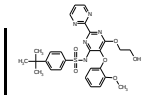	C27H29N5O6S	551.63	Store at room temperature	147536-97-8	Cardiovascular	Vasodilator
Prestw-1266	15G04	Gemcitabine	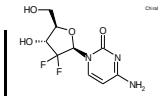	C9H11F2N3O4	263.20	Store at room temperature	95058-81-4	Oncology	Antineoplastic
Prestw-1190	15G05	Olmesartan	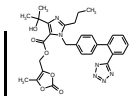	C29H30N6O6	558.60	Store at room temperature	144689-63-4	Cardiovascular	Antihypertensive
Prestw-1480	15G06	Racepinephrine HCl	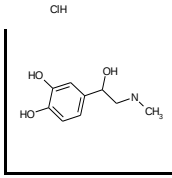	C9H14ClNO3	219.67	Store at -20°C	329-63-5	Cardiovascular	Bronchodilator
								Respiratory	Vasoconstrictor
Prestw-1189	15G07	Montelukast	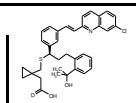	C35H36ClNO3S	586.20	Store at room temperature	158966-92-8	Respiratory	Antiasthmatic
Prestw-1180	15G08	Docetaxel	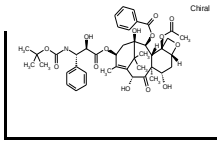	C43H53NO14	807.90	Store at room temperature	114977-28-5	Oncology	Antineoplastic

Prestw-1376	15G09	Cilnidipine	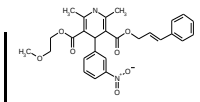	C27H28N2O7	492.53	Store at room temperature	132203-70-4	Cardiovascular	Antihypertensive
Prestw-1291	15G10	Imiquimod		C14H16N4	240.31	Store at room temperature	99011-02-6	Dermatology	Antiviral
								Immunology	
								Infectiology	
								Oncology	
Prestw-1423	15G11	Fosinopril	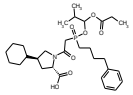	C30H46NO7P	563.68	Store at room temperature	98048-97-6	Cardiovascular	Antihypertensive
Prestw-1290	15H02	Imatinib		C29H31N7O	493.62	Store at room temperature	152459-95-5	Oncology	Antineoplastic
Prestw-1446	15H03	Moxifloxacin	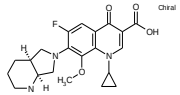	C21H24FN3O4	401.44	Store at room temperature	151096-09-2	Infectiology	Antibacterial
								Metabolism	
Prestw-1421	15H04	Formoterol fumarate	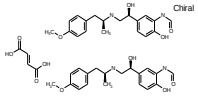	C42H52N4O12	804.90	Store at room temperature	43229-80-7	Respiratory	Antiasthmatic
Prestw-1338	15H05	Rufloxacin	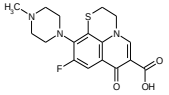	C17H18FN3O3S	363.41	Store at room temperature	101363-10-4	Infectiology	Antibacterial
								Metabolism	

Prestw-1319	15H06	Pravastatin	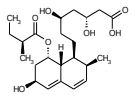	C23H36O7	424.54	Store at room temperature	81093-37-0	Metabolism	Antilipemic
Prestw-1337	15H07	Rosiglitazone Hydrochloride	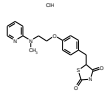	C18H20ClN3O3S	393.90	Store at room temperature	122320-73-4	Metabolism	Antidiabetic
Prestw-1334	15H08	Rivastigmine	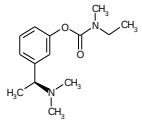	C14H22N2O2	250.34	Store at room temperature	123441-03-2	Central Nervous System	
Prestw-1342	15H09	Sildenafil	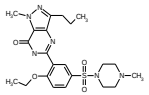	C22H30N6O4S	474.59	Store at room temperature	139755-83-2	Cardiovascular	Antihypertensive
									Erectile dysfunction treatment
Prestw-1207	15H10	Acetylsalicylic acid	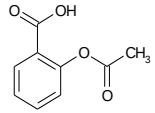	C9H8O4	180.16	Store at -20°C	50-78-2	Central Nervous System	Analgesic
									Anti-inflammatory
									Antipyretic
Prestw-1472	15H11	Hexachlorophene	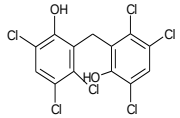	C13H6Cl6O2	406.91	Store at -20°C	70-30-4	Infectiology	Antiseptic